On distributed control analysis and design for Multi-Agent systems subject to limited information

Laura Dal Col

THÈSE

En vue de l'obtention du

DOCTORAT DE L'UNIVERSITÉ FÉDÉRALE TOULOUSE MIDI-PYRÉNÉES

Délivré par :

l'Institut National des Sciences Appliquées de Toulouse (INSA de Toulouse)

Présentée et soutenue le *25/10/2016* **par :**

Laura Dal Col

On Distributed Control Analysis and Design for Multi-Agent Systems subject to Limited Information

---

JURY

Maria D. Di Benedetto	Professor	Rapporteur
Matthew C. Turner	Professor	Rapporteur
Sophie Tarbouriech	Directeur de Recherche	Examinateur
Luca Zaccarian	Directeur de Recherche	Examinateur
Paolo Frasca	Chargé de Recherche	Examinateur
Dimos Dimarogonas	Associate Professor	Examinateur
Michel Kieffer	Professeur	Examinateur

École doctorale et spécialité :
EDSYS : Automatique

Unité de Recherche :
Laboratoire d'Analyse et d'Architecture des Systèmes

Directeurs de Thèse :
Sophie Tarbouriech et *Luca Zaccarian*

Rapporteurs :
Maria Domenica Di Benedetto et *Matthew C. Turner*

Université de Toulouse
Institut National des Sciences Appliquées de Toulouse

DOCTORAT DE L'UNIVERSITÉ FÉDÉRALE
TOULOUSE MIDI-PYRÉNÉES

On Distributed Control Analysis and Design for Multi-Agent Systems subject to Limited Information

Doctoral Dissertation of:
Laura Dal Col

Advisors:
Sophie Tarbouriech and **Luca Zaccarian**

Reviewers:
Prof. Maria Domenica Di Benedetto and **Prof. Matthew C. Turner**

25 October 2016

Abstract

Multi-agent systems are dynamical systems composed of multiple interacting elements known as *agents*. Each agent is a dynamical system with two characteristics. First, it is capable of autonomous action—that is, it is able to evolve according to a self-organised behavior, which is not influenced by the external environment. Second, it is able to exchange information with other agents in order to accomplish complex tasks, such as coordination, cooperation, and conflict resolution.

One commonly studied problem in multi-agent systems is synchronization. The agents are *synchronized* when their time evolutions converge to a common trajectory. Many real-world applications, such as flocking and formation control, can be cast as synchronization problems.

Agent synchronization can be achieved using different approaches. In this thesis, we propose distributed and centralized control paradigms for the synchronization of multi-agent systems. We develop necessary and sufficient conditions for the synchronization of multi-agent systems, composed by identical linear time-invariant agents, using a Lyapunov-based approach. Then we use these conditions to design distributed synchronization controllers. Then, we extend this result to multi-agent systems subject to external disturbances enforcing disturbance rejection with H_∞ control techniques. Furthermore, we extend the analysis to multi-agent systems with actuator constraints using LMI-based anti-windup techniques.

We test the proposed control design strategies in simulated examples among which two are inspired by real-world applications. In the first, we study airplane formation control as a synchronization problem. In the second, we analyze the delivery of video streams as a synchronization problem and we compare the results to existing controllers.

Résumé

Les systèmes multi-agents sont des systèmes dynamiques composés par plusieurs éléments qui interagissent entre eux. Ces éléments sont appelés agents. Un *agent* est un système dynamique caractérisé par deux propriétés. La première est que les agents sont autonomes—c'est-à-dire qu'ils ne sont pas dirigés par l'environnement extérieur et ils peuvent évoluer selon un comportement auto-organisé. La seconde est que les agents sont capables de communiquer entre eux pour accomplir des tâches complexes, telles que la coopération, la coordination et la résolution de conflits.

L'un des problèmes courants concernant les systèmes multi-agents est la synchronisation. Les agents sont *synchronisés* lorsque leur évolution dans le temps converge vers une trajectoire commune. Plusieurs applications du monde réel peuvent être conceptualisés comme des problèmes de synchronisation des systèmes multi-agents : par exemple, l'alignement en vitesse (*flocking* en anglais), et le contrôle de la formation du mouvement de groupes cohérents.

La synchronisation des systèmes multi-agents peut être obtenue grâce à différentes techniques de contrôle. Dans cette thèse nous proposons des méthodes de contrôle centralisées et distribuées pour la synchronisation des systèmes multi-agents. Nous développons des conditions nécessaires et suffisantes pour la synchronisation des systèmes multi-agents, composés par des agents identiques et linéaires qui ne changent pas dans le temps, en utilisant une approche Lyapunov. Ces conditions sont utilisées pour la conception de lois de contrôles distribuées. Ensuite, nous étendons les résultats aux systèmes multi-agents soumis à des perturbations externes, assurant un niveau de performance désiré grâce à une technique de contrôle de type H_∞. Enfin, nous étendons l'analyse aux systèmes multi-agents avec contraintes sur les actionneurs, en utilisant des techniques de contrôle anti-windup.

Nous évaluons l'efficacité et les performances des stratégies de contrôle proposées dans plusieurs simulations, dont deux d'entre elles sont inspirées par des applications issues du monde réel. La première est le contrôle du vol en formation d'avions, et la seconde est l'analyse de la transmission de contenus vidéo comme un problème de synchronisation. Nous comparons aussi les résultats obtenus avec des techniques de contrôle alternatives.

Contents

Acknowledgements **ix**

Notation **xi**

1 Introduction **1**
1.1 The Synchronization Problem 2
1.2 Centralized, Distributed and Decentralized Design 4
1.3 Statement of Contributions 5

2 State Synchronization **9**
2.1 Problem Formulation 10
2.2 The Synchronization Set 13
2.3 Necessary and Sufficient Conditions for Synchronization 15
2.4 ILMI Static Output Feedback Design 24
2.5 Summary 33

3 H_∞ State Synchronization **35**
3.1 Problem Formulation 36
3.2 Distributed Dynamic Output Feedback 38
3.3 The Synchronization Set 40
3.4 Sufficient Conditions for State Synchronization 40
3.5 H_∞ State Synchronization Design 46
3.6 ILMI Dynamic Output Feedback Design 49
3.7 Summary 54

4 Synchronization under Saturation Constraints **59**
4.1 Problem Formulation 60
4.2 Dynamic Output Feedback with Anti-Windup Loop 63
4.3 Decoupling Change of Coordinates 66

4.4 Extended Sector Condition 68
4.5 Global State Synchronization Analysis 69
4.6 Global H_∞ State Synchronization Design 71
4.7 Optimal H_∞ Control Design 74
4.8 Summary and Local State Synchronization 78

5 Synchronization in Quality-Fair Video Delivery 83
5.1 Overview 84
5.2 Necessary and Sufficient conditions for Quality-Fair Video Delivery 91
5.3 Optimal Design of PI Controllers 94
5.4 Simulations 105
5.5 Summary 107

6 Conclusions 111

A Graph Theory 113

B Technical Proofs for Chapter 2 117
B.1 Proof of Lemmas 2.1 and 2.4 117
B.2 Proof of Proposition 2.1 120

C Technical Proof for Chapter 5 123

Bibliography 127

Acknowlegements

First, I would like to thank my supervisors Sophie Tarbouriech and Luca Zaccarian, for their guidance and for all the things they taught me during these three years as a doctoral student.

I would like to thank Dimos Dimarogonas, for welcoming me at the Royal Institute of Technology during my visiting period and to be a member of the committee of my doctoral defense.

I want to thank Maria Domenica di Benedetto and Matthew Turner, for being reviewers of this manuscript, and Paolo Frasca and Michel Kieffer for being members of the committee of my doctoral defense.

There are many people that I want to thank! All the people in the MAC group and in the automatic control department of KTH. I thank my friends Sofia and Alicia, for being so special to me. I thank my climbing mates for all the exciting moments spent together. I thank my parents for being amazing. I thank Riccardo for being always by my side. I also thank him for the accurate proofreading of my thesis and for his precious advice.

Finally, I thank all of the people that will read my thesis!

Notation

Abbreviations

ILMI Iterative Linear Matrix Inequality

LMI Linear Matrix Inequality

LTI Linear Time-Invariant

MIMO Multi-Input Multi-Output

ODE Ordinary Differential Equation

SISO Single-Input Single-Output

Real and Complex Numbers

$|x|$ the magnitude or absolute value of $x \in \mathbb{C}$

$|\mathcal{V}|$ cardinality of the discrete set $\mathcal{V}$

$\mathbb{C}$ complex numbers

$\mathbf{Im}(z)$ imaginary part of $z \in \mathbb{C}$

$\mathbb{N}$ natural numbers

$\mathbf{Re}(z)$ real part of $z \in \mathbb{C}$

$\mathbb{R}$ real numbers

Symbols

$\otimes$ the Kronecker product of two matrices (cf. [45])

$\lambda_i(M)$ the i-th eigenvalue of a matrix $M \in \mathbb{R}^{k\times k}$

$\lambda_{\max}(M)$ ($\lambda_{\min}(M)$) the eigenvalue with the largest (smallest) real part of a symmetric matrix $M \in \mathbb{R}^{k\times k}$

m agent control input dimension

N number of agents

n agent state dimension

p agent output dimension

q agent disturbance input dimension

$\mathcal{N}$ agent index set

Matrices and Norms

$\mathbf{0}_N$ vector of zeros of dimension N

$\mathbf{1}_N$ vector of ones of dimension N

$M^\top$ the transpose of a matrix $M \in \mathbb{R}^{k\times j}$

$\mathrm{diag}(M_i)$ the block-diagonal matrix with M_i, for $i = 1, \ldots, k$ on the diagonal

$\mathbb{R}^k$ the k-dimensional Euclidean space

$\mathrm{He}(M) = M + M^\top$

$\mathrm{im}(M)$ the image of matrix $M \in \mathbb{R}^{k\times j}$

I_k identity matrix of dimensions $k \times k$

$\ker(M)$ the kernel of matrix $M \in \mathbb{R}^{k\times j}$

$|M|$ induced 2-norm of the matrix $M \in \mathbb{R}^{k\times j}$

$|x|_1$ 1-norm of the vector $x \in \mathbb{R}^k$

$|x|$ 2-norm of the vector $x \in \mathbb{R}^k$

$M > 0$ ($M < 0$) the square matrix $M \in \mathbb{R}^{k\times k}$ is positive (negative) definite

$\mathcal{S}^\perp$ orthogonal complement of subspace $\mathcal{S}$

$p_M(z)$ characteristic polynomial of matrix $M \in \mathbb{R}^{k\times k}$

$M \geq 0$ $(M \leq 0)$ the square matrix $M \in \mathbb{R}^{k\times k}$ is positive (negative) semi-definite

$\bar{\sigma}(M)$ maximum singular value of $M \in \mathbb{R}^{k\times j}$, namely $\max_i \sqrt{\lambda_i(MM^\top)}$

$\mathbb{R}^{k\times j}$ space of real matrices of dimensions $k \times j$

$\rho(M)$ spectral radius of the matrix $M \in \mathbb{R}^{k\times j}$, namely $\max_i |\lambda_i(M)|$

$*$ symmetric block in a partitioned matrix

Chapter 1

Introduction

> "*At the heart of the universe is a steady, insistent beat, the sound of cycles in sync. Along the tidal rivers of Malaysia, thousands of fireflies congregate and flash in unison;* [...] *our hearts depend on the synchronous firing of ten thousand pacemaker cells. While the forces that synchronize the flashing of fireflies may seem to have nothing to do with our heart cells, there is in fact a deep connection.*"
>
> — Strogatz, *Sync*

In his book [92], Strogatz describes the beauty of *synchrony*. He describes how components of animate and inanimate systems reach *sync* as a mathematical consequence of their individual behaviors. We start this thesis with this quote because it reveals how synchronization is *everywhere* in our life, from the behaviour of massed fireflies, to the functioning of our hearts. The quote serves as motivation and inspiration for this work, and to see it in the bigger picture. The contribution of this thesis is to give an improved analytical description of the class of phenomena summarized with the term *synchronization*. The word synchronization is composed by the prefix *syn*—that is, *together*— and the word *khronos*—the ancient Greek Immortal Being, the God of Time. Therefore, synchronization refers to individuals reaching a *temporal coincidence* of some events. Another common concept that come along with synchronization is *consensus*, which instead refers to *spatial coincidence*—that is, to be at the same point. These terms are closely related to each other, since consensus at each time instant is synchronization, and synchronization to a constant trajectory is consensus.

With the industrial revolution came the need to synchronize clocks in adjacent towns in order to maintain arrival and departure timetables for trains. Today, high-speed transport and communication signals need the alignment of remote clocks and oscillators.

When we consider the synchronization problem in control system theory, it is easy to find examples of phenomena relying on this principle.

Synchronization and consensus problems have a long history in computer science and form the foundation of the field of distributed computing (see [3], [6], [108], and [103]). The range of examples of consensus and synchronization in modern control engineering is wide. Recently, consensus have been used to control the delivery of multimedia contents in [26], for network clock synchronization in [10] and [11], for steering control of self-directed underwater gliders in [52], and to control the data flow and the failures in multi-hop control networks in [30], just to name a few.

In the current literature, the synchronization problem in collections (also called *network*) of dynamical systems (also called *agents*) is called *synchronization of multi-agent systems*. An overview of the key results of theory of synchronization of multi-agent systems, such as coordinated motion of mobile agents, is proposed by [35], [71], [72], and [76]. The underlying intuition behind these works is that the stability properties so far developed for a single dynamical system (see [42] for the linear case, and [40] for the nonlinear and hybrid case) could be extended to networks of multi-agent systems by looking at the differential evolution of the agent states. An interesting aspect behind the study of multi-agent systems is that there is an interesting interplay between Lyapunov theory and algebraic graph theory (see [39], [37]), once we realize that the communication pattern among the agents can be represented using a graph.

1.1 The Synchronization Problem

In this thesis, we want to study the synchronization problem of multi-agent systems from a theoretical point of view. As specified in the previous section, synchronization refers to the temporal agreement on a quantity of interest. Before moving to the synchronization problem, we must define what a multi-agent system is and provide the tools to describe it.

We can identify three main independent objects that exhaustively describe a multi-agent system.

Agent Model An agent is a dynamical system. Then, the Agent Model is a set of Ordinary Differential Equations (ODEs) that describes the dynamics of a single agent in the network. We can distinguish between homogeneous networks (in which the model is the same for every agent) and heterogeneous networks (in which the agents have different models). Moreover, depending on the nature of the set of ODEs, we can distinguish between linear models and nonlinear models. The stability properties of dynamical systems can be analyzed using Lyapunov stability theory. The consensus problem has been studied in the literature for particular classes of dynamical systems, such as single- or double-integrator agents (see [77], [78], and [72]) and coupled oscillators (see [89], [31], and references therein). More recently, consensus and synchronization problems for multi-agent system with high-order dynamics have received an arising attention (see [69], [114], [79], [109], and [83]).

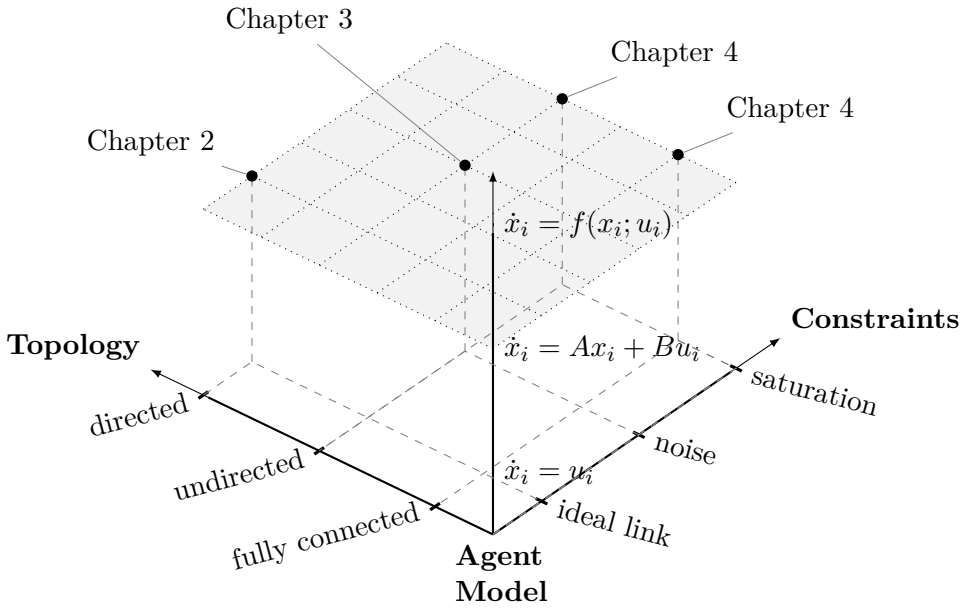

Figure 1.1: 3D coordinate system representing the multi-agent systems obtained varying the network descriptors: the agent model, the communication topology and the communication constraints. The gray surface represents all the networks having the same agent model $\dot{x}_i = Ax_i + Bu_i$. The bullets that lay in the gray surface represent the multi-agent systems considered in this thesis.

Communication Topology Communication topology answers to the questions "who talks to whom?" and "who listens to whom?"—that is, it describes the interconnections among the agents by means of a graph (see [34]). If the graph does not vary with time, the topology is fixed, otherwise we call it time-varying. While considering fixed topologies, we can distinguish between directed graphs and undirected graphs [66, Chapter 3]. Directed graphs are characterized by oriented communication links, and undirected graphs are characterized by bidirectional communication links among the agents. The algebraic properties of graphs are detailed in Appendix A, see also [68].

Communication Constraints The coupling between agents is usually subject to communication constraints, such as noise, limited signal ranges, packet losses, and delays. In particular, few works address the synchronization problem with performance specifications in terms of noise rejection. In [120] and [60], the authors consider networks of high-order agents subject to external disturbances affecting both the states and the measured outputs. Discrete-time results are also summarized in [62, §3.2.3]. Another important constraint in many real-life applications is the limitation of the actuators used in control systems, and in particular input magnitude saturation. Several works have studied the stability and stabilization of isolated linear systems with input

saturations (see, for example, [98], [118], [46] and references therein). For multi-agent systems, saturations have been taken into account indirectly in the context of binary feedback addressed by [12] and [29]. A few works have been published by considering the saturated state feedback consensus in [64], which focuses on global consensus with neutrally stable linear agents and double-integrator agents under fixed and switching network topologies. In [116], discrete-time parallel derivations are presented. In [87], the problem of continuous-time single-integrator agents with saturation constraints and time-varying topology is studied. In [95], sufficient conditions are given for global state synchronization via relative state feedback controllers. In [93], semi-global consensus is achieved using a low-gain feedback strategy. All of the above mentioned schemes address the case with saturation and full state measurements across the interconnection network.

Figure 1.1 shows, in a graphical representation, the positions of the contributions of this thesis among the problems obtained varying the three characteristics presented above. In this thesis, we analyze multi-agent system synchronization problems with different topology and communication constraints. Each chapter is identified by a triple, that characterizes the network of agents considered in the specific problem. As we can see from the figure, we consider homogeneous networks of identical LTI dynamical systems of any order and fixed topology. Synchronization and consensus research mainly focuses either on topological complexity or on system complexity, or on communication complexity, but rarely all at the same time. We will explore the trade-off among these characteristics and we will get over this limitation.

1.2 Centralized, Distributed and Decentralized Design

In order to achieve synchronization of multi-agent systems, we need to design controllers that regulate the agents inputs in order to obtain the desired behavior. There are three options for the design of controllers for multi-agent systems: centralized, distributed, and decentralized strategy (see [97] for a detailed analysis of the three strategies). In centralized control, the design of the policies for each controller is done with a common knowledge of the policies of the others. In the distributed control, some of the controllers do not know the policies of the others. In decentralized control, there is no communication at all among the controllers. Figure 1.2 represents the three strategies. In this work we are considering mainly distributed strategies, but we also develop centralized control strategies. Distributed control strategies are convenient in terms of scalability, since they favor local communications instead of requiring the bandwidth capacity of an all-to-all communication strategy. However, in some practical applications (see, among others, [67], [15], [75], and [91]), a centralized architecture is convenient when we want to compute fast a global parameter of the network (for example, the maximum or the average value of a variable). This may take longer if the calculations are performed in a distributed fashion.

Besides the centralized, distributed, and decentralized nature of the controller, a further classification is based on the available information to compute the synchronization algorithm. Most work on multi-agent systems control has focused on consensus proto-

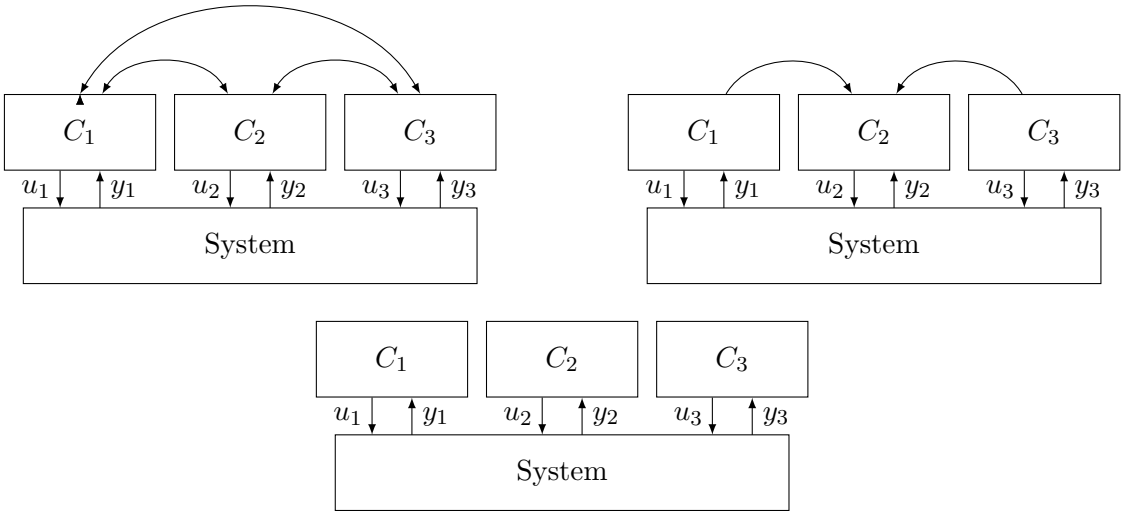

Figure 1.2: Example of a centralized control scheme (top left), distributed control scheme (top right), and decentralized control scheme (bottom) in a network of three agents (examples from EECI-HYCON2 course on Decentralized and Distributed Control, M. Farina, G. Ferrari Trecate).

cols that require the knowledge of the whole agent states. In the linear context, state feedback scenarios are studied in [114], [104], and [55].

When the full agent states are not accessible, we can use an observer-controller structure (see [83], [56], and [44]), or a direct output feedback scheme (see [119], [59], and [85]).

1.3 Statement of Contributions

This thesis is based on the work carried out over three years as a PhD student. In this section, we summarize the results of this work. We present our contributions to the development of a distributed control theory for synchronization of homogeneous networks of agents—that is, multi-agent systems where the agents are identical dynamical high-order linear systems. We explore the effects of limited information on the synchronization of distributed systems. Moreover, we develop suitable analysis and synthesis methods for distributed control algorithms for high-order multi-agent systems subject to limited information.

Chapter 2: State Synchronization In Chapter 2, we address the most fundamental distributed control task of multi-agent systems: state synchronization. We consider networks of identical LTI agents with directed information topology and ideal communication links. We give necessary and sufficient conditions for exponential state syn-

chronization of multi-agent systems, and we provide a converse Lyapunov theorem for synchronization stability. We also give an iterative algorithm to design a distributed output feedback controller that guarantees state synchronization of the agents. The theoretical results presented in this chapter serve as building blocks for the more sophisticated problems addressed in the subsequent chapters. Parts of this section are based on

Dal Col, L., Tarbouriech, S., Zaccarian, L., and Kieffer, M. "Equivalent conditions for synchronization of identical linear systems and application to quality-fair video delivery". *HAL-01116971 document* (2015)

Dal Col, L., Tarbouriech, S., Zaccarian, L., and Kieffer, M. "A linear consensus approach to quality-fair video delivery". *Proc. Conf. Decis. Control*. Dec. 2014

Chapter 3 : H_∞ State Synchronization In Chapter 3, we take a step beyond state synchronization and we address the H_∞ state synchronization problem in presence of exogenous perturbations. We consider networks of identical LTI agents with undirected information topology. We suppose that the multi-agent system dynamics is affected by additive disturbance signals of bounded energy. We quantify the attenuation level of the synchronization against the exogenous disturbances with the $\mathcal{L}_2$ gain performance index. Combining the Lyapunov synchronization theory developed in Chapter 2 and the $\mathcal{L}_2$ gain condition for synchronization, we convert the H_∞ synchronization problem into the feasibility problem of a set of matrix inequalities. Finally, we implement an iterative algorithm, based on a suitable relaxation of the synchronization analysis conditions, to design a dynamic output feedback controller. Parts of this section are based on

Dal Col, L., Tarbouriech, S., and Zaccarian, L. "H_∞ control design for synchronization of multi-agent systems". *Submitted to Int. J. Control* (2016)

Chapter 4: Synchronization under Input Saturation Constraints In Chapter 4, we include the input saturation constraints in the agent model. We consider networks of identical LTI agents with undirected and fully connected information topology—that is, all the agents are in direct communication. We suppose that the agents are affected by exogenous perturbations and input saturation constraints. We want to guarantee exponential state synchronization of the saturated multi-agent system for any initial condition of the state space. We formulate a novel incremental sector condition to bound the saturation nonlinearity. This condition, combined with the Lyapunov synchronization stability theory and the performance specifications developed respectively in Chapters 2 and 3, allows us to derive suitable synchronization conditions in terms of Linear Matrix Inequalities (LMIs). We also give insights on the state synchronization problem of saturated multi-agent systems with unstable open-loop dynamics. In this case, if the open-loop system contains eigenvalues in the open right-half plane, only local asymptotic state synchronization can be achieved. Parts of this chapter are based on

Dal Col, L., Tarbouriech, S., and L., Z. "Global H_∞ synchronization control of linear multi-agent systems with input saturation". *Proc. American Control Conf.* 2016

Dal Col, L., Tarbouriech, S., and Zaccarian, L. "Local H_∞ synchronization of multi-agent systems under input saturation". *Submitted to IEEE Trans. Autom. Control.* 2016

Chapter 5: Application of Consensus to Quality-Fair Video Delivery In Chapter 5, we present an application of the theoretical results of this thesis. We consider the problem of delivering video contents to users through a broadcast channel with limited capacity. The objective is to provide users with similar video quality. This problem is cast in terms of consensus among the quality measure of the delivered videos. The necessary and sufficient conditions for synchronization presented in Chapter 2 are used to provide an algebraic synchronization criterion. We propose two different control design techniques for this problem. The first one is a heuristic approach, based on Jury's roots criterion. The second method is an iterative algorithm for centralized output feedback design for agents' with discrete-time dynamics. Parts of this chapter are based on

Dal Col, L., Tarbouriech, S., Zaccarian, L., and Kieffer, M. "A linear consensus approach to quality-fair video delivery". *Proc. Conf. Decis. Control.* Dec. 2014

Dal Col, L., Tarbouriech, S., and Zaccarian, L. "A consensus approach to PI gains tuning for quality-fair video delivery". *Submitted to Int. J. Robust Nonlinear Control* (2016)

Chapter 6: Conclusions In Chapter 6, we summarize the main results of this thesis and we indicate possible future lines of research.

Appendix A: Graph Theory Appendix A contains the basic concepts of Graph Theory for synchronization, which are used throughout this thesis.

Appendix B: Technical Proofs for Chapter 2 Some technical proofs of Chapter 2 are deferred to Appendix B in order to improve readability.

Appendix C: Technical Proofs for Chapter 5 The proof of Lemma 5.1 is deferred to Appendix C in order to improve readability.

Chapter 2

State Synchronization

This chapter is dedicated to the state synchronization problem of multi-agent systems consisting of identical LTI systems. The importance of the results presented in this chapter lies in the fact that it serves as a building block of the theoretical results presented in the remainder of this thesis and it is instrumental for the development of control algorithms for more sophisticated tasks. In this chapter, the state synchronization problem of multi-agent systems is presented, analyzed, and solved.

First, we present a Lyapunov synchronization stability result that extends the classical Lyapunov stability notions for isolated systems (see, for example, [42]). In fact, when analyzing the state synchronization problem, the Lyapunov stability theory is applicable to the incremental dynamics among the agent states. Based on this observation, Lyapunov synchronization stability theory should be regarded as an upgrade of classical Lyapunov stability theory in the multi-agent systems context. The most outstanding features of Lyapunov synchronization stability presented in this chapter are:

1 The stability of the single system is not required. The synchronization trajectory can be of any kind (constant value, bounded trajectory, or unbounded trajectory).

2 Synchronization stability is a relative stability, meaning that we are looking at the mismatch among the states of the agents.

3 Many synthesis problems, such as robust synchronization problems, regulation or tracking problems, observer, filter, state and parameter estimation and identification, can be unified in the framework of synchronization stability theory. As classical Lyapunov stability theory has promoted the development of automatic control of isolated systems, Lyapunov synchronization stability theory will promote the development of automatic control theory of interconnected multi-agent systems.

Second, we propose a method to design a distributed static output feedback controller that guarantees state synchronization among multi-agent systems. The presented procedure is based on iterative linear matrix inequality (ILMI) optimization. Since the problem of finding a static output feedback controller is intrinsically nonconvex, the proposed algorithm is not guaranteed to converge and to find a global optimal solution. Nevertheless it shows desirable properties that make it a promising tool for distributed static output feedback control design.

2.1 Problem Formulation

According to the discussion in Chapter 1, the first stage of the formulation of a problem regarding a network of multi-agent systems consists in the definition of the agent model and the information structure. In the following, these elements are specified.

Agent Model We consider multi-agent systems consisting of N identical LTI systems of order n. The index subscript i identifies an agent in the network, and it takes values in $\mathcal{N} = \{1, \dots, N\}$, where $N > 1$ is the number of agents in the network. The dynamics of each agent is regulated by the following state-space representation

$$\begin{aligned} \delta x_i &= Ax_i + Bu_i \\ y_i &= Cx_i, \end{aligned} \qquad i \in \mathcal{N}, \tag{2.1}$$

where $x_i \in \mathbb{R}^n$ is the *agent state*, $u_i \in \mathbb{R}^m$ is the *agent input*, $y_i \in \mathbb{R}^p$ is the *agent output*, and A, B, C are matrices of appropriate dimensions. The operation δx is defined as follows: $\delta x = \dot{x}$ for continuous-time agents, and $\delta x = x^+$ for discrete-time agents.

Information Topology The agents have communication capabilities. The communication among the agents is represented by a directed graph $\mathcal{G} = (\mathcal{V}, \mathcal{E})$. An edge $(i, j) \in \mathcal{E}$ in the graph $\mathcal{G}$ means that agent j receives information from agent i. In this chapter, we make the following assumption on the graph $\mathcal{G}$.

Assumption 2.1. *The communication graph $\mathcal{G}$ associated with the multi-agent system* (2.1) *contains a directed spanning tree. Moreover, the Laplacian matrix $L \in \mathbb{R}^{N \times N}$ associated with $\mathcal{G}$ has only real eigenvalues.*

Assumption 2.1 assures that the graph $\mathcal{G}$ is directed and connected—that is, there exists a directed spanning tree, consisting of $N - 1$ arcs selected so that the arcs define a unique directed path from a designated root node to every other node. The basic notions of graph theory are summarized in Appendix A (for more details, see [68]).

The definitions of state synchronization and of the state synchronization problem we intend to address, as given in [111, Definition 3.1], are as follows.

Definition 2.1. (State Synchronization) *The agents* (2.1) *are said to achieve asymptotic state synchronization if, for any initial state* $x_i(0) \in \mathbb{R}^n$, $i \in \mathcal{N}$, *there exists a trajectory* $\bar{x}$ *such that*

$$\lim_{t \to +\infty} x_i(t) - \bar{x}(t) = \mathbf{0}_n \tag{2.2}$$

holds for every $i \in \mathcal{N}$. *In this case,* $\bar{x}$ *is called* synchronization trajectory.

Problem 2.1. (State Synchronization Problem) *Consider the multi-agent system* (2.1) *with interconnection described by* $\mathcal{G}$. *The state synchronization problem consists in finding a control law* u_i, *with* $i \in \mathcal{N}$, *such that, for any initial condition* $x_i(0) \in \mathbb{R}^n$, $i \in \mathcal{N}$, (2.2) *is satisfied.*

In the next section, we will see that the synchronization trajectory $\bar{x}$ of the multi-agent system (2.1) can be a constant value (in this case, the agents are said to achieve *consensus*), or a possibly unbounded trajectory. The synchronization trajectory is a result of self-organization, as it depends on the dynamics and the initial states of the agents, and it is not prescribed by any external signal.

Once the multi-agent system is specified and the problem is set, we choose the control strategy we want to adopt. For this problem we use a distributed control scheme—that is, the control input u_i of agent i depends on the information of its neighboring agents. More formally, a distributed control law is defined as follows.

Definition 2.2. (Distributed Control Law) *A distributed control law is an algorithm that computes the control input* u_i *of agent* i *locally, based on the information available from its direct neighbors according to the graph* $\mathcal{G}$.

In particular, we apply the following distributed static output feedback law to the multi-agent system (2.1)

$$u_i := K \tfrac{1}{|\mathcal{N}_i|} \sum_{j \in \mathcal{N}_i} (y_j - y_i), \qquad i \in \mathcal{N}, \tag{2.3}$$

where $\mathcal{N}_i$ is the set of neighbors of agent i, $|\mathcal{N}_i|$ is the number of elements in this set, and $K \in \mathbb{R}^{m \times p}$ is the feedback gain matrix. The design of the matrix K in order to guarantee state synchronization among of the multi-agent system (2.1) is presented in Section 2.4. The block diagram representation of the closed-loop system is shown in Figure 2.1, on page 12.

Within this setting, we want to establish suitable conditions to guarantee synchronization among systems (2.1), with the static output feedback interconnection (2.3).

We want to give a compact representation of the multi-agent system (2.1) with interconnection (2.3). To this purpose, a useful tool to represent the aggregate dynamics of identical linear multi-agent systems is the Kronecker product (or tensor product),

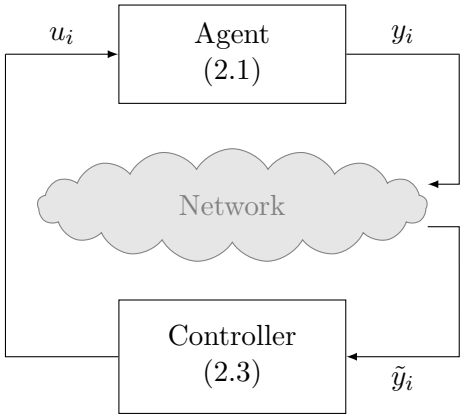

Figure 2.1: Block diagram of the closed-loop system of agents (2.1) with input (2.3). The coupling signal among the agents is $\tilde{y}_i = y_i - \frac{1}{|\mathcal{N}_i|}\sum_{j\in\mathcal{N}_i} y_j$, that is, the difference between the system output y_i and the average output of the neighboring agents $\frac{1}{|\mathcal{N}_i|}\sum_{j\in\mathcal{N}_i} y_j$.

whose definition and properties are summarized in [45]. We denote with

$$\begin{aligned} x &:= \begin{bmatrix} x_1^\top & \cdots & x_N^\top \end{bmatrix}^\top \in \mathbb{R}^{Nn}, \\ y &:= \begin{bmatrix} y_1^\top & \cdots & y_N^\top \end{bmatrix}^\top \in \mathbb{R}^{Np}, \\ u &:= \begin{bmatrix} u_1^\top & \cdots & u_N^\top \end{bmatrix}^\top \in \mathbb{R}^{Nm}, \end{aligned} \tag{2.4}$$

the aggregate state, output and input vectors, obtained stacking the states, outputs and input vectors of systems (2.1), respectively. Using the associative properties of the Kronecker product, the aggregate dynamics of the interconnected system (2.1) and (2.3) is

$$\delta x = (I_N \otimes A)x + (I_N \otimes B)u \tag{2.5}$$
$$y = (I_N \otimes C)x \tag{2.6}$$
$$u = -(L \otimes K)y = -(L \otimes K)(I_N \otimes C)x = -(L \otimes KC)x, \tag{2.7}$$

where $L \in \mathbb{R}^{N\times N}$ is the Laplacian matrix associated to $\mathcal{G}$. Substituting (2.7) into (2.5), we obtain the following compact form for the dynamics of the multi-agent system (2.1) and (2.3):

$$\delta x = (I_N \otimes A - L \otimes BKC)x. \tag{2.8}$$

The key idea to derive suitable synchronization properties for the multi-agent system (2.1) and (2.3) (or, equivalently, (2.8)), is to perform a change of coordinates in order to decouple the aggregate closed-loop dynamics (2.8). We will see in the next section that there exists a coordinate transformation such that the resulting closed-loop dynamics (2.8) is block upper-triangular.

2.2 The Synchronization Set

In this section we introduce and characterize the *synchronization set* of system (2.1), that is, the set where the states of the agents (2.1) have the same value. More formally, the synchronization set $\mathcal{S}$ is defined as follows

$$\mathcal{S} := \left\{ x = \begin{bmatrix} x_1 \\ \vdots \\ x_N \end{bmatrix} \in \mathbb{R}^{Nn} : x_1 = x_2 = \cdots = x_N \right\}, \tag{2.9}$$

where $x \in \mathbb{R}^{Nn}$ is the column vector in (2.4)—that is, the vector obtained by stacking the agent states (2.1). Denote with $\mathcal{S}^{\perp}$ the orthogonal complement of $\mathcal{S}$.

In this section, we want to define and characterize the uniform global exponential stability of the set $\mathcal{S}$ with respect to dynamics (2.1) and (2.3), or equivalently (2.8). The rigorous definition of uniform global exponential stability of a set uses the concept of the distance of a point $x \in \mathbb{R}^{Nn}$ to this set. Therefore, we first need to define and characterize the distance-to-the-set $\mathcal{S}$ function. The definition of distance to a closed set [40, Definition 3.5], is reported below. For each $x \in \mathbb{R}^{Nn}$, we denote with

$$|x|_{\mathcal{S}} := d(x, \mathcal{S}) =: \inf\{d(x, s), s \in \mathcal{S}\} \tag{2.10}$$

the standard point-to-set distance, and the point-to-point distance is taken as the Euclidean norm $d(x, s) = |x - s|$. We emphasize that $\mathcal{S}$ is convex, closed and unbounded. The next lemma shows that in any closed, convex set $\mathcal{S} \subset \mathbb{R}^{Nn}$ there is a unique closest point to $x \in \mathbb{R}^{Nn}$. The proof of this lemma can be found in [81, Theorem 12.3].

Lemma 2.1. (Uniqueness of the projection onto $\mathcal{S}$) *Given a closed, convex set $\mathcal{S} \subset \mathbb{R}^{Nn}$ and any vector $x \in \mathbb{R}^{Nn}$, there exists a unique point $s^\star \in \mathcal{S}$ satisfying*

$$s^\star = \arg\min\{d(x, s), s \in \mathcal{S}\}, \tag{2.11}$$

and $s^\star$ is the orthogonal projection of x onto $\mathcal{S}$.

From Lemma 2.1 and relation (2.10), it follows that

$$|x|_{\mathcal{S}} = \min\{d(x, s), s \in \mathcal{S}\} = d(x, s^\star) = |x - s^\star|. \tag{2.12}$$

In particular, when considering the specific convex, closed set $\mathcal{S}$ in (2.9), we can give the explicit expression of the orthogonal projection of $x \in \mathbb{R}^{Nn}$ onto $\mathcal{S}$. This result is contained in the following lemma, whose proof is given in Appendix B.

Lemma 2.2. (Distance to the set $\mathcal{S}$) *Given set $\mathcal{S}$ in (2.9), the distance of $x \in \mathbb{R}^{Nn}$ to $\mathcal{S}$ is equal to*

$$|x|_{\mathcal{S}}^2 = |x - \mathbf{1}_N \otimes \bar{x}|^2 = \textstyle\sum_{i=1}^{N} |x_i - \bar{x}|^2, \tag{2.13}$$

where $\bar{x} := \frac{1}{N}\sum_{k=1}^{N} x_k = \frac{1}{N}(\mathbf{1}_N^\top \otimes I_n)x$ is the average vector of the components $x_i \in \mathbb{R}^n$ of $x \in \mathbb{R}^{Nn}$.

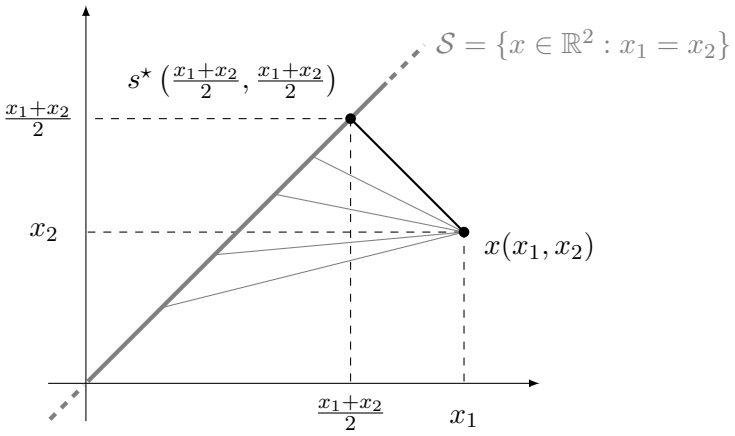

Figure 2.2: the synchronization set $\mathcal{S}$ in $\mathbb{R}^2$ (gray line), and the orthogonal projection $s^\star$ of a vector $x \in \mathbb{R}^2$ onto $\mathcal{S}$. The gray lines connect x to several point of $s \in \mathcal{S}$, with $d(x, s) > d(x, s^\star)$.

In other words, Lemma 2.2 states that the orthogonal projection of any vector $x \in \mathbb{R}^{Nn}$ is $s^\star = \mathbf{1}_N \otimes \bar{x}$, a vector whose *vector components* $x_i \in \mathbb{R}^n$ are all equal to the average value of the vector components of x. Figure 2.2 shows the synchronization set in $\mathbb{R}^2$ and the unique point $s^\star$ of $\mathcal{S}$ closest to a point $x \in \mathbb{R}^2$.

The main goal of this chapter is to establish suitable conditions to guarantee the uniform global exponential stability of the set $\mathcal{S}$ with respect to dynamics (2.1) and (2.3). We recall below the definition of uniform global exponential stability of a set, conveniently reported from [40, Definition 3.6], for the special case of continuous- and discrete-time linear systems.

Definition 2.3. *Consider the multi-agent system* (2.1) *and* (2.3)*, or equivalently* (2.8)*. A closed set $\mathcal{S} \subset \mathbb{R}^{Nn}$ is said to be uniformly globally exponentially stable if there exist positive constants $\beta, M > 0$ such that any solution to* (2.8) *satisfies*

$$|x(t)|_{\mathcal{S}} \leq M e^{-\beta t} |x(0)|_{\mathcal{S}}, \tag{2.14}$$

for all $t \geq 0$. The largest constant β such that (2.14) *is satisfied is called* synchronization rate*.*

Combining (2.14) with (2.13), we deduce that (2.9) is uniformly globally exponentially stable if there exist positive constants $\beta, M > 0$ such that any solution to (2.8) satisfies

$$|x(t) - \mathbf{1}_N \otimes \bar{x}(t)| \leq M e^{-\beta t} |x(0) - \mathbf{1}_N \otimes \bar{x}(0)|, \tag{2.15}$$

for all $t \geq 0$, where $\bar{x}$ is the synchronization trajectory in (2.2).

Problem 2.1 amounts to the stabilization of the synchronization set (2.9) by means of the control protocol (2.3). In fact, by guaranteeing uniform global exponential stability

of $\mathcal{S}$, we guarantee, in particular, that all the states converge to the same value, thus proving (2.2).

As we will see in the next section, the projection of the closed-loop dynamics (2.1) and (2.3) onto the synchronization set $\mathcal{S}$ allows us to derive the synchronization conditions for this system and to characterize the synchronization trajectory defined in (2.2).

2.3 Necessary and Sufficient Conditions for Synchronization

In the previous section, we introduced the synchronization set $\mathcal{S}$, we characterized the distance of any point $x \in \mathbb{R}^{Nn}$ to this set, and we have determined the expression of the orthogonal projection of $x \in \mathbb{R}^{Nn}$ onto $\mathcal{S}$.

In this section, we introduce a decoupling change of coordinates that allows us to project the closed-loop dynamics (2.1) and (2.3) (or equivalently, (2.8)) onto the synchronization set $\mathcal{S}$ and its orthogonal complement $\mathcal{S}^{\perp}$. We will see that the uniform global exponential stability of the projected dynamics onto $\mathcal{S}^{\perp}$ is equivalent to the uniform global exponential synchronization of the agents (2.1) with interconnection (2.3) (or equivalently, (2.8)). This allow us to derive suitable synchronization conditions encapsulated in Theorem 2.1.

2.3.1 Decoupling Change of Coordinates

The decoupling change of coordinates introduced in this section is induced by a specific unitary matrix operating on the Laplacian matrix L of the graph $\mathcal{G}$. This matrix transforms L into its Frobenius canonical form, and highlights the algebraic properties of the Laplacian matrix.

In our setting, the information topology is encoded by a directed graph $\mathcal{G}$ with a rooted spanning tree. Based on Assumption 2.1, we can state the following Lemma, whose proof directly follows from [45, Theorem 2.3.1].

Lemma 2.3. (Frobenius Canonical Form of L) *Consider the Laplacian $L \in \mathbb{R}^{N\times N}$ of a directed graph $\mathcal{G}$ with a directed spanning tree, and assume that L has real eigenvalues. Let $0 = \lambda_1 < \lambda_2 \leq \cdots \leq \lambda_N$ denote the ordered eigenvalues of L. Define the unitary vector $\nu_1 = \frac{\mathbf{1}_N}{\sqrt{N}} \in \mathbb{R}^N$ such that $L\nu_1 = \lambda_1\nu_1 = \mathbf{0}_N$. There exists a unitary matrix $T := \begin{bmatrix}\nu_1 & T_2\end{bmatrix}$—that is, $T^\top T = I_N$— where $\nu_1 \in \mathbb{R}^N$ and $U_2 \in \mathbb{R}^{N\times(N-1)}$ such that*

$$\bar{L} := T^\top L T = \begin{bmatrix} 0 & \bar{L}_{12} & \cdots & \bar{L}_{1N} \\ 0 & \lambda_2 & \cdots & \bar{L}_{2N} \\ \vdots & \vdots & \ddots & \vdots \\ 0 & 0 & \cdots & \lambda_N \end{bmatrix} \tag{2.16}$$

is upper triangular, and the diagonal entries of $\bar{L}$ are the eigenvalues of L.

Remark 2.1. According to Gershgorin theorem [45], all the eigenvalues of a Laplacian matrix L are located in a closed disc centered at $\Delta + i0$ with a radius Δ equal to the maximum in-degree of the graph. This implies that the eigenvalues of L satisfy $\mathbf{Re}(\lambda_i) \geq 0$ for all $i = 1, \ldots, N$.

We now apply the coordinates transformation

$$z := (T^\top \otimes I_n)x \tag{2.17}$$

to the aggregate closed-loop dynamics (2.8), obtaining

$$\delta z = (T^\top \otimes I_n)(I_N \otimes A - L \otimes BKC)(T \otimes I_n)z,$$

and using the associative properties of the Kronecker product, we have

$$\delta z = (T^\top T \otimes A - T^\top L T \otimes BKC)z = (I_N \otimes A - \bar{L} \otimes BKC)z. \tag{2.18}$$

We want to provide further insight into the nature of this particular transformation and explain the intuition behind the forthcoming Lyapunov theory for synchronization stability. The state matrix in (2.18) can be rewritten highlighting its block upper-triangular structure as follows

$$I_N \otimes A - \bar{L} \otimes BKC = \begin{bmatrix} A & A_{12} & \cdots & A_{1N} \\ 0 & A_2 & \cdots & A_{2N} \\ \vdots & \vdots & \ddots & \vdots \\ 0 & 0 & \cdots & A_N \end{bmatrix}, \tag{2.19}$$

where $A_i := A - \lambda_i BKC$, and $A_{ij} := A - \bar{L}_{ij} BC$ for $i = 2, \ldots, N$ and $j > i$. Note that the dynamics of the vector components $z_i \in \mathbb{R}^n$ of the transformed state vector z in (2.17) is

$$\delta z_1 = A z_1 + A_{12} z_2 + \cdots + A_{1N} z_N, \tag{2.20}$$

and

$$\begin{aligned} \delta z_2 &= A_2 z_2 + \cdots + A_{2N} z_N \\ \delta z_3 &= A_3 z_3 + \cdots + A_{3N} z_N \\ &\vdots \\ \delta z_N &= A_N z_N. \end{aligned} \tag{2.21}$$

From the structure of matrix T in (2.16), we deduce that the first component of z is $z_1 = (\nu_1^\top \otimes I_n)x = \frac{1}{\sqrt{N}} \sum_{i=1}^N x_i$. From Lemma 2.2 we see that the vector $\frac{z_1}{\sqrt{N}}$ is the orthogonal projection of the aggregate state vector $x \in \mathbb{R}^{Nn}$ onto the synchronization set $\mathcal{S}$ in (2.9). From this observation, we deduce that (2.20) is the orthogonal projection of the closed-loop dynamics (2.8) onto $\mathcal{S}$ in (2.9). On the other hand, (2.21) is the projection of the closed-loop dynamics (2.8) onto $\mathcal{S}^\perp$.

In particular, if $A-\lambda_i BKC$, for $i=2,\dots,N$ are stable matrices—that is, Hurwitz in the continuous-time case, and Schur-Cohn in the discrete-time case, from the particular cascaded structure of dynamics (2.21), we have

$$\lim_{t\to\infty} z_i = 0, \quad i=2,\dots,N. \tag{2.22}$$

In this situation, dynamics (2.20) asymptotically reduces to

$$\delta z_1 = A z_1, \tag{2.23}$$

and dynamics (2.18) is exhaustively described in the subspace $\mathcal{S}$ by (2.23). From these observations, the key idea to reach state synchronization is to guarantee the stability of the dynamics (2.21) by adequately designing K in (2.3). This intuition is formalized in the theoretical treatment of the state synchronization analysis contained in the forthcoming section.

2.3.2 State Synchronization Analysis

In this Section, we state necessary and sufficient conditions for state synchronization of the multi-agent system (2.1) with controller (2.3), based on Lyapunov stability theory results and the decoupling change of coordinates introduced in Section 2.3.1.

We recall that the uniform global exponential stability of a closed set entails the property that suitable quadratic functions (the Lyapunov function and its derivative along the solutions to the system) are bounded, and the bounds are expressed in terms of the distance of the solutions to the set (see Definition 2.3).

The following lemma, which is instrumental for the proof of the main theorem of this section, provides the bounds of a specific quadratic function in terms of the distance to the synchronization set $\mathcal{S}$. The proof of this lemma is summarized in Appendix B.1.

Lemma 2.4. *Consider any unitary matrix $T \in \mathbb{R}^{N\times N}$ whose first column is $\nu_1 = \frac{\mathbf{1}_N}{\sqrt{N}}$ and the diagonal matrix $\Lambda := I_N - e_1 e_1^\top$, where $e_1 := [1\ 0\ \cdots\ 0]^\top \in \mathbb{R}^N$ is the first vector of the Euclidean basis. For any $n\in\mathbb{N}$, there exist scalars $c_1, \bar{c}_1, c_2, \bar{c}_2 > 0$ such that for any $x := [x_1^\top\ \cdots\ x_N^\top]^\top \in \mathbb{R}^{Nn}$, where $x_k \in \mathbb{R}^n$, $\forall k = 1,\dots,N$, we have:*

$$\begin{aligned} \bar{c}_1 |x|_{\mathcal{S}}^2 = \ & c_1 \textstyle\sum_{k=2}^N |x_1 - x_k|^2 \le x^\top (T\Lambda T^\top \otimes I_n) x, \\ \bar{c}_2 |x|_{\mathcal{S}}^2 = \ & c_2 \textstyle\sum_{k=2}^N |x_1 - x_k|^2 \ge x^\top (T\Lambda T^\top \otimes I_n) x. \end{aligned} \tag{2.24}$$

We are ready to state the fundamental result of this chapter. The following theorem states the equivalence among four conditions that characterize the uniform global exponential stability of the set $\mathcal{S}$ for the closed-loop dynamics (2.1) and (2.3). The proof combines the stability results in [35] with the output feedback coupling approach of [83]. Parts of the following result can be found in the literature, possibly with different assumptions on the Laplacian L. For example, necessary and sufficient conditions in the form (i) for formation stability were given in [35, Theorem 3]; implication (i) $\implies$ (iii) is established in an equivalent formulation in [112, Theorem 1] and [85, Theorem 1] for the

convergence part. In [110], the equivalence (i) $\iff$ (iv) is proven for the continuous-time case. With this theorem, we want to give a complete, self-contained proof of a Lyapunov synchronization stability result for multi-agent systems.

Theorem 2.1. (State Synchronization Analysis) *Consider the continuous-time (respectively, discrete-time) multi-agent system* (2.1) *with distributed static output feedback interconnection* (2.3)*, and the synchronization set* $\mathcal{S}$ *in* (2.9)*. If the graph* $\mathcal{G}$ *has a directed spanning tree, and the Laplacian matrix* L *in* (2.3) *has real eigenvalues, the following statements are equivalent:*

(i) Matrices

$$A_k := A - \lambda_k BKC, \qquad k = 2, \ldots, N, \tag{2.25}$$

are Hurwitz in the continuous-time case (respectively, Schur-Cohn in the discrete-time case).

(ii) There exist a strict quadratic Lyapunov function $V(x)$ *and positive constants* α_1*,* α_2 *and* β *satisfying:*

$$\alpha_1 |x|_{\mathcal{S}}^2 \leq V(x) \leq \alpha_2 |x|_{\mathcal{S}}^2 , \tag{2.26}$$

$$\delta V(x) \leq -\beta |x|_{\mathcal{S}}^2 , \tag{2.27}$$

where $\delta V(x) := \dot{V}(x)$ *in the continuous-time case, and* $\delta V(x) := \Delta V(x) = V(x^+) - V(x)$ *in the discrete-time case.*

(iii) The synchronization set $\mathcal{S}$ *in* (2.9) *is uniformly globally exponentially stable for the interconnected multi-agent system* (2.1) *and* (2.3)*.*

(iv) The interconnected multi-agent system (2.1) *and* (2.3) *is such that the agent states* $x_i \in \mathbb{R}^n$*, with* $i \in \mathcal{N}$*, uniformly globally exponentially synchronize to the unique solution to the initial value problem*

$$\delta\bar{x} = A\bar{x}, \quad \bar{x}(0) = \tfrac{1}{|p|_1}(p^\top \otimes I_n)x(0) = \tfrac{1}{|p|_1}\textstyle\sum_{k=1}^{N} p_k^\top x_k(0), \tag{2.28}$$

where $p = [p_1 \ \ldots \ p_N]^\top$ *satisfies* $p^\top L = 0$*.*

Proof. We prove the theorem in four steps: (i) $\implies$ (ii), (ii) $\implies$ (iii), (iii) $\implies$ (iv), and (iv) $\implies$ (i).

In the proof, the superscript letters C and D characterize the variables of the continuous- and the discrete-time case, respectively. The two cases are treated in parallel in the proof. The equations for the continuous-time case are presented first and the corresponding equations for the discrete-time case follow in parenthesis in the next line.

Before starting the proof of this theorem we consider the following recursive partition of the closed-loop state matrix $I_N \otimes A - \bar{L} \otimes BKC$ in (2.19).

$$I_N \otimes A - \bar{L} \otimes BKC = \left[\begin{array}{c|c} A & M_1 \\ \hline 0 & \bar{A}_1 \end{array}\right] = \left[\begin{array}{c|c|c} A & \multicolumn{2}{c}{M_1} \\ \hline 0 & A_2 & M_2 \\ \hline & 0 & \bar{A}_2 \end{array}\right] = \left[\begin{array}{c|c|c} A & \multicolumn{2}{c}{M_1} \\ \hline 0 & \multicolumn{2}{c}{\begin{array}{c|c} A_2 & M_2 \\ \hline 0 & \begin{array}{c|c} A_3 & M_3 \\ \hline 0 & \bar{A}_3 \end{array} \end{array}} \end{array}\right] = \bar{A}. \quad (2.29)$$

In (2.29) the matrices in the diagonal blocks are $A_k = A - \lambda_k BKC$, for $i = 2, \ldots, N$, and we introduce the following notation

$$\bar{A}_k := \begin{bmatrix} A_{k+1} & A_{k+1,k+2} & \cdots & A_{k+1,N} \\ 0 & A_{k+2} & \cdots & A_{k+2,N} \\ 0 & 0 & \ddots & \vdots \\ 0 & 0 & 0 & A_N \end{bmatrix}, \quad (2.30)$$

$$M_k := \begin{bmatrix} A_{k,k+1} & \cdots & A_{k,N} \end{bmatrix}, \quad (2.31)$$

for $k = 1, \ldots, N-1$. Notice that, $\bar{A}_{N-1} = A_N$.
Proof of (i) $\implies$ (ii). Suppose that (2.25) holds. There exist matrices $P_k = P_k^\top > 0$, $k = 2, \ldots, N$, such that

$$A_k^\top P_k + P_k A_k = -2I_n, \ k = 2, \ldots, N. \quad (2.32)$$

$$\text{(respectively, } A_k^\top P_k A_k - P_k = -2I_n, \ k = 2, \ldots, N.) \quad (2.33)$$

Consider the following block diagonal matrix, which is recursively defined as

$$\begin{aligned} \bar{P}^C &:= \operatorname{diag}\left(0, \rho_2^C P_2, \bar{P}_2^C\right) = \operatorname{diag}\left(0, \rho_2^C P_2, \rho_3^C P_3, \bar{P}_3^C\right) \\ &= \operatorname{diag}(0, \rho_2^C P_2, \ldots, \rho_{N-1}^C P_{N-1}, \rho_N^C P_N), \end{aligned} \quad (2.34)$$

where $\rho_2^C, \ldots, \rho_N^C$ are positive scalars recursively defined as follows

$$\rho_k^C := \begin{cases} \bar{\rho}_{k+1}^C & \text{if } |P_k M_k| = 0 \\ \frac{\bar{\rho}_{k+1}^C}{2|P_k M_k|^2} & \text{if } |P_k M_k| \neq 0 \end{cases} \quad k = 2, \ldots, N-1, \quad (2.35)$$

where we have defined

$$\bar{\rho}_k^C := \min(\rho_k^C, \bar{\rho}_{k+1}^C), \quad k = 2, \ldots, N-1, \quad (2.36)$$

and $\rho_N^C := \bar{\rho}_N^C = 1$. Matrices $\bar{P}_k^C$ in (2.34) are defined as follows

$$\bar{P}_k^C := \operatorname{diag}(\rho_{k+1}^C P_{k+1}, \ldots, \rho_N^C P_N), \quad k = 1, \ldots, N-1. \quad (2.37)$$

Note that $\bar{P}^C_{N-1} = \rho^C_N P_N = P_N$. Similarly, consider the block diagonal matrix $\bar{P}^D$, recursively defined as follows

$$\begin{aligned}\bar{P}^D &:= \operatorname{diag}\left(0, \rho^D_2 P_2, \bar{P}^D_2\right) = \operatorname{diag}\left(0, \rho^D_2 P_2, \rho^D_3 P_3, \bar{P}^D_3\right) \\ &= \operatorname{diag}(0, \rho^D_2 P_2, \ldots, \rho^D_{N-1} P_{N-1}, \rho^D_N P_N),\end{aligned} \tag{2.38}$$

where $\rho^D_2, \ldots, \rho^D_N$ are positive scalars recursively defined as follows

$$\rho^D_k := \begin{cases} \bar{\rho}^D_{k+1} & \text{if } \left|A_k^\top P_k M_k\right| = 0 \\ \frac{\bar{\rho}^D_{k+1}}{2\left|A_k^\top P_k M_k\right|^2} & \text{if } \left|A_k^\top P_k M_k\right| \neq 0 \end{cases} \quad \text{for } k = 2, \ldots, N-1, \tag{2.39}$$

where we have defined

$$\bar{\rho}^D_k := \min(\rho^D_k, \bar{\rho}^D_{k+1}), \quad k = 2, \ldots, N-1, \tag{2.40}$$

and $\rho^D_N = \bar{\rho}^D_N = 1$. Matrices $\bar{P}^D_k$ in (2.38) are defined as follows

$$\bar{P}^D_k := \operatorname{diag}(\rho^D_{k+1} P_{k+1}, \ldots, \rho^D_N P_N), \quad k = 1, \ldots, N-1. \tag{2.41}$$

Note that, $\bar{P}^D_N = \rho^D_N P_N = P_N$.

Consider the family of functions $\Phi^C_k, \Phi^D_k : \mathbb{R}^{(N-k)n} \to \mathbb{R}$, defined as follows

$$\Phi^C_k(z) := \bar{z}_k^\top \left(\bar{A}_k^\top \bar{P}^C_k + \bar{P}^C_k \bar{A}_k\right) \bar{z}_k, \quad k = 1, \ldots, N-1, \tag{2.42}$$

$$\Phi^D_k(z) := \bar{z}_k^\top \left(\bar{A}_k^\top \bar{P}^D_k \bar{A}_k - \bar{P}^D_k\right) \bar{z}_k, \quad k = 1, \ldots, N-1, \tag{2.43}$$

where $\bar{z}_k = \begin{bmatrix} z_{k+1}^\top & \cdots & z_N^\top \end{bmatrix}^\top$, for $k = 1, \ldots, N-1$. The next proposition states a useful property of the functions Φ^C_k and Φ^D_k, that will be used in the sequel of the proof. The proof of this proposition is given in Section B.2 of Appendix B.

Proposition 2.1. *The functions $\Phi^C_k(z)$ and $\Phi^D_k(z)$ in (2.42) and (2.43) satisfy the following inequalities:*

$$\Phi^C_k(z) \leq -\bar{\rho}^C_k \bar{z}_k^\top \bar{z}_k, \quad \textit{for} \quad k = 1, \ldots, N-1 \tag{2.44}$$

$$\Phi^D_k(z) \leq -\bar{\rho}^D_k \bar{z}_k^\top \bar{z}_k, \quad \textit{for} \quad k = 1, \ldots, N-1 \tag{2.45}$$

where $\bar{\rho}^C_k$ and $\bar{\rho}^D_k$ are defined in (2.36) *and* (2.39)*, respectively.*

Define the Lyapunov function candidate:

$$V(x) := x^\top (T \otimes I_n) \bar{P}^C (T^\top \otimes I_n) x = \textstyle\sum_{k=2}^N \rho^C_k z_k^\top P_k z_k. \tag{2.46}$$

$$\text{(respectively, } V(x) := x^\top (T \otimes I_n) \bar{P}^D (T^\top \otimes I_n) x = \textstyle\sum_{k=2}^N \rho^D_k z_k^\top P_k z_k.\text{)} \tag{2.47}$$

From (2.34) and (2.19), the derivative of (2.46) along the solutions to (2.8) is

$$\dot{V}(x) = z^\top (\bar{P}^C \bar{A} + \bar{A}^\top \bar{P}^C) z = \bar{z}_1^\top (\bar{P}^C_1 \bar{A}_1 + \bar{A}_1^\top \bar{P}^C_1) \bar{z}_1 = \Phi^C_1(z). \tag{2.48}$$

Similarly, from (2.38) and (2.19), the increment of (2.47) along the solutions to (2.8) is

$$\Delta V(x) = z^\top(\bar{A}^\top \bar{P}^D \bar{A} - \bar{P}^D)z = \bar{z}_1^\top(\bar{A}_1 \bar{P}_1^D \bar{A}_1 - \bar{P}_1^D)\bar{z}_1 = \Phi_1^D(z). \tag{2.49}$$

Combining (2.48) (respectively, (2.49)) with (2.44) (respectively, (2.45)) in Proposition 2.1, we obtain

$$\begin{aligned} \dot{V}(x) &\leq -\bar{\rho}_1^C \bar{z}_1^\top \bar{z}_1. \\ \text{(respectively, } \Delta V(x) &\leq -\bar{\rho}_1^D \bar{z}_1^\top \bar{z}_1.) \end{aligned} \tag{2.50}$$

On the other hand, defining $\Lambda = \text{diag}(0, 1, \ldots, 1) \in \mathbb{R}^{N\times N}$, and using (2.17), the product in (2.50) can be rewritten as follows

$$\begin{aligned} \bar{z}_1^\top \bar{z}_1 &= \textstyle\sum_{k=2}^N |z_k|^2 = z^\top(\Lambda \otimes I_n)z \\ &= \Big((T^\top \otimes I_n)x\Big)^\top (\Lambda \otimes I_n)(T^\top \otimes I_n)x = x^\top(T\Lambda T^\top \otimes I_n)x. \end{aligned} \tag{2.51}$$

We now combine Lemma 2.4 (after noticing that matrices T and Λ in (2.51) satisfy the hypothesis of this lemma), (2.50), (2.51), the positive definiteness of P_k, for $k = 2, \ldots N$, and the positivity of the scalars ρ_k^C in (2.35) (respectively, ρ_k^D in (2.39)), obtaining the following bounds for the Lyapunov function candidate in (2.46) (respectively, (2.47))

$$V(x) \leq \bar{\rho}^C \underbrace{\max_{h\in\{2,\ldots,N\}} \lambda_{\max}(P_h)}_{:=\bar{p}} \textstyle\sum_{k=2}^N |z_k|^2 = \bar{\rho}^C \bar{p} x^\top (T\Lambda T^\top \otimes I_n)x \leq \bar{\rho}^C \bar{p} \bar{c}_2 \, |x|_{\mathcal{S}}^2 , \tag{2.52}$$

$$V(x) \geq \underline{\rho}^C \underbrace{\min_{h\in\{2,\ldots,N\}} \lambda_{\min}(P_h)}_{:=\underline{p}} \textstyle\sum_{k=2}^N |z_k|^2 = \underline{\rho}^C \underline{p} x^\top (T\Lambda T^\top \otimes I_n)x \geq \underline{\rho}^C \underline{p} \bar{c}_1 \, |x|_{\mathcal{S}}^2 , \tag{2.53}$$

(respectively,

$$V(x) \leq \bar{\rho}^D \max_{h\in\{2,\ldots,N\}} \lambda_{\max}(P_h) \textstyle\sum_{k=2}^N |z_k|^2 = \bar{\rho}^D \bar{p} x^\top (T\Lambda T^\top \otimes I_n)x \leq \bar{\rho}^D \bar{p} \bar{c}_2 \, |x|_{\mathcal{S}}^2 , \tag{2.54}$$

$$V(x) \geq \underline{\rho}^D \min_{h\in\{2,\ldots,N\}} \lambda_{\min}(P_h) \textstyle\sum_{k=2}^N |z_k|^2 = \underline{\rho}^D \underline{p} x^\top (T\Lambda T^\top \otimes I_n)x \geq \underline{\rho}^D \underline{p} \bar{c}_1 \, |x|_{\mathcal{S}}^2 ,) \tag{2.55}$$

where we have defined

$$\bar{\rho}^C := \max_{k=2,\ldots,N} \rho_k^C, \quad \underline{\rho}^C := \min_{k=2,\ldots,N} \rho_k^C. \tag{2.56}$$

$$\text{(respectively, } \bar{\rho}^D := \max_{k=2\ldots,N} \rho_k^D, \quad \underline{\rho}^D := \min_{k=2,\ldots,N} \rho_k^D.) \tag{2.57}$$

Thus (2.26) is proven with $\alpha_1 = \bar{c}_1 \underline{p} \underline{\rho}^C$ and $\alpha_2 = \bar{c}_2 \bar{p} \bar{\rho}^C$ (respectively, $\alpha_1 = \bar{c}_1 \underline{p} \underline{\rho}^D$ and $\alpha_2 = \bar{c}_2 \bar{p} \bar{\rho}^D$). Finally, using (2.50), (2.51) and Lemma 2.4, we obtain

$$\dot{V}(x) \leq \bar{\rho}_1^C \bar{z}_1^\top \bar{z}_1 = \bar{\rho}_1^C x^\top (T\Lambda T^\top \otimes I_n)x \leq -\bar{\rho}_1^C \bar{c}_1 \, |x|_{\mathcal{S}} , \tag{2.58}$$

$$\text{(respectively, } \Delta V(x) \leq \bar{\rho}_1^D \bar{z}_1^\top \bar{z}_1 = \bar{\rho}_1^D x^\top (T\Lambda T^\top \otimes I_n)x \leq -\bar{\rho}_1^D \bar{c}_1 \, |x|_{\mathcal{S}} ,) \tag{2.59}$$

which coincides with (2.27) with $\beta = \bar{\rho}_1^C \bar{c}_1$ (respectively, $\beta = \bar{\rho}_1^D \bar{c}_1$).
Proof of (ii) $\implies$ (iii). Based on (2.26)-(2.27), the uniform global exponential stability of $\mathcal{S}$ in (2.9) follows from standard Lyapunov results for noncompact attractors (see, e.g., the discrete- and continuous-time special cases of the hybrid results in [101, Theorem 1]).
Proof of (iii) $\implies$ (iv). By assumption, the vector p satisfies $p^\top L = 0$ and $p^\top \mathbf{1}_N = 1$. Since the graph $\mathcal{G}$ contains a rooted directed spanning tree, the components of p are strictly positive, implying $|p| = \sum_{i=1}^N p_k = |p|_1$, where $|p|_1$ denotes the 1-norm of p. Consider the vector $s := \mathbf{1}_N \otimes \bar{x} \in \mathcal{S}$, where

$$\bar{x} := \tfrac{1}{|p|_1}(p^\top \otimes I_n)x = \tfrac{1}{|p|_1}\textstyle\sum_{k=1}^N p_k x_k. \tag{2.60}$$

According to (2.8), the time evolution of s is

$$\begin{aligned}\delta s &= (\mathbf{1}_N \otimes p^\top \otimes I_n)\delta x = \tfrac{1}{|p|_1}(\mathbf{1}_N \otimes p^\top \otimes I_n)(1 \otimes I_N \otimes A - 1 \otimes L \otimes BKC)x \\ &= \tfrac{1}{|p|_1}(\mathbf{1}_N \otimes p^\top \otimes A)x - (\mathbf{1}_N \otimes \underbrace{p^\top L}_{=0} \otimes BKC)x = \tfrac{1}{|p|_1}(\mathbf{1}_N \otimes p^\top \otimes A)x \\ &= (I_N \otimes 1 \otimes A)(\mathbf{1}_N \otimes \tfrac{p^\top}{|p|_1} \otimes I_n)x = (I_N \otimes A)s\end{aligned} \tag{2.61}$$

Thus, the vector components $\bar{x}$ of s evolve autonomously according to

$$\delta\bar{x}(t) = A\bar{x}(t), \quad \bar{x}(0) = \tfrac{1}{|p|_1}\textstyle\sum_{k=1}^N p_k x_k(0). \tag{2.62}$$

Notice that $\bar{x}$ corresponds to the weighted average of the agent states x_k, where the weights are given by the corresponding components of p (which are all positive). Since $\mathcal{S}$ is globally exponentially stable, there exists a trajectory x_∞ such that, for all $k \in \mathcal{N}$

$$\lim_{t\to\infty} x_k(t) - x_\infty(t) = \mathbf{0}_n. \tag{2.63}$$

Therefore, using (2.60), we have

$$\begin{aligned}\lim_{t\to\infty} \bar{x}(t) - x_k(t) &= \lim_{t\to\infty} \tfrac{1}{|p|_1}\textstyle\sum_{k=1}^N p_k x_k(t) - x_k(t) \\ = \lim_{t\to\infty} \left(\tfrac{1}{|p|_1}\textstyle\sum_{k=1}^N p_k\right) x_k(t) - x_k(t) &= \lim_{t\to\infty} x_\infty(t) - x_k(t) = \mathbf{0}_n,\end{aligned} \tag{2.64}$$

where we have used $|p|_1 = \sum_{k=1}^N p_k$, which holds from the positivity of p_k.
Proof of (iv) $\implies$ (i). We prove this step by contradiction. Assume that one of matrices A_k in (2.25) is not Hurwitz (respectively, Schur-Cohn), and assume without loss of generality that it is A_N. Consider the coordinate system in (2.18), characterized by the state matrix (2.19). From the block upper-triangular structure of $I_N \otimes A - \bar{L} \otimes BKC$, there exists a vector $\omega^* \in \mathbb{R}^n$ (an eigenvector of one of the non-converging natural modes) such that the solution to (2.18) from $z^*(0) = \begin{bmatrix} 0 \\ \vdots \\ 0 \\ 1 \end{bmatrix} \otimes \omega^\star$ corresponds to $z^*(t) =$

$\begin{bmatrix} 0 \\ \vdots \\ 0 \\ 1 \end{bmatrix} \otimes z_N^\star(t)$, where $z_N^\star(t)$ does not converge to zero. As a consequence, the Lyapunov function in (2.46) (respectively (2.47)) along this solution takes the following values

$$V(x^*(t)) = V((T \otimes I_n)z^*(t)) = z_N^\top(t) P_N^C z_N(t), \tag{2.65}$$

$$\text{(respectively, } V(x^*(t)) = V((T \otimes I_n)z^*(t)) = z_N^\top(t) P_N^D z_N(t), \text{)} \tag{2.66}$$

which, from linearity, remains bounded away from zero. Then, using (2.52) (respectively, (2.54)), we conclude that $|x^*(t)|_{\mathcal{S}}$ is bounded away from zero, namely the solution $x^*(t)$ does not converge to the synchronization set $\mathcal{S}$. In other words, the components of $x^*(t)$ do not synchronize, which contradicts item (iv). The proof of Theorem 2.1 is completed. □

Item (i) of Theorem 2.1 establishes the equivalence between synchronization among agents (2.1) with interconnection (2.3), and the stability of $N-1$ LTI systems of dimension n corresponding to

$$\begin{aligned} \delta x_i &= Ax_i + Bu_i \\ u_i &= \lambda_i KCx_i \end{aligned} \qquad i = 2, \ldots, N, \tag{2.67}$$

parameterized by the nonzero eigenvalues $\lambda_2, \ldots, \lambda_N$ of L. Therefore, the problem of finding a suitable controller K that guarantees state synchronization of the multi-agent system (2.1) is a simultaneous stabilization problem.

The part (i) $\implies$ (ii) of Theorem 2.1 is a converse Lyapunov function theorem for uniform global exponential stability of the synchronization set $\mathcal{S}$ in (2.9) for dynamics (2.1) and (2.3).

Remark 2.2. According to Assumption 2.1, the Laplacian L has real eigenvalues. This assumption is necessary to have a real-valued Lyapunov function (2.46), (respectively, (2.47)). This allow us to include our problem in the classical Lyapunov stability theory framework.

Remark 2.3. We point out that there are some major technical issues while studying the stability of unbounded, closed sets. In fact, the attractivity property of stability is not uniform in general (further details on non-uniform attractivity are contained in [40, Chapter 3]).

Remark 2.4. As a consequence of Theorem 2.1, nontrivial state synchronization only happens either when the autonomous dynamics of the agents is not asymptotically stable—that is, when A in (2.1) is not Hurwitz (respectively, Schur-Cohn). However, when A in (2.1) is Hurwitz (respectively, Schur-Cohn), the theorem is still useful to prove that the agents reach state synchronization with a certified synchronization rate. In fact, if we consider multi-agent systems composed by asymptotically stable agents, consensus would be trivially achieved with the zero controller. This second situation is studied in detail in Chapter 4, where we address the global state synchronization problem under input saturation constraints and certified synchronization rate.

Remark 2.5. *(State Synchronization: existence of K)* When we consider the static output feedback interconnection (2.3), we do not have sufficient conditions for the existence of the static output feedback gain K. Indeed, the static output feedback design is known to be a difficult problem, for which no sufficient conditions are known [94]. Moreover, the simultaneous stabilization problem is known to be NP-hard [4].

However, the design of the feedback matrix K in (2.3) can be carried out using suitable relaxations. In the next section, we propose an iterative algorithm based on bisection and Linear Matrix Inequalities (LMIs) to perform the design of K. Although this method is not guaranteed to converge, nor to find a solution to the problem, it exhibits useful properties that make it a valuable design tool.

When we consider state synchronization via distributed state feedback, that is, if we replace (2.3) by

$$u_i := K\frac{1}{|\mathcal{N}_i|}\sum_{i\in\mathcal{N}_i}(x_j - x_i), \tag{2.68}$$

the stabilizability of (A, B) and the connectedness of $\mathcal{G}$ are necessary and sufficient conditions for synchronization. This result is proven in [104]. This property does not carry over to output synchronizability. A useful account for this is given by [113].

2.4 ILMI Static Output Feedback Design

In this section, we address the problem of finding a design procedure to select the value of the controller gain K in (2.3) to guarantee state synchronization among systems (2.1). As we point out in Remark 2.5, this design problem is a challenging open problem in linear control theory. The proposed design is based on an Iterative Linear Matrix Inequality (ILMI) algorithm, based on the Finsler lemma (see [73, Lemma 2]) and bisection methods. These techniques allow us to overcome the intrinsic nonlinear nature of the controller design conditions arising from the Lyapunov synchronization stability analysis that we carried out in the previous section.

In order to apply the proposed algorithm we make an additional assumption on the multi-agent system (2.1). We assume that matrix C is in the form $C = [I_p\ 0]$.

Remark 2.6. There is no loss of generality in considering systems in the form $(A, B, [I_p\ 0])$ in Algorithm 2.1 when C is a full-row rank matrix. For a system in a general form (A, B, C), where matrix C is full-row rank, there always exists a nonsingular matrix U such that $CU^{-1} = [I_p\ 0]$. Using U as a similarity transformation we obtain

$$(U^{-1}AU, U^{-1}B, CU) = (\bar{A}, \bar{B}, [I_p\ 0]).$$

In particular, we want to strengthen the synchronization requirement by maximizing the synchronization rate of the multi-agent system, as defined in (2.15). In other words, we want to find the maximum value of $\beta > 0$, such that (2.15) is satisfied. We want to obtain a characterization of this optimization problem in terms of linear matrix inequalities. In the previous section we have seen that (2.20) describes the synchronous

behavior of the multi-agent system, while (2.21) describes the synchronization error dynamics. Note that synchronization is achieved exponentially fast with synchronization rate $\beta > 0$ if the $N-1$ subsystems (2.21) converge to zero with decay rate $\beta > 0$. This observation is formalized in the following proposition, which follows from standard Lyapunov stability results for linear systems (see, for instance, [42]) and from convexity of (2.69) in λ_i.

Proposition 2.2. (State synchronization with Synchronization Rate Constraints) *If there exist a positive definite matrix $W = W^\top \in \mathbb{R}^{N\times N}$, and a scalar $\beta > 0$ such that*

$$(A - \lambda_i BKC)W + W(A - \lambda_i BKC)^\top \leq -2\beta W, \qquad i = 2, \ldots, N, \tag{2.69}$$

then, the closed-loop system (2.1) *and* (2.3) *satisfies* (2.15) *with $\epsilon = \beta$, for some $M > 0$ and for any initial condition $x(0)$.*

Lemma 2.5. *If* (2.69) *holds for $i = 2$ and $i = N$, then it holds for all $i = 3, \ldots, N-1$.*

Proof. If

$$\begin{aligned}(A - \lambda_2 BKC)W + W(A - \lambda_2 BKC)^\top &\leq -2\beta W\\ (A - \lambda_N BKC)W + W(A - \lambda_N BKC)^\top &\leq -2\beta W\end{aligned}$$

then, any convex combination $\lambda_i := \mu_i\lambda_2 + (1-\mu_i)\lambda_N$ of λ_2, λ_N, where $0 \leq \mu_i \leq 1$, is also a solution to (2.34). In fact

$$\begin{aligned}-2\beta(\mu_i + 1 - \mu_i)W &\geq \mu_i \mathrm{He}[(A - \lambda_2 BKC)W] + (1-\mu_i)\mathrm{He}[(A - \lambda_N BKC)W]\\ &= \mathrm{He}[(\mu_i + 1 - \mu_i)A - (\mu_i\lambda_2 + (1-\mu_i)\lambda_N)BKC)W]\\ &= (A - \lambda_i BKC)W + W(A - \lambda_i BKC)^\top.\end{aligned}$$

Since any eigenvalue of a Laplacian matrix L satisfying Assumption 2.1 can be rewritten as a convex combination of the largest and smallest eigenvalues of L, the statement is proved. □

Remark 2.7. Note that in (2.69) we choose a common Lyapunov matrix $W_2 = \cdots = W_N = W$. Thus, conditions (2.69) induce a certain conservatism in the state synchronization solution. However, they have the advantage of only depending on the smallest and largest eigenvalues of L, according to Lemma 2.5.

We recall that condition (2.15) states that the agent states x_i in (2.1) reach synchronization with synchronization rate less or equal than β. The larger is the value of β, the faster the agents reach state synchronization. This condition set the stage for the development of our design method. The introduction of the new parameter β has two beneficial consequences. First, it allows to give a better description of the multi-agent system behavior. Second, it allows for the initialization of the proposed algorithm for any system data (see item (i) of Proposition 2.3).

Summarizing, the problem we want to solve in this section is the following optimization problem

$$\begin{aligned} \beta^\star := \quad & \max_{W,K,\beta} \quad \beta, \\ & \text{s.t.} \quad (2.69),\ W > 0. \end{aligned} \tag{2.70}$$

Note that conditions (2.69) contain a nonlinear term $BKCW$ and a bilinear term βW. As a consequence, (2.70) is not a convex problem and can not be solved by a general off-the-shelf numerical package or algorithm. In order to overcome this problem, we present a systematic procedure in order to obtain more numerically tractable conditions to solve optimization (2.70). Consider the constraint (2.69). Applying Finsler Lemma [73, Lemma 2], we obtain that (2.69) is equivalent to

$$\begin{bmatrix} 2\beta W + \mathrm{He}((A-\lambda_i BKC)G) & -G^\top + (A-\lambda_i BKC)G + W \\ * & -G - G^\top \end{bmatrix} \leq 0, \tag{2.71}$$

for $i = 2, N$, for some multiplier $G \in \mathbb{R}^{2n\times 2n}$, and $W = W^\top > 0$. Note that in condition (2.71), the Lyapunov function matrix W is now decoupled from the controller matrix K. In fact, the introduction of the multiplier G adds an extra degrees of freedom to the problem, which is exploited in the controller design. Moreover, we suppose that the multiplier G has the following block diagonal structure

$$G = \begin{bmatrix} G_{11} & G_{11}M \\ G_{21} & G_{22} \end{bmatrix}, \quad G_{11} \in \mathbb{R}^{p\times p} \text{ nonsingular}, \tag{2.72}$$

where $M \in \mathbb{R}^{p\times 2n-p}$ is a given matrix, $G_{11} \in \mathbb{R}^{p\times p}$, and G_{21}, G_{22} are unconstrained matrices of suitable dimensions. Combining (2.71) with (2.72), we obtain that

$$(A-\lambda_i BKC)G = AG - \lambda_i BK[I_p\ 0]G = AG - \lambda_i BKG_{11}[I_p\ M]. \tag{2.73}$$

Based on (2.73), with G as in (2.72), we can rewrite (2.71) as follows

$$\begin{bmatrix} 2\beta W + \mathrm{He}(AG - \lambda_i BX) & -G^\top + AG - \lambda_i BX + W \\ * & -G - G^\top \end{bmatrix} \leq 0, \tag{2.74}$$

$$X := X_1 \begin{bmatrix} I_p & M \end{bmatrix}, \quad X_1 := KG_{11}. \tag{2.75}$$

Based on these observations, we can conclude that if there exists a solution to the following optimization problem

$$\begin{aligned} \beta_1 := & \max_{W>0,\,\beta,\,G_{11}>0,\,G_{22},\,G_{21},\,X_1} \quad \beta \\ & \text{s.t.} \quad (2.74),\ \ (2.72),\ \ (2.75), \end{aligned} \tag{2.76}$$

for a given M, then the resulting controller $K := X_1 G_{11}^{-1}$, satisfies (2.69) with $\beta = \beta_2 \geq \beta_1$. The gap between β_2 and β_1 is due to the constraint (2.72) imposed on G, which may introduce some conservatism in the solution.

Remark 2.8. We provide a relaxation of the constraints (2.69) using Finsler Lemma, obtaining the linear formulation (2.76). The price to pay for linearity is the conservatism introduced in (2.72), by constraining the multiplier G to have a predetermined structure. However, enforcing the structure of the multipliers is always less conservative than constraining the Lyapunov function matrix, and in some cases it happens without loss of generality [28]. The advantage of considering the relaxation (2.76) instead of (2.69) relies on its mathematical tractability.

We want to analyze the solution obtained solving (2.76). This analysis can be carried out by plugging the resulting controller $K = X_1 G_{11}^{-1}$ into (2.71), and solving the resulting optimization (2.70)—which is quasi convex for a fixed controller—using bisection over β. The optimal value is then obtained due to the fact that (2.76) is a generalized eigenvalue problem (see [8]) for a fixed controller. If β_1 computed from (2.76) is less or equal to the value β_2 obtained solving Problem (2.70) with $K = G_{11}^{-1} X_1$, this means that we could possibly obtain a tighter bound on β by recomputing the controller matrix.

This observation suggests a two-steps procedure, that consists of a *synthesis step*, in which the controller K is computed according to (2.76), and an *analysis step*, in which a tighten bound on β is obtained after by solving (2.70) fixing the controller matrix. If the values β_1, β_2 of β computed respectively by the analysis and the synthesis steps are not equal within a desired tolerance, we want to iterate the procedure. A way to find a not worse solution is as follows. We perform a Schur complement to (2.70), obtaining

$$\begin{bmatrix} 2\beta W + \mathrm{He}((A - \lambda_i BKC)W) & -W^\top + (A - \lambda_i BKC)W + W \\ * & -W - W^\top \end{bmatrix} \leq 0, \tag{2.77}$$

for $i = 2, N$, which corresponds to (2.71) with $G = G^\top = W > 0$. Partition the Lyapunov matrix as $W := \left[\begin{smallmatrix} W_{11} & W_{12} \\ W_{21} & W_{22} \end{smallmatrix}\right]$, according to the same partition of G in (2.72). Comparing the two expressions, and as $W_{11} > 0$, we conclude that (2.75) is solved setting $M := W_{11}^{-1} W_{12}$, will provide a value of β that can not be worse.

The overall procedure is summarized in Algorithm 2.1, on page 28. At each step, the variable β is maximized, obtaining a non-decreasing sequence of sub-optimal values (see item (ii) of Proposition 2.3). Note that, in both optimization problems (2.70) and (2.76) we do not constrain the optimization variable β to take positive values. If at the end of the optimization process, the value of β is positive, then the corresponding K is a stabilizing static output feedback matrix.

The properties of Algorithm 2.1 are stated in Proposition 2.3.

Proposition 2.3. (Properties of Algorithm 2.1) *The following statements hold:*

(i) Initialization*: Given any input $(A, B, [I_p\ 0])$, Laplacian matrix L and tolerance $\delta > 0$, the pair of scalars $(\beta_L, \beta_H) = (\beta_L^0, \beta_H^0)$ defined in the Initialization step of Algorithm 2.1 is an admissible pair for* (2.79) *(in the sense specified in the Initialization step of the algorithm).*

(ii) Feasibility*: Given any admissible pair $(\beta_{L_1}, \beta_{H_1})$ from Step 1, the pair $(\beta_{L_2}, \beta_{H_2})$ obtained from the subsequent Step 2 always satisfies $\beta_{L_2} \geq \beta_{L_1}$, and vice versa.*

Algorithm 2.1 Static output feedback controller design for state synchronization

Input: Matrices A, B, $C = [I_p\ 0]$, the Laplacian matrix L, and a tolerance $\delta > 0$.
Initialization: Set $M = 0$ and initialize the pair $(\beta_L, \beta_H) = (\beta_L^0, \beta_H^0)$, where, using $\bar{\sigma}(A + I_n)$ to denote the maximum singular value of $A + I_n$, we select

$$\beta_L^0 := \tfrac{1}{2} - \tfrac{1}{2}\bar{\sigma}^2(A + I_n), \quad \beta_H^0 := \tfrac{1}{2} - \max\ \mathbf{Re}(\mathrm{eig}(A)). \tag{2.78}$$

Pair (β_L, β_H) is *admissible* for (2.79), in the sense that (2.79) is feasible with $\beta = \beta_L$ and infeasible with $\beta = \beta_H$ for some G, W and X.
Iteration

Step 1: Given M and pair (β_L, β_H) from the previous step, solve the following optimization problem, using bisection method with tolerance $\delta > 0$.

$$\begin{aligned} \max_{W, G_{11}, G_{21}, G_{22}, X_1, \beta} \quad & \beta \\ \text{s.t.} \quad & (2.74),\ (2.72),\ (2.75),\ i = 2, N. \end{aligned} \tag{2.79}$$

In particular, determine an admissible pair (β_L, β_H) such that $\beta_H - \beta_L \leq \delta$. Pick the (sub)optimal solution $\bar{G}_{11}$, $\bar{X}_1$ corresponding to β_L, and set $\bar{K} := \bar{G}_{11}^{-1}\bar{X}_1$ for the next step.

Step 2: Given $\bar{K}$ and pair (β_L, β_H) from the previous step, solve the following optimization problem, using bisection method with tolerance $\delta > 0$.

$$\begin{aligned} \max_{W = W^\top > 0, \beta} \quad & \beta \\ \text{s.t.} \quad & (2.69),\ i = 2, N. \end{aligned} \tag{2.80}$$

In particular, determine an admissible pair (β_L, β_H) such that $\beta_H - \beta_L \leq \delta$. Pick the (sub)optimal solution $\bar{W} = \begin{bmatrix} \bar{W}_{11} & \bar{W}_{12} \\ \bar{W}_{21} & \bar{W}_{22} \end{bmatrix}$ (where W has the partition induced by G) corresponding to α_L, and set $M := \bar{W}_{11}^{-1}\bar{W}_{12}$ for the next step.
until β_L does not increase more than δ over three consecutive steps.
Output: $K_{out} = \bar{K}$ and $\beta_{out} = \beta_L$.

(iii) Guarantees*: Any solution* (K_{out}, β_{out}) *resulting from Algorithm 2.1 is such that the eigenvalues of* $A - \lambda_i B K_{out}[I_p \ 0]$ *have real part less or equal to* $-\beta_{out}$*. In particular, if* $\beta_{out} > 0$*, the static output feedback protocol* (2.3) *with* $K = K_{out}$ *is such that the multi-agent system* (2.1) *with data* $(A, B, [I_p \ 0])$ *satisfies* (2.15) *with* $\beta = \beta_{out}$*.*

Proof. Proof of (i). First, we prove that (β_L^0, β_H^0) in (2.78) is an admissible pair for (2.79), in the sense clarified in the Initialization step. To show that (2.79) is feasible with $\beta = \beta_L^0$ and infeasible with $\beta = \beta_H^0$, select $G_{11} = I_p$, $G_{22} = I_{n-p}$, $G_{21} = 0$, $X_1 = 0$, and $W = I_n$. By applying the Schur complement, (2.79) is equivalent to

$$2\beta I_n + A + A^\top + \tfrac{1}{2} A A^\top \leq 0. \tag{2.81}$$

Since

$$2\beta I_n + A + A^\top + \tfrac{1}{2} A A^\top \leq 2\beta I_n + A + A^\top + A A^\top = (2\beta - 1) I_n - (A + I_n)(A^\top + I_n), \tag{2.82}$$

by choosing $\beta = \beta_0^L$, it is verified that the second member in (2.82) is negative definite, thus assuring the feasibility of (2.79). We now prove that (2.79) is infeasible with $\beta = \beta_H^0$. For this particular choice of the variables, the first diagonal block of (2.79) is $2\beta I_n + A + A^\top$, that is positive definite by choosing $\beta = \beta_L^0$, thus completing the proof.
Proof of (ii). [From Step 1 to Step 2]. By substituting the solution β_{L_1}, $\bar{K}$ obtained from Step 1 in (2.79) we get that

$$\begin{bmatrix} 2\beta_{L_1} W + \mathrm{He}((A - \lambda_i B \bar{K} C) G) & -G^\top + (A - \lambda_i B \bar{K} C) G + W \\ * & -G - G^\top \end{bmatrix} \leq 0, \quad i = 2, N \tag{2.83}$$

has a feasible solution. By applying [73, Theorem 1], feasibility of (2.83) is equivalent to feasibility of

$$W (A - \lambda_i B \bar{K} C)^\top + (A - \lambda_i B \bar{K} C) W \leq -2\beta_{L_1} W, \quad i = 2, N. \tag{2.84}$$

Comparing (2.84) with (2.80), it follows that the subsequent solution β_{L_2} to Step 2 satisfies $\beta_{L_2} \geq \beta_{L_1}$.
[From Step 2 to Step 1]. Substitute the solution α_{L_2}, M obtained from Step 2 in (2.80) and perform the Schur complement to get

$$\begin{bmatrix} 2\beta_{L_2} W + \mathrm{He}((A - \lambda_i B \bar{K} C) W) & -W^\top + (A - \lambda_i B \bar{K} C) W + W \\ * & -W - W^\top \end{bmatrix} \leq 0, \quad i = 2, N, \tag{2.85}$$

which corresponds to (2.79) with $G = W$. It follows that the subsequent solution β_{L_1} to Step 1 satisfies $\beta_{L_1} \geq \beta_{L_2}$.
Proof of (iii). From linear systems theory (see, e.g., [42]), we deduce that both solutions at Step 1 and Step 2 provide a certificate that matrices $A - \lambda_i B K_{out} C$ for $i = 2, N$ have eigenvalues with real part less or equal than β_{out}. By virtue of Proposition 2.2, (2.15) is satisfied with $\beta = \beta_{out}$. □

Remark 2.9. Note that in Step 1 and Step 2 of Algorithm 2.1, we do not constrain the sign of β, allowing for possible negative solutions. As a consequence, the intermediate solutions to (2.79) and (2.80), are not necessarily solutions to (2.70). As stated in item (iii) of Proposition 2.3, if at the end of the optimization process the value of β is positive, then the corresponding solution to (2.79) and (2.80) is also solution to (2.70).

Example 2.1. We present an example in which a suitable static output feedback controller is designed, in order to synchronize the states of a specific multi-agent system, consisting of a group of three Grumman X-29A aircraft. This example is borrowed from [58]. In particular, we consider a network of identical LTI agents described by the following state-space representation.

$$\begin{aligned} \dot{x}_i &= A_{\text{X-29A}} x_i + B_{\text{X-29A}} u_i \\ y_i &= \begin{bmatrix} I_2 & 0 \end{bmatrix} x_i \end{aligned} \qquad i = 1, 2, 3, \tag{2.86}$$

where

$$A_{\text{X-29A}} = \begin{bmatrix} -0.59 & 0.997 & -16.55 & 0 \\ -0.1023 & -0.0679 & 6.779 & 0 \\ -0.0603 & -0.9928 & -0.1645 & 0.04413 \\ 1 & 0.07168 & 0 & 0 \end{bmatrix}, B_{\text{X-29A}} = \begin{bmatrix} 1.347 & 0.2365 \\ 0.09164 & -0.07056 \\ -0.0006141 & 0.0006866 \\ 0 & 0 \end{bmatrix}.$$

The model (2.86) describes the lateral dynamics of a Grumman X-29A aircraft (see Figure 2.3 (right)), where the state vector is given by $x_i = [p_i \; r_i \; \beta_i \; \phi_i]^\top \in \mathbb{R}^4$, for $i = 1, 2, 3$. p_i, and r_i are the roll and yaw rate and β_i, ϕ_i are sideslip and bank (roll) angle of aircraft i, respectively. The detailed linearised model of this aircraft is presented in [7], and the parameters in (2.86) correspond to the ND-UA flight mode at an altitude of 20000 ft with 0.7 Mach forward velocity. The control inputs are $u_i = [\delta_{F_i} \; \delta_{R_i}]^\top \in \mathbb{R}^2$, that represent the flaperon and rudder control, respectively. The second equation in (2.86) says that we can measure the states p_i and r_i through the outputs $y_i \in \mathbb{R}^2$. The aircraft are interconnected according to the graph $\mathcal{G}$ depicted in Figure 2.3 (left). The nonzero eigenvalues of the Laplacian matrix are $\lambda_1 = 0.382$ and $\lambda_2 = 2.681$.

We want to design a suitable output feedback control matrix $K \in \mathbb{R}^{2\times 2}$, such that the control protocol (2.3) synchronizes the states of the aircraft (2.86). The decentralized output feedback controller is designed using Algorithm 2.1. The algorithm is implemented in MATLAB, and solved with the YALMIP toolbox and the MOSEK solver. Algorithm 2.1 is run with tolerance $\delta = 10^{-4}$. Figure 2.4 shows the maximization of β during the iterations of the algorithm. The algorithm converges after 103 iterations and gives a sub-optimal value $\beta_{out} = 0.0793 > 0$. According to item (iii) of Proposition 2.3 the controller (2.3), with K selected as

$$K_{out} = \begin{bmatrix} 10.6934 & 18.5936 \\ -51.0669 & -91.8875 \end{bmatrix} \tag{2.87}$$

assures uniform global exponential synchronization of the agents (2.86), with synchronization rate at least β_{out}.

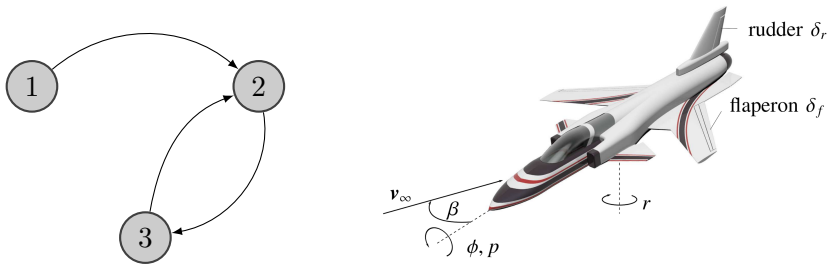

Figure 2.3: The left figures shows the network interconnections of the aircraft Grumman X-29A. The right figure shows a representation of a Gummar X-29A aircraft. (Credit Kim D. Listmann, [58] © IEEE 2016.)

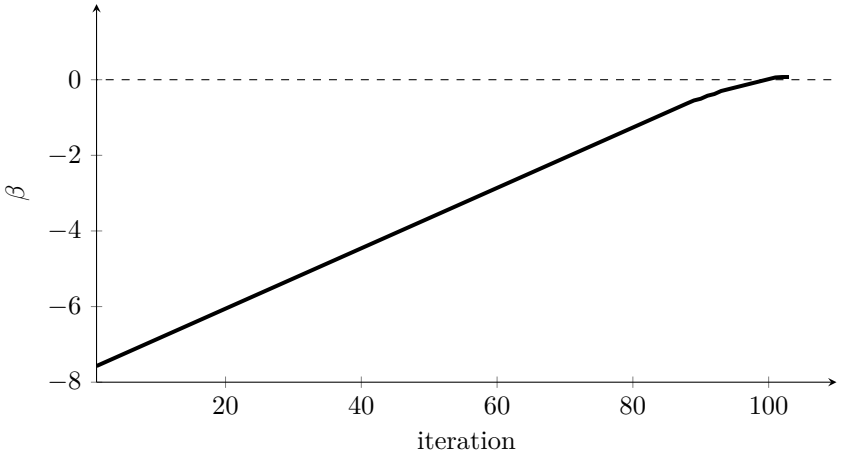

Figure 2.4: Optimization of the parameter β during the iterations of Algorithm 2.1. The sub-optimal value determined by the algorithm is $\beta_{out} = 0.0793$, after 103 iterations.

The interconnected systems (2.86) and (2.3) with $K = K_{out}$ as in (2.87) have been implemented in the MATLAB environment. The resulting simulations are shown in Figure 2.5. In all the plots, different colors identify different agents. We can see from the pictures that all the agents reach state synchronization. In particular, the last components ϕ_i, for $i = 1, 2, 3$, in Figure 2.5 (bottom), take significantly more time to synchronize as compared to the others. The simulations show the effectiveness of the proposed algorithm in the static output feedback control design. In particular, this control scheme is such that the agent states in (2.86) synchronize with the same synchronization rate as in [58], except for the last state vector component ϕ_i.

This is because in [58] a different control scheme is used—that is, a state feedback synchronizing control. The state feedback control scheme uses the knowledge all of the state variables $p_i, r_i, \beta_i, \phi_i$; the presented output feedback controller, instead, only needs the knowledge of the first two states p_i and r_i. The simulations we have performed indicate that the full state feedback has a better performance; this is possibly, because there is information in the state vector that is not available in the output

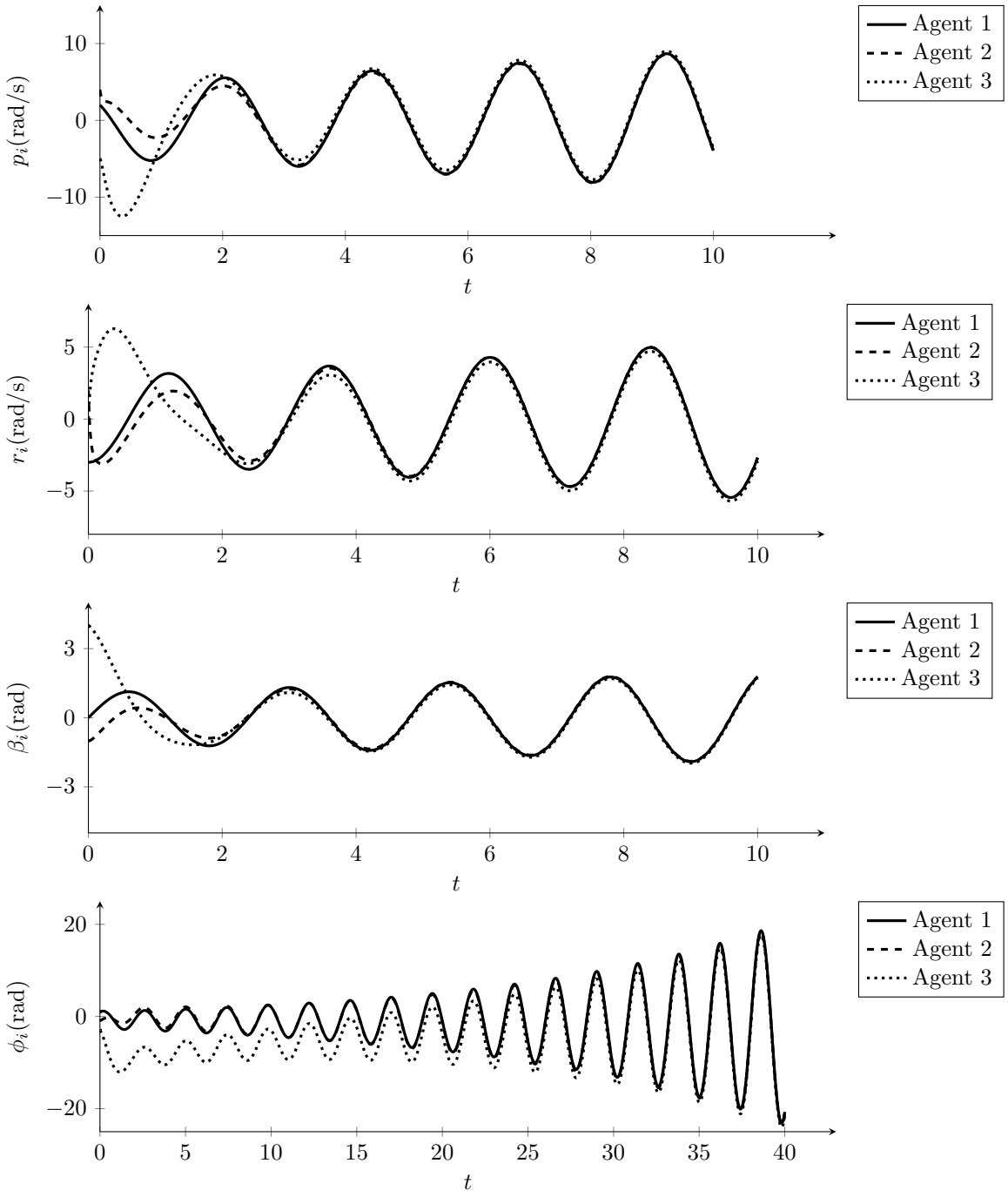

Figure 2.5: Time evolution of the state components p_i, r_i, β_i, ϕ_i of model (2.86).

2.5 Summary

Chapter 2 addressed the state synchronization problem of multi-agent systems connected according to a directed, connected topology. The multi-agent system under consideration was constituted by N identical continuous- or discrete-time linear systems. The state synchronization is achieved via distributed static output feedback control. The synchronization problem is solved by defining a Lyapunov function, and the static output feedback gain was designed by an algorithm based on Finsler Lemma. The proposed design method allows to include performance specifications in terms of synchronization rate, denoted by β in the chapter. The results are supported by a numerical example, that shows the effectiveness of the presented control design method. The results of this chapter pave the path for the introduction of more challenging control problems for multi-agent systems subject to limited information.

Chapter 3

H_∞ State Synchronization

In this chapter, we address the state synchronization problem considering the effects of exogenous disturbances. In many practical applications, the multi-agent system (2.1) is not sufficient for an exhaustive description of the behavior of the agents. In this chapter, we take into account the presence of external perturbations in the Agent Model. As these external disturbances affect the synchronization performance, rejection to external disturbances is demanded for the controller design.

The notion of $\mathcal{L}_2$ gain allows to quantify robustness properties or to design control laws to achieve desired robustness margins. In the case of isolated linear systems, the $\mathcal{L}_2$ gain stability extends the notion of asymptotic stability [106]. In this chapter we will define a $\mathcal{L}_2$ gain condition involving suitable incremental signals, such that the corresponding $\mathcal{L}_2$ gain synchronization stability comprises the notion of asymptotic synchronization.

Combining the synchronization stability results presented in Chapter 2 and a suitable $\mathcal{L}_2$ gain condition, we prove finite $\mathcal{L}_2$ synchronization stability for the case of additive noise in the agent open-loop dynamics.

More precisely, we give a matrix inequality characterization of the state synchronization problem with exogenous disturbances. We know from standard linear systems theory, that the $\mathcal{L}_2$ gain condition for a linear system is equivalent to a bound on the H_∞ norm of the transfer function from the disturbance signal to the performance signal. For this reason, the synthesis of a suitable controller to achieve stabilization with guaranteed performance is called H_∞ design. The further relaxation of the conditions for the state synchronization analysis, allows us to provide sufficient conditions for robust state synchronization in terms of Bilinear Matrix Inequalities (BMIs). Those relaxed conditions allow us to perform the H_∞ design of a distributed dynamic output feedback compensator, based on a suitable ILMI procedure.

3.1 Problem Formulation

We start this chapter by defining the Agent Model and the Information Topology of the multi-agent systems in consideration.

Agent Model We consider multi-agent systems consisting of N identical LTI continuous-time plant of order n. Each agent in the network is identified by the subscript index $i \in \mathcal{N} = \{1, \dots, N\}$, where $N > 1$ is the number of agents. The dynamics of each agent is described by the following linear state-space model

$$\begin{array}{rcll} \dot{x}_{pi} & = & A_p x_{pi} + B_{pu}\tilde{u}_i + B_{pw} w_i & \\ y_i & = & C_p x_{pi} + D_{pw} w_i & i \in \mathcal{N}, \\ z_i & = & C_{zp} x_{pi} + D_{zw} w_i, & \end{array} \tag{3.1}$$

where $x_{pi} \in \mathbb{R}^n$ is the *agent state*, $\tilde{u}_i \in \mathbb{R}^m$ is the *agent input*, $y_i \in \mathbb{R}^p$ is the *agent output*, and $z_i \in \mathbb{R}^\ell$ is the *agent performance output*. $w_i \in \mathbb{R}^q$ is the exogenous *agent disturbance* (e.g., measurement noise, plant disturbances). The system matrices A_p, B_{pu}, B_{pw}, C_p, D_{pw}, C_{zp} and D_{zp} are known matrices of appropriate dimensions. With the goal of studying disturbance attenuation requirements, we define the *differential inputs* and the *differential outputs*

$$\tilde{z}_i := z_i - \tfrac{1}{|\mathcal{N}_i|}\textstyle\sum_{j\in\mathcal{N}_i} z_j, \quad \tilde{w}_i := w_i - \tfrac{1}{|\mathcal{N}_i|}\textstyle\sum_{j\in\mathcal{N}_i} w_j \quad i \in \mathcal{N}, \tag{3.2}$$

where $\mathcal{N}_i$ denotes the set of neighbors of agent i in the graph $\mathcal{G}$. The signals $\tilde{z}_i$ and $\tilde{w}_i$ are respectively the relative performance variable and relative disturbance of the agent i with respect to the average of its neighboring agents. The variable $\tilde{w}_i$ in (3.2) is supposed to be limited in energy—that is, function of $\mathcal{L}_2[0,\infty)$. More precisely, we suppose that $\tilde{w}_i$ is a piecewise-continuous signal defined in $[0,\infty)$ such that

$$\textstyle\sum_{i=1}^N \|\tilde{w}_i\|_2^2 = \sum_{i=1}^N \int_0^\infty \tilde{w}_i(t)^\top \tilde{w}_i(t) dt < \infty, \quad i \in \mathcal{N}. \tag{3.3}$$

We will use the shorthand notation $\mathcal{L}_2$ instead of $\mathcal{L}_2[0,\infty)$, as there is no ambiguity on the underlying domain and range of the function $\tilde{w}_i$. For more details about $\mathcal{L}_p$ spaces and dissipative systems theory, the interested reader can refer to [106].

Information Topology The agents have communication capabilities. The communication topology in the multi-agent systems (3.1), is described by an undirected graph $\mathcal{G} = (\mathcal{V}, \mathcal{E})$. Every node $v_i \in \mathcal{V}$ is associated with one agent $i \in \mathcal{N}$ in the group. Every edge $(v_j, v_i) \in \mathcal{E}$ corresponds to a bidirectional link between agent i and agent j in the network. We assume that the undirected graph $\mathcal{G}$ is connected. The basic notions of graph theory are summarized in Appendix A. We choose to work with undirected graphs because the diagonalizability of the Laplacian matrix leads to simple derivations. However, using the techniques presented in Chapter 2, the results of this chapter can be extended to directed graphs satisfying Assumption 2.1.

We want to define a suitable $\mathcal{L}_2$ gain index for the multi-agent system (3.1), as a measure of the disturbance attenuation level. We first notice that the agent performance output $\tilde{z}_i$ in (3.2) can be rewritten as

$$\tilde{z}_i = C_{zp}\left(x_i - \tfrac{1}{|\mathcal{N}_i|}\textstyle\sum_{j\in\mathcal{N}_i} x_j\right) + D_{zw}\left(w_i - \tfrac{1}{|\mathcal{N}_i|}\textstyle\sum_{j\in\mathcal{N}_i} w_j\right) = C_{zp}\tilde{x}_i + D_{zi}\tilde{w}_i, \tag{3.4}$$

where we have defined the relative state vector $\tilde{x}_i$ as follows

$$\tilde{x}_i = x_i - \tfrac{1}{|\mathcal{N}_i|}\textstyle\sum_{j\in\mathcal{N}_i} x_j, \quad i \in \mathcal{N}. \tag{3.5}$$

From (3.4), we can see that smaller values of the $\mathcal{L}_2$ norm of $\tilde{z}_i$ indicate a desirable behavior. Two factors cause small values of the $\mathcal{L}_2$ norm of $\tilde{z}_i$. The first one is that the states of the multi-agent system (3.1) have similar values at the same time instants, that is, intuitively speaking, they are close to synchronization. The second one is that the system (3.1) is robust with respect to the relative noise signals $\tilde{w}_i$. This last property is formalized in the following definition.

Definition 3.1. ($\mathcal{L}_2$ gain for synchronization) *The multi-agent system* (3.1) *has finite (linear)* $\mathcal{L}_2$ *gain, with gain bound* $\gamma > 0$ *if all solutions starting from* $x_{pi}(0) = \mathbf{0}_n$ *satisfy*

$$\textstyle\sum_{i=1}^{N} \|\tilde{z}_i\|_2^2 \leq \gamma^2 \sum_{i=1}^{N} \|\tilde{w}_i\|_2^2, \tag{3.6}$$

for all $\tilde{w}_i \in \mathcal{L}_2$, *and* $i \in \mathcal{N}$.

In other words, Definition 3.1 says that, for any relative disturbance signal $\tilde{w}_i$ in $\mathcal{L}_2$, the response of the multi-agent system (3.1) starting from initial states $x_i(0) = \mathbf{0}_n$, is defined for all $t \geq 0$, and produces a performance variable $\tilde{z}_i$ that is a function in $\mathcal{L}_2$, for all $i \in \mathcal{N}$. Moreover, the ratio between the $\mathcal{L}_2$ norm of the relative performance signals $\{\tilde{z}_i,\ i \in \mathcal{N}\}$ and the relative disturbance signals $\{\tilde{w}_i,\ i \in \mathcal{N}\}$, is bounded by $\gamma > 0$. Note that the functions in $\mathcal{L}_2$ represent signals having finite energy over the infinite time interval $[0, +\infty)$. Therefore the number γ in inequality (3.6) can be interpreted as an upper bound on the ratio between the energy of the relative performance variables $\{\tilde{z}_i,\ i \in \mathcal{N}\}$ over the energy of the relative disturbances $\{w_i,\ i \in \mathcal{N}\}$. We will see in the next section that the fulfillment of inequality (3.6) is guaranteed by the fulfillment of suitable matrix inequalities involving the systems data, the controller data, the number γ, the Lyapunov matrix, and the topological parameters of the network.

The main goal of this chapter is to design a distributed control law $\tilde{u}_i$ (in the sense specified in Definition 2.2), that ensures synchronization among systems (3.1), and attenuates the effect of the exogenous disturbance on the state synchronization. The definition of state synchronization, as given in Definition 2.1, is recalled below.

Definition 3.2. (State Synchronization) *The multi-agent system* (3.1) *is said to achieve asymptotic state synchronization if, for any initial state* $x_{pi}(0) \in \mathbb{R}^n$, $i \in \mathcal{N}$, *there exists a trajectory* $\bar{x}_p$ *such that*

$$\lim_{t\to+\infty} (x_{pi}(t) - \bar{x}_p(t)) = \mathbf{0}_n \tag{3.7}$$

holds for every $i \in \mathcal{N}$, *and* $\bar{x}_p$ *is called* synchronization trajectory.

The problem we intend to address throughout the chapter is summarized as follows.

Problem 3.1. (Robust State Synchronization) *Consider the multi-agent system* (3.1)*, with interconnection described by* $\mathcal{G}$*. The robust synchronization problem consists in finding a control law* $\tilde{u}_i$ *such that*

(i) if $w_i = \mathbf{0}_q$ *for all* $i \in \mathcal{N}$*, there exists a trajectory* $\bar{x}_p$ *such that* (3.7) *is satisfied—that is, the multi-agent system* (3.1) *reaches asymptotic state synchronization.*

(ii) if $w_i \neq \mathbf{0}_q$ *for some* $i \in \mathcal{N}$*, and from initial conditions* $x_{pi}(0) = \mathbf{0}_n$*, for* $i \in \mathcal{N}$*, the multi-agent system* (3.1) *has finite* $\mathcal{L}_2$ *gain, with prescribed gain bound* $\gamma > 0$*, that is,* (3.6) *is satisfied.*

3.2 Distributed Dynamic Output Feedback

To solve Problem 3.1, we choose as control protocol, a distributed dynamic output feedback in the form

$$\dot{x}_{ci} = A_k x_{ci} + B_k y_i \tag{3.8a}$$
$$u_i = C_k x_{ci} \tag{3.8b}$$
$$\tilde{u}_i = u_i - \tfrac{1}{|\mathcal{N}_i|}\textstyle\sum_{j\in\mathcal{N}_i} u_j, \tag{3.8c}$$

where $x_{ci} \in \mathbb{R}^{n_k}$ is the *controller state*, and A_k, B_k and C_k are unknown matrices to be designed. In the following, we suppose that the controller state and the plant state have the same dimensions $n = n_k$. Note that the coupling signal among the closed-loop multi-agent system (3.1) and (3.8) is the relative input $\tilde{u}_i$, that represents the difference between the controller output of the single agent u_i and the average controller output of the neighboring agents $\frac{1}{|\mathcal{N}_i|}\sum_{j\in\mathcal{N}_i} u_j$ (see Figure 3.1).

Remark 3.1. Note that the structure of the proposed controller has no direct feed-through term—that is, $D_k = 0$. This choice leads to useful simplifications in the iterative LMI relaxation proposed next.

We want to give a compact representation of the interconnected system (3.1), and (3.8). To this end, we define the extended state vectors

$$x_i := \begin{bmatrix} x_{pi} \\ x_{ci} \end{bmatrix} \in \mathbb{R}^{2n}, \quad i \in \mathcal{N}. \tag{3.9}$$

The extended dynamics is obtained from (3.1) and (3.8), and corresponds to

$$\begin{aligned} \dot{x}_i &= \begin{bmatrix} A_p & 0 \\ B_k C_p & A_k \end{bmatrix} x_i + \begin{bmatrix} B_{pu} \\ 0 \end{bmatrix} \tilde{u}_i + \begin{bmatrix} B_{pw} \\ B_k D_{pw} \end{bmatrix} w_i \\ u_i &= \begin{bmatrix} 0 & C_k \end{bmatrix} x_i \\ z_i &= \begin{bmatrix} C_{zp} & 0 \end{bmatrix} x_i + D_{zw} w_i, \\ \tilde{u}_i &= u_i - \tfrac{1}{|\mathcal{N}_i|}\textstyle\sum_{j\in\mathcal{N}_i} u_j, \end{aligned} \tag{3.10}$$

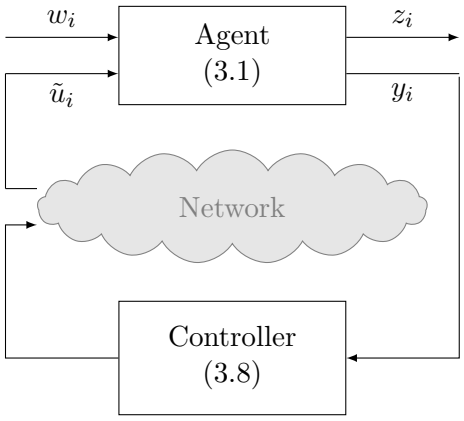

Figure 3.1: Block diagram of the closed-loop system of agents (3.1), with input (3.8) and coupling signal $\tilde{u}_i$.

We want to derive the collective dynamics of the closed-loop system (3.10). To this end, it is convenient to use the Kronecker product (or tensor product) to describe the aggregate dynamics. We define the aggregate vectors:

$$\begin{aligned} x &:= \begin{bmatrix} x_1^\top & \dots & x_N^\top \end{bmatrix}^\top \in \mathbb{R}^{2Nn} \\ u &:= \begin{bmatrix} u_1^\top & \dots & u_N^\top \end{bmatrix}^\top \in \mathbb{R}^{Nm} \\ w &:= \begin{bmatrix} w_1^\top & \dots & w_N^\top \end{bmatrix}^\top \in \mathbb{R}^{Nq} \\ z &:= \begin{bmatrix} z_1^\top & \dots & z_N^\top \end{bmatrix}^\top \in \mathbb{R}^{N\ell}, \end{aligned} \tag{3.11}$$

and similarly define the vectors $\tilde{x}$, $\tilde{u}$, $\tilde{w}$ and $\tilde{z}$. These last vectors can be rewritten in function of the ones defined in (3.11) according to (3.2), (3.5), and (3.8c) as

$$\tilde{x} = (L \otimes I_{2n})x, \quad \tilde{u} = (L \otimes I_m)u, \quad \tilde{w} = (L \otimes I_q)w, \quad \tilde{z} = (L \otimes I_\ell)z, \tag{3.12}$$

where $L \in \mathbb{R}^{N \times N}$ is the Laplacian matrix associated with $\mathcal{G}$. Combining (3.10), (3.11), and (3.12), we obtain the following collective closed-loop dynamics for the multi-agent system (3.1) and (3.8)

$$\begin{aligned} \dot{x} &= Ax + B_w w \\ z &= C_z x + D_z w \end{aligned} \tag{3.13}$$

where the structure of A, B_w, C_z, D_z is

$$\left(\begin{array}{c|c} A & B_w \\ \hline C_z & D_z \end{array}\right) = \left(\begin{array}{c|c} I_N \otimes \begin{bmatrix} A_p & 0 \\ B_k C_p & A_k \end{bmatrix} + L \otimes \begin{bmatrix} 0 & B_{pu} C_k \\ 0 & 0 \end{bmatrix} & I_N \otimes \begin{bmatrix} B_{pw} \\ B_k D_{pw} \end{bmatrix} \\ \hline I_N \otimes \begin{bmatrix} C_{zp} & 0 \end{bmatrix} & I_N \otimes D_{zw} \end{array}\right). \tag{3.14}$$

In Section 3.4, we will introduce a coordinates transformation for system (3.13), based on the spectral decomposition of the Laplacian matrix L of the network graph $\mathcal{G}$. This

new coordinates system, like the one introduced in Section 2.3 of Chapter 2, allows us to decouple the closed-loop dynamics into subsystems of smaller size. In Chapter 2, we obtained a block upper-triangular form for the state matrix of the closed-loop system. In this chapter, we will see that the symmetry property of the Laplacian matrix allows to define a suitable change of coordinates such that the state matrix of the closed-loop multi-agent system (3.13) is block diagonal, and each diagonal block is parameterized by the eigenvalues of the Laplacian matrix L.

3.3 The Synchronization Set

In this Section we introduce the synchronization set $\mathcal{S}_e$ for the multi-agent system (3.1) and (3.8), that is, the set of the extended space $\mathbb{R}^{2Nn}$ in which the agent states in (3.1) and the controller states in (3.8) coincide. This set is mathematically defined as follows

$$\mathcal{S}_e := \left\{ x \in \mathbb{R}^{2Nn} : \begin{bmatrix} x_{pi} \\ x_{ci} \end{bmatrix} - \begin{bmatrix} x_{pj} \\ x_{cj} \end{bmatrix} = 0,\ i, j \in \mathcal{N} \right\}, \tag{3.15}$$

where we denote with $x \in \mathbb{R}^{2Nn}$ the column vector obtained stacking the extended state vectors x_i in (3.9). Denote with $\mathcal{S}_e^\perp$ the orthogonal complement of $\mathcal{S}_e$.

Observe that, with respect to the synchronization set $\mathcal{S}$ in (2.9), the set $\mathcal{S}_e$ includes also the state of the controllers (3.8). Note that, item (i) of Problem 3.1 amounts to the stabilization of the synchronization set $\mathcal{S}_e$, with respect to the unperturbed closed-loop dynamics (3.1) and (3.8) with $w_i = \mathbf{0}_q$, for all $i \in \mathcal{N}$.

As for the synchronization set $\mathcal{S}$ in Chapter 2, we define the same distance-to-the-set $\mathcal{S}_e$ function as in (2.10). Moreover, Lemmas 2.1 and 2.2 hold while considering the set $\mathcal{S}_e$, once we replace the state space $\mathbb{R}^{Nn}$ with the extended state space $\mathbb{R}^{2Nn}$.

In the next section, we will see that the projection of the aggregate dynamics (3.13) onto $\mathcal{S}_e$ and its orthogonal complement $\mathcal{S}_e^\perp$ allows us to deduce conditions for robust state synchronization for the multi-agent system (3.1) and (3.8).

3.4 Sufficient Conditions for State Synchronization

In this section we want to provide conditions to solve Problem 3.1 in terms of matrix inequalities, involving the projection of the aggregate vectors (3.11) onto $\mathcal{S}_e^\perp$.

First, we suppose that the controller matrices A_k, B_k, C_k in (3.8) are given, and we look at a suitable Lyapunov function to perform the $\mathcal{L}_2$ synchronization stability analysis. The problem of designing a suitable controller in the form (3.8) to solve Problem 3.1 is then addressed in Section 3.6.

To perform the robust state synchronization analysis, we follow the same steps as in Chapter 2: we introduce a suitable coordinates transformation that projects the closed-loop dynamics (3.13) onto the synchronization set $\mathcal{S}_e$ and its orthogonal complement $\mathcal{S}_e^\perp$. Moreover, we translate the $\mathcal{L}_2$ gain condition (3.6) in the new coordinates.

3.4.1 Decoupling Change of Coordinates

Let us introduce a suitable change of coordinates for the closed-loop system (3.13) (see, for example, [35]). This coordinate transformation is induced by a specific unitary matrix U, related to the Laplacian matrix L. In our setting, the information topology of the considered multi-agent system is encoded by an undirected and connected graph $\mathcal{G}$. As shown in Appendix A, zero is a simple eigenvalue of L if and only if $\mathcal{G}$ is connected. Under these assumptions we can state the following lemma, which is a well-established result in the consensus and synchronization literature (see, e.g., [57] for more details).

Lemma 3.1. *Let $L = L^\top \in \mathbb{R}^{N\times N}$ be the symmetric Laplacian matrix of an undirected and connected graph $\mathcal{G}$. Let $0 = \lambda_1 < \lambda_2 \leq \cdots \leq \lambda_N$ denote the ordered eigenvalues of L. The set of eigenvectors $\nu_1, \nu_2, \ldots, \nu_N$ corresponding to $\lambda_1, \lambda_2, \ldots, \lambda_N$ forms an orthonormal basis of $\mathbb{R}^N$, and $\nu_1 := \frac{\mathbf{1}_N}{\sqrt{N}}$.*

Define the unitary matrix $U := \begin{bmatrix}\nu_1 & U_2\end{bmatrix}$, where $U_2 := \begin{bmatrix}\nu_2 & \ldots & \nu_N\end{bmatrix} \in \mathbb{R}^{N\times(N-1)}$, such that $U^\top U = UU^\top = I_N$. Then, based on Lemma 3.1, we can decompose the Laplacian matrix L as follows

$$\Delta := \begin{bmatrix} 0 & * \\ \mathbf{0}_{N-1} & \Delta_1 \end{bmatrix} = U^\top L U, \tag{3.16}$$

where $\Delta_1 := \operatorname{diag}(\lambda_2, \ldots, \lambda_N) \in \mathbb{R}^{(N-1)\times(N-1)}$ is positive definite.

We are ready to introduce the following coordinate transformation

$$\hat{x} := (U^\top \otimes I_{2n})x, \quad \hat{w} := (U^\top \otimes I_q)w, \quad \hat{z} := (U^\top \otimes I_\ell)\tilde{z}. \tag{3.17}$$

Consider now the following partition of vectors (3.17)

$$\begin{aligned}
\hat{x} &= \begin{bmatrix}(\nu_1^\top \otimes I_{2n})x \\ (U_2^\top \otimes I_{2n})x\end{bmatrix} := \begin{bmatrix}\hat{x}_1 \\ \hat{x}_2\end{bmatrix} \in \mathbb{R}^{2n} \times \mathbb{R}^{2(N-1)n}, \\
\hat{w} &= \begin{bmatrix}(\nu_1^\top \otimes I_q)w \\ (U_2^\top \otimes I_q)w\end{bmatrix} := \begin{bmatrix}\hat{w}_1 \\ \hat{w}_2\end{bmatrix} \in \mathbb{R}^{q} \times \mathbb{R}^{(N-1)q}, \\
\hat{z} &= \begin{bmatrix}(\nu_1^\top \otimes I_\ell)\tilde{z} \\ (U_2^\top \otimes I_\ell)\tilde{z}\end{bmatrix} := \begin{bmatrix}\hat{z}_1 \\ \hat{z}_2\end{bmatrix} \in \mathbb{R}^{\ell} \times \mathbb{R}^{(N-1)\ell},
\end{aligned} \tag{3.18}$$

where $\hat{x}, \hat{w}, \hat{z}$ have the same partition as U in (3.16). Applying the transformation (3.17) to (3.13), we obtain the following dynamics of the closed-loop system

$$\begin{aligned}
\dot{\hat{x}} &= \hat{A}\hat{x} + \hat{B}_w\hat{w} \\
\hat{z} &= \hat{C}_z\hat{x} + \hat{D}_z\hat{w},
\end{aligned} \tag{3.19}$$

where the structure of $\hat{A}$, $\hat{B}_w$, $\hat{C}_z$, $\hat{D}_z$ is as follows:

$$\left(\begin{array}{c|c} \hat{A} & \hat{B}_w \\ \hline \hat{C}_z & \hat{D}_z \end{array}\right) = \left(\begin{array}{c|c} I_N \otimes \begin{bmatrix} A_p & 0 \\ B_k C_p & A_k \end{bmatrix} + \Delta \otimes \begin{bmatrix} 0 & B_{pu}C_k \\ 0 & 0 \end{bmatrix} & I_N \otimes \begin{bmatrix} B_w \\ B_k D_{pw} \end{bmatrix} \\ \hline \Delta \otimes \begin{bmatrix} C_{zp} & 0 \end{bmatrix} & \Delta \otimes D_{zw} \end{array}\right), \tag{3.20}$$

where we have used the orthonormality of U and relation (3.16) for the derivations, together with the associative properties of the Kronecker product. In the new coordinates system, the matrices (3.20) have a block diagonal structure. Based on this observation, using the partitioned vectors in (3.18), we can decouple the closed-loop dynamics (3.19) is equivalent to the following subsystems

$$\begin{aligned} \dot{\hat{x}}_1 &= \begin{bmatrix} A_p & 0 \\ B_k C_p & A_k \end{bmatrix} \hat{x}_1 + \begin{bmatrix} B_w \\ B_k D_{pw} \end{bmatrix} \hat{w}_1 \\ \hat{z}_1 &= \mathbf{0}_\ell, \end{aligned} \tag{3.21}$$

and

$$\begin{aligned} \dot{\hat{x}}_2 &= \left(I_{N-1} \otimes \begin{bmatrix} A_p & 0 \\ B_k C_p & A_k \end{bmatrix} + \Delta_1 \otimes \begin{bmatrix} 0 & B_{pu} C_k \\ 0 & 0 \end{bmatrix} \right) \hat{x}_2 + \left(I_{N-1} \otimes \begin{bmatrix} B_w \\ B_k D_{pw} \end{bmatrix} \right) \hat{w}_2 \\ \hat{z}_i &= \left(\Delta_1 \otimes \begin{bmatrix} C_{zp} & 0 \end{bmatrix} \right) \hat{x}_2 + \left(\Delta_1 \otimes D_{zw} \right) \hat{w}_2, \end{aligned} \tag{3.22}$$

Note that, from the structure of matrix U in (3.16), the first component of $\hat{x}$ in (3.17) is

$$\hat{x}_1 = (\nu_1^\top \otimes I_{2n}) x = \tfrac{1}{\sqrt{N}} \textstyle\sum_{i=1}^N \begin{bmatrix} x_{pi} \\ x_{ci} \end{bmatrix}. \tag{3.23}$$

From Lemma 2.2, we see that vector $\frac{\hat{x}_1}{\sqrt{N}}$ is the orthogonal projection of the aggregate state vector $x \in \mathbb{R}^{2Nn}$ in (3.12) onto the synchronization set $\mathcal{S}_e$ in (3.15), and (3.21) is the projection of the closed-loop dynamics (3.13) onto $\mathcal{S}_e^\perp$. We note that, when the Laplacian matrix L is symmetric, the vector ν_1 exhaustively describes the projected dynamics of (3.13) onto $\mathcal{S}_e$, for every time instant. Instead, when considering directed networks, this property does not hold for any finite time (compare (3.21) with (2.20)), but only asymptotically, and only if the projected closed-loop dynamics onto $\mathcal{S}_e^\perp$ is asymptotically stable (see equation (2.23)).

The $N-1$ subsystems in (3.22) correspond to the projection of the closed-loop dynamics (3.13) onto $\mathcal{S}_e^\perp$, that is, the subspace generated by $\nu_2 \otimes I_{2n}, \ldots, \nu_N \otimes I_{2n}$, where $\nu_2, \ldots, \nu_N$ are the eigenvectors of L corresponding to $\lambda_2, \ldots, \lambda_N$. The $N-1$ decoupled systems (3.22) are obtained from (3.1) and (3.8), replacing (3.8c) with the input $\tilde{u}_i = \lambda_i u_i$, for $i = 2, \ldots, N$.

We want to write the $\mathcal{L}_2$ bound as a (3.6) in function of the transformed variables (3.17). The $\mathcal{L}_2$ gain condition (3.6) can be written in the aggregate vectors $\tilde{z}$ and $\tilde{w}$ in (3.12) as follows

$$\|\tilde{z}\|_2^2 = \textstyle\sum_{i=1}^N \|\tilde{z}_i\|_2^2 \leq \gamma^2 \sum_{i=1}^N \|\tilde{w}_i\|_2^2 = \gamma^2 \|\tilde{w}\|_2^2, \tag{3.24}$$

Consider the variable $\hat{z}$ in (3.17). Since from (3.12) and the properties of the Laplacian L, we have that the first component $\hat{z}_1$ of $\hat{z}$ satisfies

$$\hat{z}_1 = (\nu_1^\top \otimes I_\ell) \tilde{z} = (\nu_1^\top L \otimes I_\ell) z = \mathbf{0}_\ell. \tag{3.25}$$

We conclude that the $\mathcal{L}_2$ norm of $\hat{z}$ satisfies

$$\|\hat{z}\|_2^2 = \|\hat{z}_2\|_2^2 \tag{3.26}$$

On the other hand, from the orthonormality of U in (3.16) and definition (3.12), we have

$$\|\tilde{z}\|_2^2 = \left\|(U^\top \otimes I_\ell)\tilde{z}\right\|_2^2 = \|\hat{z}\|_2^2 = \|\hat{z}_1\|_2^2 + \|\hat{z}_2\|_2^2 = \|\hat{z}_2\|_2^2\,, \tag{3.27}$$

Consider now the disturbance variable $\hat{w}$ in (3.17) and $\tilde{w}$ in (3.12). Using (3.16), we have

$$(U^\top \otimes I_q)\tilde{w} = (U^\top L U \otimes I_q)\hat{w} = (\Delta \otimes I_q)\hat{w}. \tag{3.28}$$

We obtain the following bound on the $\mathcal{L}_2$ norm of the variables of subsystem (3.22)

$$\begin{aligned}\|\hat{w}_2\|_2^2 &= \left\|(\Delta_1^{-1}\Delta_1 \otimes I_q)\hat{w}_2\right\|_2^2 \leq \lambda_2^{-2}\,\|(\Delta_1 \otimes I_q)\hat{w}_2\|_2^2 \\ &= \lambda_2^{-2}\,\|(\Delta \otimes I_q)\hat{w}\|_2^2 = \lambda_2^{-2}\,\|\tilde{w}\|_2^2\,,\end{aligned} \tag{3.29}$$

where we used relation (3.28), and the fact that the positive entries of Δ are smaller than λ_2^{-1}—that is, the inverse of the smallest eigenvalue of the Laplacian matrix L. We conclude that the $\mathcal{L}_2$ gain property

$$\|\hat{z}_2\|_2^2 \leq \hat{\gamma}^2\,\|\hat{w}_2\|_2^2\,, \tag{3.30}$$

where $\hat{\gamma}^2 = \lambda_2^2\gamma^2$, ensures that the desired $\mathcal{L}_2$ gain property (3.6) is satisfied. In fact, combining (3.26), (3.27), (3.29) and (3.24), we obtain

$$\|\tilde{z}\|_2^2 = \|\hat{z}_2\|_2^2 \leq \hat{\gamma}^2\,\|\hat{w}_2\|_2^2 \leq \gamma^2\lambda_2^2\,\|\hat{w}_2\|_2^2 \leq \gamma^2\,\|\tilde{w}\|_2^2\,. \tag{3.31}$$

Note that, inequality (3.31) only involves the variables of subsystem (3.22), that is, the projections of the aggregate variables (3.11) onto $\mathcal{S}_e^\perp$.

3.4.2 State Synchronization Analysis

In this section we characterize a way to solve Problem 3.1 in terms of matrix inequalities. These conditions are obtained by using the decoupling change of coordinates (3.17), the $\mathcal{L}_2$ gain condition (3.30) for synchronization stability in the new coordinates, the Lyapunov synchronization stability result contained in Theorem 2.1 of Chapter 2. We point out that the presented conditions for state synchronization analysis are only sufficient, due to the conservatism introduced in the $\mathcal{L}_2$ bounds (3.26) and (3.29).

The result provided in the theorem below is an extension to the multi-agent framework of the well-known results on $\mathcal{L}_2$ gain stability, and H_∞ control for isolated LTI systems (see, for example, [84]).

Theorem 3.1. *Given a desired bound $\gamma > 0$, if there exist matrices $A_k \in \mathbb{R}^{n\times n}$, $B_k \in \mathbb{R}^{n\times p}$, $C_k \in \mathbb{R}^{m\times n}$, $N-1$ positive definite matrices $P_i = P_i^\top \in \mathbb{R}^{2n\times 2n}$, $i = 2,\ldots,N$ such that the following matrix inequalities*

$$\begin{bmatrix} \mathrm{He}\left(P_i \begin{bmatrix} A_p & \lambda_i B_{pu} C_k \\ B_k C_p & A_k \end{bmatrix}\right) & P_i \begin{bmatrix} B_{pw} \\ B_k D_{pw} \end{bmatrix} & \begin{bmatrix} \lambda_i C_{zp}^\top \\ 0 \end{bmatrix} \\ * & -I_q & \lambda_i D_{zw}^\top \\ * & * & -\hat{\gamma}^2 I_\ell \end{bmatrix} < 0, \tag{3.32}$$

for $i = 2,\ldots,N$ are satisfied, where $\hat{\gamma}^2 = \lambda_2^2\gamma^2$, then the controller (3.8) with $x_{ci}(0) = \mathbf{0}_n$, for $i \in \mathcal{N}$, solves Problem 3.1.

Proof. To prove Theorem 3.1, we invoke Theorem 2.1 of Chapter 2, once we observe that the Laplacian L and the graph $\mathcal{G}$ satisfy the hypothesis of this Theorem. First, we consider the case $w_i = \mathbf{0}_q$ for $i \in \mathcal{N}$. From (3.32) we have, in particular, that the first $2n \times 2n$ block of the $N-1$ inequalities (3.32) is negative definite, that is

$$\mathrm{He}\left(P_i \begin{bmatrix} A_p & \lambda_i B_{pu} C_k \\ B_k C_p & A_k \end{bmatrix}\right) < 0, \quad i = 2,\ldots,N. \tag{3.33}$$

Since P_i are positive definite matrices, (3.33) is equivalent to matrices

$$\begin{bmatrix} A_p & \lambda_i B_{pu} C_k \\ B_k C_p & A_k \end{bmatrix}$$

being Hurwitz, for $i = 2,\ldots,N$. From the equivalence between items (i) and (ii) of Theorem 2.1, we conclude that there exists a Lyapunov function $V(x)$ for dynamics (3.22), such that

$$\begin{aligned} \alpha_1 |x|_{\mathcal{S}_e}^2 \leq V(x) \leq \alpha_2 |x|_{\mathcal{S}_e}^2 \\ \dot{V}(x) \leq -\beta |x|_{\mathcal{S}_e}^2 , \end{aligned} \tag{3.34}$$

for some positive scalars α_1, α_2, and β. Furthermore, Theorem 2.1 gives the expression of the Lyapunov function in (2.32), for the continuous-time case. Since for symmetric Laplacian matrices, the off-diagonal blocks in (2.19) are all equal to zero, thus implying that matrices M_k in (2.31) are equal to zero, for $k = 1,\ldots,N-1$, we deduce from (2.35) that $\rho_k^C = 1$ for all $k = 2,\ldots,N$. Moreover, since L is symmetric, its Frobenius normal form (2.16) is diagonal, and reduces to (3.16). According to these observations, the Lyapunov function (2.32) when L is symmetric and $\mathcal{G}$ is connected (and undirected), reduces to

$$V(x) = x^\top (U \otimes I_{2n}) \bar{P} (U^\top \otimes I_{2n}) x = \hat{x}_2^\top \mathrm{diag}(P_i) \hat{x}_2, \tag{3.35}$$

where $\bar{P} := \mathrm{diag}(0, P_i)$, for $i = 2,\ldots,N$, and $U \in \mathbb{R}^{N\times N}$ is the unitary matrix in (3.16). The uniform global exponential stability of the consensus set $\mathcal{S}_e$ in (3.15) with respect to the unperturbed dynamics (3.1) and (3.8) (or, equivalently (3.13)) with $w_i = \mathbf{0}_q$ for all $i \in \mathcal{N}$, follows from the equivalence between (i) and (iii) of Theorem 2.1. This implies,

in particular, the convergence of the state of the agents (3.1) to a common trajectory, that is, (3.7) is satisfied.

Consider now the case where there exists an index i, such that $w_i \neq \mathbf{0}_q$. Denote with $\hat{x}_2^{(i)}, \hat{z}_2^{(i)}, \hat{w}_2^{(i)} \in \mathbb{R}^n$, for $i = 1, \ldots, N-1$, the vector components of $\hat{x}_2$, $\hat{z}_2$, $\hat{w}_2$ in (3.18). By applying the Schur complement to (3.32) and pre- and post-multiplying by $[\hat{x}_2^{(i)\top} \ \hat{w}_2^{(i)\top}]^\top$ and its transpose, we obtain

$$\begin{aligned}\hat{x}_2^{(i)\top} \mathrm{He}\left(P_i \begin{bmatrix} A_p & \lambda_i B_{pu} C_k \\ B_k C_p & A_k \end{bmatrix}\right) + \hat{x}_2^{(i)} \\ - \hat{w}_2^{(i)\top} \hat{w}_2^{(i)} + 2\hat{x}_2^{(i)\top} P_i \begin{bmatrix} B_{pw} \\ B_k D_{pw} \end{bmatrix} \hat{w}_2^{(i)} + \tfrac{1}{\hat{\gamma}^2} \hat{z}_2^{(i)\top} \hat{z}_2^{(i)} < 0, \ i = 2, \ldots, N. \end{aligned} \tag{3.36}$$

Stacking the $N-1$ inequalities in (3.36), from (3.22) we obtain

$$\tfrac{d}{dt}\left(\hat{x}_2^\top \mathrm{diag}(P_i) \hat{x}_2\right) + \tfrac{1}{\hat{\gamma}^2} \hat{z}_2^\top \hat{z}_2 - \hat{w}_2^\top \hat{w}_2 < 0, \tag{3.37}$$

By integration of (3.37) over the interval $[0, T]$, with $T > 0$, and from (3.35), we obtain

$$V(x(T)) - V(x(0)) + \tfrac{1}{\hat{\gamma}^2} \int_0^T \hat{z}_2^\top \hat{z}_2 - \int_0^T \hat{w}_2^\top \hat{w}_2 < 0. \tag{3.38}$$

Since from the first equation in (3.34), $V(x(T)) \geq 0$ for all $T > 0$, and the hypothesis $x_i(0) = \begin{bmatrix} x_{pi}(0) \\ x_{ci}(0) \end{bmatrix} = \mathbf{0}_{2n}$ for all $i = 1, \ldots, N$, implies $V(x(0)) = 0$, taking the limit of (3.38) for $T \to \infty$ we obtain

$$\|\hat{z}_2\|_2^2 \leq \hat{\gamma}^2 \, \|\hat{w}_2\|_2^2 \,. \tag{3.39}$$

Hence, by using (3.24), (3.30) and (3.31), it follows that the $\mathcal{L}_2$ gain property (3.6) is satisfied, and then item (ii) of Problem 3.1 is solved. This completes the proof. □

We are now interested in characterizing the synchronization trajectory $\bar{x}_p$ in (3.7). This is possible only when the dynamics in (3.1) and (3.8) is not perturbed. To this end we state the following result, that is obtained particularizing Theorem 3.1 when $w_i = \mathbf{0}_q$, $i \in \mathcal{N}$.

Corollary 3.1. (Characterization of the Synchronization Trajectory) *If $w_i = \mathbf{0}_q$ for all $i \in \mathcal{N}$, and there exist matrices $A_k \in \mathbb{R}^{n \times n}$, $B_k \in \mathbb{R}^{n \times p}$, $C_k \in \mathbb{R}^{m \times n}$, $N-1$ positive definite matrices $P_i = P_i^\top \in \mathbb{R}^{2n \times 2n}$ such that*

$$\mathrm{He}\left(P_i \begin{bmatrix} A_p & \lambda_i B_{pu} C_k \\ B_k C_p & A_k \end{bmatrix}\right) < 0, \quad i = 2, \ldots, N, \tag{3.40}$$

then, for any initial condition $x_i(0) = \begin{bmatrix} x_{pi}(0)^\top & x_{ci}(0)^\top \end{bmatrix}^\top \in \mathbb{R}^{2n}$, the trajectories of the closed-loop system (3.1), (3.8) *asymptotically synchronize to the solution to the following initial values problem:*

$$\dot{\bar{x}} = \begin{bmatrix} A_p & 0 \\ B_k C_p & A_k \end{bmatrix} \bar{x}, \tag{3.41}$$

where $\bar{x} = \begin{bmatrix} \bar{x}_p \\ \bar{x}_c \end{bmatrix}$, *and* $\bar{x}(0) = \frac{1}{N}\sum_{i=1}^{N} \begin{bmatrix} x_{pi}(0) \\ x_{ci}(0) \end{bmatrix}$.

Proof. Consider the dynamics of the state $\bar{x}(t) = \frac{1}{N}\sum_{i=1}^{N} x_i(t) = \frac{1}{N}(\mathbf{1}_N^\top \otimes I_{2n})x(t)$. Based on (3.13), (3.14), the time evolution of $\bar{x}$ is

$$\begin{aligned}
\dot{\bar{x}} &= \tfrac{1}{N}(\mathbf{1}_N^\top \otimes I_{2n}) \left[\left(I_N \otimes \begin{bmatrix} A_p & 0 \\ B_k C_p & A_k \end{bmatrix} \right) + \left(L \otimes \begin{bmatrix} 0 & B_{pu} C_k \\ 0 & 0 \end{bmatrix} \right) \right] x \\
&= \tfrac{1}{N} \left(\mathbf{1}_N^\top I_N \otimes \begin{bmatrix} A_p & 0 \\ B_k C_p & A_k \end{bmatrix} \right) x = \tfrac{1}{N} \left(\mathbf{1}_N^\top \otimes \begin{bmatrix} A_p & 0 \\ B_k C_p & A_k \end{bmatrix} \right) x \\
&= \begin{bmatrix} A_p & 0 \\ B_k C_p & A_k \end{bmatrix} \tfrac{1}{N}(\mathbf{1}_N^\top \otimes I_{2n}) x = \begin{bmatrix} A_p & 0 \\ B_k C_p & A_k \end{bmatrix} \bar{x}, \qquad (3.42)
\end{aligned}$$

where we used the relation $\mathbf{1}_N^\top L = 0$, and $\bar{x}(0) = \frac{1}{N}(\mathbf{1}_N^\top \otimes I_{2n})x(0) = \frac{1}{N}\sum_{i=1}^{N} x_i(0)$. From item (iv) of Theorem 2.1, the agents' state exponentially synchronize to the same trajectory, described by (3.42), once we notice that $p = \mathbf{1}_N$ for symmetric Laplacian matrices. □

Note that, taking the first component of the vector $\bar{x}$ of (3.41), we obtain

$$\dot{\bar{x}}_p = A_p \bar{x}_p, \quad \bar{x}_p(0) = \tfrac{1}{N}\sum_{i=1}^{N} x_{pi}(0). \qquad (3.43)$$

Moreover, from Corollary 3.1, we deduce that also the controller states x_{ci} in (2.3) converge to a common trajectory $\bar{x}_c$, that is the solution to

$$\dot{\bar{x}}_c = B_k C_p \bar{x}_p + A_k \bar{x}_c, \quad \bar{x}_c(0) = \tfrac{1}{N}\sum_{i=1}^{N} x_{ci}(0). \qquad (3.44)$$

If the controller matrices A_k, B_k, C_k are given, the conditions (3.32) and (3.40) are convex in the Lyapunov matrices P_i, $i = 2, \ldots, N$. However, if we consider the controller matrices as variables of the problem, (3.32) and (3.40) become nonlinear matrix inequalities, and then these conditions cannot straightforwardly be used for the controller design. Nevertheless, using some relaxation techniques, (3.32) and (3.40) can be converted to BMI feasibility problems in the controller matrices and the Lyapunov matrices. Feasibility problems involving BMIs can be solved using iterative approaches, in the same way as we did for the controller design in Chapter 2.

3.5 H_∞ State Synchronization Design

In this Section we use some relaxation techniques in order to convert (3.32) and (3.40) into BMI feasibility problems. In fact, conditions (3.32) and (3.40) are hardly tractable from a numerical standpoint, because the controller parameters A_k, B_k, C_k are coupled with the Lyapunov matrices P_i for $i = 2, \ldots, N$ and this leads to a possible NP-hard problem without desirable design guarantees. More precisely, the nonlinear term $P_i \left[\begin{smallmatrix} \lambda_i B_{pu} & 0 \\ 0 & I_n \end{smallmatrix}\right] \left[\begin{smallmatrix} 0 & C_k \\ B_k & A_k \end{smallmatrix}\right] \left[\begin{smallmatrix} C_p & 0 \\ 0 & I_n \end{smallmatrix}\right]$ in the first diagonal block of (3.32) has been

a long-standing obstacle to the derivation of suitable conditions for the dynamic output-feedback design (see [18]). Thus, in general, the direct design of the controller matrices solving (3.32) and (3.40) is unlikely doable. Note that we have already encountered this problem for the distributed static output feedback control design in Section 2.4. As we pointed out in Chapter 2, the output feedback design problem is a cumbersome one. Nevertheless, we are able to provide a dynamic H_∞ design technique, that is effective in practice in satisfying the requirements of Problem 3.1.

Based on a suitable congruence transformation of the controller variables (see, e.g., [63] and [36]), and relaxation techniques, we give sufficient conditions for (3.32) and (3.40). These new conditions are bilinear in the unknown variables. Although those conditions are not convex, they are more tractable from a numerical point of view, and they provide a first step towards a design algorithm for the proposed controller, which is presented in Section 3.6. The relaxed robust synchronization conditions are contained in the following theorem.

Theorem 3.2. *Given a desired performance bound $\gamma > 0$, if there exist symmetric positive definite matrices $Y, W \in \mathbb{R}^{n\times n}$, matrices $\hat{A} \in \mathbb{R}^{n\times n}$, $\hat{B} \in \mathbb{R}^{n\times p}$, $\hat{C} \in \mathbb{R}^{m\times n}$, a positive definite matrix $M \in \mathbb{R}^{2n\times 2n}$, a matrix $H \in \mathbb{R}^{2n\times 2n}$ and a scalar λ_c such that*

$$\begin{bmatrix} \Gamma & H & \hat{W}M & \begin{bmatrix} B_{pw} \\ WB_{pw} - \hat{B}D_{pw} \end{bmatrix} & \lambda_i \begin{bmatrix} Y \\ I_n \end{bmatrix} C_{zp}^\top \\ * & \delta_i\Sigma - M & 0 & 0 & 0 \\ * & * & -M & 0 & 0 \\ * & * & * & -I_q & \lambda_i D_{zw}^\top \\ * & * & * & * & -\hat{\gamma}^2 I_\ell \end{bmatrix} < 0, \quad i = 2, N \tag{3.45}$$

where we have defined:

$$\Gamma := \mathrm{He}\left(\begin{bmatrix} A_pY + \lambda_i B_{pu}\hat{C} & 0 \\ \hat{A} & WA_p - \hat{B}C_p \end{bmatrix} + \hat{W}H \right), \tag{3.46}$$

$$\hat{W} := \begin{bmatrix} I_n & 0 \\ 0 & W \end{bmatrix}, \quad \Sigma := \mathrm{He}\left(\begin{bmatrix} 0 & 0 \\ B_{pu}\hat{C} & 0 \end{bmatrix} \right), \quad \delta_i := \lambda_c - \lambda_i, \quad \hat{\gamma}^2 := \lambda_2^2\gamma^2, \tag{3.47}$$

then the controller (3.8) *with $x_{ci}(0) = \mathbf{0}_n$ and*

$$\begin{aligned} C_k &: = \hat{C}Z^{-1} \\ B_k &: = W^{-1}\hat{B} \\ A_k &: = -\hat{A}YZ^{-1} - B_kC_pYZ^{-1} + \lambda_c B_{pu}C_k + W^{-1}A_p^\top Z^{-1}, \end{aligned} \tag{3.48}$$

where $Z := Y - W^{-1}$, solves Problem 3.1.

Proof. We want to prove that (3.45) implies (3.32). Suppose that a solution to (3.45) exists with variables Y, W, $\hat{A}$, $\hat{B}$ $\hat{C}$, M, H, λ_c. Applying the Schur complement to (3.45), we obtain

$$\begin{bmatrix} \Gamma_1 & \begin{bmatrix} B_{pw} \\ WB_{pw} - \hat{B}D_{pw} \end{bmatrix} & \lambda_i \begin{bmatrix} Y \\ I_n \end{bmatrix} C_{zp}^\top \\ * & -I_q & \lambda_i D_{zw}^\top \\ * & * & -\hat{\gamma}^2 I_\ell \end{bmatrix} < 0 \tag{3.49}$$

with

$$\Gamma_1 = \mathrm{He}\left(\begin{bmatrix} A_pY + \lambda_i B_{pu}\hat{C} & 0 \\ \hat{A} & WA_p - \hat{B}C_p \end{bmatrix} + \hat{W}H\right) + \hat{W}M\hat{W} + H^\top (M - \delta_i\Sigma)^{-1}H. \tag{3.50}$$

Since from (3.45) we have that $M - \delta_i\Sigma > 0$ and $M > 0$, Γ_1 satisfies

$$\Gamma_1 \geq \Gamma_2 := \mathrm{He}\left(\begin{bmatrix} A_pY + \lambda_i B_{pu}\hat{C} & 0 \\ \hat{A} & WA_p - \hat{B}C_p \end{bmatrix}\right) + \delta_i \hat{W}^\top \Sigma \hat{W}, \tag{3.51}$$

and from (3.49) and (3.51) we obtain

$$\begin{bmatrix} \Gamma_2 & \begin{bmatrix} B_{pw} \\ WB_{pw} - \hat{B}D_{pw} \end{bmatrix} & \lambda_i \begin{bmatrix} Y \\ I_n \end{bmatrix} C_{zp}^\top \\ * & -I_q & \lambda_i D_{zw}^\top \\ * & * & -\hat{\gamma}^2 I_\ell \end{bmatrix} < 0. \tag{3.52}$$

By substituting the expressions of (3.48) into (3.52) and by defining the matrix

$$P = P^\top = \begin{bmatrix} Y & Z \\ Z & Z \end{bmatrix}^{-1} = \begin{bmatrix} W & -W \\ -W & W + Z^{-1} \end{bmatrix}, \tag{3.53}$$

where $Z = Z^\top > 0$ $W = (Y - Z)^{-1}$, and $\Pi := \left[\begin{smallmatrix} Y & Z \\ I_n & 0 \end{smallmatrix}\right]$, and noticing that $\Pi P = \left[\begin{smallmatrix} I_n & 0 \\ W & -W \end{smallmatrix}\right]$, we obtain that (3.52) is equivalent to

$$\begin{bmatrix} \mathrm{He}\left(\Pi P \begin{bmatrix} A_p & \lambda_i B_{pu} C_k \\ B_k C_p & A_k \end{bmatrix} \Pi^\top\right) & \Pi P \begin{bmatrix} B_{pw} \\ B_k D_{pw} \end{bmatrix} & \Pi \begin{bmatrix} \lambda_i C_{zp}^\top \\ 0 \end{bmatrix} \\ * & -I_q & \lambda_i D_{zw}^\top \\ * & * & -\hat{\gamma}^2 I_\ell \end{bmatrix} < 0. \tag{3.54}$$

Finally, by pre- and post- multiplying (3.54) by $\mathrm{diag}(\Pi^{-1}, I_q, I_\ell)$ and its transpose, we obtain (3.32) with $P_i = P$ for $i = 2, N$. To prove (3.32) for $i = 3, \ldots, N-1$ it is sufficient to perform convex combinations of (3.54). □

Remark 3.2. In the matrix inequalities formulation (3.45) we specify P_i as a common Lyapunov matrix, i.e., $P_i = P$ for $i = 2, \ldots, N$, when the controller is parameterized as in (3.48). This choice is conservative with respect to the matrix inequality formulation in (3.32). However, this choice allows restricting these inequalities to the cases $i = 2, N$—namely, the smallest and larger positive eigenvalues of L.

Remark 3.3. There is no loss of generality by parameterizing P as (3.53), because this particular structure does not lead any conservatism (see [115, Lemma 1]).

Remark 3.4. In the nonlinear matrix inequalities formulation (3.32), the Lyapunov function matrices P_i involved in (3.35), are coupled with the controller matrices A_k, B_k, C_k in (3.32). On the other hand, in the relaxed formulation (3.45), the transformed controller matrices $\hat{A}$, $\hat{B}$, $\hat{C}$, obtained from (3.48), are decoupled from the Lyapunov matrices Y and W. This decoupling technique arises from the completion of squares (3.50), in which the slack variables H and M are introduced, providing an extra degree of freedom and relaxing the structure of the constraints (3.32). This makes the constraints (3.45) more tractable than (3.32) from a numerical standpoint, and they allow to design the iterative solving algorithm presented in Section 3.6.

The following result provides a relaxation of conditions (3.40) for the noiseless case $w_i = \mathbf{0}_q$, for all $i \in \mathcal{N}$.

Corollary 3.2. *If $w_i = \mathbf{0}_q$ for all $i \in \mathcal{N}$, and there exist positive definite matrices $Y, W \in \mathbb{R}^{n\times n}$, matrices $\hat{A} \in \mathbb{R}^{n\times n}$, $\hat{B} \in \mathbb{R}^{n\times p}$, $\hat{C} \in \mathbb{R}^{m\times n}$, a positive definite matrix $M \in \mathbb{R}^{2n\times 2n}$, a matrix $H \in \mathbb{R}^{2n\times 2n}$ and a scalar λ_c such that*

$$\Upsilon_i := \begin{bmatrix} \mathrm{He}\left(\begin{bmatrix} A_pY + \lambda_i B_{pu}\hat{C} & 0 \\ \hat{A} & WA_p - \hat{B}C_p \end{bmatrix} + \hat{W}H\right) & H & \hat{W}M \\ * & \delta_i\Sigma - M & 0 \\ * & * & -M \end{bmatrix} < 0, \tag{3.55}$$

for $i = 2, N$, where $\hat{W}$, Σ, δ_i are defined in (3.47)*. Then, for any initial condition $x_i(0) = \begin{bmatrix} x_{pi}(0)^\top & x_{ci}(0)^\top \end{bmatrix}^\top \in \mathbb{R}^{2n}$, the resulting trajectories of the closed-loop system* (3.1)*,* (3.8) *asymptotically synchronize.*

Proof. Tracing the proof of Theorem 3.2 we prove that (3.55) is a sufficient condition for (3.40). □

3.6 ILMI Dynamic Output Feedback Design

In this section we address the problem of designing suitable matrices A_k, B_k, C_k of the distributed dynamic output feedback compensator (3.8) that solves Problem 3.1. As shown in the previous sections, the proposed robust output feedback design problem cannot be characterized by a convex formulation, but it inherently leads to a nonlinear formulation.

The controller synthesis is obtained based on feasible solutions of the relaxed BMI conditions (3.45). In fact, according to Theorem 3.2, any solution to (3.45) provides suitable controller matrices to solve Problem 3.1. Furthermore, we investigate through a numerical example the gap between the solution to the relaxed feasibility problem (3.45), and the original nonlinear one (3.32).

Of course, we would like to go one step further asking whether it is possible to optimize the distributed compensator (3.8) for better disturbance rejection, which amounts

to minimizing the performance bound γ in (3.6). Moreover, taking γ as an additional decision variable allows us to increase the number of feasible solutions to (3.45), making it easier to find the solution to Problem 3.1.

More precisely, the problem we want to solve in this section is the following optimization problem

$$\begin{aligned}(\gamma^\star)^2 := \quad & \min_{W,Y,\hat{A},\hat{B},\hat{C},H,M,\lambda_c,\gamma^2} \quad \gamma^2, \\ & \text{s.t.} \quad (3.45),\ W>0,\ Y>0,\ \gamma^2>0.\end{aligned} \tag{3.61}$$

If the solution to (3.61) gives a value $\gamma^\star$ less or equal to the bound prescribed in (3.6), then, the corresponding controller solves Problem 3.1. Note that the controller matrices A_k, B_k, C_k in (3.8) are obtained from the solution $\hat{A}$, $\hat{B}$, $\hat{C}$ to (3.61) by applying the change of coordinates (3.48).

It is well known that BMI problems, like the one we are considering, are NP-hard, and so far there is no polynomial algorithm to compute the optimal solutions [102]. Since in (3.45) there are product terms (also known as *complicating variables*) between the Lyapunov parameters and the slack variables (i.e., $\hat{W}H$ and $\hat{W}M$), and the controller matrices and the slack variables (i.e., $\lambda_c\hat{C}$), our approach to solve the non-convex optimization problem (3.61) is based on an ILMI procedure. The proposed algorithm, quite similar to the one presented in Section 2.4, alternates between two different LMI problems: (3.61) fixing the set of variables $\{\lambda_c, H, M\}$, and (3.61) fixing the set of variables $\{W, \hat{C}\}$. At each iteration the value of γ^2 is minimized, and a controller with increasing robustness is determined.

The procedure of alternating between the LMI problems is an iterative approach allowing to solve nonconvex problems, without a clear guarantee of convergence. Moreover, using the proposed relaxation technique, we can provide only sub-optimal solutions, and consequently a sub-optimal controller. However, this algorithm has been tested in several examples and it is effective in practice in determining a suitable controller for Problem 3.1.

As most local approaches, the proposed method requires an initially feasible solution from which the suboptimal process starts. In the next section we will provide a method for choosing the values of a set of variables to initialize the algorithm, and we give a detailed description of the algorithm.

Algorithm Initialization and Description

In this section we provide a preliminary procedure to compute initial values of the variables to initialize the design algorithm. Since the size of the optimization problem (3.61) is large, and the random choice of the initial variables might lead to infeasible solutions to (3.45), we introduce a preliminary initialization problem, that makes it more likely to find an initial feasible solution to (3.61). This preliminary procedure consists in finding solutions to the following optimization problem

$$t^\star := \min_{W,Y,\hat{A},\hat{B},\hat{C},H,M,\lambda_c,t} \quad t, \tag{3.62}$$

$$\text{s.t.} \quad \Upsilon_i - tI_{6n} < 0,\ i = 2, N,\ W > 0,\ Y > 0,$$

where Υ_i is defined in (3.55), and corresponds to the first $6n \times 6n$ diagonal block in (3.45). Intuitively speaking, we are finding a solution to Problem 3.1 in the noiseless case $w_i = \mathbf{0}_q$. Problem (3.62) is bilinear in the decision variables and can be solved with the ILMI procedure described above. Note that problem (3.62) performs the minimization of the variable t. In fact, for any choice of the parameters, $\Upsilon_i - tI < 0$, for $i = 2, N$, is always satisfied for t sufficiently large.

If a solution to (3.62) exists with $t^\star < 0$, then Υ_i, for $i = 2, \ldots, N$ are negative definite and the resulting controller guarantees synchronization of the controlled multi-agent system (3.1) and (3.8), according to Corollary 3.2. We will call such a controller a *synchronizing* controller. The detailed algorithm to solve (3.62) is described in Algorithm 3.2 (page 56).

This preliminary procedure is convenient because the synchronizing controller design requires the iterative solution to a set of BMIs of smaller size as compared to conditions (3.45). Moreover, the existence of a synchronizing controller is necessary for the existence of a sub-optimal controller. The algorithm for the sub-optimal controller design to solve (3.61) is presented in Algorithm 3.3 (page 57). The solution to (3.62) is taken as a starting point.

Remark 3.5. If no synchronizing controller is found in Algorithm 3.2, no sub-optimal controller can be found either, because Υ_i in (3.40) would not be negative definite for some i, and (3.45) is violated.

Example 3.1. We provide an illustrative example to show the effectiveness of the controller design presented in Section 3.6. Consider a multi-agent system composed by $N = 6$ agents, each of them described by (3.1), and the following data

$$\begin{gathered} A_p = \begin{bmatrix} 0.05 & 0.9 \\ -0.9 & 0.05 \end{bmatrix}, B_{pu} = \begin{bmatrix} 0 \\ 1 \end{bmatrix}, B_{pw} = \begin{bmatrix} 1 \\ 0 \end{bmatrix}, C_p = \begin{bmatrix} 0 & 1 \end{bmatrix}, \\ C_{zp} = \begin{bmatrix} 1 & 1 \end{bmatrix}, D_{pw} = D_{zw} = 0. \end{gathered} \tag{3.63}$$

The interconnection graph depicted in Figure 3.2, on page 52, represents the communications among the agents in the network. Algorithm 3.2 and Algorithm 3.3 are implemented in MATLAB and solved using the YALMIP toolbox [61], and the MOSEK solver [70].

Algorithm 3.2 is run with tolerance $\delta = 10^{-4}$, and gives $t^\star = -0.61$, see Figure 3.3 (left), on page 3.3. Algorithm 3.3 can therefore be initialized, and the minimization of γ^2 is shown in Figure 3.3 (right). The resulting sub-optimal controller matrices are:

$$A_k = \begin{bmatrix} -0.52 & 5.38 \\ 0.72 & -25.78 \end{bmatrix}, \quad B_k = \begin{bmatrix} -0.054 \\ 2.686 \end{bmatrix}, \quad C_k = \begin{bmatrix} 0.37 & -1.37 \end{bmatrix} \tag{3.64}$$

and $(\gamma^\star)^2 = 39.4$. We consider the following piecewise constant disturbance $w_i \in \mathcal{L}_2$, for all $i \in \mathcal{N}$

$$w_i = \begin{cases} w_{0i} & \text{if } 20s \leq t \leq 25s \\ 0 & \text{otherwise,} \end{cases} \qquad i \in \mathcal{N}, \tag{3.65}$$

with w_{0i} constant values randomly chosen in the interval $[-1, 1]$.

The time responses of the closed-loop multi-agent system (3.1) with data (3.63), and (3.8) with data (3.64), and $w_i = \mathbf{0}_q$ for all $i \in \mathcal{N}$, are depicted in Figure 3.4, on page 53. Each plot represents the time evolution of the components $x_{pi}^{(1)}$ and $x_{pi}^{(2)}$ of the states $x_{pi} \in \mathbb{R}^2$, for all the agents $i = 1, \ldots, 6$. Each agent is identified by a colour in the plots. We observe that the agents reach state synchronization, and from Corollary 3.1,

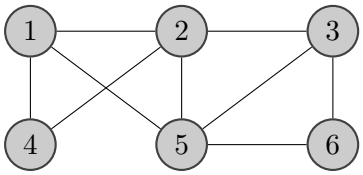

Figure 3.2: Network interconnections of the multi-agent system (3.1) with data (3.63) in Example 3.1.

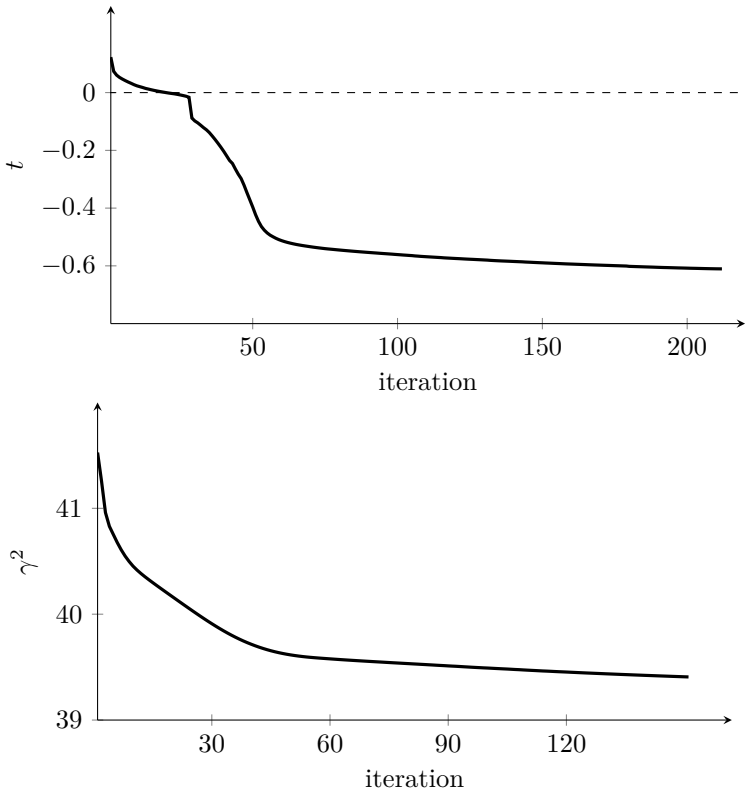

Figure 3.3: Minimization of the value of t (left) and γ (right) performed by Algorithm 3.2 and Algorithm 3.3, respectively. The minimum values of t and γ are $t^\star = -0.61$ and $(\gamma^\star)^2 = 39.4$, respectively.

we know that they synchronize to the solution to

$$\dot{\bar{x}}_p = A_p \bar{x}_p, \quad \bar{x}_p(0) = \tfrac{1}{N}\textstyle\sum_{i=1}^{3} x_i(0), \tag{3.66}$$

which is,

$$\bar{x}_p(t) = e^{0.05t}\left(k_1 \begin{bmatrix} \frac{1}{\sqrt{2}}\cos(0.9t) \\ \frac{1}{\sqrt{2}}\sin(0.9t) \end{bmatrix} + k_2 \begin{bmatrix} \frac{1}{\sqrt{2}}\sin(0.9t) \\ -\frac{1}{\sqrt{2}}\cos(0.9t) \end{bmatrix}\right), \tag{3.67}$$

where k_1, k_2 are constants that depends on the initial conditions $x_{pi}(0)$, with $i \in \mathcal{N}$. We observe that the synchronization trajectory is unbounded.

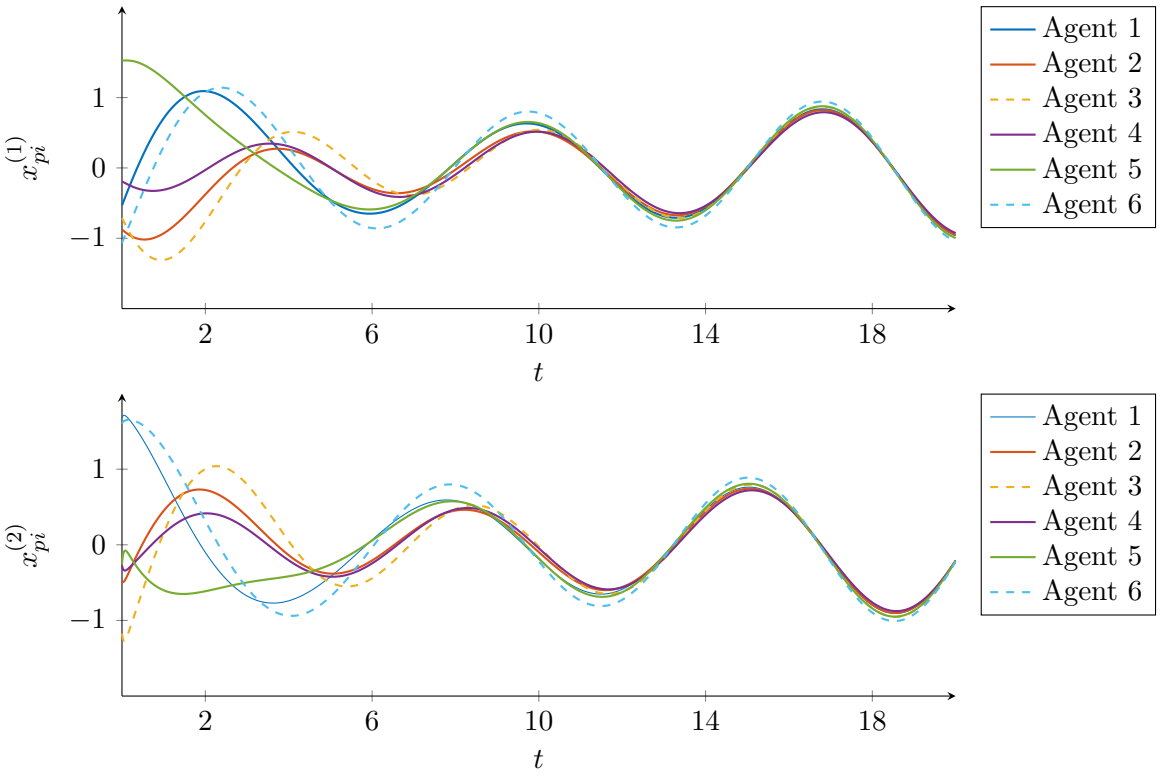

Figure 3.4: Time evolution of the agent state components $x_{pi}^{(1)}$ (top) and $x_{pi}^{(2)}$ (bottom), for all the agents $i \in \mathcal{N}$. Each colour in the plots identifies an agent of the network. The agents synchronize to the trajectory characterized in (3.67).

The same example is revisited with the addition of noise w_i as in (3.65), as per (3.1) with data (3.63), with dynamic output feedback compensator (3.8) with data (3.64). Figure 3.5, on page 3.5, shows the time responses of the state components of the vector x_p, and of the norm of the performance variable $\tilde{z}$ involved in the $\mathcal{L}_2$ gain condition (3.6). We can see that the agents initially reach state synchronization. As the perturbation is applied for $t = 20s$, the agent trajectories drift away from the desired synchronization trajectory (3.67), due to the noise term. When the disturbances vanish, that is, for $t > 25s$, state synchronization is achieved again.

From both scenarios presented in Figures 3.4 and 3.5, we conclude that the proposed controller guarantees robust state synchronization.

We want to conclude this example by providing further insight on the conservatism introduced by the relaxed conditions (3.45) for the H_∞ design. To this end we want to compare the sub-optimal solution given by (3.61) with the analysis conditions given in (3.32). More precisely, we plug the controller matrices A_k, B_k, C_k into conditions (3.32), and we compute the minimum value of γ^2, such that (3.32) is satisfied. This procedure gives an optimal value of $\gamma^2 = 37.4$, that is close to the one obtained with Algorithm 3.3 (see Figure 3.3). Although the numerical gap between the nonlinear conditions (3.32) and (3.45) cannot be mathematically quantified, this qualitative analysis suggests that the relaxation performed in Section 3.6, is a good alternative to the nonlinear formulation (3.32).

3.7 Summary

Chapter 3 considered the state synchronization problem of multi-agent systems subject to additive perturbations. As a consequence of the effect of the uncontrolled perturbations, the synchronization stability cannot be guaranteed. Based on some relaxation techniques, we proposed an ILMI algorithm for the H_∞ control design. This iterative procedure, although heuristic, is effective in practice in designing a distributed dynamic output feedback compensator that meets the requirements of the proposed problem. The next challenge in the same line of the topic presented in this chapter, is to take into account the saturation of the agent input in the multi-agent system dynamics.

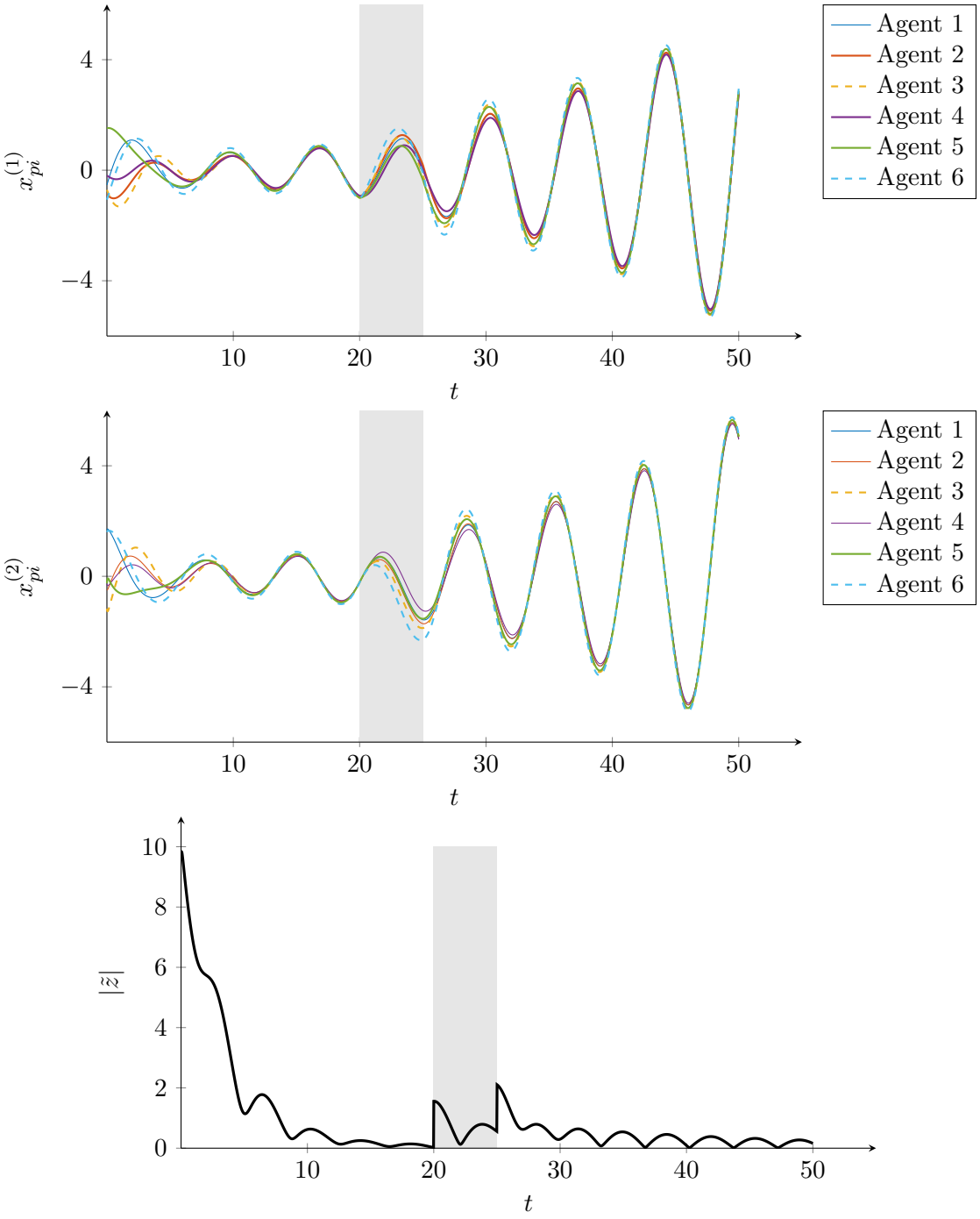

Figure 3.5: Time evolution of the agent state components. The top and the middle plots show the time evolution of the components of the state x_p. The bottom plot represents the time evolution of the norm of the performance variable $\tilde{z}$ involved in (3.6). The gray dotted lines delimit the time interval $20s \leq t \leq 25s$, in which the disturbances w_i in (3.65) are nonzero.

Algorithm 3.2 Initialization of Algorithm 3.3

Input: Matrices A_p, B_{pu}, C_p, Laplacian L, and a tolerance $\delta > 0$.
Initialization: Set $\lambda_c = 0$, $H = 0$ and $M = 0$ in (3.55), and solve the LMI

$$\Upsilon_i - tI_{6n} < 0, \quad i = 2, \ldots, N, \tag{3.56}$$

in the variables $Y = Y^\top > 0$, $W = W^\top > 0$, $\hat{C}$, $\hat{A}$, $\hat{B}$, t. Determine the values of $\hat{C}$ and W, correspondent to the solution to (3.56).
Iteration

Step 1: Given $\hat{C}$ and W from the previous step, solve the convex optimization problem

$$\begin{aligned} &\min_{Y,\hat{A},\hat{B},H,M,\lambda_c,t} \quad t, \\ &\text{s.t.} \quad \Upsilon_i - tI_{6n} < 0,\ i = 2, \ldots, N,\ Y = Y^\top > 0. \end{aligned} \tag{3.57}$$

Pick the optimal solution M, H, λ_c corresponding to the minimum value of t for the next step.

Step 2: Given M, H and λ_c from the previous step, solve the convex optimization problem

$$\begin{aligned} &\min_{W,Y,\hat{A},\hat{B},\hat{C},t} \quad t, \\ &\text{s.t.} \quad \Upsilon_i - tI_{6n} < 0,\ i = 2, \ldots, N,\ W = W^\top > 0,\ Y = Y^\top > 0. \end{aligned} \tag{3.58}$$

Pick the optimal solution $\hat{C}$ and W corresponding to the minimum value of t for the next step.
until t does not decrease more than δ over three consecutive steps.
Output: $\hat{A}, \hat{B}, \hat{C}, W, Y, H, M, \lambda_c$ and $t^\star = t$.

Algorithm 3.3 Dynamic output feedback controller design for state synchronization

Input: Matrices A_p, B_{pu}, C_p, B_{pw}, D_{pw}, C_{zp}, D_{zw}, the output parameters of Algorithm 3.2, Laplacian L, and a tolerance $\delta > 0$.

if $t^\star > 0$ **then**

no sub-optimal controller

else

Initialization

end if

Initialization: Fix the variables $\hat{C}$ and W as in **Input**.

Iteration

Step 1: Given $\hat{C}$ and W from the previous step, solve the convex optimization problem

$$\begin{aligned} &\min_{Y,\hat{A},\hat{B},H,M,\lambda_c,\gamma^2} \quad \gamma^2, \\ &\text{s.t.} \quad (3.45),\ Y = Y^\top > 0,\ \gamma^2 > 0. \end{aligned} \tag{3.59}$$

Pick the optimal solution M, H, λ_c corresponding to the minimum value of γ^2 for the next step.

Step 2: Given M, H and λ_c from the previous step, solve the convex optimization problem

$$\begin{aligned} &\min_{W,Y,\hat{A},\hat{B},\hat{C},\gamma^2} \quad \gamma^2, \\ &\text{s.t.} \quad (3.45),\ W = W^\top > 0,\ Y = Y^\top > 0,\ \gamma^2 > 0. \end{aligned} \tag{3.60}$$

Pick the optimal solution $\hat{C}$ and W corresponding to the minimum value of γ^2 for the next step.

until γ^2 does not decrease more than δ over three consecutive steps.

Compute A_k, B_k, C_k from (3.48).

Output: A_k, B_k, C_k and $(\gamma^\star)^2 = \gamma^2$.

Chapter 4

Synchronization under Saturation Constraints

In Chapter 3, we discussed and analyzed the state synchronization problem for multi-agent systems subject to external disturbances. In real-life applications, the information exchanged among the agents is subject to constraints that come from physical limitations in the agents or uncertain communication channels. Realistic examples are, among others, in the synchronization of vehicles with limited speed and working space [32], or the control of smart buildings with temperature and humidity in a specific range [41]. In this chapter, we suppose that the multi-agent systems under consideration have communication channel constraints, and more precisely, input saturation constraints. In addition, each agent gathers a limited information of the synchronizing control policy and, in addition, is affected by external disturbances. As these two factors—input saturation constraints and external disturbances—affect the synchronization performance, the resulting control strategy is a synchronizing control under limited-input constraints.

The described setting joins several challenging problems. There exist several approaches to tackle the saturation problems for isolated systems (see [46], [100] and [98]). In this chapter we aim at extending the saturated control strategies presented in [98] to the multi-agent scenario. More precisely, we include in the proposed control scheme an anti-windup loop so that, when saturation occurs, that anti-windup loop becomes active and acts to modify the closed-loop behavior such that it is more resilient to saturation (see [98], [118], and [105]). The control strategy used in this chapter is a centralized dynamic output feedback with a static anti-windup loop. The goal is to ensure global exponential synchronization of the multi-agent system.

The proposed approach builds on the theoretical results on synchronization stability and performance specifications presented in the previous chapters; however, there is an intrinsic limitation of this kind of approach, which is directly related to the stability

properties of the agent model: using the proposed controller, global exponential synchronization can be achieved only with exponentially stable plants. This is a necessary condition for global exponential stabilizability with bounded inputs (see [98] and [88]). However, we propose a controller for which the synchronization happens in the transient, before the global decay to zero (see Remark 2.4).

The contribution of this chapter is twofold. First, we give sufficient conditions for state synchronization for multi-agent systems under input saturation constraints. The conditions are obtained by globally bounding the saturation with an incremental sector condition and by enforcing synchronization rate constraints. Second, we propose a method to perform the synthesis of a centralized output feedback controller with static anti-windup loop, based on an LMI feasibility problem. Finally, we end the chapter by providing some insight on the extension to the local state synchronization problem with input saturation constraints.

4.1 Problem Formulation

We start this chapter by defining the agent model and the information topology of the multi-agent system under consideration.

Agent Model We consider multi-agent systems consisting of continuous-time identical systems subject to external disturbances and input magnitude saturation. Each agent is identified by the subscript index i, taking values in the index set $\mathcal{N} = \{1, \dots, N\}$, where $N > 1$ is the number of agents in the network. The ith agent dynamics is described by the following model

$$\begin{aligned} \dot{x}_{pi} &= A_p x_{pi} + B_{pu}\mathrm{sat}(\tilde{u}_i) + B_{pw} w_i \\ y_i &= C_p x_{pi} + D_p w_i \qquad\qquad i \in \mathcal{N}, \\ \tilde{z}_i &= x_{pi} - \tfrac{1}{N}\textstyle\sum_{j=1}^{N} x_{pj}, \end{aligned} \tag{4.1}$$

where $x_{pi} \in \mathbb{R}^n$ is the *agent state*, $\tilde{u}_i \in \mathbb{R}^m$ is the *agent input*, $y_i \in \mathbb{R}^p$ is the *agent output*, $w_i \in \mathbb{R}^q$ is the *agent disturbance*, and $\tilde{z}_i \in \mathbb{R}^n$ is the *agent performance output*. The matrices A_p, B_{pu}, B_{pw}, C_p, D_p are known matrices of appropriate dimensions. The function sat is the vector-valued saturation function defined as

$$\mathrm{sat}(\tilde{u}_i)_{(j)} := \mathrm{sat}(\tilde{u}_{i(j)}) = \begin{cases} \tilde{u}_{0(j)} & \text{if} \quad \tilde{u}_{i(j)} > \tilde{u}_{0(j)} \\ \tilde{u}_{i(j)} & \text{if} \quad -\tilde{u}_{0(j)} \le \tilde{u}_{i(j)} \le \tilde{u}_{0(j)} \\ -\tilde{u}_{0(j)} & \text{if} \quad \tilde{u}_{i(j)} < -\tilde{u}_{0(j)}, \end{cases} \tag{4.2}$$

for $j = 1, \dots, m$, and $i \in \mathcal{N}$. $\tilde{u}_{0(j)} \ge 0$, $j = 1, \dots, m$, is the level of saturation of the j-th component of $\tilde{u}_i$. For simplicity, in the remainder of this chapter, we assume that these levels are symmetric and uniform over all the agents, but this property is not required in the proofs of the results. Figure 4.1 shows the saturation function defined in (4.2).

We make the following assumption regarding the agent model.

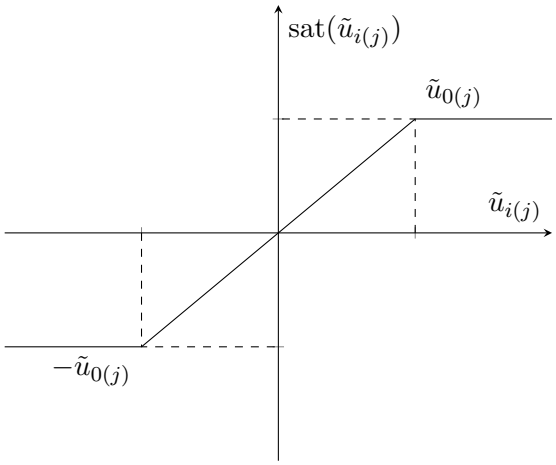

Figure 4.1: The saturation function.

Assumption 4.1. *A_p is Hurwitz.*

This condition is necessary for global exponential stabilizability with bounded inputs (see [88]).

Information Topology The communication links of the multi-agent system (4.1) are described by an undirected graph $\mathcal{G} = (\mathcal{V}, \mathcal{E})$. Every node $v_i \in \mathcal{V}$ is associated with the ith agent (4.1) in the network. Each edge $(v_i, v_j) \in \mathcal{E}$ identifies a bidirectional link between the ith and the jth agent. In this chapter we make the following assumption on the graph $\mathcal{G}$.

Assumption 4.2. *The graph $\mathcal{G}$ is undirected and fully connected.*

We recall that a graph $\mathcal{G}$ is fully connected if there exists a link between every pair of nodes. The basic definitions and properties of graph theory are summarized in Appendix A (for more details see [68]).

We want to define a suitable $\mathcal{L}_2$ gain condition to describe the performance specifications of the multi-agent system (4.1) with respect to the agent disturbances. Define the incremental agent disturbance

$$\tilde{w}_i := w_i - \tfrac{1}{N}\textstyle\sum_{j=1}^{N} w_j, \quad i \in \mathcal{N}. \tag{4.3}$$

We suppose that $\tilde{w}_i \in \mathbb{R}^q$ is an external disturbance bounded in energy—that is, $\tilde{w}_i$ belongs to $\mathcal{L}_2[0, +\infty)$. We suppose that the agent disturbance $\tilde{w}_i$ is a piecewise-continuous signal defined in $[0, \infty)$ such that

$$\textstyle\sum_{i=1}^{N} \|\tilde{w}_i\|_2^2 = \sum_{i=1}^{N} \int_0^\infty \tilde{w}_i(t)^\top \tilde{w}_i(t) dt < \infty, \quad i \in \mathcal{N}, \tag{4.4}$$

and we use the shorthand notation $\mathcal{L}_2$, instead of $\mathcal{L}_2[0, \infty)$, as there is no ambiguity on the underlying domain and range of the function $\tilde{w}_i$.

Consider the agent performance output $\tilde{z}_i$ in (4.1). Smaller values of the norm of $\tilde{z}_i$ indicates a desirable behavior of the multi-agent system: they mean that the agent states are close to each other—that is, the multi-agent system (4.1) is reaching state synchronization. In this chapter, we use the same $\mathcal{L}_2$ gain condition as in Chapter 4, contained in Definition 3.1 and reported below.

Definition 4.1. ($\mathcal{L}_2$ gain for synchronization) *The multi-agent system* (4.1) *has finite* $\mathcal{L}_2$ *gain, with gain bound* $\gamma > 0$ *if*

$$\sum_{i=1}^{N} \|\tilde{z}_i\|_2^2 \leq \gamma^2 \sum_{i=1}^{N} \|\tilde{w}_i\|_2^2 , \tag{4.5}$$

for all initial conditions $x_{pi}(0) = \mathbf{0}_n$*, all* $\tilde{w}_i \in \mathcal{L}_2$*, and* $t \geq 0$*,* $i \in \mathcal{N}$*.*

Condition (4.5) is a measure of how much the incremental agent disturbances $\tilde{w}_i$ affect the synchronization of the agent states x_i, and ensures that the ratio between the $\mathcal{L}_2$ norm of the agent disturbances $\{\tilde{w}_i,\ i \in \mathcal{N}\}$ and the agent performance outputs $\{\tilde{z}_i,\ i \in \mathcal{N}\}$ is bounded by $\gamma > 0$.

In this chapter we will use a centralized control scheme, according to the fully interconnected interaction of the multi-agent system (4.1), as stated in Assumption 4.2. A centralized control law has the following definition.

Definition 4.2. (Centralized Control Law) *A centralized control law is an algorithm that computes the control input* $\tilde{u}_i$ *of the agent* i*, globally, based on the knowledge of all the agent inputs* $\tilde{u}_j$*,* $j \in \mathcal{N}$ *of the network.*

Centralized control policies are alternative to distributed policies (compare Definitions 4.2 and 2.2, and see Section 1.2).

The goal of this chapter is to design a centralized control law $\tilde{u}_i$ that ensures exponential state synchronization among multi-agent systems (4.1), that attenuates the effects of the agent disturbances $\tilde{w}_i$, and that compensates for the limits imposed by the saturation to the synchronization seeking. Moreover, we want the multi-agent system (4.1) to reach exponential state synchronization with a prescribed synchronization rate. The definition of state synchronization has been formulated in Definition 2.1, and is recalled below.

Definition 4.3. (State Synchronization) *The multi-agent system* (4.1) *is said to achieve asymptotic state synchronization if, for any initial state* $x_{pi}(0) \in \mathbb{R}^n$*,* $i \in \mathcal{N}$*, there exists a trajectory* $\bar{x}_p$ *such that*

$$\lim_{t \to +\infty} x_{pi}(t) - \bar{x}_p(t) = \mathbf{0}_n \tag{4.6}$$

holds for every $i \in \mathcal{N}$*.*

If the multi-agent system is synchronized, the trajectory $\bar{x}_p(t)$ is called the *synchornization trajectory.*

The problem addressed in this chapter is summarized as follows.

Problem 4.1. (Global State Synchronization) *Consider the multi-agent system* (4.1)*, subject to external disturbances and input saturation constraints, with interconnection described by* $\mathcal{G}$*. The global state synchronization problem consists in finding a control law* $\tilde{u}_i$ *such that*

(i) if $w_i = \mathbf{0}_q$ *for all* $i \in \mathcal{N}$*, there exists a trajectory* $\bar{x}_p$ *such that the agent states* x_{pi} *in* (4.1) *satisfy* (4.6)*—that is the multi-agent system* (4.1) *reaches state synchronization. Moreover, if the initial condition is small enough so that the solution does not saturate, the synchronization rate is at least* β*.*

(ii) if $w_i \neq \mathbf{0}_q$ *for some* $i \in \mathcal{N}$*, and zero initial conditions* $x_{pi}(0) = \mathbf{0}_n$*, for* $i \in \mathcal{N}$*, relation* (4.5) *is satisfied for some* $\gamma > 0$*.*

Remark 4.1. In item (i) of Problem 4.1, the synchronization requirement is strengthened by imposing a prescribed local synchronization rate β (local meaning that this synchronization rate is fulfilled by all the solutions that do not exceed the saturation threshold). This additional constraint is added to control the synchronization rate with respect to the trivial case of zero controller—which is a trivial solution since A_p is Hurwitz according to Assumption 4.1.

4.2 Dynamic Output Feedback with Anti-Windup Loop

In order to solve Problem 4.1, we adopt the following centralized output feedback compensator with a static anti-windup loop. The dynamics of the ith compensator obeys

$$\begin{array}{rcll} \dot{x}_{ci} & = & A_k x_{ci} + B_k y_i + E_k \mathrm{dz}\,(\tilde{u}_i) & \\ u_i & = & C_k x_{ci} + D_k y_i & i \in \mathcal{N}, \\ \tilde{u}_i & = & u_i - \frac{1}{N}\sum_{j=1}^{N} u_j, & \end{array} \tag{4.7}$$

where we denote with x_{ci} the *controller state* and we assume that it has the same dimensions as the agent state—that is, $x_{ci} \in \mathbb{R}^n$. $u_i \in \mathbb{R}^m$ is the *controller output*, and $\mathrm{dz}(\cdot) : \mathbb{R}^m \to \mathbb{R}^m$ is the deadzone function defined as

$$\mathrm{dz}(\tilde{u}_i) := \tilde{u}_i - \mathrm{sat}(\tilde{u}_i), \tag{4.8}$$

or, equivalently

$$\mathrm{dz}(\tilde{u}_i)_{(j)} := \mathrm{dz}(\tilde{u}_{i(j)}) = \begin{cases} \tilde{u}_{i(j)} - \tilde{u}_{0(j)} & \text{if} \quad \tilde{u}_{i(j)} > \tilde{u}_{0(j)} \\ 0 & \text{if} \quad -\tilde{u}_{0(j)} \leq \tilde{u}_{i(j)} \leq \tilde{u}_{0(j)} \\ \tilde{u}_{i(j)} + \tilde{u}_{0(j)} & \text{if} \quad \tilde{u}_{i(j)} < -\tilde{u}_{0(j)}, \end{cases} \tag{4.9}$$

for $j = 1, \ldots, m$, and $i \in \mathcal{N}$. The architecture of the closed-loop system (4.1) and (4.7) is shown in Figure 4.2, on page 64. The compensator (4.7) is fed by the static anti-windup loop, which corresponds to the term $E_k \mathrm{dz}(\tilde{u}_i)$. From (4.9), we can see that the signal $\mathrm{dz}(\tilde{u}_i)$ activates the anti-windup action whenever necessary—that is, when the

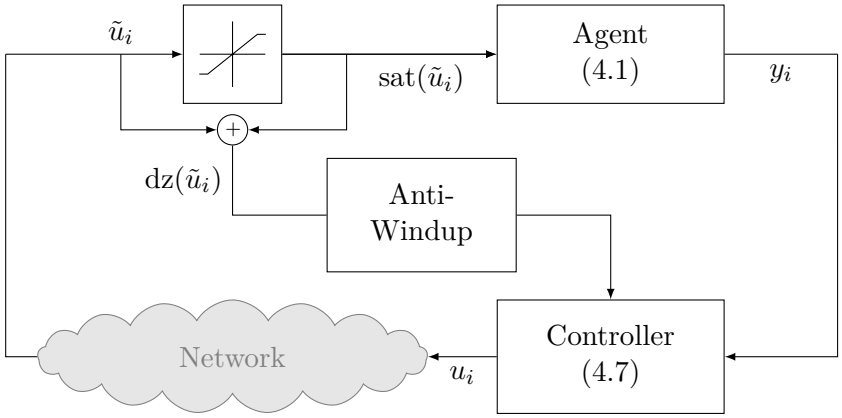

Figure 4.2: Block diagram representation of the closed-loop system (4.1) and (4.7).

agent input $\tilde{u}_i$ saturates. Note that controller (4.7) can be viewed as an extension of a classical dynamic output feedback controller including an anti-windup term, Such a controller is studied in the context of isolated LTI continuous-time systems subject to input magnitude saturation (see, for example, [21], [82], [98], and references therein).

Remark 4.2. Although the control law is *centralized*, in the sense that each agent input $\tilde{u}_i$ is computed based on the knowledge of all agent inputs, each agent only receives one input and does not need any global information. The global information is present in the network that computes $\tilde{u}_i$ for each agent (see Figure 4.2). This architecture allows for distributed generalizations of this approach, as in our recent submission [25].

We want now to give a compact representation of the closed-loop system (4.1) and (4.7), and to rewrite the multi-agent system (4.1) by replacing the saturation function (4.2) with the deadzone nonlinearity (4.8)—or, equivalently, (4.9). This procedure allows us to derive a convenient system representation and to formulate suitable synchronization conditions.

Consider the aggregate state vector

$$x_i := \begin{bmatrix} x_{pi} \\ x_{ci} \end{bmatrix} \in \mathbb{R}^{2Nn}, \quad i \in \mathcal{N}, \tag{4.10}$$

which includes the agent state in (4.1) and the controller state in (4.7). The dynamics of (4.10) is determined by combining (4.1), (4.7), and (4.8), and has the following expression

$$\dot{x}_i = \begin{bmatrix} A_p & 0 \\ B_k C_p & A_k \end{bmatrix} x_i + \begin{bmatrix} B_{pu} \\ 0 \end{bmatrix} \tilde{u}_i + \begin{bmatrix} -B_{pu} \\ E_k \end{bmatrix} \mathrm{dz}(\tilde{u}_i) + \begin{bmatrix} B_{pw} \\ B_k D_{pw} \end{bmatrix} w_i. \tag{4.11}$$

We want to give a compact representation of the closed-loop system. To this end, we

define the aggregate vectors

$$\begin{aligned} x &:= \begin{bmatrix} x_1^\top & \cdots & x_N^\top \end{bmatrix}^\top \in \mathbb{R}^{2Nn}, \\ y &:= \begin{bmatrix} y_1^\top & \cdots & y_N^\top \end{bmatrix}^\top \in \mathbb{R}^{Np}, \\ w &:= \begin{bmatrix} w_1^\top & \cdots & w_N^\top \end{bmatrix}^\top \in \mathbb{R}^{Nq}, \\ \mathrm{Dz}(\tilde{u}) &:= \begin{bmatrix} \mathrm{dz}(\tilde{u}_1)^\top & \cdots & \mathrm{dz}(\tilde{u}_N)^\top \end{bmatrix}^\top \in \mathbb{R}^{Nm}. \end{aligned} \tag{4.12}$$

Define $\tilde{z}$, $\tilde{u}$ and $\tilde{w}$, which are in relation with the vectors in (4.12) according to

$$\tilde{z} = (L_c \otimes I_{2n})x, \quad \tilde{u} = (L_c \otimes I_m)u, \quad \tilde{w} = (L_c \otimes I_q)w, \tag{4.13}$$

where we used the last equations in (4.1) and (4.7), and (4.3), and L_c is the Laplacian matrix associated with graph $\mathcal{G}$. From Assumption 4.2 and [34, Section 5], the Laplacian matrix L_c of a complete graph $\mathcal{G}$ has the following expression

$$[L_c]_{(i,j)} = \begin{cases} \frac{N-1}{N}, & \text{if} \quad i = j \\ -\frac{1}{N}, & \text{if} \quad i \neq j \end{cases} \quad i, j \in \mathcal{N}. \tag{4.14}$$

Using (4.12) and (4.13), the aggregate dynamics of (4.11) can be written as

$$\begin{aligned} \dot{x} &= Ax + B_w w + B_u \mathrm{Dz}(\tilde{u}) \\ u &= C_u x + D_u w \\ \tilde{z} &= C_z x, \end{aligned} \tag{4.15}$$

where A, B_w, B_u, C_u, D_u, and C_z are defined as

$$\begin{aligned} A &= I_N \otimes \begin{bmatrix} A_p & 0 \\ B_k C_p & A_k \end{bmatrix} + L_c \otimes \begin{bmatrix} B_{pu} D_k C_p & B_{pu} C_k \\ 0 & 0 \end{bmatrix}, \quad B_u = I_N \otimes \begin{bmatrix} -B_{pu} \\ E_k \end{bmatrix}, \\ B_w &= I_N \otimes \begin{bmatrix} B_w \\ B_k D_{pw} \end{bmatrix} + L_c \otimes \begin{bmatrix} B_{pu} D_k D_p \\ 0 \end{bmatrix}, \\ C_u &= I_N \otimes \begin{bmatrix} D_k C_p & C_k \end{bmatrix}, \quad D_u = I_N \otimes D_k D_p, \quad C_z = L_c \otimes \begin{bmatrix} I_n & 0 \end{bmatrix}, \end{aligned} \tag{4.16}$$

where we used the properties of the Kronecker product for the derivations. Before moving to the next section, in which we propose a coordinate transformation for the closed-loop system (4.15), it is useful to recall the definition of the extended synchronization set $\mathcal{S}_e$ given in (3.15). The synchronization set

$$\mathcal{S}_e := \left\{ x \in \mathbb{R}^{2Nn} : x_1 = x_2 = \cdots = x_N \right\}. \tag{4.17}$$

is the subset of the extended state space $\mathbb{R}^{2Nn}$ in which the agent states and the controller states coincide. The results on exponential stability of the set $\mathcal{S}_e$, which are presented in Chapter 2, constitute one of the main ingredients for solving Problem 4.1.

4.3 Decoupling Change of Coordinates

In this section we want to apply the change of coordinates proposed in Section 3.4.1, in order to project the dynamics (4.15) onto the synchronization set $\mathcal{S}_e$ (4.17) and its orthogonal complement $\mathcal{S}_e^{\perp}$. The following lemma particularizes Lemma 3.1 for networks characterized by a fully connected graph $\mathcal{G}$, for which the Laplacian matrix has the particular form (4.14) (see [57]).

Lemma 4.1. *Consider the Laplacian L_c in* (4.14)*. The eigenvalues of L_c are $\frac{N}{N-1}$ with multiplicity $N-1$ and 0 with multiplicity 1. Furthermore, there exists an orthonormal matrix $U_c = [\nu_1\ U_2] \in \mathbb{R}^N \times \mathbb{R}^{N\times(N-1)}$ —that is, $U_c^\top U_c = I_N$— such that:*

$$\Delta_c := \begin{bmatrix} 0 & 0 \\ * & \Delta_1 \end{bmatrix} = U_c^\top L_c U_c, \tag{4.18}$$

where $\Delta_1 := \frac{N}{N-1} I_N = \frac{N}{N-1} \otimes I_{N-1}$.

Using Lemma 4.1, we can define the coordinate transformation

$$\begin{aligned} \hat{x} &:= (U_c^\top \otimes I_{2n})x, \qquad & \hat{w} &:= (U_c^\top \otimes I_q)w, \\ \hat{z} &:= (U_c^\top \otimes I_n)\tilde{z}, \qquad & \hat{u} &:= (U_c^\top \otimes I_m)u, \end{aligned} \tag{4.19}$$

and

$$\hat{\mathrm{Dz}}(\hat{u}) := (U_c^\top \otimes I_m)\mathrm{Dz}((L_c U_c \otimes I_m)\hat{u}). \tag{4.20}$$

Consider now the following partition of the vectors (4.19) and (4.20)

$$\begin{aligned} \hat{x} &= \begin{bmatrix} (\nu_1^\top \otimes I_{2n})x \\ (U_2^\top \otimes I_{2n})x \end{bmatrix} := \begin{bmatrix} \hat{x}_1 \\ \hat{x}_2 \end{bmatrix} \in \mathbb{R}^{2n} \times \mathbb{R}^{2(N-1)n}, \\ \hat{u} &= \begin{bmatrix} (\nu_1^\top \otimes I_m)u \\ (U_2^\top \otimes I_m)u \end{bmatrix} := \begin{bmatrix} \hat{u}_1 \\ \hat{u}_2 \end{bmatrix} \in \mathbb{R}^{m} \times \mathbb{R}^{(N-1)m}, \\ \hat{w} &= \begin{bmatrix} (\nu_1^\top \otimes I_q)w \\ (U_2^\top \otimes I_q)w \end{bmatrix} := \begin{bmatrix} \hat{w}_1 \\ \hat{w}_2 \end{bmatrix} \in \mathbb{R}^{q} \times \mathbb{R}^{(N-1)q}, \\ \hat{z} &= \begin{bmatrix} (\nu_1^\top \otimes I_{2n})z \\ (U_2^\top \otimes I_{2n})z \end{bmatrix} := \begin{bmatrix} \hat{z}_1 \\ \hat{z}_2 \end{bmatrix} \in \mathbb{R}^{2n} \times \mathbb{R}^{2(N-1)n}, \\ \hat{\mathrm{Dz}}(\hat{u}) &= \begin{bmatrix} (\nu_1^\top \otimes I_m)\mathrm{Dz}((L_c U_c \otimes I_m)\hat{u}) \\ (U_2^\top \otimes I_m)\mathrm{Dz}((L_c U_c \otimes I_m)\hat{u}) \end{bmatrix} := \begin{bmatrix} \hat{\mathrm{Dz}}_1(\hat{u}) \\ \hat{\mathrm{Dz}}_2(\hat{u}) \end{bmatrix} \in \mathbb{R}^{m} \times \mathbb{R}^{(N-1)m}, \end{aligned} \tag{4.21}$$

where $\hat{x}$, $\hat{u}$, $\hat{w}$, $\hat{z}$, and $\hat{\mathrm{Dz}}(\hat{u})$ have the same partition as U_c in (4.14).

In the transformed coordinates, the closed-loop dynamics (4.15) becomes

$$\begin{aligned} \dot{\hat{x}} &= \hat{A}\hat{x} + \hat{B}_w\hat{w} + \hat{B}_u\hat{\mathrm{Dz}}(\hat{u}) \\ \hat{u} &= \hat{C}_u\hat{x} + \hat{D}_u\hat{w} \\ \hat{z} &= \hat{C}_z\hat{x} \end{aligned} \tag{4.22}$$

where the matrices $\hat{A}$, $\hat{B}_w$, $\hat{B}_u$, $\hat{C}_u$, $\hat{D}_u$, $\hat{C}_z$ are defined as follows

$$\begin{aligned}
\hat{A} &= I_N \otimes \begin{bmatrix} A_p & 0 \\ B_k C_p & A_k \end{bmatrix} + \Delta_c \otimes \begin{bmatrix} B_{pu} D_k C_p & B_{pu} C_k \\ 0 & 0 \end{bmatrix}, \quad \hat{B}_u = I_N \otimes \begin{bmatrix} -B_{pu} \\ E_k \end{bmatrix}, \\
\hat{B}_w &= I_N \otimes \begin{bmatrix} B_w \\ B_k D_{pw} \end{bmatrix} + \Delta_c \otimes \begin{bmatrix} B_{pu} D_k D_p \\ 0 \end{bmatrix}, \\
\hat{C}_u &= I_N \otimes \begin{bmatrix} D_k C_p & C_k \end{bmatrix}, \quad \hat{D}_u = I_N \otimes D_k D_p, \quad \hat{C}_z = \Delta_c \otimes \begin{bmatrix} I_n & 0 \end{bmatrix}.
\end{aligned} \tag{4.23}$$

Note that to obtain (4.23) we used the associative properties of the Kronecker product, and we replaced $U_c^\top L_c U$ with Δ_c, defined in (4.18), in several places. Furthermore, due to the block diagonal structure of matrices in (4.23), it is immediate to verify that the aggregate dynamics in (4.22) can be decomposed into the two independent subsystems

$$\begin{aligned}
\dot{\hat{x}}_1 &= \begin{bmatrix} A_p & 0 \\ B_k C_p & A_k \end{bmatrix} \hat{x}_1 + \begin{bmatrix} B_w \\ B_k D_p \end{bmatrix} \hat{w}_1 + \begin{bmatrix} -B_{pu} \\ E_1 \end{bmatrix} \hat{\mathrm{D}}\mathrm{z}_1(\hat{u}) \\
\hat{u}_1 &= \begin{bmatrix} D_k C_p & C_k \end{bmatrix} \hat{x}_1 + D_k D_p \hat{w}_1 \\
\hat{z}_1 &= \mathbf{0}_n,
\end{aligned} \tag{4.24}$$

and

$$\begin{aligned}
\dot{\hat{x}}_2 &= \hat{A}^2 \hat{x}_2 + \hat{B}_w^2 \hat{w}_2 + \hat{B}_u^2 \hat{\mathrm{D}}\mathrm{z}_2(\hat{u}) \\
\hat{u}_2 &= \hat{C}_u^2 \hat{x}_2 + \hat{D}_u^2 \hat{w}_2 \\
\hat{z}_2 &= \hat{C}_z^2 \hat{x}_2,
\end{aligned} \tag{4.25}$$

where $\hat{A}^2$, $\hat{B}_w^2$, $\hat{B}_u^2$, $\hat{C}_u^2$, $\hat{D}_u^2$, and $\hat{C}_z^2$ are defined as

$$\begin{aligned}
\hat{A}^2 &= I_{N-1} \otimes \begin{bmatrix} A_p + \frac{N}{N-1} B_{pu} D_k C_p & \frac{N}{N-1} B_{pu} C_k \\ B_k C_p & A_k \end{bmatrix}, \quad \hat{B}_u^2 = I_{N-1} \otimes \begin{bmatrix} -B_{pu} \\ E_k \end{bmatrix}, \\
\hat{B}_w^2 &= I_{N-1} \otimes \begin{bmatrix} B_w + \frac{N}{N-1} B_{pu} D_k D_p \\ B_k D_{pw} \end{bmatrix} \\
\hat{C}_u^2 &= I_{N-1} \otimes \begin{bmatrix} D_k C_p & C_k \end{bmatrix}, \quad \hat{D}_u^2 = I_{N-1} \otimes D_k D_p, \quad \hat{C}_z^2 = I_{N-1} \otimes \begin{bmatrix} \frac{N}{N-1} I_n & 0 \end{bmatrix}.
\end{aligned} \tag{4.26}$$

Using the same reasoning as in Section 3.4.1, we see that system (4.24) corresponds to the projection of the closed-loop dynamics (4.15) onto the synchronization space $\mathcal{S}_e$, defined in (4.17), and that the $N-1$ identical subsystems (4.25) correspond to the projection of dynamics (4.15) onto $\mathcal{S}_e^\perp$. The control strategy consists in solving Problem 4.1 for dynamics (4.25), thereby ensuring asymptotic synchronization of the multi-agent system (4.1).

We want to rewrite the $\mathcal{L}_2$ bound (4.5) in terms of the variables of subsystem (4.25)—that is, the projection of the variables (4.12) and (4.13) onto $\mathcal{S}_e^\perp$. This result is the first

main tool for solving Problem 4.1. Consider the variables $\tilde{z}$ and $\tilde{w}$ in (4.13). From definition (4.19), the orthonormality of U_c in (4.18), and (3.21), we obtain that

$$\|\tilde{z}\|_2^2 = \left\|(U_c^\top \otimes I_n)\tilde{z}\right\|_2^2 = \|\hat{z}\|_2^2 = \|\hat{z}_1\|_2^2 + \|\hat{z}_2\|_2^2 = \|\hat{z}_2\|_2^2\,, \tag{4.27}$$

where we used the fact that $\hat{z}_1$ in (4.24) is identically zero. Consider now the vectors $\tilde{w}$ in (4.13) and $\hat{w}$ in (4.19). Using a similar reasoning as before, and considering the diagonal structure of Δ_c in (4.18), we get

$$(U_c^\top \otimes I_q)\tilde{w} = (U_c^\top L_c U_c \otimes I_q)\hat{w} = (\Delta_c \otimes I_q)\hat{w} = \left(\begin{bmatrix} 0 & 0 \\ 0 & \Delta_1 \end{bmatrix} \otimes I_q\right) \begin{bmatrix} \hat{w}_1 \\ \hat{w}_2 \end{bmatrix} = (\Delta_1 \otimes I_q)\hat{w}_2, \tag{4.28}$$

where Δ_c is defined in (4.18). Hence, from (4.28), we obtain

$$\|\tilde{w}\|_2^2 = \|(\Delta_1 \otimes I_q)\hat{w}_2\|_2^2 = \left(\tfrac{N}{N-1}\right)^2 \|\hat{w}_2\|_2^2\,. \tag{4.29}$$

We conclude that the $\mathcal{L}_2$ gain property

$$\|\hat{z}_2\|_2^2 \leq \hat{\gamma}^2 \|\hat{w}_2\|_2^2\,, \tag{4.30}$$

with $\hat{\gamma}^2 := \left(\tfrac{N}{N-1}\gamma\right)^2$, ensures that the desired $\mathcal{L}_2$ gain property (4.5) for the multi-agent system (4.1) is satisfied. In fact, combining (4.5), (4.27), (4.29), and (4.30), we obtain

$$\sum_{i=1}^N \|\tilde{z}_i\|_2^2 = \|\tilde{z}\|_2^2 = \|\hat{z}_2\|_2^2 \leq \hat{\gamma}^2 \|\hat{w}_2\|_2^2 = \left(\tfrac{\gamma N}{N-1}\right)^2 \|\hat{w}_2\|_2^2 = \gamma^2 \|\tilde{w}\|_2^2 = \gamma^2 \sum_{i=1}^N \|\tilde{w}_i\|_2^2\,. \tag{4.31}$$

4.4 Extended Sector Condition

In this section, we want to extend the concept of classical sector condition of isolated systems (see, for example, [98]) to the multi-agent system scenario. In particular, we want to define a sector condition for the function $\hat{D}z_2(\hat{u})$—that is, the partition of $\hat{\mathrm{D}}\mathrm{z}(\hat{u})$ defined in (4.21). In particular, we want to derive a sector narrowing condition which holds globally on the extended state space $\mathbb{R}^{2Nn}$. This condition is one of the main ingredients to solve Problem 4.1.

Lemma 4.2. *Given the nonlinearity* $\hat{\mathrm{D}}\mathrm{z}(\hat{u})$ *defined in* (4.20)*, for each* $\hat{u} = \begin{bmatrix} \hat{u}_1 \\ \hat{u}_2 \end{bmatrix} \in \mathbb{R}^m \times \mathbb{R}^{(N-1)m}$*, we have*

$$\hat{\mathrm{D}}\mathrm{z}_2(\hat{u})^\top (I_{N-1} \otimes S^{-1})(\hat{\mathrm{D}}\mathrm{z}_2(\hat{u}) - (\Delta_1 \otimes I_m)\hat{u}_2) \leq 0, \tag{4.32}$$

for any diagonal positive definite matrix $S^{-1} \in \mathbb{R}^{m\times m}$*, where* $\hat{\mathrm{D}}\mathrm{z}_2(\hat{u})$ *is defined in* (4.21)*, and* Δ_1 *is defined in Lemma 4.1.*

Proof. The nonlinear function $\mathrm{dz}(\tilde{u}_i)$, defined in (4.8), satisfies the following global sector property (see, for example, [99]):

$$\mathrm{dz}(\tilde{u}_i)^\top S^{-1}(\mathrm{dz}(\tilde{u}_i) - \tilde{u}_i) \leq 0 \qquad i \in \mathcal{N}, \tag{4.33}$$

for all $\tilde{u}_i \in \mathbb{R}^m$, and any diagonal positive definite matrix $S^{-1} \in \mathbb{R}^{m\times m}$. In the aggregate variables $\mathrm{Dz}(\tilde{u})$ and $\tilde{u}$ in (4.12), and (4.13), respectively, the classical sector bound condition (4.33) reads

$$\mathrm{Dz}(\tilde{u})^\top (I_N \otimes S^{-1})(\mathrm{Dz}(\tilde{u}) - \tilde{u}) \leq 0. \tag{4.34}$$

Select $\tilde{u} = (L_c U \otimes I_m)\hat{u}$. Then from (4.34) we have

$$\begin{aligned} 0 \geq & \mathrm{Dz}^\top((L_c U \otimes I_m)\hat{u})(I_N \otimes S^{-1})\left[\mathrm{Dz}((L_c U_c \otimes I_m)\hat{u}) - (L_c U_c \otimes I_m)\hat{u}\right] \\ = & \hat{\mathrm{Dz}}^\top(\hat{u})(U_c^\top \otimes I_m)(I_N \otimes S^{-1})\left[(U_c \otimes I_m)\hat{\mathrm{Dz}}(\hat{u}) - (L_c U_c \otimes I_m)\hat{u}\right] \\ = & \hat{\mathrm{Dz}}(\hat{u})^\top(U_c^\top U_c \otimes S^{-1})\left[\hat{\mathrm{Dz}}(\hat{u}) - (U_c^\top L_c U_c \otimes I_m)\hat{u}\right]. \end{aligned} \tag{4.35}$$

From Lemma 4.1, by substituting $U_c^\top U_c = I_N$ and $U_c^\top L_c U_c = \Delta_c$, since $I_N \otimes S^{-1}$ and Δ_c, defined in (4.18), are block diagonal matrices, relation (4.35) is equivalent to

$$\hat{\mathrm{Dz}}_2(\hat{u})^\top(I_{N-1} \otimes S^{-1})(\hat{\mathrm{Dz}}_2(\hat{u}) - (\Delta_1 \otimes I_m)\hat{u}_2)) + \hat{\mathrm{Dz}}_1(\hat{u})S^{-1}\hat{\mathrm{Dz}}_1(\hat{u}) \leq 0, \tag{4.36}$$

Since $\hat{\mathrm{Dz}}_1(\hat{u})S^{-1}\hat{\mathrm{Dz}}_1(\hat{u}) \geq 0$, the first term in (4.36) is negative semidefinite and relation (4.32) is obtained. □

4.5 Global State Synchronization Analysis

In this section, we characterize Problem 4.1 in terms of a matrix inequality feasibility problem. The conditions presented in this section are obtained combining three main ingredients. First, the Lyapunov synchronization conditions presented in Theorem 2.1; second, the $\mathcal{L}_2$ gain condition (4.30), and finally, the extended sector bound condition in Lemma 4.2. In this first analysis step, we suppose that the controller matrices A_k, B_k, C_k, D_k, E_k are known and we derive the constraint on the Lyapunov function matrix. The synthesis of the controller is addressed in Section 4.6.

This theorem is a result for global state synchronization with guaranteed local convergence rate for the closed-loop multi-agent system (4.1) and (4.7).

Theorem 4.1. (Necessary Sufficient Conditions for Global State Synchronization) *Given the desired bounds $\gamma^2 > 0$ and $\beta > 0$, if there exist matrices $A_k \in \mathbb{R}^{n\times n}$, $B_k \in \mathbb{R}^{n\times p}$, $C_k \in \mathbb{R}^{m\times n}$, $D_k \in \mathbb{R}^{m\times p}$, $E_k \in \mathbb{R}^{m\times m}$, a positive definite matrix $P = P^\top \in \mathbb{R}^{2n\times 2n}$, and a positive definite diagonal matrix $S^{-1} \in \mathbb{R}^{m\times m}$ such that the following matrix inequalities*

$$\begin{bmatrix} He(P\mathbb{A}) & P\mathbb{B}_2 + \frac{N}{N-1}\mathbb{C}_1^\top S^{-1} & P\mathbb{B}_1 & \mathbb{C}_2^\top \\ * & -2S^{-1} & \frac{N}{N-1}S^{-1}\mathbb{D}_1 & 0 \\ * & * & -I_q & 0 \\ * & * & * & -\hat{\gamma}^2 I_n \end{bmatrix} < 0, \tag{4.37}$$

$$\mathrm{He}(P\mathbb{A}) + 2\beta P \leq 0, \tag{4.38}$$

with

$$\begin{aligned} \mathbb{A} &:= \begin{bmatrix} A_p + \frac{N}{N-1} B_{pu} D_k C_p & \frac{N}{N-1} B_{pu} C_k \\ B_k C_p & A_k \end{bmatrix}, \mathbb{B}_1 := \begin{bmatrix} \frac{N}{N-1} B_{pu} D_k D_p + B_{pw} \\ B_k D_p \end{bmatrix}, \\ \mathbb{B}_2 &:= \begin{bmatrix} -B_{pu} \\ E_k \end{bmatrix}, \mathbb{C}_1 := \begin{bmatrix} D_k C_p & C_k \end{bmatrix}, \mathbb{D}_1 := D_k D_p, \mathbb{C}_2 := \begin{bmatrix} \frac{N}{N-1} I_n & 0 \end{bmatrix} \end{aligned} \tag{4.39}$$

and $\hat{\gamma}^2 = \left(\frac{N\gamma}{N-1}\right)^2$*, are satisfied, then the controller* (4.7) *with* $x_{ci}(0) = \mathbf{0}_n$*, for* $i \in \mathcal{N}$*, solves Problem 4.1.*

Proof. Consider the Lyapunov function candidate

$$V(\hat{x}_2) = x^\top (U_c \otimes I_{2n}) \operatorname{diag}(0, \underbrace{P, \ldots, P}_{N-1}) (U_c^\top \otimes I_{2n}) x = \hat{x}_2^\top (I_{N-1} \otimes P) \hat{x}_2. \tag{4.40}$$

From Theorem 2.1, such a function satisfies

$$\alpha_1 |x|_{\mathcal{S}_e}^2 \leq V(\hat{x}_2) \leq \alpha_2 |x|_{\mathcal{S}_e}^2 \tag{4.41}$$

for positive scalars α_1 and α_2, where $\mathcal{S}_e$ is the synchronization set defined in (4.17). Denote with $\hat{x}_2^{(i)} \in \mathbb{R}^n, \hat{\mathrm{D}}\mathrm{z}_2(\hat{u})^{(i)} \in \mathbb{R}^m, \hat{z}_2^{(i)} \in \mathbb{R}^n, \hat{w}_2^{(i)} \in \mathbb{R}^q$ for $i = 1, \ldots, N-1$ the vector components of $\hat{x}_2$, $\hat{\mathrm{D}}\mathrm{z}_2(\hat{u})$, $\hat{z}_2$, $\hat{w}_2$ in (4.21), respectively. By pre- and post-multiplying (4.37) by $[\hat{x}_2^{(i)\top} \hat{\mathrm{D}}\mathrm{z}_2(\hat{u})^{(i)\top} \hat{w}_2^{(i)\top} \hat{z}_2^{(i)\top}]^\top$ and its transpose, we obtain that (4.37) is equivalent to

$$\begin{aligned} 2\hat{x}_2^{(i)\top} P \left(\mathbb{A}\hat{x}_2^{(i)} + \mathbb{B}_2 \hat{\mathrm{D}}\mathrm{z}_2(\hat{u})^{(i)} + \mathbb{B}_1 \hat{w}_2^{(i)} \right) + \tfrac{1}{\hat{\gamma}^2} \hat{z}_2^{(i)\top} \hat{z}_2^{(i)} - \hat{w}_2^{(i)\top} \hat{w}_2^{(i)} \\ -2\hat{\mathrm{D}}\mathrm{z}_2(\hat{u})^{(i)\top} S^{-1} \left(\hat{\mathrm{D}}\mathrm{z}_2(\hat{u})^{(i)} - \tfrac{N}{N-1} (\mathbb{C}_1 \hat{x}_2^{(i)} + \mathbb{D}_1 \hat{w}_2^{(i)}) \right) < 0 \end{aligned} \tag{4.42}$$

Stacking the inequalities (4.42) for every $i = 2, \ldots, N$, noticing that (4.39) are related to (4.26) according to

$$\begin{aligned} \hat{A}_2 = I_{N-1} \otimes \mathbb{A}, \quad \hat{B}_u^2 = I_{N-1} \otimes \mathbb{B}_2, \quad \hat{B}_w^2 = I_{N-1} \otimes \mathbb{B}_1, \\ \hat{C}_u^2 = I_{N-1} \otimes \mathbb{C}_1, \quad \hat{D}_u^2 = I_{N-1} \otimes \mathbb{D}_1, \quad \hat{C}_z^2 = I_{N-1} \otimes \mathbb{C}_2, \end{aligned}$$

and combining (4.18), (4.25), and (4.40), we obtain that (4.42) is equivalent to

$$\dot{V}(\hat{x}_2) + \tfrac{1}{\hat{\gamma}^2} \hat{z}_2^\top \hat{z}_2 - \hat{w}_2^\top \hat{w}_2 - 2\hat{\mathrm{D}}\mathrm{z}_2(\hat{u})^\top (I_{N-1} \otimes S^{-1}) \left[\hat{\mathrm{D}}\mathrm{z}_2(\hat{u}) - (\Delta_1 \otimes I_m) \hat{u}_2 \right] < 0. \tag{4.43}$$

Similarly, pre- and post-multiplying (4.38) by $\hat{x}_2^{(i)\top}$ and its transpose and combining (4.40) and (4.25), we obtain that (4.38) is equivalent to

$$\dot{V}(\hat{x}_2) \leq -2\beta V(\hat{x}_2). \tag{4.44}$$

Consider the case $w_i = \mathbf{0}_q$, for all $i \in \mathcal{N}$. Setting $\hat{w}_2 = (U_c^\top \otimes I_q)w = \mathbf{0}_{(N-1)q}$ in (4.43) and using Lemma 4.2, we obtain $\dot{V}(\hat{x}_2) < 0$; however this condition is already implied by (4.44).

If the initial conditions of the closed-loop system are such that the input $\tilde{u}_i$ does not saturate for all the time—that is, the closed-loop system behaves like a linear system—from linear systems theory (see, for example, [42]), condition (4.44) is equivalent to the exponential stability of subsystem (4.25) with decay rate β. Applying Theorem 2.1 we can conclude that the synchronization set $\mathcal{S}_e$ in (4.17) is exponentially stable—that is, if the initial conditions are such that the closed-loop system does not saturate, the multi-agent system (4.1) and (4.7) reaches exponential state synchronization with local synchronization rate β. This proves that item (i) of Problem 4.1 is solved. If $w_i \neq \mathbf{0}_q$ for some $i \in \mathcal{N}$, we apply Lemma 4.2 to (4.43) obtaining

$$\dot{V}(\hat{x}_2) + \tfrac{1}{\hat{\gamma}^2}\hat{z}_2^\top \hat{z}_2 - \hat{w}_2^\top \hat{w}_2 < 0, \tag{4.45}$$

We now apply the same technique used in Theorem 3.1. By integration of (4.45) over the interval $[0, T]$, with $T > 0$, we obtain

$$V(\hat{x}_2(T)) - V(\hat{x}_2(0)) + \tfrac{1}{\hat{\gamma}^2}\int_0^T \hat{z}_2^\top(t)\hat{z}_2(t)dt - \int_0^T \hat{w}_2^\top(t)\hat{w}_2(t)dt < 0. \tag{4.46}$$

Since from (4.41), $V(\hat{x}_2(T)) \geq 0$ for all $T > 0$, and from the hypothesis $x_i(0) = \begin{bmatrix} x_{pi}(0) \\ x_{ci}(0) \end{bmatrix} = \mathbf{0}_{2n}$ for all $i = 1, \ldots, N$, that implies $V(\hat{x}_2(0)) = 0$, taking the limit of (4.46) as $T \to \infty$, we obtain

$$\|\hat{z}_2\|_2^2 \leq \hat{\gamma}^2 \|\hat{w}_2\|_2^2 . \tag{4.47}$$

Hence, by using (4.30) and (4.31), it follows that the $\mathcal{L}_2$ gain property (4.5) is satisfied, and then item (ii) of Problem 4.1 is solved. This completes the proof. □

Note that, if the controller matrices A_k, B_k, C_k, D_k, E_k are known, then (4.37) and (4.38) are linear matrix inequalities in the decision variable $P = P^\top > 0$. However, if we consider the controller matrices as decision variables, then relations (4.37) and (4.38) are nonconvex matrix inequalities. For this reason, (4.37) and (4.38) can not be easily used for controller design. In the next section, we introduce a suitable coordinate transformation to obtain LMI conditions for the global H_∞ state synchronization design.

4.6 Global H_∞ State Synchronization Design

In this section, we addresses the design of the dynamic output feedback compensator with anti-windup loop (4.7) to solve Problem 4.1. In order to provide a convex procedure for the controller design, we use the linearising congruence transformation presented in [84]. The following theorem contains the LMI characterization of the saturated H_∞ control design with guaranteed local synchronization rate for the closed-loop system (4.1) and (4.7).

Theorem 4.2. *Given a desired local synchronization rate $\beta > 0$, if there exist two positive definite matrices $X = X^\top \in \mathbb{R}^n$, $Y = Y^\top \in \mathbb{R}^n$ a positive definite diagonal matrix $S \in \mathbb{R}^{m\times m}$, a scalar $\gamma^2 > 0$ and four matrices $W \in \mathbb{R}^{n\times n}$, $F \in \mathbb{R}^{n\times p}$, $L \in \mathbb{R}^{m\times n}$, $H \in \mathbb{R}^{m\times p}$ such that*

$$\begin{bmatrix} \mathrm{He}\left(\begin{bmatrix} A_pY + B_{pu}L & A_p + B_{pu}HC_p \\ W & XA_p + FC_p \end{bmatrix}\right) & \begin{bmatrix} -B_{pu}S + L^\top \\ Q + C_p^\top H^\top \end{bmatrix} & \begin{bmatrix} B_{pw} + B_{pu}HD_p \\ XB_{pw} + FD_p \end{bmatrix} & \begin{bmatrix} Y \\ I_n \end{bmatrix} \\ * & -2S & HD_p & 0 \\ * & * & -I_q & 0 \\ * & * & * & -\hat{\gamma}^2 I_n \end{bmatrix} < 0 \quad (4.48)$$

$$\mathrm{He}\left(\begin{bmatrix} A_pY + B_{pu}L & A_p + B_{pu}HC_p \\ W & XA_p + FC_p \end{bmatrix}\right) + 2\beta \begin{bmatrix} Y & I_n \\ I_n & X \end{bmatrix} \leq 0 \quad (4.49)$$

$$\begin{bmatrix} Y & I_n \\ I_n & X \end{bmatrix} > 0, \quad (4.50)$$

where $\hat{\gamma}^2 = \left(\frac{N\gamma}{N-1}\right)^2$, are satisfied, then controller (4.7) solves Problem 4.1 with $x_{ci}(0) = \mathbf{0}_n$, for $i \in \mathcal{N}$ and

$$\begin{array}{rcl} D_k & := & \frac{N-1}{N} H \\ C_k & := & \frac{N-1}{N}(L - HC_pY)V^{-\top} \\ B_k & := & G(F - XB_{pu}H) \\ A_k & := & G^{-1}(W - XA_pY - XB_{pu}L - GB_kC_pY)V^{-\top} \\ E_k & := & G^{-1}(XB_{pu} + QS^{-1}), \end{array} \quad (4.51)$$

where V and G are nonsingular matrices that satisfy $V^\top = G^{-1}(I_n - XY)$.

Proof. We want to prove that (4.48) is equivalent to (4.37). Consider condition (4.37). We apply the linearizing change of variables introduced in [84]. Consider the following partition of the Lyapunov matrix P and its inverse

$$P = \begin{bmatrix} X & G \\ * & \hat{X} \end{bmatrix}, \qquad P^{-1} = \begin{bmatrix} Y & V \\ * & \hat{Y} \end{bmatrix}. \quad (4.52)$$

Define $\mathbb{J} := \begin{bmatrix} Y & V \\ I_n & 0 \end{bmatrix}$. Note that $\mathbb{J}P = \begin{bmatrix} I_n & 0 \\ X & G \end{bmatrix}$, and $\mathbb{J}P\mathbb{J}^\top = \begin{bmatrix} Y & I_n \\ I_n & X \end{bmatrix}$. Then, the satisfaction of relation (4.50) guarantees that P is positive definite. Moreover, from (4.52) and (4.50) and (4.52), it follows that $X - Y^{-1} > 0$, which implies that $I_n - XY$ is nonsingular. Pre- and post-multiplying (4.37) by $\mathrm{diag}(\mathbb{J}, S, I, I)$ and its transpose. We define the following controller matrices transformation

$$\begin{bmatrix} W & F \\ L & H \end{bmatrix} := \begin{bmatrix} XA_pY & 0 \\ 0 & 0 \end{bmatrix} + \begin{bmatrix} G & \frac{N}{N-1}XB_{pu} \\ 0 & \frac{N}{N-1}I_m \end{bmatrix} \begin{bmatrix} A_k & B_k \\ C_k & D_k \end{bmatrix} \begin{bmatrix} V^\top & 0 \\ C_pY & I_p \end{bmatrix}, \quad (4.53)$$

and $Q := (-XB_{pu} + GE_k)S$. Since $I_n - XY$ is nonsingular, it is always possible to compute two square and nonsingular matrices V and G satisfying $GV^\top = I_n - XY$.

This fact also ensures that $\mathbb{J}$ is nonsingular. The nonsingularity of $\mathbb{J}$ guarantees that the transformation is invertible. After some calculations we obtain that (4.37) coincides with (4.48). Now we want to prove that (4.49) is equivalent to (4.38). Pre- and post-multiplying (4.38) by $\mathbb{J}$ and its transpose, and using the change of variables (4.53), after some calculations, we obtain that (4.38) coincides with (4.49). This ends the proof. □

Theorem 4.2 allows us to design the matrices A_k, B_k, C_k, D_k, E_k of the proposed control architecture in such a way that the performance level γ guarantees the desired disturbance rejection against the external disturbances, while guaranteeing a certified local convergence rate β. As a result, all the solutions of the distributed closed loop have the $\mathcal{L}_2$ gain property in (4.5) in the presence of external disturbances $\tilde{w}_i$ and zero initial conditions. In addition, for the case of disturbances w_i equal to zero and linear behavior, all the solutions exponentially synchronize, with guaranteed local synchronization rate β—that is, β has the meaning of synchronization rate of the multi-agent system only if the initial conditions are such that the system does not saturate.

Remark 4.3. The matrix inequality (4.48) for the global H_∞ control design is convex in the decision variables. This property is related to the centralized nature of the network interconnection, as per (4.14). When we consider general undirected topologies (see Section 3.5) this property does not hold and we need to relax the problem in order to perform the control design. This makes the proposed all-to-all interconnection topology interesting from a theoretical point of view.

Remark 4.4. As pointed out in the introduction, the proposed solution to the global state synchronization problem is feasible only if the open-loop system is exponentially stable—that is, matrix A_p is Hurwitz. This condition follows from classical results on global exponential stabilizability with bounded inputs (see, for example, [49] and [88]). Therefore, the synchronization requirement can be enforced by selecting the design parameter β smaller than the minimum real part of the eigenvalues of A_p, meaning that the multi-agent system synchronizes fasten than decaying to zero. This situation is studied in detail in Section 4.7.

The following corollary characterizes the synchronization trajectory of the multi-agent system (4.1) and (4.7) in the linear, unperturbed case—that is, in the context of item (i) of Problem 4.1.

Corollary 4.1. (Characterization of the Synchronization Trajectory) *Given a desired local synchronization rate $\beta > 0$, if $w_i = \mathbf{0}_q$ for all $i \in \mathcal{N}$, and initial conditions $x_i(0) = \begin{bmatrix} x_{pi}(0)^\top & x_{ci}(0)^\top \end{bmatrix}^\top \in \mathbb{R}^{2n}$ are such that the closed-loop system does not saturate—that is, $dz(\tilde{u}_i) = 0$ for all $i \in \mathcal{N}$—and there exist matrices $A_k \in \mathbb{R}^{n\times n}$, $B_k \in \mathbb{R}^{n\times p}$, $C_k \in \mathbb{R}^{m\times n}$, $D_k \in \mathbb{R}^{m\times p}$, a positive definite matrix $P = P^\top \in \mathbb{R}^{2n\times 2n}$ such that*

$$\mathrm{He}\left(P \begin{bmatrix} A_p + \frac{N}{N-1} B_{pu} D_k C_p & \frac{N}{N-1} B_{pu} C_k \\ B_k C_p & A_k \end{bmatrix}\right) < -2\beta P, \tag{4.54}$$

then, the trajectories of the closed-loop system (4.1) *and* (4.7) *exponentially synchronize to the solution to the following initial value problem*

$$\dot{\bar{x}} = \begin{bmatrix} A_p & 0 \\ B_k C_p & A_k \end{bmatrix} \bar{x}, \tag{4.55}$$

where $\bar{x} = \begin{bmatrix} \bar{x}_p \\ \bar{x}_c \end{bmatrix}$, *and* $\bar{x}(0) = \frac{1}{N}\sum_{i=1}^{N} \begin{bmatrix} x_{pi}(0) \\ x_{ci}(0) \end{bmatrix}$, *with local synchronization rate* β.

Proof. Consider the dynamics of the state $\bar{x}(t) = \frac{1}{N}\sum_{i=1}^{N} x_i(t) = \frac{1}{N}(\mathbf{1}_N^\top \otimes I_{2n})x(t)$. Based on (4.15) and (4.16), the time evolution of $\bar{x}$ is

$$\begin{aligned} \dot{\bar{x}} &= \tfrac{1}{N}(\mathbf{1}_N^\top \otimes I_{2n}) \left[\left(I_N \otimes \begin{bmatrix} A_p & 0 \\ B_k C_p & A_k \end{bmatrix} \right) + \left(L_c \otimes \begin{bmatrix} B_{pu} D_k C_p & B_{pu} C_k \\ 0 & 0 \end{bmatrix} \right) \right] x \\ &= \tfrac{1}{N} \left(\mathbf{1}_N^\top I_N \otimes \begin{bmatrix} A_p & 0 \\ B_k C_p & A_k \end{bmatrix} \right) x = \tfrac{1}{N} \left(\mathbf{1}_N^\top \otimes \begin{bmatrix} A_p & 0 \\ B_k C_p & A_k \end{bmatrix} \right) x \\ &= \begin{bmatrix} A_p & 0 \\ B_k C_p & A_k \end{bmatrix} \tfrac{1}{N}(\mathbf{1}_N^\top \otimes I_{2n}) x = \begin{bmatrix} A_p & 0 \\ B_k C_p & A_k \end{bmatrix} \bar{x}, \end{aligned} \tag{4.56}$$

where we used the relation $\mathbf{1}_N^\top L_c = 0$. Tracing the proof of Theorem 4.1 for $w_i = \mathbf{0}_q$ for all $i \in \mathcal{N}$, condition (4.54) guarantees that the multi-agent system reaches exponential state synchronization with local synchronization rate equal to β. Then item (iv) of Theorem 2.1 ensures that the agents exponentially synchronize to the solution to (4.56), once we notice that $p = \mathbf{1}_N$ for symmetric Laplacian matrices. □

Remark 4.5. Note that Corollary 4.1 ensures exponential synchronization of the multi-agent system to the solution to (4.55), but it does not ensure that the synchronization trajectory remains bounded. It becomes then relevant to investigate whether the synchronization solution (4.55) remains or not bounded for each initial condition. This question is answered by noticing that the eigenvalues of the state matrix in (4.55) are the union of the eigenvalues of A_p and A_k—that is, the agent and controller matrices, respectively. Recalling that A_p must be Hurwitz, the solution to (4.55) remains bounded if and only if A_k is Hurwitz too. The stability of the controller is in general not a requirement. Stabilization of systems using stable controllers is often called in the literature as *strong stabilization* (see, among others, the Parity Interlacing Property characterized in [117]).

4.7 Optimal H_∞ Control Design

In this section, we give an example of how to use the synchronization conditions contained in Theorem 4.2 to design a suitable compensator in the form (4.7) to solve Problem 4.1. In fact, we want to go one step further and ask if it possible to determine an optimal compensator (4.7) that maximizes the disturbance rejection and the synchronization rate.

This corresponds to minimizing the $\mathcal{L}_2$ gain γ^2, while maximizing the parameter β. In particular, we require β to be larger than the convergence rate of A_p (see Remark 4.4)—that is, larger than the absolute value of the maximum real part of the eigenvalues of A_p. Note that, if we take $\beta > 0$ in (4.50) as a variable of the problem, then (4.48) (4.50) define a quasi-convex optimization problem. In fact, all the variables X, Y, W, F, L, H, V, S, γ^2 enter linearly in the conditions, except for β, due to the product term $\beta \begin{bmatrix} Y & I_n \\ I_n & X \end{bmatrix}$, and since from (4.50) we have that $\begin{bmatrix} Y & I_n \\ I_n & X \end{bmatrix} > 0$, then the bilinearity in (4.49) is quasi-convex and is characterized by a well defined feasibility bound β.

This multi-objective problem can be tackled as follows. We can fix the value of β in the interval $(0, \bar{\beta}]$, where $\bar{\beta} \geq \max_i \ |\mathbf{Re}(\lambda_i(A_p))|$. In this way, the conditions (4.48)–(4.50) are linear in the remaining variables, and we can compute the sub-optimal solution to the problem minimizing γ^2. The optimal solution to the overall problem will lay on the trade-off curve (β, γ^2). The choice of the particular operating point depends on the requirements of the multi-objective control design. For instance, we may prefer large disturbance rejection, at the cost of a slow convergence rate, or we may require a fast convergence rate, at the cost of larger sensitivity to external disturbances. Summarizing, the proposed optimized control design can be mathematically formulated as follows

$$\begin{array}{ll} \min\limits_{X,Y,F,L,H,V,S,\gamma^2} & \gamma^2 \\ \text{s.t.} & (4.50), (4.49), (4.48), \end{array} \tag{4.57}$$

for a sampled selection of β in the interval $(0, \bar{\beta}]$, and $\bar{\beta} \geq \max_i \ |\mathbf{Re}(\lambda_i(A_p))|$. This is the strategy adopted in the next example.

Example 4.1. Consider $N = 6$ agents, each of them described by (4.1) and the following data

$$A_p = \begin{bmatrix} 0 & 1 \\ -1 & -0.6 \end{bmatrix}, B_{pu} = B_{pw} = \begin{bmatrix} 0 \\ 10 \end{bmatrix}, C_p = \begin{bmatrix} 1 & 0 \end{bmatrix}, D_p = 0, \tag{4.58}$$

with the level of saturation $u_0 = 0.1$. Note that the open-loop plant is asymptotically stable, since the eigenvalues of A_p are $\lambda_i(A_p) = -0.3000 \pm 0.9539i$. The output feedback compensator with anti-windup loop (4.7) is designed using the optimized procedure summarized in (4.57).

The optimization problem described in (4.57) has been implemented in MATLAB and solved numerically using the YALMIP toolbox and the MOSEK solver (see [61] and [70], respectively). Figure 4.3 shows the trade-off curve between γ^2 and β. For each value of β in the range $(0, \bar{\beta}]$, with $\bar{\beta} = 0.5 > 0.3 = \max_i \ |\mathbf{Re}(\lambda_i(A_p))|$, the parameter γ^2 is minimized according to (4.57). Notice that, increasing the local convergence rate leads to a less effective attenuation of external disturbances.

To determine an optimized controller selection, we may choose β in the range $[0.3, 0.5]$. Lower values of β would lead to synchronization rate slower then the rate of converge to zero. Larger values of β lead to unacceptable disturbance rejection (see Figure 4.3). The interval in which we make our selection is contained in the gray area of Figure 4.3. Requiring synchronization rates larger than $\beta = 0.4$ leads, in this example, to ill-conditioned

solutions; therefore, we choose $(\beta, \gamma^2) = (0.4, 2.5 \cdot 10^3)$ as operating point (represented by a black dot in Figure 4.3). The resulting optimized controller matrices are

$$\begin{aligned} A_k &= \begin{bmatrix} -0.81 & 10.76 \\ -13.9 & -20.47 \end{bmatrix}, \; B_k = \begin{bmatrix} -0.25 \\ -42.19 \end{bmatrix}, \; E_k = \begin{bmatrix} 2.05 \\ 5 \end{bmatrix}, \\ C_k &= \begin{bmatrix} -0.07 & 1.5 \end{bmatrix}, \; D_k = 0.48. \end{aligned} \tag{4.59}$$

Note that for this example we obtain that A_k is Hurwitz, thereby guaranteeing boundedness of all solutions (see Remark 4.5). We consider the following piecewise constant disturbances $w_i \in \mathcal{L}_2$

$$w_i = \begin{cases} w_{0i} & \text{if} \quad 5s \leq t \leq 7s, \\ 0 & \text{otherwise} \end{cases} \tag{4.60}$$

for $i = 1, \ldots, 5$ with w_{0i} constant values uniformly chosen in the interval $[-0.5, 0.5]$. The closed-loop system (4.1) with data (4.58), and the controller (4.7) with data (4.59) have been simulated in MATLAB environment. The obtained closed-loop responses are shown in Figure 4.4 in the case of unperturbed dynamics ($w_i = \mathbf{0}_q$). Each agent is identified by a colour in the plots. From the figure, we can see that the system does not saturate, so that the hypothesis of Corollary 4.1 are satisfied. Furthermore, the agent states (and outputs) synchronize with rate $\beta = 0.4$, and then they decay to zero.

The simulation is then repeated with addition of the noise w_i as in (4.60), with the same data for the agent model and compensator. The obtained responses are represented in Figures 4.5, 4.6, and 4.7, respectively. Figure 4.7 represents the agent outputs and inputs without any feedback controller, nor interconnection among the agents. Figure 4.6 represents the ideal unconstrained closed-loop agent outputs and inputs if the saturation

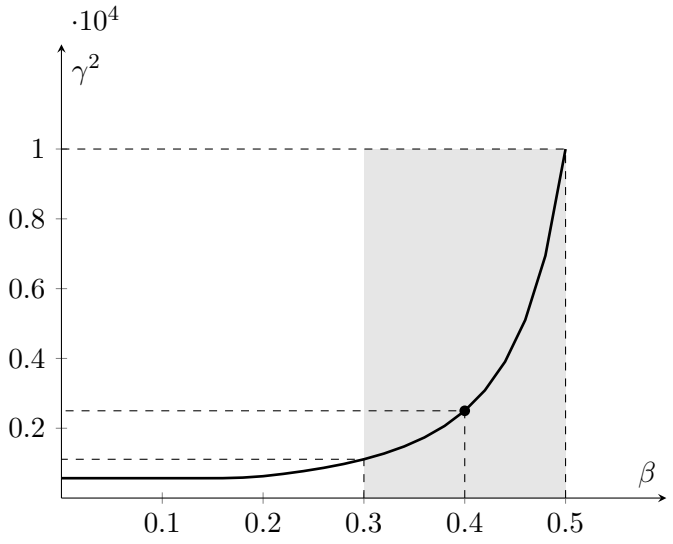

Figure 4.3: Trade-off curve (β, γ^2).

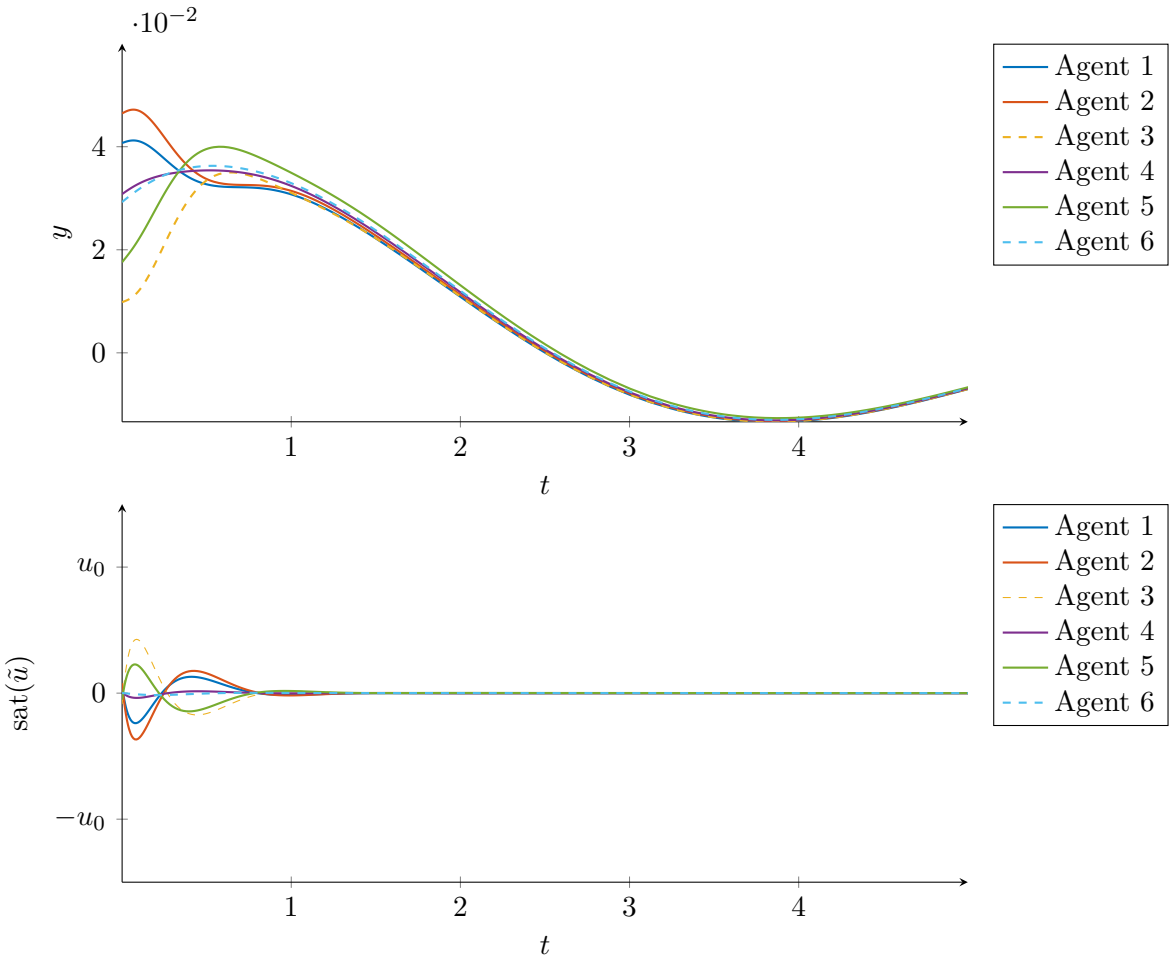

Figure 4.4: Evolution of the agent outputs (top) and the agent inputs (bottom) in the noiseless case $w_i = \mathbf{0}_q$.

is not in place—that is $\mathrm{sat}(\tilde{u}_i) = \tilde{u}_i$, for all $i \in \mathcal{N}$. Finally, Figure 4.5 represents the agent outputs and inputs with saturation constraints. In all the figures, the gray area delimits the time interval in which the noise w_i in (4.60) is nonzero.

Comparing the plots in Figures 4.5 and 4.7, we see that the controller design is effective at speeding up the synchronization of the agents (as certified by β in Theorem 4.2 and the numerical procedure described in this section). From Figure 4.5 we can notice that, despite the inevitable limits imposed by saturation, which slows down the transient, the closed-loop behavior is still significantly better than the open-loop response in Figure 4.7, in which the outputs drift apart.

The plots in Figures 4.5, and 4.6 are also effective at illustrating the closed-loop behavior with exogenous signals in light of the performed $\mathcal{L}_2$ gain optimization. One can see that, in Figure 4.7, for $t \geq 5s$ the perturbation has a strong effect on the open-loop response, causing the agents to drift away from one another. This effect is

significantly reduced in the closed-loop dynamics: in Figure 4.5 the dynamics is less sensitive to the same perturbation. Furthermore, the responses in Figure 4.5 and 4.6 are identical for $t \geq 7s$ because the saturation level does not affect the control input signal.

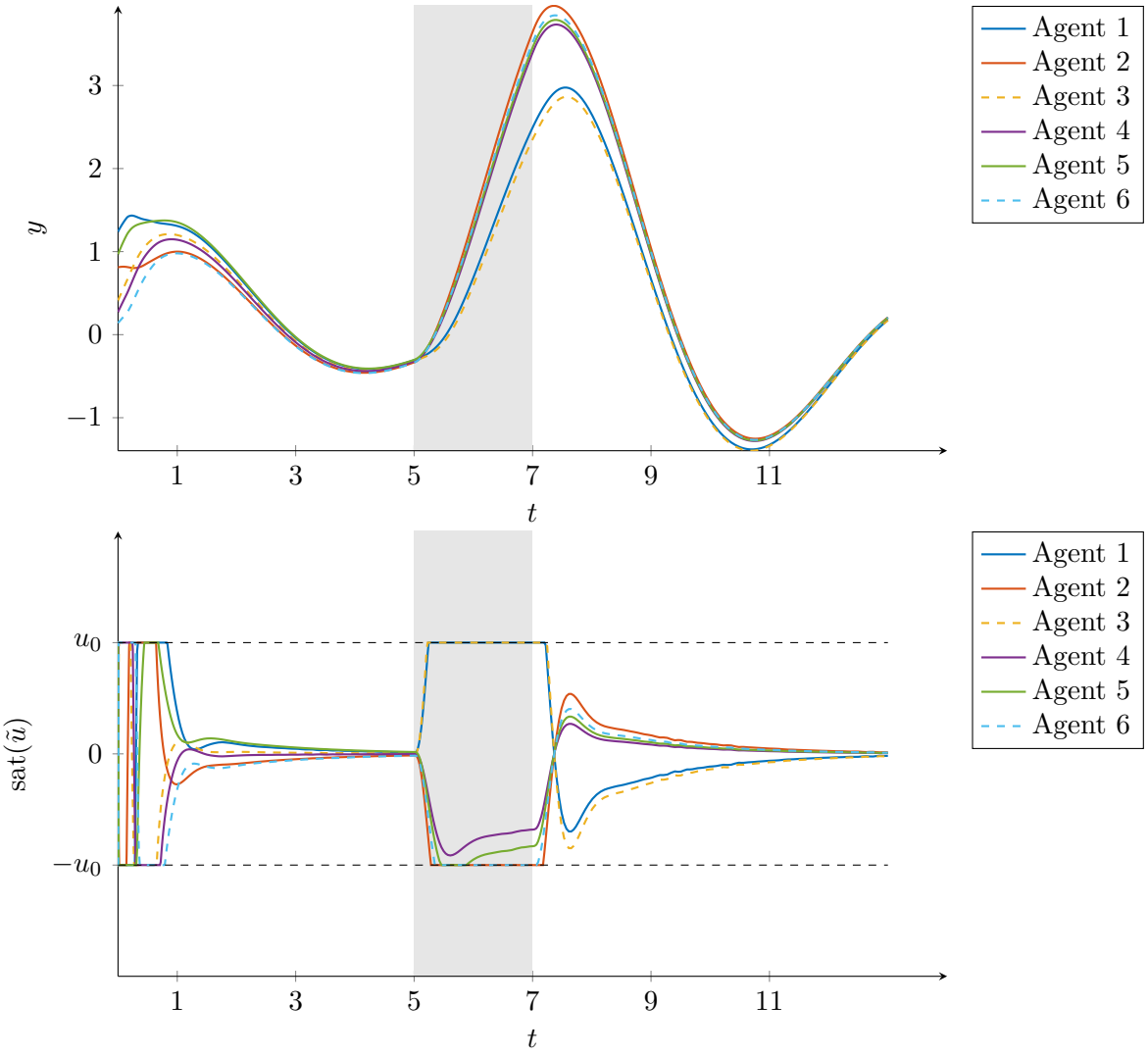

Figure 4.5: Evolution of the agent outputs (top) and inputs (bottom) in the closed-loop saturated case.

4.8 Summary and Local State Synchronization

In this chapter, we addressed the problem of global synchronization of a network of agents corresponding to identical linear continuous-time systems within a fully connected net-

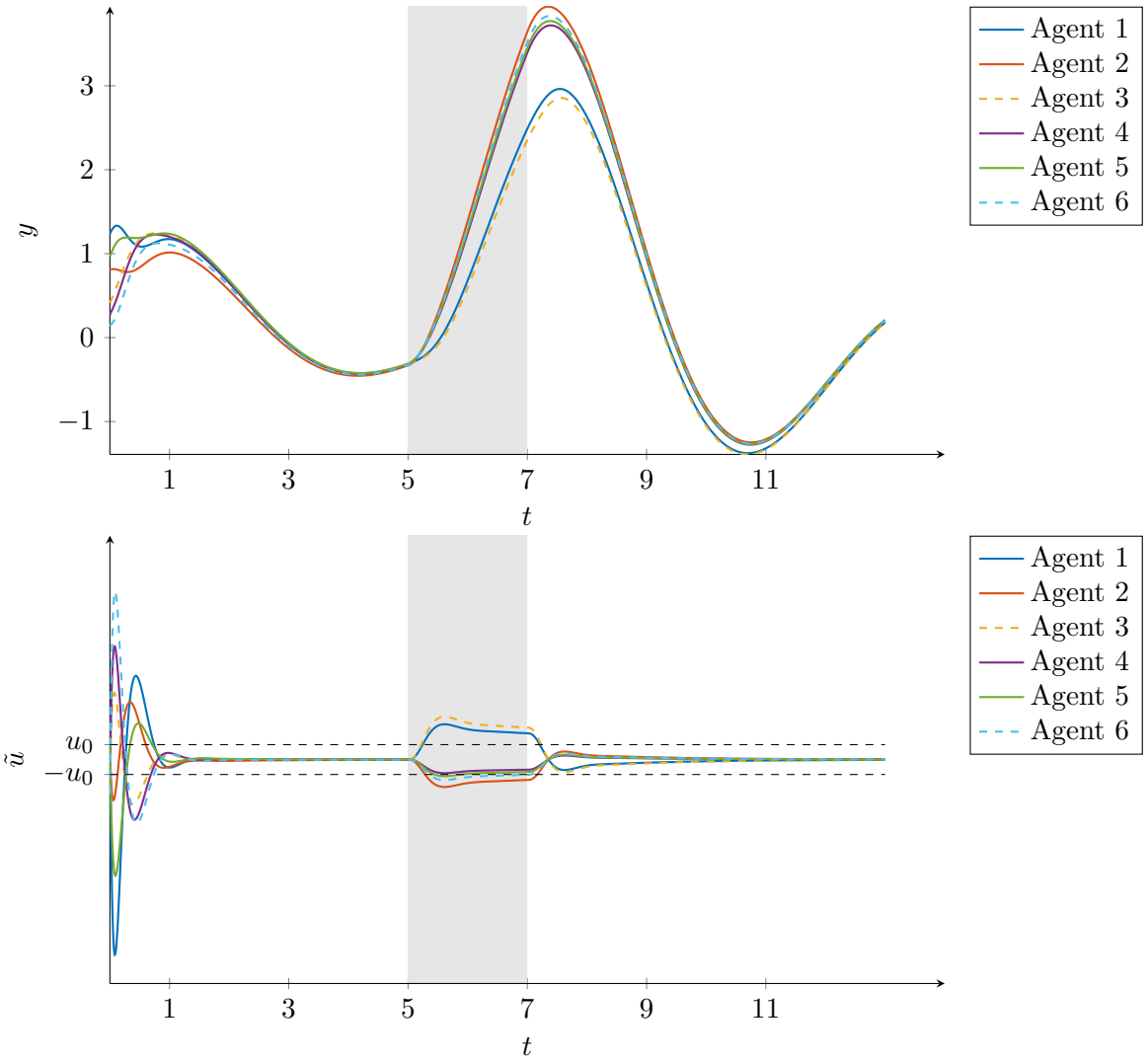

Figure 4.6: Evolution of the agent outputs (top) and the agent inputs (bottom) in the unconstrained case $\text{sat}(\tilde{u}_i) = \tilde{u}_i$.

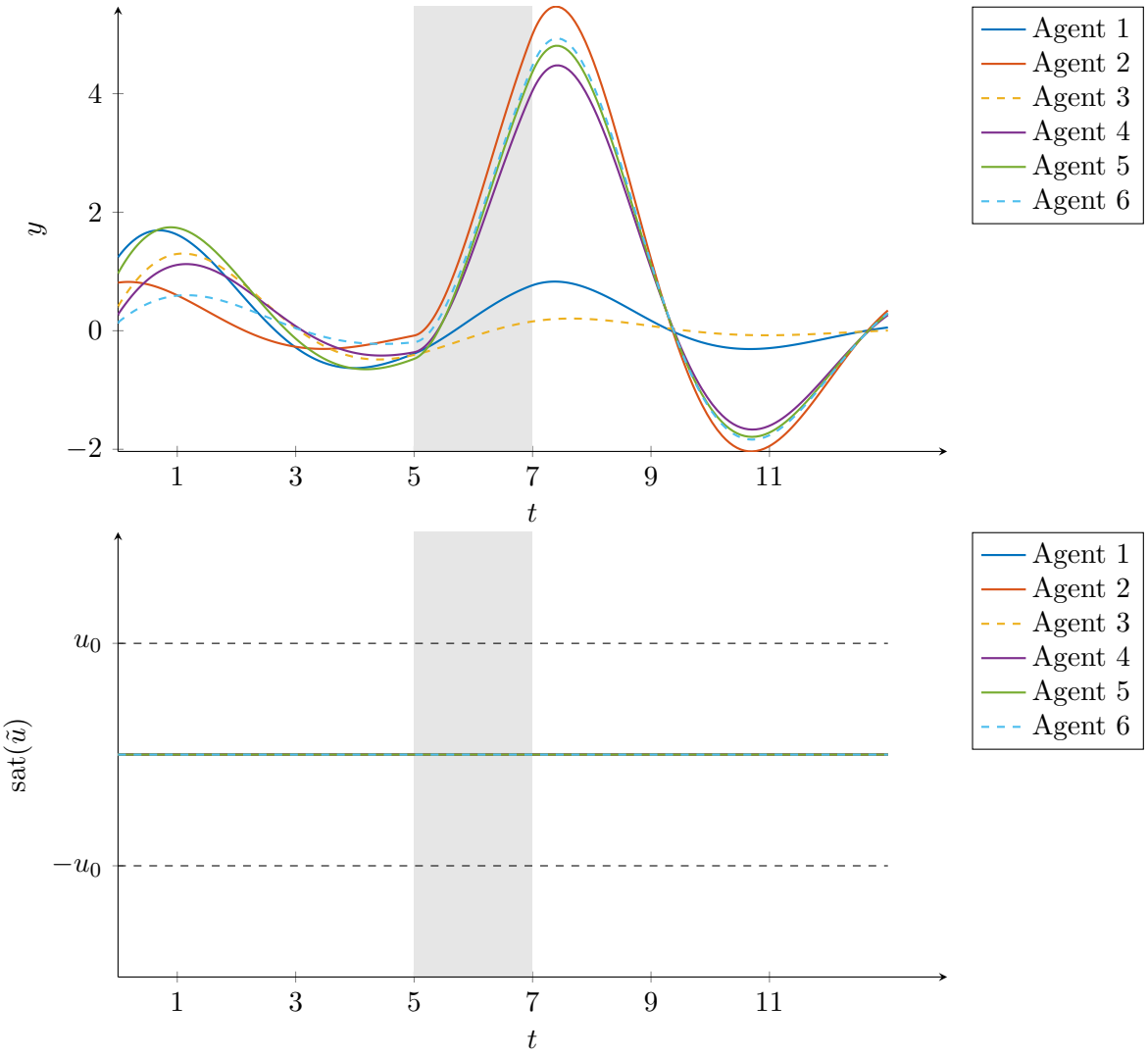

Figure 4.7: Evolution of the agent outputs (top) and the agent inputs (bottom) in the open-loop case.

work, and in the presence of saturation constraints. Each agent is subject to control input magnitude saturation and is affected by an $\mathcal{L}_2$ bounded disturbance. To solve the state synchronization problem we designed a dynamic output feedback compensator with static anti-windup loop. This problem has been characterized by linear matrix inequality conditions that ensure global state synchronization, a guaranteed and optimized H_∞ performance level, and a guaranteed local synchronization rate. Simulation results confirmed the effectiveness of the proposed solution.

The results presented in this chapter have been extended considering the following observations. It is interesting to relax the assumption on the asymptotic stability of matrix A_p. From the result for stabilizability of linear systems with bounded signals (see, e.g, [88] and [49]), we know that if the plant is exponentially unstable, then the null controllability region is bounded and global results cannot be achieved. The same concept applies in the multi-agent system context. If matrix A_p in (4.1) is exponentially unstable, only local state synchronization can be achieved. In this case, we need to determine the set of admissible states $\mathcal{X}_0 \subset \mathbb{R}^{Nn}$ in which the closed-loop system can be initialized in order to guarantee synchronization. Hence, our goal in this local context, is to design a controller in the form (4.7) in such a way that along solutions to the distributed closed-loop system satisfy

$$\lim_{t\to+\infty} x_{pi}(t) - x_{pj}(t) = \mathbf{0}_n,\ \forall i, j \in \mathbb{N} \tag{4.61}$$

as long as the initial conditions are sufficiently close to the synchronization set $\mathcal{S}_e$ in (4.17). More specifically, we are interested in establishing synchronization conditions that guarantee local asymptotic stability of $\mathcal{S}_e$ in (4.17) with a certain guaranteed region of attraction $\mathcal{X}_0$ containing set $\mathcal{S}_e$ in its interior.

If we take into account performance specifications, such as disturbance rejection, the following problem can be stated.

Problem 4.2. (Local State Synchronization Problem) *Consider the multi-agent system* (4.1) *subject to exogenous disturbances and input saturation constraints. Given the set*

$$\tilde{\mathcal{W}} = \left\{ \tilde{w}_i \in \mathcal{L}_2 : \textstyle\sum_{i=1}^{N} \|\tilde{w}_i\|_2^2 \leq \delta^{-2} \right\}, \tag{4.62}$$

the local consensus problem consists in finding a control law $\tilde{u}_i$ such that for any initial condition $x_{pi}(0) \in \mathcal{X}_0$

- *if $\tilde{w}_i = \mathbf{0}_q$ for all $i \in \mathcal{N}$, there exists a trajectory $\bar{x}_p$ such that the agent states x_{pi} in* (4.1) *satisfy* (4.61).
- *if $\tilde{w}_i \neq \mathbf{0}_q$ for some $i \in \mathcal{N}$, and any $\tilde{w}_i \in \mathcal{W}$, the relation* (4.5) *is satisfied for a prescribed bound $\gamma > 0$.*

The main difficulties in solving Problem 4.2 rely in providing a generalized sector condition extending the global results stated in Lemma 4.2. Moreover, the definition of a local sector condition allows to characterize the certified stability region $\mathcal{X}_0$—namely, the estimate of the region of attraction. Note that, if we use the sector narrowing technique

in [22], we are not able to provide an explicit estimate of the region of attraction $\mathcal{X}_0$. In fact, the energy of the perturbation is directly related to the size of the set $\mathcal{X}_0$. Intuitively speaking, for significant perturbations we expect the synchronization region to be smaller. Moreover, when considering the local synchronization context, the matrix inequality condition (4.37) must be completed by using the generalized sector condition, and a new inclusion condition must be added in order to guarantee that the set

$$\mathcal{E}(P,\hat{\delta}) := \left\{ x \in \mathbb{R}^{2Nn} : \textstyle\sum_{1\leq i<j\leq N} (x_i - x_j)^\top P (x_i - x_j) \leq (\lambda_2 \delta^{-2}) \right\}$$

is a region of local synchronization, where $P = P^\top > 0$ is solution to a Lyapunov-type inequality, and λ_2 is the second smallest eigenvalue of the Laplacian matrix.

Moreover, it is also interesting to generalize the state synchronization problem of multi-agent systems under input saturation constraints considering more generic interconnection topologies—that is, relax Assumption 4.2 to undirected distributed interconnections. As pointed out in Remark 4.3, the convexity of the synchronization conditions is related to the fully connected topology of the network. This means that, if we consider undirected topologies, the change of coordinates (4.53) can not be applied, and the resulting matrix inequalities conditions are not convex. To cope with this problem, we may apply the relaxation technique introduced in Section 3.5 to perform the control design.

The aforementioned elements—namely, the local state synchronization problem with input saturation constraints and energy-bounded perturbations, has been addressed in the work [25], which is currently under review.

Chapter 5

Synchronization in Quality-Fair Video Delivery

This chapter deals with the application of synchronization concepts in multimedia traffic. The rapid advances in communication and storage technologies have heralded a new era of multimedia traffic. There are still many open problems in terms of how to efficiently provide quality of service requirements for mobile users. One particularly challenging problem is multimedia streaming, where demand for better quality and small transmission delays needs to be reconciled with limited communication resources. The main technical difficulties for media streaming include the following:

(i) Media streaming usually has large volume of data, and the volume of data may vary with time. For instance, the sources for most video streaming application are sequences with high bit-rates. However, wireless networks have limited bandwidth. In order to support media streaming over limited capacity networks, the rate at which the contents are transmitted needs to be adapted. As an example, media resources can be compressed and encoded, and then sent to limited-capacity links.

(ii) Media streaming has stringent delay requirements. Media streaming cannot tolerate much variation in delay if the buffer starves: once the playout starts, it needs to keep playing.

(iii) Different media content segments have different rate-distortion characteristics. For example, some segment may be part of an action movie and requires a lot of bits to encode, while others may be part of a video with less bits to encode, such as a scene of news broadcast. In a system supporting many users, this type diversity in content-rate distortion characteristics also needs to be accounted for.

In this chapter, we propose a new controller design based on Proportional Integral (PI) loops to regulate the delivery of multimedia contents over a limited capacity channel. We want to provide mobile users with similar quality of service, keeping the controlled network stable and robust. The difficulties described above are taken into account, discussed, and overcome. The problem we want to solve is a quality-fair delivery problem, which can be cast into a synchronization problem, by noticing that the goal is to reach an agreement in terms of quality of service of the delivered videos. Once the goal is set, we can exploit the mathematical methodology developed in Chapter 2. Let us first provide an overview of the literature related to the quality-fair delivery problem under consideration in this chapter.

5.1 Overview

In recent years, video-on-demand has emerged as one of the most important applications of multimedia. The delivery of compressed videos has increased rapidly with the development of wireless networks and the widespread use of smartphones [48]. Among all multimedia applications, videos require the largest amount of bandwidth. Being a scarce resource, efficient bandwidth utilization is the main concern in video broadcasting schemes. Moreover, operators have to satisfy application-layer quality-of-service constraints, which are more challenging than traditional network-layer quality-of-service constraints.

In this chapter, we consider the problem of the parallel delivery of multiple encoded video streams to mobile users through a dedicated broadcast channel of limited capacity. We want to provide the users with video contents of similar qualities. A blind-source allocation may lead to unacceptable quality for high-complexity video compared to lower-complexity ones. For this reason, it is necessary to apply a resource allocation criterion.

In this scenario, we introduce the concepts of *utility* and *fairness*. The utility function is a measure of users' happiness of the quality of service [86]. There are several metrics to describe the utility measure, like Peak Signal-to-Noise Ratio (PSNR) and Structural SIMilarity (SSIM) [107]. In this application we measure the utility in terms of video PSNR. Fairness is one of the main concerns for resource allocation when many users are sharing limited network resources; in this application we consider fairness in utility of the delivered contents.

Several protocols and design philosophies have been proposed in the literature for resource allocation in multimedia traffic. We can consider utility max-min fair sharing, which amounts to the maximization of the minimum utility. The utility max-min fair criterion is discussed in [9], [19], and references therein. Nevertheless, this scheme does not consider the temporal variability of the rate-utility characteristics (RUCs) of the contents nor the delays introduced by the network and the buffers of the delivery system. As pointed out previously, the control of the communication delays is a crucial requirement in multimedia streaming.

For video contents competing bandwidth in networks, the content-aware networking approach brings the intelligence of video source coding at the application layer and

network resource engineering together. The work [54] presents a content-aware video delivery scheme that optimizes the max-min distortion fairness of many users sharing a network. For video contents, the utility function is time-varying and it is hard to estimate it accurately on the fly. For this reason, [54] assumes that the utility of each frame is known in advance. This content-aware scheme can be used for the streaming of stored videos. Similarly, [20] proposes a cross-layer method that maximizes the sum of the achievable rates while minimizing the distortion difference among the received video sequences.

Using a different approach, [14] performs the encoding rate control together with the buffer level control. The average quality of the streams is maximized. This scheme considers constraints on the transmission rate and on the Peak Signal-to-Noise Ratio (PSNR) discrepancy of the delivered videos. This multi-objective problem is formulated by means of Lagrange decomposition and stochastic programming. Both approaches in [20] and [14] require to gather all RUCs of the streams at the control unit.

In [17], the user experience is accurately modeled by the subjective cumulative distribution function of the predicted video quality. In contrast with conventional average-quality maximized rate-adaptation algorithm, the work [17] adopts a different control strategy. This strategy is a threshold-based admission policy, that blocks users whose empirical cumulative quality distribution is not likely to satisfy their quality constraint.

In this chapter, we adopt the control method presented in [13], [15]. The heuristic control approach used in these works is based on PI control loops. The controllers are used to regulate the encoding rate of video servers and the transmission rate of the video streams towards the channel. We do this joint control because, if the videos are encoded at a constant bit-rate, the quality may change significantly with the variations of the characteristics of the contents. On the other hand, if the contents are encoded at a variable bit-rate, the buffering delay may increase significantly, leading to unacceptable delivery fluctuations. The joint actions of the controllers provide the desirable effect in terms of video-fairness: videos with utility below the average are drained faster through the corresponding buffers, and the encoding rate of such streams is then increased to improve the quality. In the scheme [13], [15] the control is performed in some Media Aware Network Element (MANE) [5] at the bottleneck of the links between the remote servers and the communication channel. The MANE is located close to the Base Station (BS), to which the clients are connected. In this *fully centralized* version of the controller, the MANE is in charge of sending the encoding rate target to each video server, based on the measure of the buffer level. On the contrary, in a *partially distributed* control architecture, the servers receive only the individual buffer discrepancies, and they are in charge of computing the encoding rate. In this specific application, a fully centralized architecture is convenient with respect to the distributed one, because we want to compute as fast as possible a global parameter of the network—that is, the mean value of the utility functions of the users. This may take longer if the calculations are performed in a distributed fashion, possibly causing freeze-ups in playback.

The aim of this chapter is to provide an optimized method to perform the gain tuning of the PI controllers for the quality-fair video streaming control proposed in [13], [15].

The nonlinear model in [13], [15] is linearised, so that we can apply the general synchronization results contained in Chapter 2. We give here necessary and sufficient conditions for the synchronization among the quality measures of the delivered video streams. This result is obtained by casting the fair-delivery requirement into a problem of synchronization for identical linear systems.

Moreover, we propose two control design strategies. The first one is a heuristic technique based on the Jury stability criterion, that consists in determining the stability of a linear discrete-time system by analyzing the coefficients of its characteristic polynomial, see [53, Section 9.9.3]. The second one is systematic and optimized PI tuning procedure, based on static output feedback design. The resulting conditions for the output feedback control design are nonlinear matrix inequalities. To perform the control design, we find the solution to these conditions using an ILMI technique, like the one described in Section 2.4. The algorithm presented in this chapter is the extension to the discrete-time case of the static output feedback design technique for continuous-time agents presented in Algorithm 2.1 in Chapter 2.

These controller design methods are based on the assumption that the linearised model of the system closely approximates the non-linear behavior observed in reality. These control strategies are then tested in the real nonlinear model, proving the effectiveness of the linear time-invariant approximation for the controller synthesis.

5.1.1 Model Description

Consider a broadcasting system, see [13], in which N encoded video streams are provided by N remote servers that share a communication channel of total transmission rate R_c, see Figure 5.1. The Media Aware Network Element (MANE) contains N dedicated buffers that temporarily store the encoded video streams, as groups of pictures (GoPs). The MANE contains the encoding rate controllers and the transmission rate controllers. The encoding rate controllers limit the deviations of the current buffer level B_i from the reference level B_c, equal for all the streams. The transmission rate controllers adjust the drain rates of the buffers, using the the quality information of the stored GoP—that is, the utility. We denote with U_i^{dd}, $i \in \mathcal{N}$ the value of the utility function of each GoP.

In the following, we assume that time is slotted with a period T and each video server is controlled synchronously, with GoPs of the same duration T. All the propagations and queues in the system are modeled as time delays of duration T. We do not model packet losses, which are handled at the MAC layer.

The above setting leads to a discrete-time state-space representation of the controlled system. Each controlled video stream is identified by the subscript index $i \in \mathcal{N} = \{1, \dots, N\}$, and described by the following set of equations (see [13, equation (22)])

$$a_i(j)^+ = a_i(j) + \delta a_i(j) \tag{5.1a}$$

$$U_i^{dd}(j)^+ = f(a_i(j), R_i^{ed}(j)) \tag{5.1b}$$

$$\Pi_i^b(j)^+ = \Pi_i^b(j) + (B_i(j) - B_c) \tag{5.1c}$$

$$R_i^{ed}(j)^+ = R_0 - \tfrac{K_P^{eb}+K_I^{eb}}{T}(B_i(j) - B_c) - \tfrac{K_I^{eb}}{T}\Pi_i^b(j) \tag{5.1d}$$

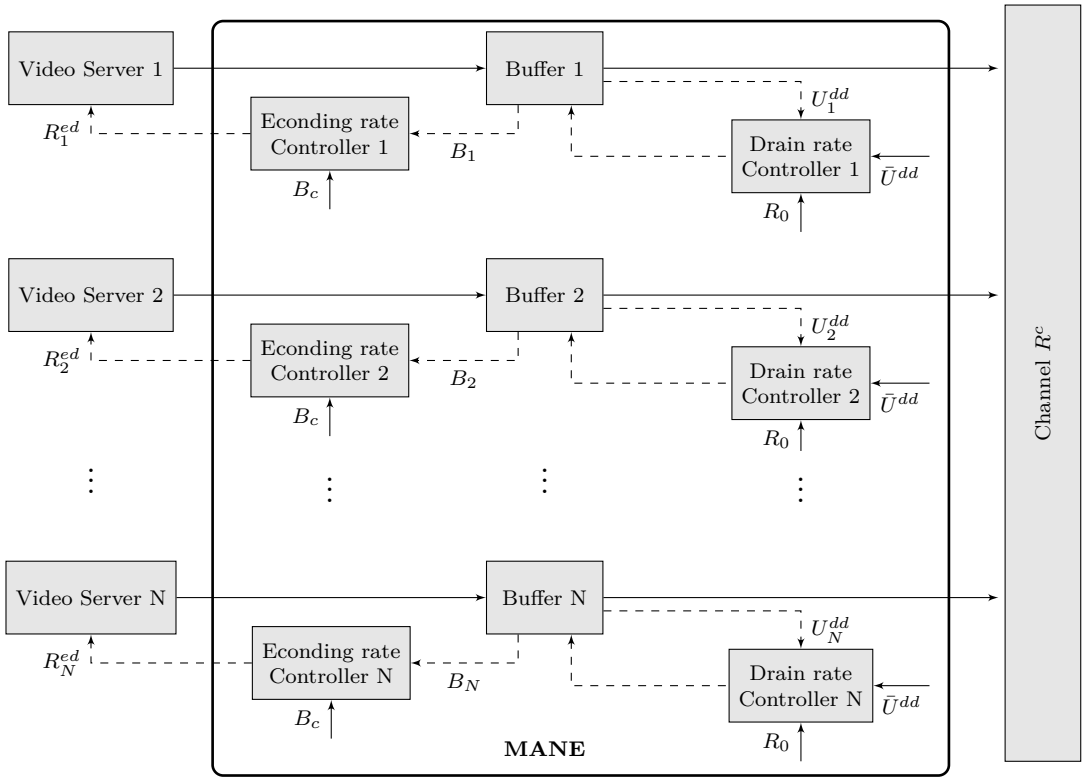

Figure 5.1: Structure of the quality-fair delivery system. N Video Servers send encoded video streams to a Channel of limited capacity R_c. The centralized controllers are located close to the bottleneck of the link. The bold line delimits the MANE, that contains the buffers, the encoding rate, and transmission rate control loops.

$$R_i^{edd}(j)^+ = R_i^{ed}(j) \tag{5.1e}$$
$$\Phi_i(j)^+ = \Phi_i(j) + \Delta U_i^{dd}(j) - U_i^{dd}(j) \tag{5.1f}$$
$$B_i(j)^+ = B_i(j) + [R_i^{edd}(j) - R_0 + (K_P^t + K_I^t)\Delta U_i^{dd}(j) - K_I^t \Phi_i(j)]T \tag{5.1g}$$
$$\Delta U_i^{dd}(j) = \bar{U}^{dd}(j) - U_i^{dd}(j), \tag{5.1h}$$

where we denote with $x^+(j) = x(j+1)$ the one-step forward shift operation for discrete-time systems. Equations (5.1a)-(5.1b) constitutes the source model, that describes the nonlinear dependence of the utility output U_i^{dd} on the video-source characteristics a_i^d and on the encoding rate R_i^{ed} through the nonlinear function f. The quantity a_i^d models the time-varying nature of the utility as a function of the encoding rate R_i^{ed}. The nonlinear function f is a continuous and increasing function of R_i^{ed}, which is the main nonlinearity of model (5.1). The encoding rate controller is characterized by (5.1c)-(5.1e), and it regulates the buffer level B_i around the reference level B_c. We assume that the reference encoding rate is $R_0 = \frac{R_c}{N}$—that is, the rate that would be allocated in a rate-fair scenario. The parameters K_P^{eb} and K_I^{eb} are the proportional and integral

controller gains, respectively, corresponding to the first two parameters to be tuned.

Finally, the drain rate controller is described by (5.1g)-(5.1h). The buffer draining rate is updated comparing the utility function U_i^{dd} of the stream, with the mean value $\bar{U}^{dd}(j) = \frac{1}{N}\sum_{k=1}^{N} U_k^{dd}(j)$ of the utilities of the overall system. The parameters K_P^t and K_I^t are the proportional and integral controller gains, respectively, corresponding to the second set of parameters to be tuned.

The goal of this chapter is to provide a method to tune the PI controllers gains K_P^{eb}, K_I^{eb}, K_P^t, K_I^t in order to guarantee the asymptotic convergence of the utilities $U_i^{dd}(j)$ in (5.1b) to a common value $\bar{U}$, that is

$$\lim_{j\to+\infty} \left| U_i^{dd}(j) - \bar{U} \right| = 0, \quad i \in \mathcal{N}. \tag{5.2}$$

Remark 5.1. We emphasize that the architecture of the MANE corresponds to a fully connected graph representation. Indeed, (5.1h) can be rewritten as

$$\Delta U_i^{dd}(j) = \tfrac{1}{N}\textstyle\sum_{k=1}^{N} \left(U_k^{dd}(j) - U_i^{dd}(j) \right) = \tfrac{1}{N}\textstyle\sum_{k=1}^{N} U_k^{dd} - U_i^{dd}, \tag{5.3}$$

which corresponds to a fully connected graph—that is, a centralized control strategy (see Definition 4.2). Using the tools presented in this chapter we can alternatively perform a distributed control strategy for the proposed video delivery system. More precisely, a distributed control policy is obtained by replacing (5.1h) with

$$\Delta U_i^{dd}(j) = \tfrac{1}{|\mathcal{N}_i|}\textstyle\sum_{k\in\mathcal{N}_i} U_k^{dd}(j) - U_i^{dd}(j), \tag{5.4}$$

where $\mathcal{N}_i$ denote the set of streams connected with the ith stream, and $\mathcal{N}_i \neq \mathcal{N}$. In this work we stick with the current fully connected architecture because it corresponds to the technological structure of MANE, and because it allows for a comparison with pre-existing works.

In the next section, we will present more in detail the control architecture, and we will introduce a convenient change of coordinates that allows us to apply the synchronization results contained in Chapter 2.

5.1.2 Two PI control loops

In this section we provide a state-space representation of model (5.1), in order to highlight the different actions performed by the encoding rate and transmission rate controllers on the network. This representation leads to a convenient formulation of the PI gains tuning, which allows us to develop the design techniques presented in this chapter. For the sake of simplicity, in the remainder of the chapter, we drop the dependence of the system variables on the time index j.

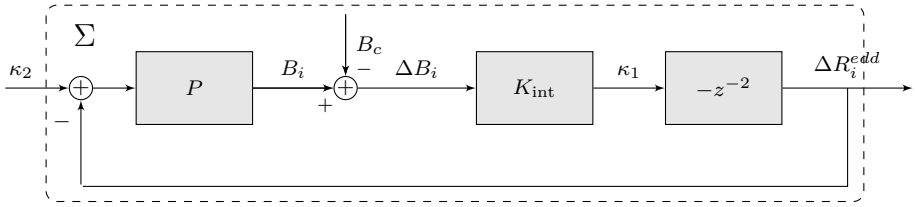

Figure 5.2: Block diagram representation of the encoding rate control loop for system (5.1). This loop is also called the *internal loop*.

The encoding rate controller (denoted by K_{int} in Figure 5.2), described by (5.1c)-(5.1e), is characterized by the following state-space representation

$$\Pi_i^{b+} = \Pi_i^b + \Delta B_i \tag{5.5a}$$
$$\kappa_1 = \tfrac{k_I^{\text{int}}}{T}\Pi_i^b + \tfrac{k_P^{\text{int}}}{T}\Delta B_i, \tag{5.5b}$$

where Π_i^b is the controller state, $\Delta B_i = B_i - B_c$ is the controller input, and $\kappa_1 = -\Delta R_i^e = -(R_i^e - R_0)$ is the controller output. The integral and proportional gains k_P^{int} and k_I^{int} are related to K_P^{eb}, K_I^{eb} according to the invertible relation

$$k_P^{\text{int}} = K_P^{eb} + K_I^{eb}, \quad k_I^{\text{int}} = K_I^{eb}. \tag{5.6}$$

The encoding rate controller acts on the system (denoted by P in Figure 5.2) whose input-output relation is

$$\Delta R_i^{ed+} = \Delta R_i^e = -\kappa_1 \tag{5.7a}$$
$$\Delta R_i^{edd+} = \Delta R_i^{ed} \tag{5.7b}$$
$$\Delta B_i^{+} = \Delta B_i + T(\Delta R_i^{edd} - \kappa_2). \tag{5.7c}$$

In the sequel we denote with Σ the controlled system (5.5)-(5.7) from κ_2 to ΔR_i^{edd} (see Figures 5.2 and 5.3).

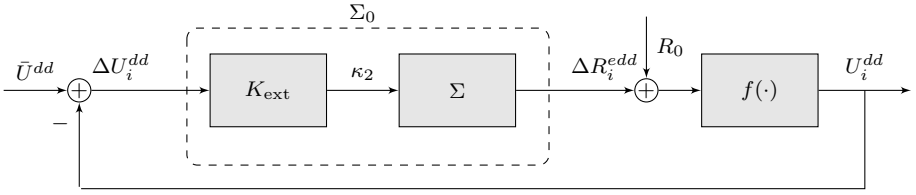

Figure 5.3: Block diagram representation of the draining rate control loop for system (5.1). This loop is also called *external loop*.

The transmission rate controller (denoted with K_{ext} in Figure 5.3), described by (5.1g)-(5.1h) and (5.3), provides the reference signal κ_2 to the closed-loop system (5.5)-(5.7) according to

$$\Phi_i^{s+} = \Phi_i^s + \tfrac{\Delta U_i^{dd}}{\nu} \tag{5.8a}$$

$$\kappa_2 \;=\; k_I^{\text{ext}}\Phi_i^s + \tfrac{k_P^{\text{ext}}}{\nu}\Delta U_i^{dd}, \tag{5.8b}$$

where $\nu > 0$ is a normalization constant, $\Phi_i^s = \frac{\Phi_i}{\nu}$ is the controller state, $\Delta U_i^{dd} = U_i^{dd} - \bar{U}^{dd}$ is the controller input, and κ_2 is the controller output, and $\bar{U}^{dd} = \frac{1}{N}\sum_{k=1}^{N} U_k^{dd}$ is the average utility among the video streams. The integral and proportional gains k_P^{ext} and k_I^{ext} are related to K_P^t, K_I^t according to the invertible relation

$$k_P^{\text{ext}} = \nu(K_P^t + K_I^t), \quad k_I^{\text{ext}} = \nu K_I^t. \tag{5.9}$$

Note that the integral actions of K_{int} and K_{ext} reject the constant reference buffer level B_c and the constant average encoding rate R_0, respectively.

From the structure of (5.5), (5.7), and (5.8), we notice that the overall system is composed by two nested control loops. The following state-space representation highlights the different separate actions performed by controllers K_{int} and K_{ext}. Denote with $(A_{\text{int}}, B_{\text{int}}, C_{\text{int}}, D_{\text{int}})$ and $(A_{\text{ext}}, B_{\text{ext}}, C_{\text{ext}}, D_{\text{ext}})$ the matrices that characterize the state-space model of Σ and K_{ext}, respectively. Then, combining (5.5) and (5.7) for Σ and (5.8) for K_{ext}, we can represent the i-th video stream dynamics using the states

$$x_{\text{int},i} = \begin{bmatrix} \frac{\Delta B_i}{T} & \frac{\Pi_i}{T} & \Delta R_i^{ed} & -\Delta R_i^{edd} \end{bmatrix}^\top, \quad x_{\text{ext},i} = \Phi_i^s. \tag{5.10}$$

With this selection, the state-space matrices of Σ and K_{ext} are

$$\left(\begin{array}{c|c} A_{\text{int}} & B_{\text{int}} \\ \hline C_{\text{int}} & D_{\text{int}} \end{array}\right) = \left(\begin{array}{cccc|c} 1 & 0 & 0 & -1 & -1 \\ 1 & 1 & 0 & 0 & 0 \\ -k_P^{int} & -k_I^{int} & 0 & 0 & 0 \\ 0 & 0 & -1 & 0 & 0 \\ \hline 0 & 0 & 0 & -1 & 0 \end{array}\right), \tag{5.11}$$

$$\left(\begin{array}{c|c} A_{\text{ext}} & B_{\text{ext}} \\ \hline C_{\text{ext}} & D_{\text{ext}} \end{array}\right) = \left(\begin{array}{c|c} 1 & \frac{1}{\nu} \\ \hline k_I^{\text{ext}} & \frac{k_P^{\text{ext}}}{\nu} \end{array}\right). \tag{5.12}$$

Consider now the cascaded interconnection of K_{ext} and Σ (denoted with Σ_0 in Figure 5.3), which establishes the linear relation from ΔU_i^{dd} to ΔR_i^{edd}. A state-space representation of Σ_0 defined through the following matrices

$$\left(\begin{array}{c|c} A_0 & B_0 \\ \hline C_0 & \end{array}\right) = \left(\begin{array}{cc|c} A_{\text{ext}} & 0 & B_{\text{ext}} \\ B_{\text{int}}C_{\text{ext}} & A_{\text{int}} & B_{\text{int}}D_{\text{ext}} \\ \hline 0 & C_{\text{int}} & \end{array}\right). \tag{5.13}$$

Note that matrix A_0 has a lower block-triangular structure, and then, the eigenvalues of A_0 are the union of the eigenvalues of the diagonal blocks A_{int} and A_{ext}. This observation suggests that the two PI controllers act separately on the system dynamics: in particular controller K_{int} performs an internal stabilization of each video stream, while controller K_{ext} performs the external synchronization of the video streams utilities of the network.

5.2 Necessary and Sufficient conditions for Quality-Fair Video Delivery

In this section we cast the quality-fair delivery problem introduced in Section 5.1.1 into a synchronization problem. More precisely, we want the network (5.1) to reach agreement on a quantity of interest—that is the utility function U_i^{dd} of the video streams.

For instance, each system in (5.1) can be associated to a node in a graph $\mathcal{G} = (\mathcal{V}, \mathcal{E})$, and it is an agent in the network. Each edge $(v_j, v_i) \in \mathcal{E}$ represents a communication link from agent i to agent j. From Remark 5.1, we deduce that the graph $\mathcal{G}$ is undirected and fully connected, as in the considered application each connection allows bidirectional and all-to-all communication between each agent. More details on graph theory are contained in Appendix A.

The coupling among the agents arises from the average utility $\bar{U}_i^{dd}$ of the video streams, acting as the reference input of the closed-loop system (see Figure 5.3). According to (5.1b), the quantity U_i^{dd} is a nonlinear function of the video-source parameters a_i^{dd} and the encoding rate R_i^{edd}. It can be expressed as

$$U_i^{dd} = f(a_i, R_i^{edd}) = f(a_i^{dd}, \Delta R_i^{edd} + R_0), \quad i \in \mathcal{N}. \tag{5.14}$$

We make the following assumption, so that a linear time-invariant analysis of the consensus algorithm can be performed.

Assumption 5.1. *For each $i = 1, \ldots, N$, a_i in (5.1a) is constant—that is, $\delta a_i = 0$—for each i. Moreover there exist scalars h_i, $i = 1, \ldots, N$ and a scalar $K_f > 0$ such that:*

$$U_i^{dd} = f(a_i, R_i^{edd}) = h_i + K_f R_i^{edd} = h_i + K_f R_0 + K_f \Delta R_i^{edd}, \quad i \in \mathcal{N}. \tag{5.15}$$

Intuitively speaking, K_f translates the variation of utility provided by a variation of the video encoding rate.

Remark 5.2. Other multimedia traffic strategies model the utility function with different nonlinear approximations. As an example, [51, Section 2.3] considers a utility function that is logarithmic with the allocated rate. Using a different approach, [96] uses a non-differentiable utility function referred to as *staircase*. Alternatively, [50] adopts a sigmoidal-like utility function. However, a linear approximation like the one we propose in (5.15) is reasonable in some practical applications, like in MPEG-FGS video coders or MPEG-2 encoding (see [47, Section 5.3.1]).

Based on Assumption 5.1 and on the integral action of controller K_{ext}, we perform a coordinate change to compensate for the action of the constant disturbance $h_i + K_f R_0$, so that the overall system can be written as an output feedback network interconnection of N identical linear systems

$$\begin{array}{rcll} x_i^+ & = & A_0 x_i + B_0 \Delta U_i^{dd} & \\ U_i^{dd} & = & K_f C_0 x_i, & i \in \mathcal{N}, \end{array} \tag{5.16}$$

where $x_i \in \mathbb{R}^n$ is the state vector and U_i^{dd} the scalar output. Define the stacked column vectors

$$U^{dd} := \begin{bmatrix} U_1^{dd} & \cdots & U_N^{dd} \end{bmatrix}^\top, \; \Delta U^{dd} := \begin{bmatrix} \Delta U_1^{dd} & \cdots & \Delta U_N^{dd} \end{bmatrix}^\top. \tag{5.17}$$

The relation between ΔU^{dd} and U^{dd} in (5.17) can be rewritten in compact form using (5.1h) as

$$\Delta U^{dd} = -LU^{dd}, \tag{5.18}$$

where $L = [L_{ij}] \in \mathbb{R}^{N \times N}$, and

$$L_{ij} := \begin{cases} \frac{N-1}{N}, & \text{if } i = j \\ -\frac{1}{N}, & \text{if } i \neq j. \end{cases} \tag{5.19}$$

The matrix L corresponds to the Laplacian matrix of the graph $\mathcal{G}$, which is *fully connected*, due to the centralized nature of the proposed control. This structure is intrinsic of the solution to the specific technological application and here we reinterpret it in a consensus framework. Define the aggregate vectors

$$x := \begin{bmatrix} x_1^\top & \cdots & x_N^\top \end{bmatrix}^\top \in \mathbb{R}^{Nn}, \quad y := \begin{bmatrix} y_1 & \cdots & y_N \end{bmatrix}^\top \in \mathbb{R}^N, \tag{5.20}$$

where $y_i = U_i^{dd}$, for $i \in \mathcal{N}$. Combining (5.16), (5.18) and (5.20), and using the Kronecker product, we obtain the following expression for the dynamics of the interconnected system

$$\begin{array}{rcl} x^+ & = & (I_N \otimes A_0)x - (L \otimes B_0)y \\ y & = & U^{dd} = (I_N \otimes K_f C_0)x, \end{array} \tag{5.21}$$

with A_0, B_0 and C_0 defined in (5.13). With the goal of establishing synchronization among the utilities U_i^{dd}, we consider the synchronization set introduced in (2.9):

$$\mathcal{S} := \{x \in \mathbb{R}^{Nn} : \; x_1 = x_2 = \cdots = x_N\}. \tag{5.22}$$

The properties of the set $\mathcal{S}$ are summarized in Section 2.2. We are ready to state a set of necessary and sufficient conditions for output synchronization for the identical discrete-time linear systems (5.16) with interconnection (5.18). As specified in (5.2), synchronization in the above model means that all the individual system utilities U_i^{dd} asymptotically reach a common, constant value $\bar{U}$. The following theorem particularizes Theorem 2.1 to discrete-time linear agents connected through an undirected and fully connected graph, in which the synchronization trajectory is a constant value.

Theorem 5.1. *Consider the closed-loop system* (5.21)*. The following statements are equivalent:*

(i) Matrices A_{int} *and*

$$A_f := A_0 - \tfrac{N}{N-1} B_0 K_f C_0 \tag{5.23}$$

are Schur-Cohn.

(ii) The synchronization set $\mathcal{S}$ in (5.22) *is uniformly globally exponentially stable for the closed-loop dynamics* (5.21)*, and matrix A_{int} is Schur-Cohn.*

(iii) The interconnected system (5.21) *is such that the states x_i uniformly globally exponentially synchronize to the unique solution to the following initial value problem*

$$x_c^+ = A_0 x_c, \quad x_c(0) = \tfrac{1}{N}\textstyle\sum_{k=1}^{N} x_k(0), \tag{5.24}$$

and A_{int} is Schur-Cohn.

(iv) Given any solution to (5.21)*, there exists a constant $\bar{U} \in \mathbb{R}$ such that the output of* (5.21) *satisfies*

$$\lim_{j\to+\infty} y_i(j) = \lim_{j\to+\infty} U_i^{dd}(j) = \bar{U}, \quad i \in \mathcal{N}. \tag{5.25}$$

Proof. We prove the theorem in four steps: (i) $\iff$ (ii), (ii) $\iff$ (iii), (iii) $\implies$ (iv), and (iv) $\implies$ (i).

Proof of (i) $\iff$ (ii) Applying the equivalence between items (i) and (ii) of Theorem 2.1 when focusing on system (5.21), item (i) of Theorem 5.1 is equivalent to having that all eigenvalues λ_k of matrix L in (5.19), except for that one related to the eigenvector $\frac{\mathbf{1}_N}{\sqrt{N}}$, are such that $A_0 - \lambda_k K_f B_0 C_0$ is Schur-Cohn. Since these eigenvalues of L are coincident and equal to $\frac{N}{N-1}$, the result is proven.

Proof of (ii) $\iff$ (iii). Applying the equivalence between items (iv) and (iii) of Theorem 2.1, and noticing that, for undirected and connected graphs $\frac{\mathbf{1}_N^\top}{\sqrt{N}} L = 0$, that is, the left and right eigenvalues of L relative to $\lambda_1 = 0$ coincide.

Proof of (iii) $\implies$ (iv) Note that system (5.24) corresponds to Σ_0, whose state-space representation is given in (5.13). The state matrix A_0 has a block diagonal structure, therefore its eigenvalues are $\lambda(A_0) = \lambda(A_{\text{ext}}) \cup \lambda(A_{\text{int}}) = \{1\} \cup \lambda(A_{\text{int}})$. Since A_{int} defined in (5.11) is Schur-Cohn, all the solutions to (5.16), (5.18) converge to a constant.

Proof of (iv) $\implies$ (i). We prove this statement by contradiction. Assume that (i) does not hold. We must analyze these two situations

- A_f is not Schur-Cohn. In this case, we notice that (i) is violated, and we can conclude that the agents do not achieve exponential state synchronization for some initial conditions. From the linear input-output relation in (5.16), we conclude that (iv) does not hold.

- A_f is Schur-Cohn and A_{int} is not Schur-Cohn. In this case, from the equivalence (i) $\iff$ (iii), the states of system (5.16) exponentially synchronize to the unique solution to (5.24). Two cases may occur: **a)** A_{int} has at least one eigenvalue with magnitude larger than 1 or at least one eigenvalue on the unit circle with multiplicity larger than 1: in this case some solutions synchronize to a diverging evolution, thus item (iv) does not hold; **b)** A_{int} has at least one eigenvalue with magnitude 1 on the unit disk. If that eigenvalue is at 1, then due to the triangular

structure, matrix A_0 has two eigenvalues in 1 (the other one coming from A_{ext} in (5.12)) and again some solutions synchronize to a diverging evolution. If that eigenvalue is anywhere else in the unit circle, then it generates a revolving non-constant mode and some solutions synchronize to a non-convergent oscillatory trajectory. In both cases **a)** and **b)**, from the linear input-output relation in (5.16), item (iv) does not hold and the proof is completed.

□

Remark 5.3. Theorem 5.1 gives us the conditions under which the synchronization trajectory (5.24) is a constant value. This additional constraint is encapsulated in the stability requirement of matrix A_{int}. This condition was not present in Theorem 2.1; there, the synchronization trajectory depends on the specific problem data and is, in general, not constant.

Remark 5.4. Note that a discrete-time dead-beat controller using the knowledge of $\bar{U}^{dd}$ could achieve (5.2) in finite time, based on the knowledge of R_0, B_c and h_i. However, the filtering action of the double PI loop proposed in [13, 15] is more effective in dealing with the actual time-varying nature of (5.15), that can be well represented by suitable additional disturbances affecting the average behavior characterized by (5.15). That points out the relevance of the PI scheme.

5.3 Optimal Design of PI Controllers

In this section, we address the problem of finding suitable PI controller gains k_P^{int}, k_I^{int}, k_P^{ext} and k_I^{ext} in order to guarantee synchronization among utility measures U_i^{dd}—that is, (5.2). Similarly to Chapter 2, we want to provide an optimized procedure for the controller selection that guarantees a minimum convergence rate to consensus. As pointed out in Section 2.4, this additional requirement is obtained by constraining the eigenvalues of the dynamics orthogonal to the synchronization set $\mathcal{S}$ in (5.22)—that is, the eigenvalues of matrix A_f in (5.23).

Moreover, in the optimized gain selection, we want also to speed up the transient of system (5.24)—that is, to make the utility converge to a constant value as fast as possible. From (5.24), this amounts to constraining the eigenvalues of A_0, or, equivalently, constraining the eigenvalues of A_{int}.

Hence, the optimized gain selection consists in minimizing the spectral radius of A_f and A_{int}. We recall that the *spectral radius* $\rho(M)$ of a matrix M is the maximum of the absolute values of its eigenvalues. Due to the nested structure of closed-loop system (5.16), a possible way to implement this optimization strategy consists of two steps. First, we consider matrix A_{int} and we select k_P^{int} and k_I^{int} such that $\rho(A_{\text{int}})$ is minimized. Second, once we have determined the optimized gains $k_P^{\text{int}\star}$ and $k_I^{\text{int}\star}$ of the internal controller, we plug these values in A_f in (5.23), and we determine with the same strategy k_P^{ext} and k_I^{ext} minimizing $\rho(A_f)$. The overall control strategy can be formulated

as follows

$$\begin{aligned}(k_P^{\text{int}\star}, k_I^{\text{int}\star}, \rho_{\min}(A_{\text{int}})) := & \quad \underset{k_P^{\text{int}}, k_I^{\text{int}}}{\arg\min} \quad \rho(A_{\text{int}}); \\ (k_P^{\text{ext}\star}, k_I^{\text{ext}\star}, \rho_{\min}(A_f)) := & \quad \underset{k_P^{\text{int}}, k_I^{\text{int}}, k_P^{\text{ext}}, k_I^{\text{ext}}}{\arg\min} \quad \rho(A_f). \\ & \quad \text{s.t.} \quad k_P^{\text{int}} = k_P^{\text{int}\star}, k_I^{\text{int}} = k_P^{\text{int}\star}\end{aligned} \tag{5.26}$$

The joint optimization of the four gains k_P^{int} and k_I^{int}, k_P^{ext} and k_I^{ext}, although possible, is more convoluted with respect to the two-steps design proposed here. We prefer mathematical elegance and simplicity in the design, to more sophisticated strategies with higher computational burden. In the next sections we propose two control strategies in order to solve (5.26).

5.3.1 Control Design based on The Jury Criterion

In this section we present a heuristic strategy for the selection of the PI gains k_P^{int}, k_I^{int}, k_P^{ext} and k_I^{ext}, solving the optimization problem (5.26). The Jury stability criterion (see [53, Section 9.9.3]) is an algebraic method that determines whether the roots of a polynomial lie within the unit circle. This test can be used in our case, after having computed the characteristic polynomial of A_{int} and A_f.

As explained at the beginning of Section 5.3, we design the inner controller gains k_P^{int}, k_I^{int} first. Once we have fixed the inner loop control gains, the selection of the outer loop controller gains k_P^{ext} and k_I^{ext} is carried out.

Consider matrix A_{int}; its characteristic polynomial $p_{A_{\text{int}}}(z)$ can be computed from (5.11) and has the following expression

$$p_{A_{\text{int}}}(z) := z^4 - 2z^3 + z^2 + k_P^{\text{int}} z + (k_I^{\text{int}} - k_P^{\text{int}}). \tag{5.27}$$

We want to determine the values of the pair $k_P^{\text{int}}, k_I^{\text{int}}$, such that the roots of the polynomial (5.27) lie within the unit circle. The following Lemma gives the explicit expression of the stability region of matrix A_{int} as a function of the PI controller gains, and is obtained applying the Jury stability criterion to (5.27). The proof of this lemma is postponed to Appendix C.

Lemma 5.1. *Matrix A_{int} in (5.11) is Schur-Cohn if and only if the following conditions hold*

$$\begin{aligned}& k_I^{int} > 0 \\ & k_P^{int} + \frac{1-\sqrt{5}}{2} \leq k_I^{int} < k_P^{int} \\ & (k_I^{int} - k_P^{int} - 1)^2 (k_I^{int} - k_P^{int}) - (k_P^{int} + 2)(2k_I^{int} - k_P^{int}) > 0.\end{aligned} \tag{5.28}$$

Constraints (5.28) implicitly define a convex set in the space $(k_P^{\text{int}}, k_I^{\text{int}})$. We can give a pictorial representation of this set performing a two-dimensional grid search on the values of the gains such that (5.28) is satisfied. The result is shown in Figure 5.4 (top).

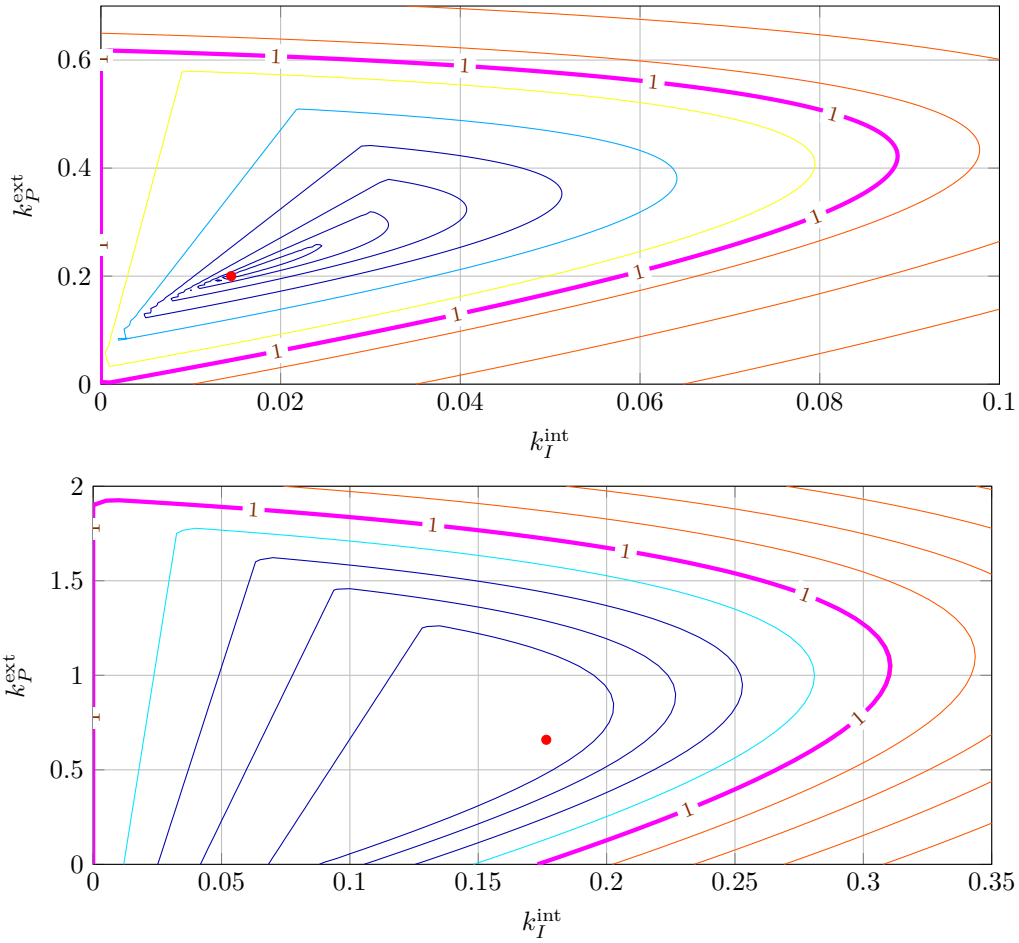

Figure 5.4: Level sets of the spectral radii $\rho(A_{\text{int}})$ (top) and $\rho(A_f)$ (bottom) as a function of the PI gains. The minimum values are $\rho_{\min}(A_{\text{int}}) = 0.7964$ and $\rho_{\min}(A_f) = 0.9399$, obtained for $k_P^{\text{int}} = 0.2$, $k_I^{\text{int}} = 0.0145$, $k_P^{\text{ext}} = 0.6590$, $k_I^{\text{ext}} = 0.1765$. In both plots, The bold magenta line delimits the stability region, and the red dots indicate the minima.

Figure 5.4 shows different level sets of the spectral radius $\rho(A_{\text{int}})$ as a function of parameters k_I^{int} and k_P^{int}. The bold magenta line represents the stability limit—that is, the set where $\rho(A_{\text{int}}) = 1$. Inspecting the level sets and performing a numerical optimization, we obtain the desired gain selection for the first controller, that corresponds to $k_I^{\text{int}\star} = 0.2$ and $k_P^{\text{int}\star} = 0.0145$.

Consider matrix A_f in (5.23). We fix the internal controller gains $k_P^{\text{int}} = k_P^{\text{int}\star}$ and $k_I^{\text{int}} = k_I^{\text{int}\star}$, according to (5.28). Conveniently choosing $\nu = K_f \frac{N-1}{N}$, so that matrix A_f does not depend on the physical parameters of the network, we get

$$A_f = \begin{bmatrix} 1 & 0 & 0 & 0 & 1 \\ -k_I^{\text{ext}} & 1 & 0 & 0 & -k_P^{ext} - 1 \\ 0 & 1 & 1 & 0 & 0 \\ 0 & -k_P^{\text{int}\star} & -k_I^{\text{int}\star} & 0 & 0 \\ 0 & 0 & 0 & -1 & 0 \end{bmatrix}. \tag{5.29}$$

Note that matrix A_f only depends on k_I^{ext} and k_P^{ext}. The stability region of A_f cannot be expressed in terms of constraints on the PI gains k_I^{ext}, k_P^{ext}. In this case, applying the Jury stability criterion to the characteristic polynomial of A_f, we do not obtain simple mathematical conditions as we did in Lemma 5.1. Therefore, we perform a grid search on the values of the gains that makes the matrix A_f Schur-Cohn. The result is shown in Figure 5.4 (bottom). Figure 5.4 (bottom) shows different level sets of the spectral radius $\rho(A_{\text{ext}})$ as a function of parameters k_I^{ext} and k_P^{ext}. The bold magenta line represents the stability limit—that is, the set where $\rho(A_{\text{ext}}) = 1$. Inspecting the level sets and performing a numerical optimization we obtain the desired gain selection for the second controller, that corresponds to $k_I^{\text{ext}\star} = 0.01765$ and $k_P^{\text{ext}\star} = 0.6590$.

5.3.2 Control Design based on ILMI Algorithm

In this section, we address the problem of finding a systematic strategy to solve (5.26) and determine the PI controller gains k_P^{int}, k_I^{int}, k_P^{ext} and k_I^{ext}. More precisely, the problem of designing the PI controller gains is translated here in terms of a static output feedback design problem. Moreover, we provide a systematic procedure to find the solution to the static output feedback design problem. The proposed solution is of general applicability (see Remark 5.5) beyond the considered fair-delivery problem and it is the extension to the discrete-time case of the ILMI design technique presented in Section 2.4 and using slack variables. Compared to the current literature, this method can be viewed as an alternative approach to coordinate descent algorithms (see [1]). The reader interested in the use of slack variables can also consult [33] and [74].

The PI gain selection consists in a two-steps optimization process in which first the controller gains k_P^{int}, k_I^{int} are designed in order to maximize the spectral radius of A_{int}, and once these are set, the same procedure is applied to the selection of k_P^{ext} and k_I^{ext}, in order to maximize the convergence rate of A_f. As pointed out in Section 5.3.1, by choosing the parameter $\nu = K_f \frac{N}{N-1}$, A_f becomes independent of the network parameters. Note

that matrices A_{int} in (5.11) and A_f in (5.23) can be conveniently rewritten as follows

$$A_{\text{int}} = A_1 - B_1 K_{\text{int}} C_1, \quad K_{\text{int}} := \begin{bmatrix} k_P^{\text{int}} & k_I^{\text{int}} \end{bmatrix} \tag{5.30}$$

$$A_f = A_2 - B_2 K_{\text{ext}} C_2, \quad K_{\text{ext}} := \begin{bmatrix} k_I^{\text{ext}} & k_P^{\text{ext}} \end{bmatrix} \tag{5.31}$$

with

$$A_1 := \begin{bmatrix} 1 & 0 & 0 & -1 \\ 1 & 1 & 0 & 0 \\ 0 & 0 & 0 & 0 \\ 0 & 0 & -1 & 0 \end{bmatrix}, \quad B_1 := \begin{bmatrix} 0 \\ 0 \\ 1 \\ 0 \end{bmatrix}, \quad C_1 := \begin{bmatrix} 1 & 0 & 0 & 0 \\ 0 & 1 & 0 & 0 \end{bmatrix},$$

$$A_2 := \begin{bmatrix} 1 & 1 & 0 & 0 & 0 \\ 0 & -1 & 0 & 0 & 1 \\ 0 & 0 & 1 & 0 & 1 \\ 0 & 0 & -k_I^{int} & 0 & -k_P^{int} \\ 0 & 0 & 0 & -1 & 0 \end{bmatrix}, \quad B_2 := \begin{bmatrix} 0 \\ 1 \\ 0 \\ 0 \\ 0 \end{bmatrix}, \quad C_2 := \begin{bmatrix} 1 & 0 & 0 & 0 & 0 \\ 0 & 1 & 0 & 0 & 0 \end{bmatrix}. \tag{5.32}$$

Within this setting, the problem described in (5.26) consists in designing suitable static output feedback matrices K_{int}, K_{ext}, such that the spectral radii of A_{int} and A_f are minimized. Using classical Lyapunov stability results, the following proposition casts (5.26) into a static output feedback problem with optimized rate of convergence.

Proposition 5.1. *Suppose that there exists a solution to the following optimization problems*

$$\begin{aligned} (k_P^{\text{int}\star}, k_I^{\text{int}\star}, \beta^{\text{int}}) = & \underset{W=W^\top>0, \beta, k_P^{\text{int}}, k_I^{\text{int}}}{} \quad \beta \\ & s.t. \quad (A_1 - B_1 K_{\text{int}} C_1) W (A_1 - B_1 K_{\text{int}} C_1)^\top - W + \beta W \leq 0, \end{aligned} \tag{5.33}$$

$$\begin{aligned} (k_P^{\text{ext}\star}, k_I^{\text{ext}\star}, \beta^{ext}) = & \underset{W=W^\top>0, \beta, k_P^{\text{int}}, k_I^{\text{int}}, k_P^{\text{ext}}, k_I^{\text{ext}}}{} \quad \beta \\ & s.t. \quad (A_2 - B_2 K_{\text{ext}} C_2) W (A_2 - B_2 K_{\text{ext}} C_2)^\top - W + \beta W \leq 0, \\ & \qquad k_P^{\text{int}} = k_P^{\text{int}\star}, k_I^{\text{int}} = k_I^{\text{int}\star}, \end{aligned} \tag{5.34}$$

where matrices A_i, B_i, C_i, for $i = 1, 2$, are defined in (5.32)*, and K_{int}, K_{ext} are defined in* (5.30) *and* (5.31)*, respectively.*

If $\beta^{\text{int}}, \beta^{ext} > 0$, then (5.26) *holds with $\rho_{\min}(A_{\text{int}}) = \sqrt{1 - \beta^{\text{int}}}$ and $\rho_{\min}(A_f) = \sqrt{1 - \beta^{\text{ext}}}$.*

Proof. From linear system stability theory (see, for example, [42]), given a matrix $A \in \mathbb{R}^{n \times n}$, there exists a solution to

$$AWA^\top - W + \beta W \leq 0$$

if and only if the eigenvalues $\lambda_i(A)$, $i = 1, \ldots, n$, of A satisfy

$$\lambda_i^2(A) - 1 + \beta \leq 0, \tag{5.35}$$

for all $i = 1, \ldots, n$—that is, $|\lambda_i(A)| \leq \sqrt{1-\beta}$, for all $i = 1, \ldots, n$. Taking the minimum of the absolute value of the eigenvalues of A, we have that the spectral radius of A satisfies

$$\rho(A) \leq \sqrt{1-\beta}, \tag{5.36}$$

thus proving the statement. □

Proposition 5.1 is the main ingredient for the development of the control design method presented in this section. Our goal is to find a solution to (5.33) and (5.34). However, conditions (5.33) and (5.34) are not numerically tractable, since they are nonlinear matrix inequalities for which there exists no analytical solution, nor a numerically efficient algorithm (see [94]). Consider the matrix inequality in (5.33). Applying a Schur complement, we obtain

$$\begin{bmatrix} -W + \beta W & (A_1 - B_1 K_{\text{int}} C_1) W \\ * & -W \end{bmatrix} \leq 0. \tag{5.37}$$

The main nonlinearity in (5.37) is the product term $B_1 K_{\text{int}} C_1 W$. The same reasoning can be applied to (5.34). We will present a procedure in order to transform conditions (5.33) and (5.34) into a numerically tractable formulation, by applying the Finsler Lemma [73, Lemma 2] and exploiting the particular structure of matrices C_1 and C_2. In the remainder of this section, such a procedure is applied to A_{int}, by manipulating (5.34). The same kind of reasoning can be followed for matrix A_f.

Consider the constraint defined in (5.33). Using the Finsler Lemma [73, Lemma 2], we obtain that the inequality in (5.33) is equivalent to

$$\begin{bmatrix} -W + \beta W & (A_1 - B_1 K_{\text{int}} C_1) G \\ * & -G - G^\top + W \end{bmatrix} \leq 0, \tag{5.38}$$

for some multiplier $G \in \mathbb{R}^{n \times n}$, and $W = W^\top > 0$. Note that, in (5.38), the Lyapunov function matrix W is now decoupled from the controller matrix K_{int}. In fact, the introduction of multiplier G adds an extra degree of freedom to the problem, that will be used for the controller design. In our case, we constrain the multiplier G to have the following block structure

$$G = \begin{bmatrix} G_{11} & G_{11} M \\ G_{21} & G_{22} \end{bmatrix}, \quad G_{11} \in \mathbb{R}^{p \times p} \text{ nonsingular}, \tag{5.39}$$

where $M \in \mathbb{R}^{p \times n-p}$ is a given matrix, $G_{11} \in \mathbb{R}^{p \times p}$, n and p are the state and the output dimensions of system (5.11), respectively, and G_{21}, G_{22} are unconstrained matrices of

suitable dimensions. In fact, by substituting (5.39) and C_1 in (5.32) into (5.38), we obtain that the off-diagonal block in (5.38) has the following expression

$$(A_1 - B_1 K_{\text{int}} C_1)G = A_1 G - B_1 K_{\text{int}} \begin{bmatrix} I_p & 0 \end{bmatrix} G = A_1 G - B_1 K_{\text{int}} G_{11} \begin{bmatrix} I_p & M \end{bmatrix}. \quad (5.40)$$

Based on (5.40), the constraint in (5.38), with G as in (5.39), can be rewritten as

$$\begin{bmatrix} -W + \beta W & A_1 G - B_1 X \\ * & -G - G^\top + W \end{bmatrix} \leq 0, \quad X := X_1 \begin{bmatrix} I_p & M \end{bmatrix}, \quad X_1 := K_{\text{int}} G_{11}. \quad (5.41)$$

Note that (5.41) is an LMI problem in the variables $W = W^\top > 0$, X_1, G_{11}, G_{21} and G_{22}. If we consider β as a decision variable of problem (5.41), another nonlinearity emerges: the bilinear term βW. However, as β is a scalar variable, and $W > 0$, the search for the maximum value of β such that (5.41) has a solution, can be carried out using the bisection method. This problem is a *generalized eigenvalue problem*. Based on these observations, we can conclude that if there exists a solution to the following optimization problem

$$\begin{aligned} \beta_1 := \max_{W>0,\, \beta,\, k_P^{\text{int}},\, k_I^{\text{int}},\, G_{11}>0,\, G_{22},\, G_{21},\, X_1} \quad & \beta \\ \text{s.t.} \quad & \begin{bmatrix} -W + \beta W & A_1 G - B_1 X \\ * & -G - G^\top + W \end{bmatrix} \leq 0, \ (5.39), \ X = X_1 \begin{bmatrix} I_p & M \end{bmatrix}, \end{aligned} \quad (5.42)$$

for a given M, then the resulting controller $K_{\text{int}} := X_1 G_{11}^{-1}$, satisfies (5.33) with $\beta = \beta_2 \geq \beta_1$. The gap between β_2 and β_1 is due to the conservative structure of G in (5.39), which breaks the equivalence between (5.33) and (5.42). We want to analyze the optimality of the solution obtained solving (5.42)—that is, determining how close we are from the optimal solution β^{int} to (5.33). As we are constraining the multiplier (2.72) to have a predetermined structure, we can not provide any guarantees of optimality. We can analyze the resulting solution to (5.42) by plugging the corresponding controller $K_{\text{int}} = X_1 G_{11}^{-1}$ into (5.33), and solving the resulting optimization problem—which is quasi convex for a fixed controller—using bisection over β. The optimal value of β is then obtained due to the fact that (5.33) is a generalized eigenvalue problem [8] for a fixed controller K_{int}.

This observation suggests a two-steps procedure, that consists of a *synthesis step*, in which the controller K_{int} is computed according to (5.42), and an *analysis step*, in which a possibly tighter bound on β is obtained by solving (5.33) after fixing the controller matrix.

If the sequence of the values of β obtained from the synthesis step does not increase more than a desired tolerance, the algorithm stops and provides a suboptimal solution to problem (5.33). Otherwise, we repeat the design, based on the analysis solution. We perform a Schur complement to (5.33), obtaining

$$\begin{bmatrix} -W + \beta W & (A_1 - B_1 K_{\text{int}} C_1) W \\ * & -W \end{bmatrix} \leq 0, \quad (5.46)$$

Algorithm 5.4 Convergence rate β and PI controller K

Input: Matrices A, B, $C = \begin{bmatrix} I_p & 0 \end{bmatrix}$, and a tolerance $\delta > 0$.

Initialization: Set $M = 0$ and initialize the pair $(\beta_L, \beta_H) = (\beta_L^0, \beta_H^0)$, where, using $\bar{\sigma}(A)$ to denote the maximum singular value of A, we select

$$\beta_0^L := 1 - \bar{\sigma}^2(A), \quad \beta_H^0 := 1.1 \tag{5.43}$$

the pair (β_L, β_H) is *admissible* for (5.44), in the sense that (5.44) is feasible with $\beta = \beta_L$ and infeasible with $\beta = \beta_H$, for some $W, G_{11}, G_{12}, G_{22}$, and M.

Iteration

Step 1: Given M and the pair (β_L, β_H) from the previous step, by using bisection with tolerance $\delta > 0$, solve

$$\begin{aligned} &\max_{W=W^\top>0, G_{11}, G_{21}, G_{22}, X_1, \beta} \quad \beta \\ &\text{s.t.} \quad \begin{bmatrix} -W + \beta W & AG - BX \\ * & -G - G^\top + W \end{bmatrix} \leq 0, \ (5.39), \ X = X_1 \begin{bmatrix} I & M \end{bmatrix}, \end{aligned} \tag{5.44}$$

Determine an admissible pair (β_L, β_H) such that $\beta_H - \beta_L \leq \delta$. Pick the suboptimal solution $\bar{G}_{11}$, $\bar{X}_1$ corresponding to β_L, and set $\bar{K} = \bar{X}_1 \bar{G}_{11}^{-1}$ for the next step.

Step 2: Given $\bar{K}$ and pair (β_L, β_H) from the previous step, by using bisection with tolerance $\delta > 0$, solve

$$\begin{aligned} &\max_{\beta, W=W^\top>0} \quad \beta \\ &\text{s.t.} \quad (A - B\bar{K}C)W(A - B\bar{K}C)^\top - W + \beta W \leq 0. \end{aligned} \tag{5.45}$$

In particular, determine an admissible pair (β_L, β_H) such that $\beta_H - \beta_L \leq \delta$. Pick the (sub)optimal solution $\bar{W} = \begin{bmatrix} \bar{W}_{11} & \bar{W}_{12} \\ \bar{W}_{12}^\top & \bar{W}_{22} \end{bmatrix}$ (where W has the partition induced by G), corresponding to β_L and set $M := \bar{W}_{11}^{-1} \bar{W}_{12}$ for the next step.

until β_L does not increase more than δ over three consecutive steps.

Output: $K_{out} = \bar{K}$ and $\beta_{out} = \beta_L$.

which corresponds to (5.38) with $G = G^\top = W > 0$. Partition the Lyapunov matrix as $W = \left[\begin{smallmatrix} W_{11} & W_{12} \\ W_{12}^\top & W_{22} \end{smallmatrix}\right]$, according to the same partition of G in (5.39). Comparing the two expressions, and as $W_{11} > 0$, we conclude that (5.42) solved setting $M := W_{11}^{-1} W_{12}$, will provide value of β greater than or equal to the one provided by the previous iteration. Iterating between the synthesis and analysis problems, we obtain a sequence of nondecreasing values of β; the corresponding W, k_P^{int}, k_P^{ext} satisfy the constraint in (5.33).

The overall general procedure is summarized in Algorithm 5.4, on page 101. Alternating between analysis and synthesis steps may reduce the conservatism of the conditions (5.42) due to the constraint (5.39) imposed on the structure of the multipliers. Nevertheless, this conservatism is unavoidable, and the iterative procedure in Algorithm 5.4 is not guaranteed to converge to the global optimum. In fact, we are solving a static output feedback design problem, which is well known to be a challenging one.

Algorithm 5.4 joins several useful properties that make it a promising tool for computing suboptimal static output feedback gains. Such properties are stated and proven next.

Proposition 5.2. *The following statements hold:*

(i) Initialization and termination: Given any input $(A, B, [I_p\ 0])$ and tolerance $\delta > 0$, the pair of scalars (β_L, β_H) defined in the Initialization step of Algorithm 5.4 is an admissible pair (in the sense specified in the initialization step). Moreover, the algorithm terminates after a finite number of steps.

(ii) Feasibility: Given any admissible pair $(\beta_{L_1}, \beta_{H_1})$ from Step 1, the pair $(\beta_{L_2}, \beta_{H_2})$ obtained from the subsequent Step 2 always satisfies $\beta_{L_2} \geq \beta_{L_1}$, and vice versa.

(iii) Guarantees: Any solution (K_{out}, β_{out}) resulting from Algorithm 5.4 satisfies

$$\rho\left(A - BK_{out}[I_p\ 0]\right) \leq \sqrt{1 - \beta_{out}}, \tag{5.47}$$

where ρ denotes the spectral radius. In particular, if $\beta_{out} > 0$, then the gain selection K_{out} is a stabilizing output feedback gain for the triple $(A, B, [I_p\ 0])$, and $\sqrt{1 - \beta_{out}}$ is the corresponding convergence rate.

Proof. Proof of (i). First, we prove that (β_L^0, β_H^0) in (5.43) is an admissible pair in the sense clarified in the Initialization step. In fact, (5.44) is infeasible with $\beta = \beta_H^0$, because the upper-left entry is positive definite. To show that (5.44) is feasible with $\beta = \beta_L^0$ as in (5.43), select $G_{11} = I_p$, $G_{22} = I_{n-p}$, $G_{21} = 0$, $X_1 = 0$, and $W = I_n$ so that, applying a Schur complement, (5.44) is feasible if

$$(\beta_L^0 - 1) I_n + AA^\top \leq 0, \tag{5.48}$$

which is ensured if $\beta_L^0 - 1 + \bar{\sigma}^2(A) \leq 0$. We now prove that the algorithm always terminates in a finite number of steps. Let $\beta_{L_1}^j$ denote the value of β_L at the j-th iteration of Step 1. From item (ii) of Proposition 5.2 the sequence $\beta_{L_1}^j$, $j \in \mathbb{N}$, is non

decreasing and upper bounded by $\beta = 1$, thus it is convergent. That is, given $\delta > 0$ there exists an index $j \in \mathbb{N}$ such that $\beta_{L_1}^{j+1} - \beta_{L_1}^{j} \leq \delta$.

Proof of (ii). [From Step 1 to Step 2]. By substituting the solution β_{L_1}, $\bar{K}$ obtained from Step 1 solving (5.44), we get that

$$\begin{bmatrix} -W + \beta_{L_1} W & (A - B\bar{K}C)G \\ * & -G - G^\top + W \end{bmatrix} \leq 0 \tag{5.49}$$

has a feasible solution. By applying the Finsler Lemma, feasibility of (5.49) is equivalent to feasibility of

$$(A - B\bar{K}C)W(A - B\bar{K}C)^\top - W \leq -\beta_{L_1} W. \tag{5.50}$$

Comparing (5.50) with (5.45), it follows that the subsequent solution β_{L_2} to Step 2 satisfies $\beta_{L_2} \geq \beta_{L_1}$.

[From Step 2 to Step 1]. Substitute the solution β_{L_2}, M obtained from Step 2 in (5.45), and perform a Schur complement to get

$$\begin{bmatrix} -W + \beta_{L_2} W & (A - BKC)W \\ * & -W \end{bmatrix} \leq 0, \tag{5.51}$$

which corresponds to (5.44) with $G = G^\top = W$. It follows that the subsequent solution β_{L_1} to Step 1 satisfies $\beta_{L_1} \geq \beta_{L_2}$.

Proof of (iii). From linear systems theory (see, e.g., [42]), we get that both solutions at Step 1 and Step 2 provide a certificate that matrix $\bar{A} = A - BK_{out}C$ has a spectral radius smaller than $\sqrt{1 - \beta_{out}}$. □

Remark 5.5. There is no loss of generality in considering systems in the form $(A, B, [I_p\ 0])$ in Algorithm 5.4. For a system in a general form (A, B, C), where matrix C is full-row rank, there always exists a nonsingular matrix T such that $CT^{-1} = [I_p\ 0]$. Using T as a similarity transformation we obtain $(T^{-1}AT, T^{-1}B, CT) = (\bar{A}, \bar{B}, [I_p\ 0])$. Thus Algorithm 5.4 can be applied to any static output feedback design problem for discrete-time systems.

Remark 5.6. Comparing the properties of Algorithm 2.1 and Algorithm 5.4, which are associated to Propositions 2.3 and 5.2, respectively, we notice that the substantial difference between the algorithms is that Algorithm 5.4 is guaranteed to converge, while Algorithm 2.1 is not. This happens because, in the continuous-time case, the sequence of β_L obtained during the iteration process is not bounded. This difference is intrinsic to the nature of the stability region for linear systems: in the continuous-time case, the eigenvalues of a Hurwitz matrix belong to the unbounded open right-half plane, while in the discrete-time case, the eigenvalues of a Schur-Cohn matrix belong to the bounded open unit circle.

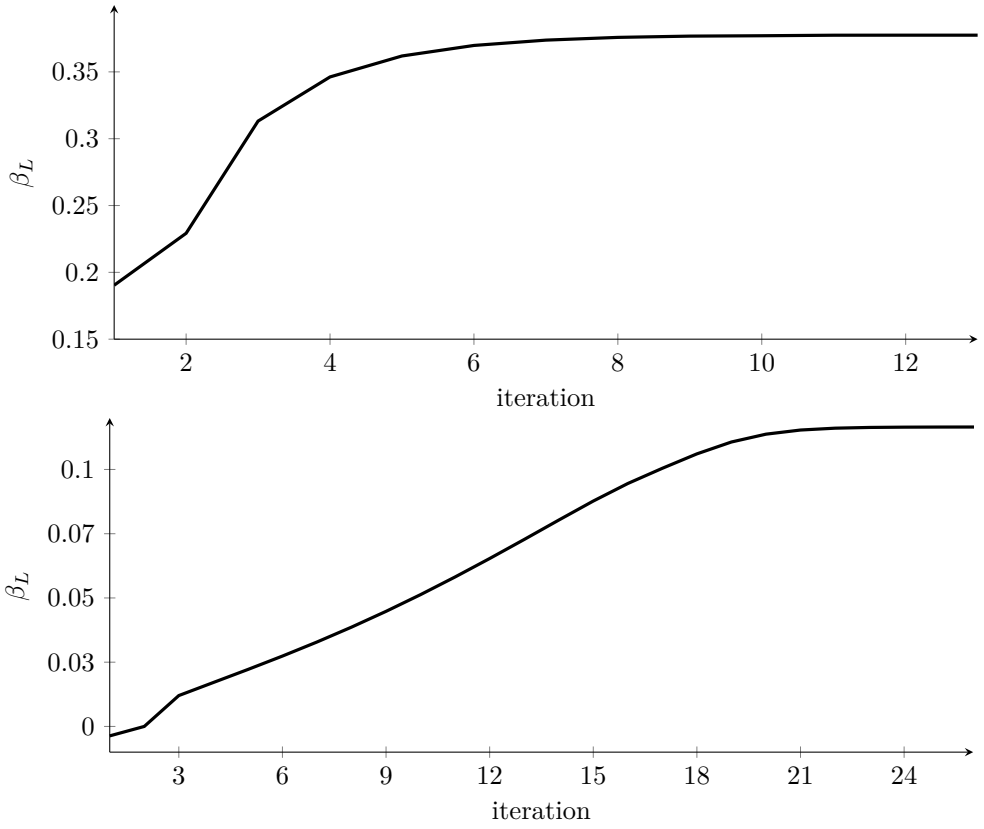

Figure 5.5: Gain selection via Algorithm 5.4. Maximization of the convergence rate β_L of A_{int} (top) and A_f (bottom).

5.3.3 Numerical Evaluation

The outer and inner PI controller gains K_{int} and K_{ext} of the quality-fair delivery problem are designed using Algorithm 5.4. The algorithm has been implemented with MATLAB and solved with the optimization environment YALMIP [61] with LMI-lab solver [38]. The algorithm is executed with data (5.32) and tolerance $\delta = 10^{-8}$. Figure 5.5 shows the optimization of the convergence rate of A_{int} and A_{ext} performed by the algorithm. Figure 5.5 (top) shows that after 13 iterations, the rate β_L of A_{int} in (5.30) converges to 0.37789, and the corresponding controller gains are $k_P^{\text{int}} = 0.19256$, and $k_I^{\text{int}} = 0.012915$. Similarly, Figure 5.5 (bottom) shows the optimization of the convergence rate β_L of A_f. After 25 iterations the value of β_L is 0.1165 and the external controller gain selection is $k_I^{\text{ext}} = 0.17645$ and $k_P^{\text{ext}} = 0.65801$. Let us summarize and compare the results of Sections 5.3.1 and 5.3.2. Denote with PI1 and PI1-bis the controller selection obtained with Algorithm 5.4 and with the numerical method in Section 5.3.1, respectively. Table 5.1, on page 105, shows the PI gains controllers selection obtained with the two strategies.

From Table 5.1 we can observe that the two methods give almost the same results, validating the effectiveness of the two methods in providing the optimized gain selection.

Method	k_I^{int}	k_P^{int}	k_I^{ext}	k_P^{ext}	$\rho_{\min}(A_{\text{int}})$	$\rho_{\min}(A_f)$
PI1	0.012915	0.19256	0.17645	0.65810	0.7887	0.9399
PI1-bis	0.0145	0.2	0.1765	0.6590	0.7964	0.9399

Table 5.1: Comparison between the gain tuning methods PI1 and PI1-bis.

Nevertheless, the second strategy is preferable to use in practice, because it is more general and it can be applied to a dynamical system of any order. Moreover, the numerical method presented in Section 5.3.1 requires the selection of the 2D interval in which the grid search for the optimum value is performed. The existence and the knowledge of this interval is a priori nontrivial, and is found in practice by trial and error. For these reasons, in the forthcoming simulations section, we will use the PI control gains determined by PI1—that is, the first line of Table 5.1.

Remark 5.7. The original system gains K_I^{eb}, K_P^t, K_I^{eb} and K_P^t in (5.1) are obtained from k_I^{int} and k_P^{int}, k_I^{ext} and k_P^{ext} using (5.6) and (5.9). In particular the values of K_I^{eb}, K_P^t depends on the selection of the constant $\nu = K_f \frac{N-1}{N}$—that is, the external controller gains depend on the video parameter K_f and the number of streams N.

5.4 Simulations

In this section we provide simulation results to demonstrate the effectiveness of the control design technique described in the previous sections.

In the simulations we consider six video streams[1] of different types, encoded during 60 s with x.264 [43] in 4CIF (704×576) format at various bit rates. The programs are Interview (Prog 1), Sport (Prog 2), Big Buck Bunny (Prog 3), Nature Documentary (Prog 4), Video Clip (Prog 5), and an extract of Spiderman (Prog 6). The frame rate is $F = 30$ frames/s. We consider GoPs of 10 frames with duration $T = 0.33$ s, for a total number of GoPs of $M = 180$. The model parameters are selected as follows: the reference bit-rate is $B_c = 1200$ kb/s to tolerate significant variations of the buffering delay, and the channel rate is $R_c = 4000$ kb/s. The considered utility function U_i is the PSNR, and we evaluate the performance of the control schemes with the metric

$$\overline{\Delta U} := \frac{1}{MN} \sum_{j=1}^{M} \sum_{k=1}^{N} \left| U_k^{dd}(j) - \overline{U}^{dd}(j) \right|, \tag{5.52}$$

that is, the time and ensemble average of the absolute value of the difference between the PSNR of each stream and the average PSNR of all the streams. A smaller value of $\overline{\Delta U}$ indicates a better performance of the control scheme, as it indicates that all the utilities are closer to the average for all the times.

We simulate the behavior of the servers, the network, the MANE, the BS, and the clients in MATLAB. In the simulations we compare the following approaches:

[1] http://www.youtube.com/watch?v=l2Y5nIbvHLs, =G63TOHluqno, =YE7VzlLtp-4, =NNGDj9IeAuI, =rYEDA3JcQqw, =SYFFVxcRDbQ.

PI1 *PI controllers with parameter tuning based on Algorithm 5.4.* We set the value of the parameter K_f in (5.15) as follows. We evaluate the time and ensemble average of the rate-PSNR characteristics for the four first streams at different constant encoding rates $R_i^{ed} = R^{ed}$, $i = 1, \ldots, 4$, in the range from 250 kb/s to 2 Mb/s. The resulting values of K_f are in the range from 0.02 dB/kb/s to 0.0025 dB/kb/s. Among these values, we select $K_f = 0.02$ dB/kb/s to avoid aggressive variations of the video encoding rate and increase robustness of the system.

PI2 *PI controllers with parameter tuning based on [15].* This tuning gives stable A_{int} but unstable A_f. Then Theorem 5.1 anticipates lack of consensus[2].

TRF *Transmission Rate Fair approach*, obtained removing the transmission rate controllers (5.1g)-(5.1h) from (5.1). The PI gains K_P^{eb}, K_I^{eb} are selected as in [15]. In this simplified architecture, the transmission rate is constant for all programs. Also in this case Theorem 5.1 anticipates lack of consensus and lack of convergence of the utilities, that is, (5.2) is not satisfied. In fact A_f in (5.23) has poles at the limit of stability (indeed the scheme corresponds to $L = \mathbf{0} \in \mathbb{R}^{N \times N}$, with only zero eigenvalues).

UMMF *Utility max-min fair approach [19].* The encoding rate for each GoP is selected to maximize the minimum utility under a total rate constraint.

CMUM *Constrained mean-utility maximization approach [14].* The encoding rate for each GoP is selected to maximize the average utility under a total rate constraint and considering also maximum utility discrepancies between programs. Compared to [14], we do not take into account temporal smoothness constraints, because the other approaches do not model them.

Method	K_I^{eb}	K_P^{eb}	K_I^t	K_P^t
PI1	0.012922	0.1797	$0.17645/\nu$	$0.418/\nu$
PI2	0.002	0.15	0.05	100
TRF	0.002	0.15	0	0

Table 5.2: Comparison between the gain tuning for the PI-based schemes PI1, PI2, TRF.

	PI1	PI2	TRF	UMMF	CMUM
Progs 1−4	2.28	2.37	4.12	0.88	1.53
Progs 3−6	3.22	–	3.66	1.45	1.19

Table 5.3: Comparison of the average absolute value of the utility discrepancy $\overline{\Delta U}$ obtained with different control schemes (values in dB).

[2] Note that the gains in [15] had been heuristically tuned without any formal guarantee of convergence.

Table 5.2, shows the values of the PI gains of system (5.1) of methods PI1, PI2, TRF. Note that the first line of Table 5.2 has been obtained from the first line of Table 5.1 via (5.6) and (5.9), once we have fixed the value of the physical constant ν.

The value of the average utility $\overline{\Delta U}$ for the simulations is given in Table 5.3, on page 106.

Figures 5.6 and 5.7, show the time evolution of the utilities U_i of the first group of videos (Programs 1–4). Figure 5.8, shows the time evolution of the utilities U_i, of the second group of videos (Programs 3–6), using the schemes PI1 (top), PI2 (middle), and TRF (bottom). We do not show the simulations using the other schemes because they give similar results as compared to the correspondent ones in Figure 5.7.

Note that both the control methods PI2 and TRF do not stabilize the consensus set. It is not surprising that the utilities obtained with these schemes diverge (see Figure 5.8 (middle)) and do not converge (see Figure 5.8 (bottom)), when sending Programs 3–6. For this reason we can not evaluate the corresponding value of $\overline{\Delta U}$ for the scheme PI2 (see Table 5.3).

From Figures 5.6, 5.7, and Table 5.3, we deduce that the UMMF and CMUM schemes give the best results in terms of PSNR discrepancies $\overline{\Delta U}$. The price to pay is the computational complexity. In fact these approaches require the availability at the MANE of the RUCs of the future GoP of each video stream, and thereby the solution at each time step of a nonlinear, non-differentiable constrained optimization problem. We observe in Figure 5.7 (bottom), that the CMUM technique causes large variations of the PSNR at some time instants. They are due to scene changes, which this scheme does not model.

Summarizing, the control design technique proposed in this chapter performs worse than the UMMF and the CMUM schemes, and better than the heuristics PI2 and TRF. However, it has a very small computational complexity. In fact, without needing the RUCs information, it provides a reasonable fairness among programs: in most of the cases we observe discrepancies among programs of less than 5 dB. In addition, the proposed control is robust to variations of the video characteristics as compared to the PI2 and TRF schemes.

5.5 Summary

In this chapter we have presented necessary and sufficient conditions for the quality-fair delivery of video contents for the considered broadcasting system. The control architecture is based on nested PI control loops that regulate the internal stream dynamics and the outer stream synchronization. Based on the proposed conditions, we presented two strategies to design the PI controller gains. The first one is based on the Jury stability criterion (see [26]), and the second one on static output feedback control design (see [23]). A general LMI-based iterative procedure has been also addressed for the design of linear output feedback static controllers. This procedure is then applied to determine suboptimal PI controller gains. Experimental results allow to point out the advantages and the drawbacks of the proposed technique with respect to results of the literature.

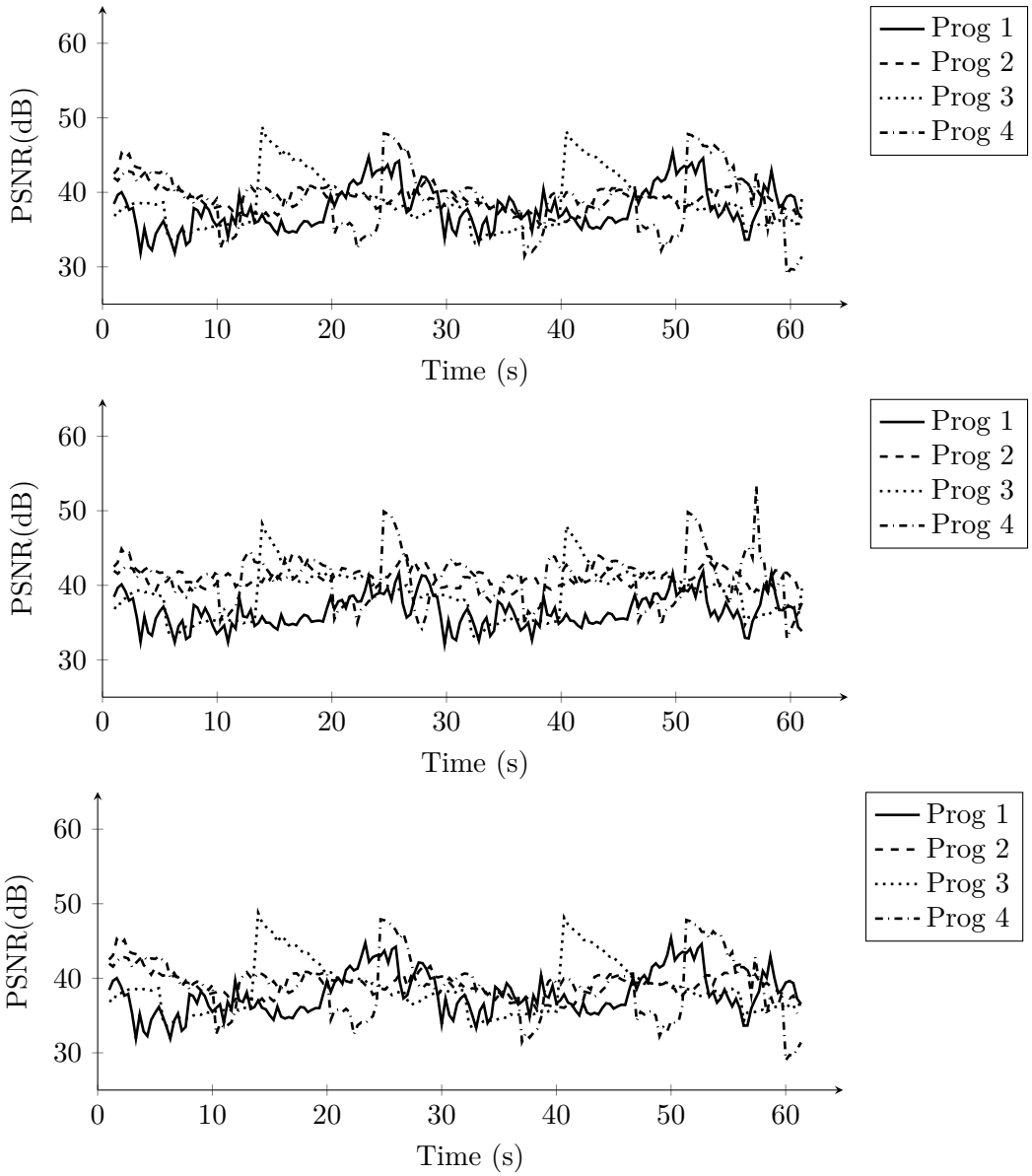

Figure 5.6: PSNR of Progs 1 to 4, comparison between different control schemes: PI1 (top), PI2 (middle), TRF (bottom).

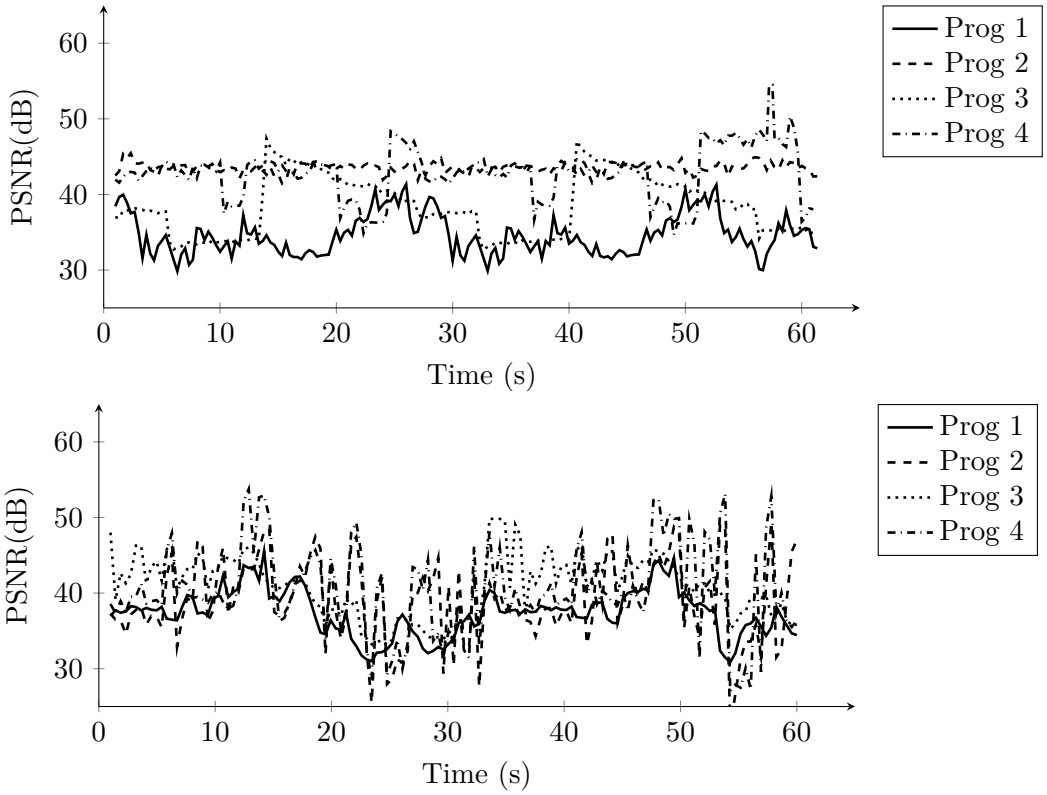

Figure 5.7: PSNR of Progs 1 to 4, comparison between different control schemes: UMMF (top), CMUM (bottom).

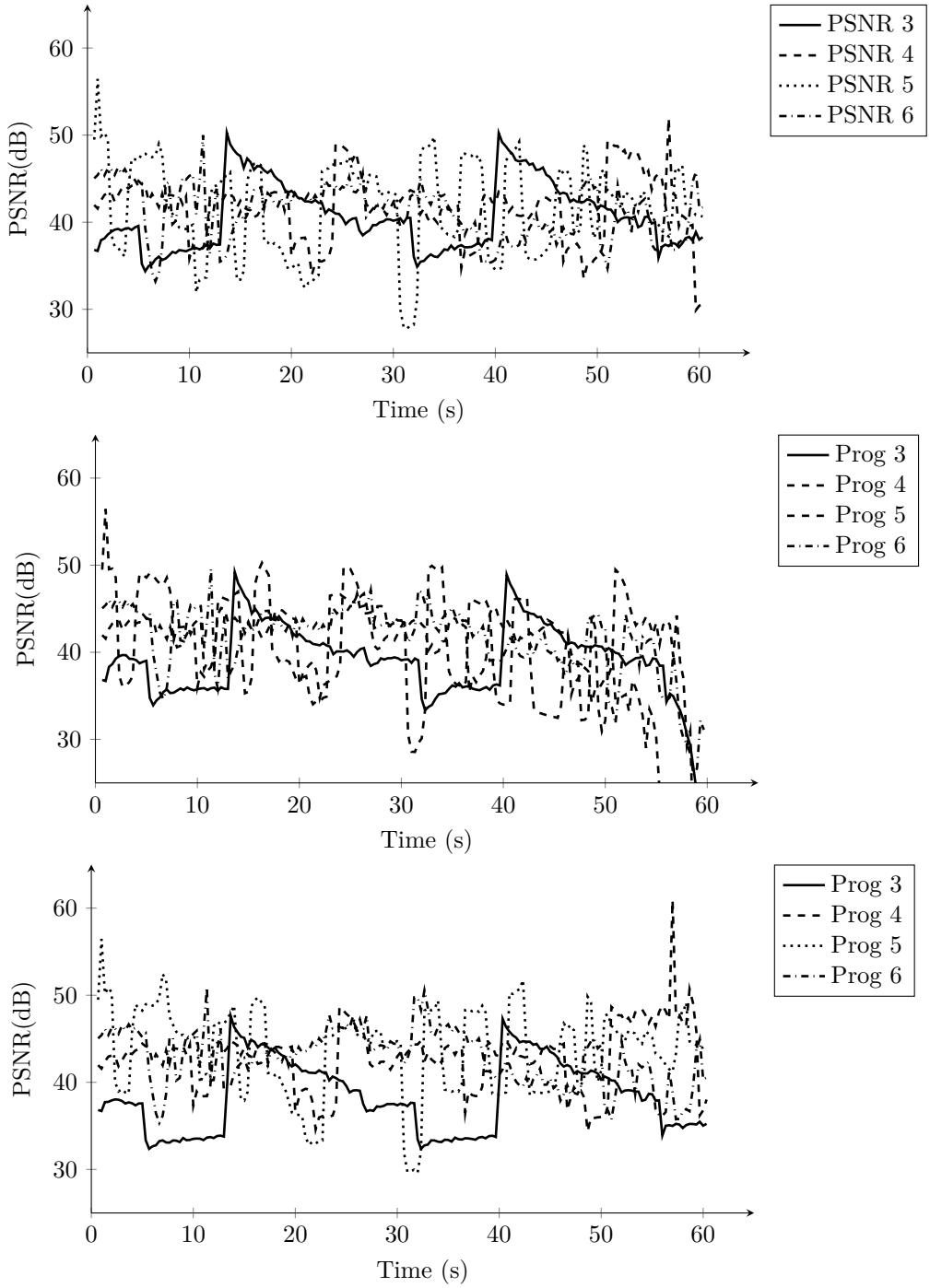

Figure 5.8: PSNR of Progs 3 to 6, comparison between the PI1 (top), PI2 (middle), and TRF (bottom).

Chapter 6

Conclusions

The large-scale networks of the modern engineering applications, along with the necessity of distributed and autonomous control, require the development of a theoretical framework for new control methods for multi-agent systems. In this thesis, we presented an improved theoretical analysis of the synchronization problem of multi-agent systems using classical Lyapunov stability tools.

Together with communication constraints, the agent model and the graph topology identify the characteristics of the class of multi-agent systems under consideration. We considered high-order linear time invariant multi-agent systems, and we derived synchronization conditions for increasing levels of topological complexity and communication constraints. Weaker assumptions on the communication graph associated with the network yields increased topological complexity. The best we were able to deal with were directed communication graphs. The communication constraints include a large variety and combinations of problems, such as noise, time delays, magnitude saturation, and packet losses.

We considered the following problems. First, we analyzed multi-agent systems with directed topology in the ideal case of noiseless communication links and unconstrained dynamics. Second, we considered multi-agent systems with undirected topologies affected by external perturbations and we formulated suitable performance requirements for synchronization. Third, we constrained the multi-agent systems dynamics taking into account actuator saturation. Finally, we presented an application of the synchronization problem to the fair-delivery control of multiple encoded videos. For each problem, we provided a control design strategy based on output-feedback control and Lyapunov techniques. We considered distributed and centralized control algorithms. Distributed controllers are preferable for the scalability and flexibility, while centralized controllers allow to compute global variables of the network rapidly. The choice of the strategy depends on the specific application. Note that, the multi-agent systems considered throughout

this thesis were composed by identical agents with linear-time invariant dynamics.

The results presented in this thesis may be extended along many future lines of research. For instance, we considered a specific definition of consensus and synchronization. Namely, we require the agent states to converge asymptotically to a common trajectory, but we did not take into consideration any specification on the synchronization trajectory. Hence, it would be interesting to include in this analysis the trajectory tracking problem. Then, the presented results could be extended to multi-agent systems composed by agents with non-identical linear dynamics. Moreover, it would be interesting to relax the assumptions on the graph connectedness and to extend our analysis to switching or time-varying graphs. Furthermore, we could take into account different communication limitations, such as communication delays and packet losses. Finally, we could implement different control strategies, such as event-triggered controllers, with the advantages of reducing the controller update frequency.

Appendix A

Graph Theory

In this appendix, we review selected concepts of graph theory for synchronization, which constitute the basis for the understanding of this thesis. For more details, an exhaustive analysis of algebraic graph theory can be found in [39] and [37].

A graph $\mathcal{G} := (\mathcal{V}, \mathcal{E})$ is defined by the *vertex set* $\mathcal{V}$ and the *edge set* $\mathcal{E}$. Let $\mathcal{N}$ be the index set $\mathcal{N} := \{1, \dots, N\}$. Each node $v_k \in \mathcal{V}$ can be associated to a dynamical system $k \in \mathcal{N}$ in the network. The edge set $\mathcal{E} \subseteq \mathcal{V} \times \mathcal{V}$ is composed by directed edges (v_j, v_k), with $j, k \in \mathcal{N}$. In the multi-agent system context, $(v_j, v_k) \in \mathcal{E}$ means that there is a communication link from agent j to agent k. The vertices v_k and v_j are called tail and head, respectively, since there is an information flow from v_j to v_k. Usually, the edges are represented by arrows going from the head to the tail. If the edges in $\mathcal{E}$ are directed, $\mathcal{G}$ is called *directed* graph. A consecutive sequence of directed edges is called *directed path*. A graph $\mathcal{G}$ is called *undirected* if $(v_j, v_k) \in \mathcal{E} \iff (v_k, v_j) \in \mathcal{E}$.

The *adjacency matrix* $A_\mathcal{G} \in \mathbb{R}^{N \times N}$ describes the graph structure. Its elements a_{kj} are defined as follows

$$a_{kj} := \begin{cases} 1 & \text{if } (v_j, v_k) \in \mathcal{E} \\ 0 & \text{otherwise.} \end{cases} \tag{A.1}$$

The representations of the adjacency matrix $A_\mathcal{G}$ depend on the specific ordering of the vertices—that is, the adjacency matrix of a graph is uniquely defined modulo vertex permutations. The spectral properties of the adjacency matrix do not depend on the particular vertex ordering. The *neighbor set* of a vertex v_k is the set $\mathcal{N}_k := \{j \in \mathcal{N} : (v_j, v_k) \in \mathcal{E}\}$ of all vertices having an ingoing edge to v_k. The *degree* d_k of a vertex v_k is the sum of all its incoming edges, that is, $d_k = \sum_{j=1}^{N} a_{kj}$. The degree matrix of $\mathcal{G}$ is defined as $D_\mathcal{G} := \operatorname{diag}(d_1, \dots, d_N)$. The *Laplacian matrix* $L \in \mathbb{R}^{N \times N}$ is defined as

$$L := A_\mathcal{G} - D_\mathcal{G}.$$

By construction, L has nonnegative off-diagonal elements, and has zero row sums—that is $L\mathbf{1}_N = \mathbf{0}_N$. As a consequence, the vector $\mathbf{1}_N$—that is, the vector whose entries are all ones—is the eigenvector corresponding to the eigenvalue $\lambda_1(L) = 0$.

We recall some notation from [16]. A graph $\mathcal{G}$ is called *weakly connected* if it contains a path (disregarding the directions) from every node to every other node in the network. A directed graph $\mathcal{G}$ is called *strongly connected* if it contains a directed path from every node to every other node in the graph. A *strongly connected component* or *bicomponent* $\hat{\mathcal{G}}$ is every maximal (by inclusion) strongly connected subgraph. In particular, the *basis bicomponent* is a bicomponent that does not have ingoing arcs, meaning that its nodes are not influenced by outer nodes. There exists at least one basis bicomponent in every graph. A graph $\mathcal{G}$ with one unique basis bicomponent is said to contain a *rooted directed spanning tree*.

The following theorem characterizes the relation between the connectivity properties of the graph $\mathcal{G}$ and the spectral properties of the Laplacian matrix L. The proof of this theorem is contained in [65].

Theorem A.1. (Connectedness and the spectrum of L). *Given any directed graph $\mathcal{G}$, all the eigenvalues of L are contained in the closed right-half plane—that is, $\mathbf{Re}(\lambda_k(L)) \geq 0$, for all $k \in \mathcal{N}$—and there exists at least one eigenvalue equal to zero.*

Moreover, the zero eigenvalue $\lambda_1(L) = 0$ is simple, and all the other eigenvalues have positive real parts—that is, $\mathbf{Re}(\lambda_k(L)) > 0$ for all $k = 2, \ldots, N$—if and only if $\mathcal{G}$ has a directed spanning tree.

As a convention, the indices of the eigenvalues of L are ordered according to the magnitude of the real parts, such that $0 = \lambda_1(L) \leq \mathbf{Re}(\lambda_2) \leq \ldots \leq \mathbf{Re}(\lambda_N)$. In the sequel and in the reminder of this thesis, the argument L will be omitted. If the graph $\mathcal{G}$ is undirected, the Laplacian matrix L is symmetric and has only real eigenvalues. In this case, the second smallest eigenvalue $\lambda_2 \geq 0$ is called *algebraic connectivity* of $\mathcal{G}$ (see [39]).

The following theorem characterizes the properties of the left eigenvector p of the Laplacian matrix L related to the zero eigenvalue. The proof of the following theorem is contained in [111].

Theorem A.2. *If $\mathcal{G}$ is weakly connected, then* $\ker(L) = \mathrm{im}(\mathbf{1}_N)$ *and the left eigenvector p of L corresponding to the eigenvalue $\lambda_1 = 0$, with $p^\top \mathbf{1}_N = 1$, is nonnegative—that is, $p^\top L = \mathbf{0}_N^\top$, and $p \geq \mathbf{0}_N$ element-wise. Moreover, if $\mathcal{G}$ has a rooted directed spanning tree, then p is positive—that is $p > \mathbf{0}_N$ element-wise.*

Sometimes, it is desirable to write the Laplacian matrix of a connected graph in a special form. This canonical form is reported, for example, in [2].

Theorem A.3. *If the graph $\mathcal{G}$ contains a directed spanning tree, then there exists a*

vertex permutation such that L reduces to the following upper block-triangular form

$$\bar{L} = \begin{bmatrix} \bar{L}_{11} & \bar{L}_{12} & \cdots & \bar{L}_{1m} \\ 0 & \bar{L}_{22} & \cdots & \bar{L}_{2m} \\ \vdots & \vdots & \ddots & \vdots \\ 0 & 0 & \cdots & \bar{L}_{mm} \end{bmatrix}, \tag{A.2}$$

where $\bar{L}_{ii}$, for $i = 1, \ldots, m$, are irreducible square matrices, and each $\bar{L}_{ii}$, for $i = 2, \ldots, m$, has at least one row with positive row sum. If $\bar{L}_{11}$ is scalar, then $\bar{L}_{11} = 0$.

Appendix B

Technical Proofs for Chapter 2

B.1 Proof of Lemmas 2.1 and 2.4

The proof of Lemma 2.1 directly follows from the following result, which is based on [90, Theorem 1.10].

Lemma B.1. *Given a closed, convex set $\mathcal{S} \subset \mathbb{R}^\nu$ and any vector $x \in \mathbb{R}^\nu$, there exists a unique point $y \in \mathcal{S}$ satisfying*

$$|x - y| = |x|_{\mathcal{S}} := \min_{a \in \mathcal{S}} |x - a| \,. \tag{B.1}$$

Moreover, $y \in \mathcal{S}$ satisfies (B.1) if and only if $x \in N_{\mathcal{S}}(y)$, where

$$N_{\mathcal{S}}(y) = \Big\{ n \in \mathbb{R}^\nu : \langle n - y, y - a \rangle \geq 0 \quad \forall a \in \mathcal{S} \Big\} \tag{B.2}$$

is the normal cone to $\mathcal{S}$ at y, and y is the orthogonal projection of x onto $\mathcal{S}$ (see [80]).

Proof. We only prove the equivalence among (B.1) and (B.2) because the existence and uniqueness of y is already proven in [81, Theorem 12.3].
Proof of (B.2) $\Rightarrow$ (B.1). If $x \in N_{\mathcal{S}}(y)$ then, $\forall a \in \mathcal{S}$ we have

$$\begin{aligned} |x - a|^2 &= |x - y + y - a|^2 \\ &= |x - y|^2 + |y - a|^2 + 2\langle x - y, y - a \rangle \geq |x - y|^2 \,. \end{aligned}$$

Proof of (B.1) $\Rightarrow$ (B.2). For all $a \in \mathcal{S}$ and for any $\eta \in (0, 1]$, we have from convexity that $\eta a + (1 - \eta) y \in \mathcal{S}$. Hence, from (B.1) we deduce

$$|x - y|^2 \;\; \leq \;\; |x - (\eta a + (1 - \eta) y)|^2 = |x - y - \eta(a - y)|^2$$

$$= \quad |x-y|^2 + 2\eta\langle x-y, y-a\rangle + \eta^2 |y-a|^2 .$$

Dividing by η, we obtain

$$2\langle x-y, y-a\rangle + \eta |y-a|^2 \geq 0.$$

Taking the limit as $\eta \to 0$, the statement is proven. □

Using Lemma B.1 we can prove Lemma 2.2.

Proof of Lemma 2.2. Select $y = \mathbf{1}_N \otimes \bar{x} \in \mathbb{R}^{Nn}$, so that $|x-y|^2 = \sum_{k=1}^{N} |x_k - \bar{x}|^2$. Then, according to Lemma B.1, the proof is completed if $x \in N_{\mathcal{S}}(y)$. Note that, since $\mathcal{S}$ is a linear subspace, for any pair of vectors $y, a \in \mathcal{S}$, we have $b := y - a \in \mathcal{S}$, so that it is sufficient to show

$$\langle x-y, b\rangle \geq 0, \quad \forall b \in \mathcal{S}. \tag{B.3}$$

Relation (B.3) can be established by first noticing that $b \in \mathcal{S}$ implies that there exists $\bar{b} \in \mathbb{R}^n$ such that $b = \mathbf{1}_N \otimes \bar{b}$, and then computing

$$\begin{aligned}
\langle x-y, b\rangle &= \langle x - \mathbf{1}_N \otimes \bar{x}, \mathbf{1}_N \otimes \bar{b}\rangle = \langle \mathbf{1}_N \otimes \bar{b}, x - \mathbf{1}_N \otimes \bar{x}\rangle \\
&= (\mathbf{1}_N \otimes \bar{b})^\top \left(x - \mathbf{1}_N \otimes \frac{1}{N}(\mathbf{1}_N^\top \otimes I_n)x \right) \\
&= \frac{1}{N}(\mathbf{1}_N^\top \otimes \bar{b}^\top) \left(NI_{Nn} - \mathbf{1}_N \otimes \mathbf{1}_N^\top \otimes I_n \right) x \\
&= \frac{1}{N}(\mathbf{1}_N^\top \otimes \bar{b}^\top) \left(\left[NI_N - \mathbf{1}_N \otimes \mathbf{1}_N^\top \right] \otimes I_n \right) x \\
&= \frac{1}{N}(\underbrace{\mathbf{1}_N^\top \left[NI_N - \mathbf{1}_N \otimes \mathbf{1}_N^\top \right]}_{=0} \otimes \bar{b}^\top)x = 0
\end{aligned}$$

which completes the proof. □

Proof of Lemma 2.4. Based on Lemma 2.2, we can now prove Lemma 2.4. Since matrix Λ has a zero in the upper left entry and ones in the remaining diagonal entries, we can write:

$$T\Lambda T^\top = \bar{T}\bar{T}^\top \tag{B.4}$$

where $\bar{T} \in \mathbb{R}^{N\times(N-1)}$, composed by the last $N-1$ columns of T, satisfies $\bar{T}^\top \mathbf{1}_N = 0$ and has $N-1$ independent columns. Therefore, $\mathrm{im}(\bar{T}) \subset (\mathbf{1}_N)^\perp$. As a consequence $\mathrm{im} \begin{bmatrix} 1 & 1 & \cdots & 1 \\ -1 & 0 & \cdots & 0 \\ 0 & -1 & \cdots & 0 \\ \vdots & \vdots & \ddots & \vdots \\ 0 & 0 & \cdots & -1 \end{bmatrix} \subset \mathrm{im}(\bar{T})$, and there exists Σ invertible such that $(\Sigma\bar{T}^\top \otimes I_n)x =$

$\tilde{x} := \begin{bmatrix} x_1 - x_2 \\ \vdots \\ x_1 - x_N \end{bmatrix} \in \mathbb{R}^{(N-1)n}$, where $\tilde{x}$ satisfies $\sum_{k=2}^{N}(x_1 - x_k)^2 = |\tilde{x}|^2$. From relation (B.4) consider now the quadratic form:

$$
\begin{aligned}
x^\top (T\Lambda T^\top \otimes I_n)x &= \begin{bmatrix} x_1 \\ \vdots \\ x_N \end{bmatrix}^\top (\bar{T}\bar{T}^\top \otimes I_n) \begin{bmatrix} x_1 \\ \vdots \\ x_N \end{bmatrix} \\
&= \left((\Sigma \bar{T}^\top \otimes I_n) \begin{bmatrix} x_1 \\ \vdots \\ x_N \end{bmatrix} \right)^\top (M \otimes I_n) \left((\Sigma \bar{T}^\top \otimes I_n) \begin{bmatrix} x_1 \\ \vdots \\ x_N \end{bmatrix} \right) \\
&= \left(\begin{bmatrix} I_n & -I_n & 0 & \cdots & 0 \\ I_n & 0 & -I_n & \cdots & 0 \\ \vdots & \vdots & \vdots & \ddots & 0 \\ I_n & 0 & 0 & \cdots & -I_n \end{bmatrix} \begin{bmatrix} x_1 \\ \vdots \\ x_N \end{bmatrix} \right)^\top (M \otimes I_n) \left(\begin{bmatrix} I_n & -I_n & 0 & \cdots & 0 \\ I_n & 0 & -I_n & \cdots & 0 \\ \vdots & \vdots & \vdots & \ddots & 0 \\ I_n & 0 & 0 & \cdots & -I_n \end{bmatrix} \begin{bmatrix} x_1 \\ \vdots \\ x_N \end{bmatrix} \right) \\
&= \tilde{x}^\top (M \otimes I_n)\tilde{x},
\end{aligned}
$$

where $\tilde{x} = \begin{bmatrix} x_1^\top - x_2^\top & \dots & x_1^\top - x_N^\top \end{bmatrix}^\top$. Then noticing that $\lambda_{\min}(M \otimes I_n) = \lambda_{\min}(M) = c_1$ and $\lambda_{\max}(M \otimes I_n) = \lambda_{\max}(M) = c_2$ we obtain the inner inequalities in (2.24). To complete the proof we need to show the outer inequalities in (2.24). To this end, it is sufficient to show that there exist positive scalars k_1 and k_2 such that for any pair n, N and any $x \in \mathbb{R}^{Nn}$

$$
k_1 |\tilde{x}|^2 \leq \textstyle\sum_{k=1}^{N} |\bar{x} - x_k|^2 \leq k_2 |\tilde{x}|^2 , \tag{B.5}
$$

and then the result follows from Lemma 2.2. To show (B.5) we first observe that $\sum\limits_{k=1}^{N} |\bar{x} - x_k|^2 = |\bar{x} \otimes \mathbf{1}_n - x|^2$ and then the straightforward relation

$$
\tilde{x} = \underbrace{\begin{bmatrix} I_n & -I_n & 0 & \cdots & 0 \\ I_n & 0 & -I_n & \cdots & 0 \\ \vdots & \vdots & \vdots & \ddots & 0 \\ I_n & 0 & 0 & \cdots & -I_n \end{bmatrix}}_{T_1} (\bar{x} \otimes \mathbf{1}_n - x) \tag{B.6}
$$

implies $|\tilde{x}|^2 = \tilde{x}^\top \tilde{x} = (\bar{x} \otimes \mathbf{1}_n - x)^\top T_1^\top T_1 (\bar{x} \otimes \mathbf{1}_n - x) \leq k_1^{-1} |\bar{x} \otimes \mathbf{1}_n - x|$, where k_1^{-1} is the maximum singular value of $T_1^\top T_1$. Similarly we have

$$
\begin{aligned}
&\frac{1}{N} \begin{bmatrix} -I_n & -I_n & \cdots & -I_n \end{bmatrix} \tilde{x} = \\
&= \frac{1}{N} \left(-(N-1)x_1 + \sum_{k=2}^{N} x_k + x_1 - x_1 \right) \\
&= \frac{1}{N} \left(-N x_1 + \sum_{k=1}^{N} x_k \right) = \bar{x} - x_1
\end{aligned} \tag{B.7}
$$

which implies:

$$\begin{aligned}\frac{1}{N}\begin{bmatrix}(N-1)I_n & -I_n & \cdots & -I_n\end{bmatrix}\tilde{x} = \\ = \bar{x} - x_1 + \frac{N}{N}(x_1 - x_2) = \bar{x} - x_2\end{aligned} \tag{B.8}$$

Using similar reasoning, one gets:

$$\bar{x}\otimes\mathbf{1}_n - x = \underbrace{\begin{bmatrix} -I_n & -I_n & -I_n & \cdots & -I_n \\ (N-1)I_n & -I_n & -I_n & \cdots & -I_n \\ \vdots & \vdots & \vdots & \ddots & \vdots \\ -I_n & -I_n & -I_n & \cdots & (N-1)I_n \end{bmatrix}}_{T_2}\tilde{x}, \tag{B.9}$$

which implies $|\bar{x}\otimes\mathbf{1}_n - x|^2 = (\bar{x}\otimes\mathbf{1}_n - x)^\top(\bar{x}\otimes\mathbf{1}_n - x) = \tilde{x}^\top T_2^\top T_2\tilde{x} \le k_2\,|\tilde{x}|^2$, where k_2 is the maximum singular value of $T_2^\top T_2$. □

B.2 Proof of Proposition 2.1

Proof of Proposition 2.1. We prove the statement by induction. First, using (2.32) for Φ_k^C and (2.33) for Φ_k^D, for $k = N-1$, we obtain:

$$\begin{aligned}\Phi_{N-1}^C(z) &= \bar{z}_{N-1}^\top\left(\bar{A}_{N-1}^\top\bar{P}_{N-1}^C + \bar{P}_{N-1}^C\bar{A}_{N-1}\right)\bar{z}_{N-1} \\ &= z_N^\top\left(A_N^\top P_N + P_N A_N\right)z_N = -2z_N^\top z_N,\end{aligned} \tag{B.10a}$$

$$\begin{aligned}\Phi_{N-1}^D(z) &= \bar{z}_{N-1}^\top\left(\bar{A}_{N-1}^\top\bar{P}_{N-1}^D\bar{A}_{N-1} - \bar{P}_{N-1}^D\right)\bar{z}_{N-1} \\ &= z_N^\top\left(A_N^\top P_N A_N - P_N\right)z_N = -2z_N^\top z_N,\end{aligned} \tag{B.10b}$$

thus (2.44) and (2.45) are verified for $k = N-1$. Assume that (2.44) and (2.45) are verified for $K \le N-1$, namely:

$$\Phi_K^C(z) = \bar{z}_K^\top(\bar{A}_K^\top\bar{P}_K^C + \bar{P}_K^C\bar{A}_K)\bar{z}_K \le -2\bar{\rho}_K\bar{z}_K^\top\bar{z}_K. \tag{B.11a}$$

$$\Phi_K^D(z) = \bar{z}_K^\top(\bar{A}_K^\top\bar{P}_K^D\bar{A}_K - \bar{P}_K^D)\bar{z}_K \le -2\bar{\rho}_K^D\bar{z}_K^\top\bar{z}_K. \tag{B.11b}$$

Using definitions (2.29), (2.34) and (2.38) we get

$$\begin{aligned}&\Phi_{K-1}^C(z) = \bar{z}_{K-1}^\top(\bar{A}_{K-1}^\top\bar{P}_{K-1}^C + \bar{P}_{K-1}^C\bar{A}_{K-1})\bar{z}_{K-1} \\ &= 2\begin{bmatrix}z_{K-1}\\ \bar{z}_{K-1}\end{bmatrix}^\top\begin{bmatrix}\rho_{K-1}^C P_{K-1} & 0\\ 0 & \bar{P}_{K-1}^C\end{bmatrix}\begin{bmatrix}A_{K-1} & M_{K-1}\\ 0 & \bar{A}_{K-1}\end{bmatrix}\begin{bmatrix}z_{K-1}\\ \bar{z}_{K-1}\end{bmatrix} \\ &= 2\rho_{K-1}^C z_{K-1}^\top P_{K-1}A_{K-1}z_{K-1} + 2\rho_{K-1}^C z_{K-1}^\top P_{K-1}M_{K-1}\bar{z}_{K-1} + 2\bar{z}_{K-1}^\top\bar{P}_K^C\bar{A}_K\bar{z}_{K-1}.\end{aligned} \tag{B.12a}$$

$$
\begin{aligned}
\Phi^D_{K-1}(z) &= \bar{z}^\top_{K-1}(\bar{A}^\top_{K-1}\bar{P}^D_{K-1}\bar{A}_{K-1} - \bar{P}^D_{K-1})\bar{z}_{K-1} \\
&= \begin{bmatrix} z_{K-1} \\ \bar{z}_{K-1} \end{bmatrix}^\top \left(\begin{bmatrix} A^\top_{K-1} & 0 \\ M^\top_{K-1} & \bar{A}^\top_{K-1} \end{bmatrix} \begin{bmatrix} \rho^D_{K-1}P_{K-1} & 0 \\ 0 & \bar{P}^D_{K-1} \end{bmatrix} \begin{bmatrix} A_{K-1} & M_{K-1} \\ 0 & \bar{A}_{K-1} \end{bmatrix} \right. \\
&\quad \left. - \begin{bmatrix} \rho^D_{K-1}P_{K-1} & 0 \\ 0 & \bar{P}^D_{K-1} \end{bmatrix} \right) \begin{bmatrix} z_{K-1} \\ \bar{z}_{K-1} \end{bmatrix} \qquad \text{(B.12b)} \\
&= \begin{bmatrix} z_{K-1} \\ \bar{z}_{K-1} \end{bmatrix}^\top \begin{bmatrix} \rho^D_{K-1}(A^\top_{K-1}P_{K-1}A_{K-1} - P_{K-1}) & \rho^D_{K-1}A^\top_{K-1}P_{K-1}M_{K-1} \\ \rho^D_{K-1}M^\top_{K-1}P^D_{K-1}A_{K-1} & \bar{A}^\top_K\bar{P}^D_K\bar{A}_K - \bar{P}^D_K \end{bmatrix} \begin{bmatrix} z_{K-1} \\ \bar{z}_{K-1} \end{bmatrix}^\top .
\end{aligned}
$$

Taking the norm of (B.12a), and using (B.11) and (2.32) we obtain the following upper bound for $\Phi^C_{K-1}(z)$

$$
\begin{aligned}
\Phi^C_{K-1}(z) \leq &- \begin{bmatrix} |z_{K-1}| \\ |\bar{z}_{K-1}| \end{bmatrix}^\top \begin{bmatrix} \rho^C_{K-1} & \rho^C_{K-1}\,|P_{K-1}M_{K-1}| \\ \star & \bar{\rho}^C_K \end{bmatrix} \begin{bmatrix} |z_{K-1}| \\ |\bar{z}_{K-1}| \end{bmatrix} \\
&- \min\{\rho^C_{K-1}, \bar{\rho}^C_K\} \begin{bmatrix} |z_{K-1}| \\ |\bar{z}_{K-1}| \end{bmatrix}^2 .
\end{aligned} \qquad \text{(B.13)}
$$

Similarly, taking the norm of (B.12b), and using (B.11) and (2.33) we obtain the following upper bound $\Phi^D_{K-1}(z)$:

$$
\begin{aligned}
\Phi^D_{K-1}(z) \leq &- \begin{bmatrix} |z_{K-1}| \\ |\bar{z}_{K-1}| \end{bmatrix}^\top \begin{bmatrix} \rho^D_{K-1} & \rho^D_{K-1}\left|A^\top_{K-1}P_{K-1}M_{K-1}\right| \\ \star & \bar{\rho}^D_K \end{bmatrix} \begin{bmatrix} |z_{K-1}| \\ |\bar{z}_{K-1}| \end{bmatrix} \\
&- \min\{\rho^D_{K-1}, \bar{\rho}^D_K\} \begin{bmatrix} |z_{K-1}| \\ |\bar{z}_{K-1}| \end{bmatrix}^2 .
\end{aligned} \qquad \text{(B.14)}
$$

Finally, we get

$$
\Phi^C_{K-1}(z) \leq -\bar{\rho}^C_{K-1}\bar{z}^\top_{K-1}\bar{z}_{K-1}, \quad \text{if} \quad \underbrace{\begin{bmatrix} \rho^C_{K-1} & \rho^C_{K-1}\,|P_{K-1}M_{K-1}| \\ \star & \bar{\rho}^C_K \end{bmatrix}}_{\Omega^C} > 0,
$$

$$
\Phi^D_{K-1}(z) \leq -\bar{\rho}^D_{K-1}\bar{z}^\top_{K-1}\bar{z}_{K-1}, \quad \text{if} \quad \underbrace{\begin{bmatrix} \rho^D_{K-1} & \rho^D_{K-1}\left|A^\top_{K-1}P_{K-1}M_{K-1}\right| \\ \star & \bar{\rho}^D_K \end{bmatrix}}_{\Omega^D} > 0,
$$

and it can be verified that Ω^C (respectively, Ω^D) is symmetric positive definite. Indeed the leading principal minors of Ω^C (respectively, Ω^D) are ρ^C_{K-1} (respectively, ρ^D_{K-1}) and $\rho^C_{K-1}(\bar{\rho}^C_K - \rho^C_{K-1}\,|P_{K-1}M_{K-1}|^2)$ (respectively, $\rho^D_{K-1}(\bar{\rho}^D_K - \rho^D_{K-1}\left|A^\top_{K-1}P_{K-1}M_{K-1}\right|^2)$), both of them being positive from the definition in (2.35) (respectively, (2.39)). □

Appendix C

Technical Proof for Chapter 5

Proof of Lemma 5.1. The characteristic polynomial $p_{A_{\text{int}}}(z)$ in (5.27) of matrix A_{int} can be conveniently rewritten as

$$p_{A_{\text{int}}}(z) = z^4 - 2z^3 + z^2 + \alpha z + \beta, \tag{C.1}$$

where we have defined the new coefficients

$$\alpha = k_P^{\text{int}}, \quad \beta = k_I^{\text{int}} - k_p^{\text{int}}. \tag{C.2}$$

We apply Jury stability criterion (see [53, Section 9.9.3]) to the polynomial (C.1), establishing whether its roots lie within the unit circle. We obtain that this condition is verified if and only if α and β satisfy

$$\alpha + \beta > 0 \tag{C.3a}$$
$$\beta - \alpha + 4 > 0 \tag{C.3b}$$
$$1 - |\beta| > 0 \tag{C.3c}$$
$$1 - \beta^2 - |\alpha + 2\beta| > 0 \tag{C.3d}$$
$$(\beta^2 - 1)^2 - (\alpha + 2\beta)^2 > \left|(\beta^2 - 1)(\beta - 1) + (\alpha + 2\beta)(\alpha\beta + 2)\right|. \tag{C.3e}$$

Define the functions $f(\alpha, \beta)$ and $g(\alpha, \beta)$ as follows

$$f(\alpha, \beta) = (\beta^2 - 1)^2 - (\alpha + 2\beta)^2 \tag{C.4a}$$
$$g(\alpha, \beta) = (\beta^2 - 1)(\beta - 1) + (\alpha + 2\beta)(\alpha\beta + 2). \tag{C.4b}$$

Note that $f(\alpha, \beta)$ and $g(\alpha, \beta)$ correspond to the left- and right-hand sides of inequality (C.3e), respectively. On the other hand, conditions (5.28) in Lemma 5.1, can be expressed as a function of α and β as

$$\alpha + \beta > 0 \tag{C.5a}$$

$$\frac{1-\sqrt{5}}{2} \leq \beta < 0 \tag{C.5b}$$

$$\beta(\beta-1)^2 - (\alpha+2\beta)(\alpha+2) > 0 \tag{C.5c}$$

The proof of Lemma 5.1 amounts to proving the equivalence between (C.3) and (C.5). Let $\mathcal{A}$ denote the set of values (α, β) satisfying inequalities (C.3), and $\mathcal{A}^*$ denote the set of values (α, β) satisfying (C.5). We want to prove that $\mathcal{A} \subseteq \mathcal{A}^*$. The reverse inclusion $\mathcal{A}^* \subseteq \mathcal{A}$ is trivial. From constraints (C.3d) and (C.3c) we get

$$\begin{cases} \alpha < -\beta^2 - 2\beta + 1 & \leq \min_\beta \left\{-\beta^2 - 2\beta + 1\right\} = 2 \\ \alpha > \beta^2 - 2\beta - 1 & \geq \max_\beta \left\{\beta^2 - 2\beta - 1\right\} = -2 \end{cases} \implies |\alpha| < 2 \tag{C.6}$$

Thus, conditions (C.6), (C.3a) and (C.3c) imply

$$\mathcal{A} \subseteq \mathcal{A}_1 := \left\{(\alpha, \beta) : |\beta| < 1,\, |\alpha| < 2,\, \alpha + \beta > 0\right\}$$

Moreover, it is trivial to prove that $(\alpha, \beta) \in \mathcal{A}_1$ satisfy the condition (C.3b). We have that, for any $(\alpha, \beta) \in \mathcal{A}_1$, the function g in (C.4b) satisfies

$$\begin{aligned} g(\alpha, \beta) &= (\beta^2-1)(\beta-1) + \underbrace{(\alpha+\beta)}_{>0}\underbrace{(\alpha\beta+2)}_{>0} + \beta(\alpha\beta+2) \\ &> (\beta^2-1)(\beta-1) + \beta(\alpha\beta+2) \\ &= -\beta^2 + \beta^3 - \beta + 1 + \alpha\beta^2 + 2\beta \\ &> -\beta^2 + \beta^3 + \beta + 1 - \beta^3 \\ &= -\beta^2 + \beta + 1, \end{aligned}$$

and we get

$$\tfrac{1-\sqrt{5}}{2} \leq \beta \leq \tfrac{1+\sqrt{5}}{2} \iff -\beta^2 + \beta + 1 \geq 0 \implies g(\alpha, \beta) > 0 \tag{C.7}$$

As a consequence, $g(\alpha, \beta)$ is positive in the set

$$\mathcal{A}^+ := \left\{(\alpha, \beta) : \tfrac{1-\sqrt{5}}{2} \leq \beta < 1,\ |\alpha| < 2,\ \alpha + \beta > 0\right\}.$$

Consider now the set

$$\mathcal{A}^- = \mathcal{A}_1 \setminus \mathcal{A}^+ = \left\{(\alpha, \beta) : -1 < \beta < \tfrac{1-\sqrt{5}}{2},\, |\alpha| < 2,\, \alpha + \beta > 0\right\}. \tag{C.8}$$

Note that $\mathcal{A}^- \cap \mathcal{A}^+ = \emptyset$ and $\mathcal{A}^- \cup \mathcal{A}^+ = \mathcal{A}_1$. We want to prove that

$$f(\alpha, \beta) < |g(\alpha, \beta)|, \tag{C.9}$$

for all $(\alpha, \beta) \in \mathcal{A}^-$. Two cases may occur:

(i) if $g(\alpha,\beta) \geq 0$ then

$$f(\alpha,\beta) - g(\alpha,\beta) < \beta^4 - 2\beta^2 - \beta = \beta(\beta+1)\left(\beta - \frac{1+\sqrt{5}}{2}\right)\left(\beta - \frac{1-\sqrt{5}}{2}\right),$$

and the following condition holds

$$-1 < \beta < \frac{1-\sqrt{5}}{2} \Longrightarrow \beta^4 - 2\beta^2 - \beta < 0 \Longrightarrow f(\alpha,\beta) - g(\alpha,\beta) < 0 \qquad \text{(C.10)}$$

(ii) If $g(\alpha,\beta) < 0$ then $|g(\alpha,\beta)| = -g(\alpha,\beta) > g(\alpha,\beta)$, and from the inequality (C.10) we have

$$f(\alpha,\beta) < g(\alpha,\beta) < -g(\alpha,\beta) = |g(\alpha,\beta)|$$

And (C.9) is verified.

We have proved that $\mathcal{A} \subseteq \mathcal{A}^+$.

Consider now $(\alpha,\beta) \in \mathcal{A}^+$. Applying the conditions (C.3e) and (C.7), we get

$$f(\alpha,\beta) > g(\alpha,\beta) > 0 \Longrightarrow f(\alpha,\beta) > 0. \qquad \text{(C.11)}$$

The function $f(\alpha,\beta)$ can be rewritten as $f(\alpha,\beta) = -(\alpha - f_1(\beta))(\alpha - f_2(\beta))$, where $f_1(\beta) = \beta^2 - 2\beta - 1$ and $f_2(\beta) = -\beta^2 - 2\beta + 1$. It can be shown that $f_1(\beta) < f_2(\beta)$ holds $\forall\beta : |\beta| < 1$. With this notation we obtain

$$f(\alpha,\beta) = -(\alpha - f_1(\beta))(\alpha - f_2(\beta)) > 0 \Longleftrightarrow \alpha < f_1(\beta) \vee \alpha > f_2(\beta). \qquad \text{(C.12)}$$

It follows that

$$\beta \underbrace{(\beta+1)}_{>0} \underbrace{(f_1(\beta) - \alpha)}_{<0} > 0 \Longrightarrow \beta < 0$$

holds for any $(\alpha,\beta) \in \mathcal{A}^+$.

Moreover, from condition (C.11), we get (C.3d). In fact

$$\begin{aligned} f(\alpha,\beta) &= (\beta^2-1)^2 - (\alpha+2\beta)^2 > 0 \\ &\Longrightarrow \left|\beta^2 - 1\right| > |\alpha + 2\beta| \\ &\Longrightarrow 1 - \beta^2 > |\alpha + 2\beta| \end{aligned}$$

holds for $(\alpha,\beta) : |\beta| < 1$. Finally, condition (C.5c) is obtained from (C.3e), (C.3c), and (C.4b) as follows

$$f(\alpha,\beta) - g(\alpha,\beta) = \beta(\beta^2-1)(\beta-1) - (\alpha+2\beta)(\alpha+2)(\beta+1) > 0$$

$$\Updownarrow$$

$$(\beta+1)\left[\beta(\beta-1)^2 - (\alpha+2\beta)(\alpha+2)\right] > 0$$

$$\Updownarrow$$

$$\beta(\beta-1)^2-(\alpha+2\beta)(\alpha+2)>0$$

We conclude that

$$\mathcal{A}\subseteq\{(\alpha,\beta):\frac{1-\sqrt{5}}{2}\leq\beta<0,\ \beta(\beta-1)^2-(\alpha+2\beta)(\alpha+2)>0,\ \alpha+\beta>0\}=\mathcal{A}^*,$$

and the statement is proven. □

Bibliography

[1] Arzelier, D. and Peaucelle, D. "An iterative method for mixed H_2/H_∞ synthesis via static output-feedback". *Proc. Conf. Decis. Control*. Vol. 3. IEEE. 2002, pp. 3464–3469.

[2] Beineke, L. W. and Wilson, R. J. *Topics in algebraic graph theory*. Vol. 102. Cambridge University Press, 2004.

[3] Benediktsson, J. A. and Swain, P. H. "Consensus theoretic classification methods". *Trans. Syst. Man Cybernet.* 22.4 (1992), pp. 688–704.

[4] Blondel, V. and Tsitsiklis, J. "NP-hardness of some linear control design problems". *SIAM J. Control Optim.* 35.6 (1997), pp. 2118–2127.

[5] Borcoci, E., Negru, D., and Timmerer, C. "A novel architecture for multimedia distribution based on content-aware networking". *IEEE Int. Conf. on Comm. Theory Reliability Quality of Service*. June 2010, pp. 162–168.

[6] Borkar, V. and Varaiya, P. "Asymptotic agreement in distributed estimation". *IEEE Trans. Autom. Control* 27.3 (1982), pp. 650–655.

[7] Bosworth, J. T. "Linearized aerodynamic and control law models of the X-29A airplane and comparison with flight data". *NASA Technical Memorandum 4356* (1992).

[8] Boyd, S. and El Ghaoui, L. "Method of centers for minimizing generalized eigenvalues". *Linear Algebra Appl* 188 (1993), pp. 63–111.

[9] Cao, Z. and Zegura, E. W. "Utility max-min: an application-oriented bandwidth allocation scheme". *Proc. of Annual Joint Conf. Computer and Comm. Societies.* Vol. 2. IEEE. 1999, pp. 793–801.

[10] Carli, R., Chiuso, A., Schenato, L., and Zampieri, S. "A PI Consensus Controller for Networked Clocks Synchronization". *Proc. IFAC World Congr. 2008*. July 2008, pp. 10289–10294.

[11] Carli, R. and Zampieri, S. "Network clock synchronization based on the second-order linear consensus algorithm". *IEEE Trans. Autom. Control* 59.2 (2014), pp. 409–422.

[12] Ceragioli, F., De Persis, C., and Frasca, P. "Discontinuities and hysteresis in quantized average consensus". *Automatica* 47.9 (2011), pp. 1916–1928.

[13] Changuel, N., Sayadi, B., and Kieffer, M. "Control of distributed servers for quality-fair delivery of multiple video streams". *Proc. ACM Int. Conf. Multimedia*. Nara, Japan, 2012.

[14] Changuel, N., Sayadi, B., and Kieffer, M. "Predictive encoder and buffer control for statistical multiplexing of multimedia contents". *IEEE Trans. Broadcast.* 58.3 (2012), pp. 401–416.

[15] Changuel, N., Sayadi, B., and Kieffer, M. "Control of multiple remote servers for quality-fair delivery of multimedia contents". *IEEE J. Select. Areas Commun.* 32.4 (Apr. 2014), pp. 746–759.

[16] Chebotarev, P. Y. and Agaev, R. P. "Coordination in multiagent systems and Laplacian spectra of digraphs". *Autom. Remote Control* 70.3 (2009), pp. 469–483.

[17] Chen, C., Zhu, X., Veciana, G. de, Bovik, A. C., and Heath, R. W. "Rate adaptation and admission control for video transmission with subjective quality constraints". *IEEE J. Sel. Top. Signal Process.* 9.1 (Feb. 2015), pp. 22–36.

[18] Chilali, M. and Gahinet, P. "H_∞ design with pole placement constraints: an LMI approach". *IEEE Trans. Autom. Control* 41.3 (Mar. 1996), pp. 358–367.

[19] Cho, J. and Chong, S. "Utility max-min flow control using slope-restricted utility functions". *IEEE Global Comm. Conf.* Dec. 2005, pp. 818–824.

[20] Cicalo, S. and Tralli, V. "Cross-layer algorithms for distortion-fair scalable video delivery over OFDMA wireless systems". *IEEE Global Comm. Conf.* Dec. 2012, pp. 1287–1292.

[21] Dai, D., Hu, T., Teel, A. R., and Zaccarian, L. "Output feedback design for saturated linear plants using deadzone loops". *Automatica* 45 (2009), pp. 2917–2924.

[22] Dal Col, L., Tarbouriech, S., and L., Z. "Global H_∞ synchronization control of linear multi-agent systems with input saturation". *Proc. American Control Conf.* 2016.

[23] Dal Col, L., Tarbouriech, S., and Zaccarian, L. "A consensus approach to PI gains tuning for quality-fair video delivery". *Submitted to Int. J. Robust Nonlinear Control* (2016).

[24] Dal Col, L., Tarbouriech, S., and Zaccarian, L. "H_∞ control design for synchronization of multi-agent systems". *Submitted to Int. J. Control* (2016).

[25] Dal Col, L., Tarbouriech, S., and Zaccarian, L. "Local H_∞ synchronization of multi-agent systems under input saturation". *Submitted to IEEE Trans. Autom. Control*. 2016.

[26] Dal Col, L., Tarbouriech, S., Zaccarian, L., and Kieffer, M. "A linear consensus approach to quality-fair video delivery". *Proc. Conf. Decis. Control*. Dec. 2014.

[27] Dal Col, L., Tarbouriech, S., Zaccarian, L., and Kieffer, M. "Equivalent conditions for synchronization of identical linear systems and application to quality-fair video delivery". *HAL-01116971 document* (2015).

[28] De Oliveira, M. C., Geromel, J. C., and Bernussou, J. "Extended H_2 and H_∞ norm characterizations and controller parametrizations for discrete-time systems". *Int. J. Control* 75.9 (2002), pp. 666–679.

[29] De Persis, C. and Frasca, P. "Hybrid coordination of flow networks". *Hybrid Systems with Constraints*. Ed. by Daafouz, J., Tarbouriech, S., and Sigalotti, M. Wiley, 2013, pp. 121–143.

[30] D'Innocenzo, A., Di Benedetto, M. D., and Serra, E. "Fault tolerant control of multi-hop control networks". *IEEE Trans. Autom. Control* 58.6 (2013), pp. 1377–1389.

[31] Dörfler, F. and Bullo, F. "Synchronization in complex networks of phase oscillators: A survey". *Automatica* 50.6 (2014), pp. 1539–1564.

[32] Drexl, M. "Synchronization in vehicle routing-A survey of VRPs with multiple synchronization constraints". *Transportation Science* 46.3 (2012), pp. 297–316.

[33] Ebihara, Y., Peaucelle, D., and Arzelier, D. *S-variable approach to LMI-based robust control*. Ed. by Springer. Springer, 2015.

[34] Fax, J. and Murray, R. "Graph Laplacians and Stabilization of Vehicle Formations". *Proc. of IFAC World Congr.* (2002), pp. 88–88.

[35] Fax, J. and Murray, R. "Information flow and cooperative control of vehicle formations". *IEEE Trans. Autom. Control* 49.9 (Sept. 2004), pp. 1465–1476. ISSN: 0018-9286.

[36] Fichera, F., Prieur, C., Tarbouriech, S., and Zaccarian, L. "A convex hybrid H_∞ synthesis with guaranteed convergence rate." *Proc. Conf. Decis. Control*. 2012, pp. 4217–4222.

[37] Fiedler, M. "Algebraic connectivity of graphs". *Czechoslovak Mathematical J.* 23.2 (1973), pp. 298–305.

[38] Gahinet, P., Nemirovskii, A., Laub, A. J., and Chilali, M. "The LMI control toolbox". *Proc. Conf. Decis. Control*. Vol. 2. 1994, pp. 2038–2038.

[39] Godsil, C. D., Royle, G., and Godsil, C. *Algebraic graph theory*. Vol. 207. Springer New York, 2001.

[40] Goebel, R., Sanfelice, R., and Teel, A. *Hybrid dynamical systems: modeling, stability, and robustness*. Princeton University Press, Mar. 2012.

[41] Gupta, S. K., Kar, K., Mishra, S., and Wen, J. T. "Distributed consensus algorithms for collaborative temperature control in smart buildings". *Proc. American Control Conf.* 2015, pp. 5758–5763.

[42] Hespanha, J. *Linear systems theory*. Princeton, New Jersey: Princeton Press, Sept. 2009.

[43] Home Page, x264. "VideoLan Organization". http://www.videolan.org/developers/x264.html. 2011.

[44] Hong, Y., Chen, G., and Bushnell, L. "Distributed observers design for leader-following control of multi-agent networks". *Automatica* 44.3 (2008), pp. 846–850.

[45] Horn, R. A. and Johnson, C. R. *Matrix analysis*. Cambridge university press, 2012.

[46] Hu, T. and Lin, Z. *Control systems with actuator saturation: analysis and design*. Springer, 2001.

[47] Ibnkahla, M. *Adaptation and Cross Layer Design in Wireless Networks*. CRC press, 2008.

[48] Index, C. V. N. *Forecast and methodology, 2009-2014*. Tech. rep. 2010.

[49] Lasserre, J. B. "Reachable, controllable sets and stabilizing control of constrained linear systems". *Automatica* 29.2 (1993), pp. 531–536.

[50] Lee, J.-W., Mazumdar, R. R., and Shroff, N. B. "Non-convex optimization and rate control for multi-class services in the Internet". *IEEE Trans. Networking* 13.4 (2005), pp. 827–840.

[51] Lee, K.-T., Tsai, W.-H., Liao, H.-Y. M., Chen, T., Hsieh, J.-W., and Tseng, C.-C. *Advances in Multimedia Modeling*. Springer, 2011.

[52] Leonard, N., Paley, D., Lekien, F., Sepulchre, R., Fratantoni, D., and Davis, R. "Collective Motion, Sensor Networks, and Ocean Sampling". *Proc. IEEE* 95.1 (2007), pp. 48–74.

[53] Levine, W. S. *The control handbook*. CRC press, 1996.

[54] Li, Y., Li, Z., Chiang, M., and Calderbank, A. "Content-aware distortion-fair video streaming in congested networks". *IEEE Trans. Multimedia* 11.6 (Oct. 2009), pp. 1182–1193.

[55] Li, Z., Duan, Z., Chen, G., and Huang, L. "Consensus of multiagent systems and synchronization of complex networks: a unified viewpoint". *IEEE Trans. Circuits Syst.* 57.1 (2010), pp. 213–224.

[56] Li, Z., Duan, Z., and Huang, L. "Leader-follower consensus of multi-agent systems". *Proc. American Control Conf.* June 2009, pp. 3256–3261.

[57] Lin, P., Jia, Y., Du, J., and Yu, F. "Distributed leadless coordination for networks of second-order agents with time-delay on switching topology". *Proc. American Control Conf.* June 2008.

[58] Listmann, K. D. "Novel conditions for the synchronization of linear systems". *Proc. Conf. Decis. Control*. 2015, pp. 5605–5612.

[59] Liu, Y., Jia, Y., Du, J., and Yuan, S. "Dynamic output feedback control for consensus of multi-agent systems: An H_∞ approach". *Proc. American Control Conf.* June 2009, pp. 4470–4475.

[60] Liu, Y. and Jia, Y. "H_∞ consensus control of multi-agent systems with switching topology: a dynamic output feedback protocol". *Int. J. Control* 83.3 (2010), pp. 527–537.

[61] Löfberg, J. "YALMIP: A toolbox for modeling and optimization in MATLAB". *Int. Symp. Computer Aided Control Syst. Design*. 2004, pp. 284–289.

[62] Massioni, P. *Decomposition methods for distributed control and identification*. PhD Thesis. TU Delft, Delft University of Technology, 2010.

[63] Masubuchi, I., Ohara, A., and Suda, N. "LMI-based controller synthesis: A unified formulation and solution". *Int. J. Robust Nonlinear Control* 8.8 (1998), pp. 669–686.

[64] Meng, Z., Zhao, Z., and Lin, Z. "On global leader-following consensus of identical linear dynamic systems subject to actuator saturation". *Systems and Control Letters* 62 (2013), pp. 132–142.

[65] Merris, R. "Laplacian matrices of graphs: a survey". *Linear Algebra Appl* 197 (1994), pp. 143–176.

[66] Mesbahi, M. and Egerstedt, M. *Graph theoretic methods in multiagent networks*. Princeton University Press, 2010.

[67] Ming-Syan, C., Philip, S. Y., and Kun-lung, W. "Optimal all-to-all broadcast schemes in distributed computing systems". *IBM Research Report, RC* 17003 (1991).

[68] Mohar, B., Alavi, Y., Chartrand, G., and Oellermann, O. "The Laplacian spectrum of graphs". *Graph theory, combinatorics, and applications* 2.871-898 (1991), p. 12.

[69] Moreau, L. "Stability of continuous-time distributed consensus algorithms". *Proc. Conf. Decis. Control*. Vol. 4. Dec. 2004, 3998–4003 Vol.4.

[70] Mosek, A. "The MOSEK optimization software". *Online at http://www. mosek. com* 54 (2010).

[71] Nair, S. and Leonard, N. "Stable synchronization of mechanical system networks". *SIAM J. Control Optim.* 47.2 (Feb. 2008), pp. 661–683.

[72] Olfati-Saber, R., Fax, J., and Murray, R. "Consensus and Cooperation in Networked Multi-Agent Systems". *Proc. IEEE* 95.1 (Jan. 2007), pp. 215–233.

[73] Oliveira, M. C. de and Skelton, R. E. "Stability tests for constrained linear systems". *Perspectives in robust control*. Springer, 2001, pp. 241–257.

[74] Pipeleers, G., Demeulenaere, B., Swevers, J., and Vandenberghe, L. "Extended LMI characterizations for stability and performance of linear systems". *Systems and Control Letters* 58.7 (2009), pp. 510–518.

[75] Rao, B., Durrant-Whyte, H. F., and Sheen, J. A. "A fully decentralized multi-sensor system for tracking and surveillance". *Int. J. of Rob. Res.* 12.1 (1993), pp. 20–44.

[76] Ren, W. "Consensus strategies for cooperative control of vehicle formations". *IET Control Theory Appl.* 1.2 (Mar. 2007), pp. 505–512.

[77] Ren, W. and Beard, R. "Consensus algorithms for double-integrator dynamics". *Distributed Consensus in Multi-vehicle Cooperative Control: Theory and Applications* (2008), pp. 77–104.

[78] Ren, W. "Collective motion from consensus with Cartesian coordinate coupling". *IEEE Trans. Autom. Control* 54.6 (2009), pp. 1330–1335.

[79] Ren, W., Moore, K., and Chen, Y. "High-Order Consensus Algorithms in Cooperative Vehicle Systems". *Int. Conf. Networking, Sensing Control*. 2006.

[80] Rockafellar, R., Wets, R., and Wets, M. *Variational Analysis*. Grundlehren der mathematischen Wissenschaften. Springer, Oct. 2011. ISBN: 9783642083044.

[81] Rudin, W. *Functional Analysis*. Mathematics series. McGraw-Hill, 1991.

[82] Sawada, K., Kiyama, T., and Iwasaki, T. "Generalized sector synthesis of output feedback control with anti-windup structure". *Systems and Control Letters* 58 (2009), pp. 421–428.

[83] Scardovi, L. and Sepulchre, R. "Synchronization in networks of identical linear systems". *Automatica* 45.11 (2009), pp. 2557–2562.

[84] Scherer, C., Gahinet, P., and Chilali, M. "Multiobjective output-feedback control via LMI optimization". *IEEE Trans. Autom. Control* 42.7 (1997), pp. 896–911.

[85] Seo, J., Shim, H., and J.Back. "Consensus of high-order linear systems using dynamic output feedback compensator: Low gain approach". *Automatica* 45.11 (Nov. 2009), pp. 2659–2664.

[86] Shenker, S. "Fundamental design issues for the future Internet". *IEEE J. Selected Areas in Comm.* 13.7 (1995), pp. 1176–1188.

[87] Shi, G. and Hong, Y. "Distributed coordination of multi-agent systems with switching structure and input saturation". *Proc. Conf. Decis. Control*. 2009, pp. 895–900.

[88] Sontag, E. D. "An algebraic approach to bounded controllability of linear systems". *Int. J. Control* 39.1 (1984), pp. 181–188.

[89] Stan, G. and Sepulchre, R. "Analysis of Interconnected Oscillators by Dissipativity Theory". *IEEE Trans. Autom. Control* 52.2 (Feb. 2007), pp. 256–270.

[90] Stefanov, S. *Separable Programming: Theory and Methods*. Applied Optimization. Springer, 2001. ISBN: 9780792368823.

[91] Strogatz, S. H. "From Kuramoto to Crawford: exploring the onset of synchronization in populations of coupled oscillators". *Physica D* 143.1 (2000), pp. 1–20.

[92] Strogatz, S. and Edwards, A. W. *Sync- how order emerges from chaos in the universe, nature, and daily life*. Vol. 27. 1. Springer, 2005, pp. 89–89.

[93] Su, H., Chen, M., Lam, J., and Lin, Z. "Semi-Global Leader-Following Consensus of Linear Multi-Agent Systems With Input Saturation via Low Gain Feedback". *IEEE Trans. Circuits Syst.* 60.7 (2013), pp. 1881–1889.

[94] Syrmos, V., Abdallah, C., Dorato, P., and Grigoriadis, K. "Static output feedback—A survey". *Automatica* 33.2 (Feb. 1997), pp. 125–137.

[95] Takaba, K. "Synchronization of linear multi-agent systems under input saturation". *Int. Symposium on Mathematical Theory of Networks and Systems*. Groningen, The Netherlands, July 2014, pp. 1076–1079.

[96] Talebi, M. S., Khonsari, A., Hajiesmaili, M. H., and Jafarpour, S. "A suboptimal network utility maximization approach for scalable multimedia applications". *IEEE Global Telecom. Conf.* 2009, pp. 1–6.

[97] Tanenbaum, A. S. and Van Steen, M. *Distributed systems*. Prentice-Hall, 2007.

[98] Tarbouriech, S., Garcia, G., Gomes da Silva Jr., J., and Queinnec, I. *Stability and Stabilization of Linear Systems with Saturating Actuators*. Springer, London (UK), 2011.

[99] Tarbouriech, S., Prieur, C., and Gomes da Silva Jr., J. "Stability analysis and stabilization of systems presenting nested saturations". *IEEE Trans. Autom. Control* 51.8 (2006), pp. 1364–1371.

[100] Tarbouriech, S. and Turner, M. "Anti-windup design: an overview of some recent advances and open problems". *IET Control Theory Appl* 3.1 (2009), pp. 1–19.

[101] Teel, A., Forni, F., and Zaccarian, L. "Lyapunov-based sufficient conditions for exponential stability in hybrid systems". *IEEE Trans. Autom. Control* 58.6 (2013), pp. 1591–1596.

[102] Toker, O. and Özbay, H. "On the NP-hardness of solving bilinear matrix inequalities and simultaneous stabilization with static output feedback". *Proc. American Control Conf.* Vol. 4. 1995, pp. 2525–2526.

[103] Tsitsiklis, J. N., Bertsekas, D. P., and Athans, M. "Distributed asynchronous deterministic and stochastic gradient optimization algorithms". *Proc. American Control Conf.* 1984, pp. 484–489.

[104] Tuna, S. "LQR-based coupling gain for synchronization of linear systems". *arXiv preprint arXiv:0801.3390* (2008).

[105] Turner, M. C. and Postlethwaite, I. "A new perspective on static and low order anti-windup synthesis". *Int. J. Control* 77.1 (2004), pp. 27–44.

[106] Van der Schaft, A. *$\mathcal{L}_2-$gain and passivity techniques in nonlinear control*. Springer Science & Business Media, 2012.

[107] Wang, Z., Bovik, A., Sheikh, H., and Simoncelli, E. "Image quality assessment: from error visibility to structural similarity". *IEEE Trans. Image Process.* 13.4 (Apr. 2004), pp. 600–612.

[108] Weller, S. C. and Mann, N. C. "Assessing rater performance without a "gold standard" using consensus theory". *Med. Decis. Making* 17.1 (1997), pp. 71–79.

[109] Wieland, P., Kim, J., Scheu, H., and Allgöwer, F. "On consensus in multi-agent systems with linear high-order agents". *Proc. IFAC World Congr.* Vol. 17. 2008, pp. 1541–1546.

[110] Wieland, P., Sepulchre, R., and Allgöwer, F. "An internal model principle is necessary and sufficient for linear output synchronization". *Automatica* 47.5 (Mar. 2011), pp. 1068–1074.

[111] Wieland, P. "From static to dynamic couplings in consensus and synchronization among identical and non-identical systems". PhD thesis. Universität Stuttgart, 2010.

[112] Xia, T. and Scardovi, L. "Synchronization conditions for diffusively coupled linear systems". *Int. Symposium on Mathematical Theory of Networks and Systems*. July 2014, pp. 1070–1075.

[113] Xia, T. and Scardovi, L. "Output-feedback synchronizibility of linear time-invariant systems". *Systems and Control Letters* 94 (Aug. 2015), pp. 152–158. eprint: 1512.01910.

[114] Xiao, F. and Wang, L. "Consensus problems for high-dimensional multi-agent systems". *IET Control Theory Appl* 1.3 (May 2007), pp. 830–837. ISSN: 1751-8644.

[115] Yang, G. and Ye, D. "Robust H_∞ dynamic output feedback control for linear time-varying uncertain systems via switching-type controllers". *IET Control Theory Appl.* 4.1 (2010), pp. 89–99.

[116] Yang, T., Meng, Z., Dimarogonas, D. V., and Johansson, K. H. "Global consensus for discrete-time multi-agent systems with input saturation constraints". *Automatica* 50 (2014), pp. 499–506.

[117] Youla, D., Bongiorno Jr, J., and Lu, C. "Single-loop feedback-stabilization of linear multivariable dynamical plants". *Automatica* 10.2 (1974), pp. 159–173.

[118] Zaccarian, L. and Teel, A. *Modern anti-windup synthesis*. Princeton University Press, 2011.

[119] Zhang, H., Lewis, F., and Das, A. "Optimal design for synchronization of cooperative systems: state feedback, observer and output feedback". *IEEE Trans. Autom. Control* 56.8 (2011), pp. 1948–1952.

[120] Zhu, J. and Yang, G. "Robust H_∞ dynamic output feedback synchronization for complex dynamical networks with disturbances". *Neurocomputing* 175 (Jan. 2016), pp. 287–292.